ABSTRACT

LI, SHUHAI. Comparing the Performance of Naturally Ventilated and Fan Ventilated Greenhouses. (Under the direction of Daniel H. Willits.)

In order to evaluate the comparative performance of natural ventilation (NV) and fan-ventilation (FV) greenhouses, several aspects of cooling were considered: fog cooling and control in NV houses; thermal stratification in FV houses; environmental comparison of NV and FV houses and their suitability under a variety of climates.

Cooling efficiency and evaporation efficiency of low-pressure and high-pressure fogging systems were compared. Data show that the high-pressure system had greater evaporation efficiency and cooling efficiency than the low-pressure system. A control strategy, NCSU control, was proposed to control both the pump and the vents in a high-pressure fogging system for naturally ventilated greenhouses. NCSU control and four other control strategies were tested. It was found that NCSU control cycled the pump less frequently and resulted in higher cooling efficiency. NCSU control was shown to be able to maintain air temperature and relative humidity simultaneously.

Thermal stratification in a fan-ventilated house was studied. Experimental data suggested that the vertical air temperature variation increased with solar radiation. Lower ventilation rates, in conjunction with evaporative pad cooling, also created greater vertical air temperature variations. The presence of a canopy reduced air temperature variation. A model was developed to predict the air temperature distribution in the vertical direction. Simulations suggested that increased ventilation reduced air temperature more in the upper part of the greenhouse. Evaporative pad cooling reduced air temperature more in the lower part of the greenhouse.

The inside environment was compared between NV and FV houses. The spatial variation of air temperature of the FV houses was more than in the NV houses and the air temperature in the NV houses underwent less variation during the course of a day. Leaf temperature was higher than air temperature when evaporative pads were used. The reverse was true when evaporative pads were not used. The cooling abilities of fan-and-pad system and high-pressure fog with natural ventilation were comparable in terms of temperature reduction. Due to lower airflow in NV houses, inside enthalpy was higher in NV houses than in FV houses.

The suitability of fan and natural ventilation with evaporative cooling (evaporative pads and high-pressure fog) was investigated with a simulation model and the weather data of selected locations. It is suggested that the suitability of various cooling technologies depends on climate, evapotranspiration and the ventilation characteristics. The geographical distribution pattern of suitable cooling technologies was examined for the U.S.

COMPARING THE PERFORMANCE OF NATURALLY VENTILATED AND FAN VENTILATED GREENHOUSES

By

SHUHAI LI

A thesis submitted to the Graduate Faculty of

North Carolina State University

in partial fulfillment of the

requirements for the Degree of

Doctor of Philosophy

BIOLOGICAL AND AGRICULTURAL ENGINEERING

Raleigh, NC

2007

APPROVED BY:

Mary M. Peet	**James H. Young**
Dan H. Willits Chair of Advisory Committee	**Jack R. Edwards Jr.** Minor Representative

BIOGRAPHY

Shuhai Li was born in Henan Province, China on July 2nd, 1978. He earned his bachelor's degree from China Agricultural University in Agricultural Structure and Environmental Engineering. He pursued his master's degree at the same university and worked on greenhouse environment modeling. In the fall of 2003, he entered the doctoral program in Controlled Environment Agriculture at NC State under Dr. Daniel H. Willits and will complete his degree in May of 2007.

ACKNOWLEDGEMENTS

It is a great relief to finally arrive at this point after a long journey of dissertation writing, feeling as if I am standing on an outlook platform after hiking a long trail. Looking back the sophisticated terrain and dense canopy behind, I realized there were so many chances I could have been lost in the forest without the invaluable guidance and assistance from the people to whom I am indebted so much.

I express my deepest gratitude to Dr. Willits, my advisor, for his guidance during the past four years. As his sole PhD student, I received much more attention and advice than otherwise possible. His integrity, persistence and self-discipline will always be an inspiration of what a scientist is supposed to be. I truly appreciate his numerous assistances during research and personal issues. It is unforgettable that he once drove me to hospital after I cut my finger accidentally.

I thank Dr. Jack Edward, Dr. Mary Peet and Dr. Jim Young for serving on my committee. The efforts they put into my exams and the multitude of suggestions they gave on my research are appreciated very much.

The person I would like to thank most is Cyrus Yunker. Over the years, we have been working side by side. The friendship we developed will be lifelong treasure to me. I also thank Justin Macialek, Chase Helms, Jessica Bradford, and Heidi Bunn for their excellent work during the project.

The financial support for my PhD study from BARD is also acknowledged.

Finally, I would like to thank my parents, Fashan Li and Chuanqin Liu and my fiancée, Ying Li for their encouragement and motivation during my four years's study.

TABLE OF CONTENTS

LIST OF TABLES

LIST OF FIGURES

Chapter 1 Introduction

1.1 Greenhouse Production in U.S. and World

Agricultural production can be categorized as either indoor or open field production. Greenhouses are a type of indoor production facility characterized by transparent covers. Greenhouse, nursery and floriculture products have become increasingly popular and have become a fast growing sector of agricultural economy of the U.S. The expenditure per household on nursery and greenhouse products increased by 54% from 1990 to 2004 (Noel, 2005). The value of vegetables, melons and other specialty crops was about $11.2 billion (National Agricultural Statistics Service, 2005). Among them, greenhouse production accounts for a significant portion.

Rapid increases in greenhouse production were seen in the past two decades across the world. Increased and year-around demand for high quality produce, and increased concern about food security, are some of the factors that have contributed to the rapid development of the greenhouse industry. Aside from the several major export countries of horticultural products such as the Netherlands and Israel, greenhouse production has become an important industry in countries such as Spain, Greece, China, South Korea and Mexico. A large portion of greenhouse production is concentrated in areas like the Mediterranean, North Europe, East Asia and North America (Enoch and Enoch, 1999). Greenhouse produce exported from these countries and regions is increasing every year.

As greenhouse production increases dramatically overseas, especially in developing countries, greenhouse growers in the U.S. face increasing competition. They are looking for all possible means to minimize costs to maintain profitability. One of the strategies is to

migrate operations to warm regions to reduce heating costs in winter, a major operational cost. However, cooling problems in summer have become of more concern because warm winters are generally accompanied by hot summers. One straightforward solution to avoiding summer cooling is to halt production during that period. However, keeping greenhouses empty is not an economical option for many growers because they will lose revenue by not fully using structures and equipment with limited lifetime (Beytes, 2006). Moreover, year-round production is an important strategy to maintain an established brand. A break of supply of several months could have a chilling effect on market share.

1.2 Greenhouse Cooling Technologies

To maintain summer production, cooling must be provided to ensure proper growth conditions for the crop. Greenhouse cooling is achieved, first of all, by the intrinsic function of plant-transpiration (Seginer *et al.*, 2000). By evaporating water through leaf surfaces, plants keep leaf temperature from rising to detrimental levels. Ventilation, the process of exchanging air inside the greenhouse with that outside (ASAE, 2003), is needed for plant transpiration to take place continually, otherwise, water vapor will be built up inside the greenhouse and transpiration will be suppressed.

Greenhouse ventilation is either driven by natural wind and/or buoyancy effect (natural ventilation) or fans (fan ventilation). Studies have suggested that natural ventilation (NV) driven by wind will be dominant over that driven by buoyancy when outdside wind speed is above 1-2 m s^{-1}. In summer, wind speeds in open areas are generally higher than that because of atmospheric activities, therefore natural ventilation in summer is primarily wind induced. For that reason, natural ventilation is unstable and unpredictable. In addition, airflow inside NV houses is complex and irregular. On the other hand, airflow is more regular

in FV houses than NV houses. Even on windy days where the performance of fans can be affected, airflow will not deviate from design condition significantly. These differences between NV and FV determine their respective cooling performance and their compatibilities with other cooling systems.

When ventilation is not sufficient to mitigate the temperature in greenhouses, evaporative cooling will generally be applied. Evaporative pad cooling and fogging are two commonly used evaporative cooling technologies.

Evaporative pads are usually made of a water absorbent material and fabricated in forms that allow air penetrating. When the pad is wetted by water supplied from above and air is pulled through the pad, part of the sensible heat of the incoming air is transformed into latent heat, resulting in reduced air temperature and increased relative humidity. Evaporative pads are generally used with fan ventilation but not with natural ventilation. The reason is that for evaporative pads to work properly, they must be installed at the air intake of a greenhouse so that cooler air leaving the pad will move into the greenhouses. In NV houses, more than one vent is generally installed so these vents can coordinate each other. When some vents function as intakes, others may function as outlets. Since wind direction is constantly changing, the vents that originally functioned as intakes may change to outlets and vice versa. There are no fixed intakes so it is impossble to determine where pads should be installed. Moreover, pads will reduce the already low ventilation rates in NV houses.

In FV houses, an evaporative pad is generally installed in an end wall and fans are installed in the opposite wall. A schematic of a fan-and-pad system is shown in Fig.1.1. The temperatures given in the schematic are for illustration purposes.

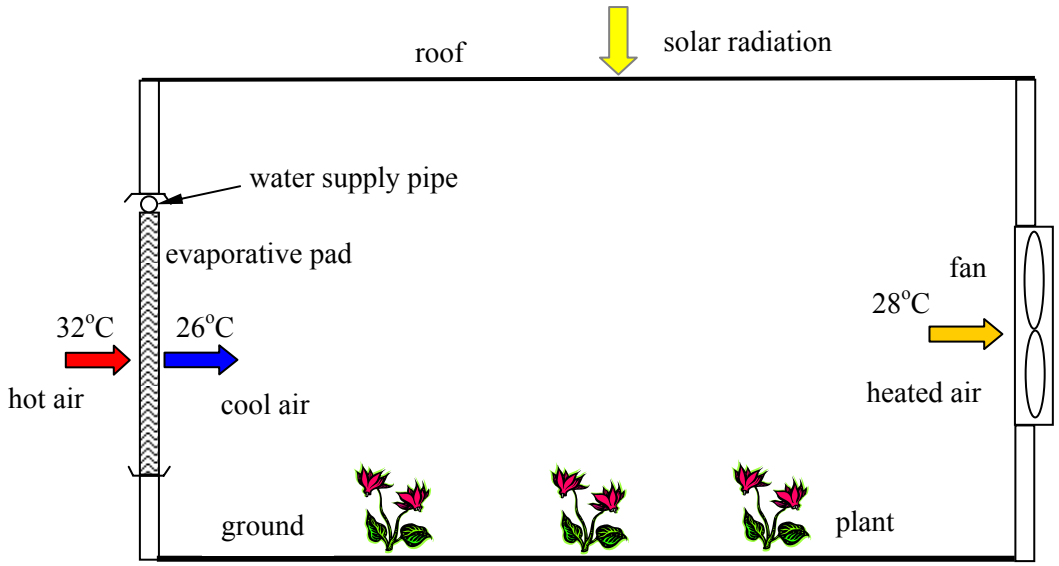

Figure 1.1 Schematic of fan and pad systems

Fogging, a second measure of evaporative cooling, cools by spraying fine water droplets into the air. During the course of drifting or falling, the droplets evaporate partially or completely, converting some sensible heat of greenhouse air into latent heat. Air temperature is thus reduced and relative humidity is increased. Based on working pressure, fogging systems can be classified as low-pressure fogging or high-pressure fogging systems. Low-pressure fogging systems typically work at the line pressure of city water supply (3-4 atm) without additional pressure boosting. The size of droplets produced by low-pressure systems is typically 50 to 100 μm. The working pressure of high-pressure systems is much higher (35-70 atm) than low-pressure systems and high-pressure pumps are typically utilized. The droplet size produced by high-pressure systems is typically 2 to 60 μm.

Fogging is not as compatible with FV systems as evaporative pads because it is difficult to keep unevaporated droplets from being blown out of the house through the fan(s). For this reason, fogging is not normally used in FV houses. Evaporative pad cooling is a

mature technology, which works very well for most FV houses. There is no reason to use fogging in FV houses. Fogging is generally used in NV houses since fogging is the only evaporative cooling technology compatible with NV. A schematic of a fogging system in a NV greenhouse is given in Fig.1.2.

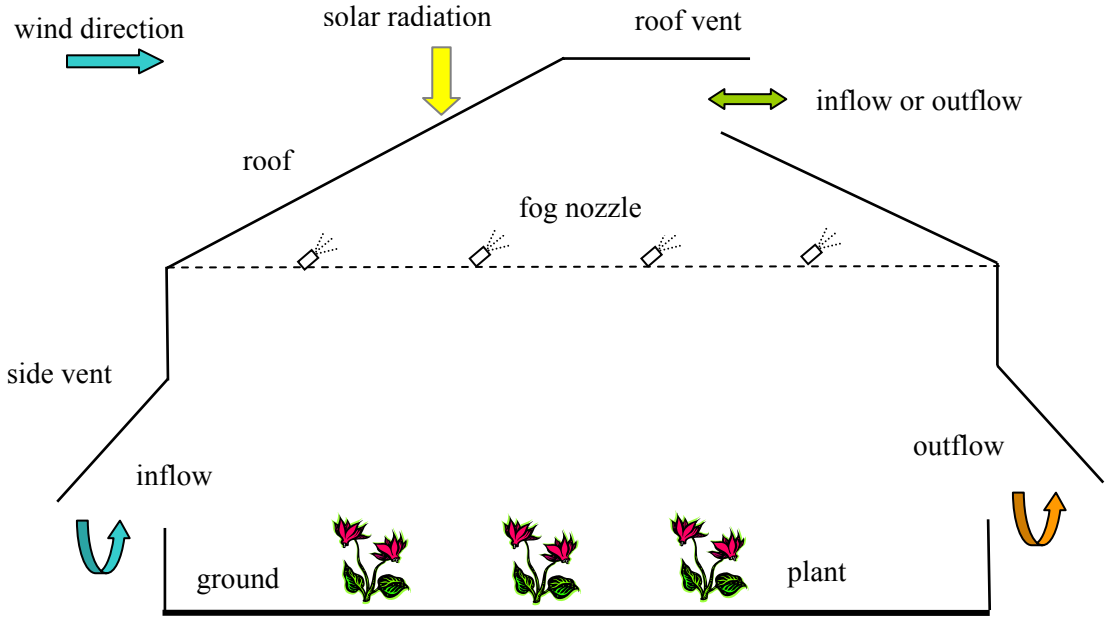

Figure 1.2 Schematic of fogging systems in naturally ventilated greenhouses

1.3 Design Limitations

As a principal method for controlling and regulating temperature, selection of the ventilation system is a key step in designing a greenhouse. Currently, four greenhouse design guidelines (ASABE, 2003; ACME, 1993; NGMA, 1998; ASHRAE, 1995) are available for designers in the U.S., but none of the guidelines provide information on the choice of a ventilation system. The selection of a greenhouse ventilation mechanism is still a practice based on rule of thumb. An improper choice may waste money and/or expose the crop to unfavorable conditions.

A controlled comparison of the performance of the two ventilation systems is a pre-requisite for making a sound choice. A literature survey shows that most studies focus on either NV or FV system (NV examples: Bot, 1983; De Jong, 1990; Lee and Short, 2000; Wang, 1998; Teitel and Tanny, 1999; Boulard and Baille, 1995. FV examples: Walker, 1965; Seginer and Livne, 1978; Willits, 2003). There have been essentially no studies on the comparative performance of the two systems.

1.4 Objectives

To address these problems, this study will focus on the thermal environment (air temperature, relative humidity and leaf temperature) of two ventilation systems, because thermal environment is the one of the most important factors that affects plant growth. In comparing the thermal environment of NV and FV systems, fogging in NV houses and thermal stratification in FV houses are recognized as two important factors that affect the comparative performance of NV and FV systems.

1.4.1 Fog Cooling in NV Houses

Fogging was chosen as a focus for this study because in order for NV houses to compete with FV houses with pads, evaporative cooling must be provided. While evaporative pads have been studied extensively and the cooling performance is well known, fogging systems have been less well studied and the cooling performance is poorly known, thus, fogging in NV houses needs to be better understood and controlled for an effective comparison of NV and FV houses.

Previous fog studies (Montero *et al*, 1990; Giacomelli *et al*, 1985; Arbel *et al*, 1999; Arbel *et al*, 2003) have certain limitations: 1) studies were conducted in a single greenhouse

without a control, so it is not possible to isolate the effect of fogging from others such as weather; 2) almost all of the studies did not consider the more fundamental charateristics of greenhouse fogging (cooling efficiency and evaporation efficiency), only air temperature and relative humidity were discussed; 3) the response of leaf temperature to fogging was not considered in most studies; and 4) the studies focused on either low-pressure or high-pressure fog, and none of them constrasted them. This study will attempt to address all of these limitations.

Fogging systems are difficult to control in NV greenhouses, because fog evaporation efficiency depends on weather conditions and ventilation rate. Since ventilation rate is dependent on the wind, spray rates are impossible to determine in advance. To resolve the difficulty, various fog control strategies will be explored and their performance will be evaluated.

1.4.2 Thermal Stratification in FV Houses

Thermal stratification was chosen as a focus of this study because during the study comparing NV and FV systems, vertical air temperature gradient in FV houses complicated the comparison. Given the significant vertical temperature gradient observed, especially at low ventilation rates, the control computer called for less cooling than required. The result was that FV houses ended up with higher temperatures than the NV houses, even through the cooling ability of the FV systems was superior to the NV systems at the time (Willits and Li, 2005).

To find out what the vertical air temperature distribution is and how weather, crop and evaporative pad cooling affect it, experiments were performed and a model was constructed to describe the thermal stratification in FV houses.

1.5 Dissertation Composition

This dissertation consists of eight chapters. Chapters 2 and 3 focus on fogging systems. In Chapter 2, cooling and evaporation efficiencies are compared for low-pressure and high-pressure fogging systems in a NV greenhouse. Chapter 3 describes a new control strategy for high-pressure fog in NV greenhouses. The new strategy, called NCSU control, along with four existing strategies, were tested in a NV greenhouse. The performance of the control strategies was evaluated and compared in terms of cooling efficiency, water use, duty circle of high-pressure pump and leaf wetness duration.

Chapters 4 and 5 focus on thermal stratification in FV greenhouses. In Chapter 4, observed airflow patterns and thermal stratification in a FV greenhouse are investigated. The effects of solar radiation, ventilation rate, evaporative cooling and canopy on vertical temperature profiles are presented. Chapter 5 describes a mechanistic model for the vertical air temperature gradient in FV houses. Model calibration, verification and simulation results are presented.

Chapters 6 and 7 compare the environment in NV and FV systems and investigate the suitability of the two systems in different locations. Chapter 6 examines the spatial and temporal variation of air temperature, leaf-air temperature difference of NV and FV systems. The cooling performance of high-pressure fog in a NV system is compared with that of fan-and-pad systems. Chapter 7 explores the suitability of various cooling technologies-NV, FV and evaporative cooling (evaporative pad vs. fogging) under various climates using a simulation model. The effects of evapotranspiration and ventilation characteristics of NV systems are discussed. The geographical disbution pattern of suitable cooling technologies is

discussed for the U.S.

Finally, Chapter 8 provides a summary for this study.

References

ACME. 1993. The greenhouse climate control book. ACME Engineering and Manufacturing Corp., Horticulture Division, Muskogee, OK

Arbel, A.; Yekutieli, O.; Barak, M. 1999. Performance of a fog system for cooling greenhouses. *Journal of Agricultural Engineering Research*, 72: 129-136

Arbel, A.; Barak, M.; Shklyar, A. 2003. Combination of forced ventilation and fogging systems for cooling greenhouses. *Journal of Agricultural Engineering Research*, 84(1): 45-55

ASAE. 2003. Heating, ventilating and cooling greenhouses. ANSI/ASAE EP406.2. American Society of Agricultural Engineers, St. Joseph, MI

ASHARE. 1995. Environment control for animals and plants. In: 1995 ASHARE handbook: heating, ventilating and air-conditioning applications. ASHARE, Atlanta, GA

Beytes, C. 2006. What makes Cheshire tick? *Grower Talks*, 70(5): 80-88

Bot, G.P.A. 1983. Greenhouse climate: from physical processes to a dynamic model. PhD dissertation. Wageningen Agricultural University, Wageningen, Netherlands

Boulard, T.; Baille, A. 1995. Modeling of air exchange rate in a greenhouse equipped with continuous roof vents. *Journal of Agricultural Engineering Research*, 61:37-48.

De Jong, T. 1990. Natural ventilation of large multi-span greenhouses. PhD dissertation. Agricultural University, Wageningen, Netherlands

Enoch, H.Z. and Enoch, Y. 1999. The history and geography of greenhouse. In: Greenhouse ecosystems. Edited by Stanhill, G. and Enoch, H.Z. Elservier. Amsterdam, Netherlands

Giacomelli, G.; Giniger, M.S.; Krass, A.E. *et al*. 1985. Improved methods of greenhouse evaporative cooling. *Acta Horticulturae*. 1974: 49-55

Lee, I.; Short T.H. 2000. Two-dimensional numerical simulation of natural ventilation in a multi-span greenhouse. *Transaction of the ASAE*, 43(3): 745-753

Kittas, C.; Bartzanas, T.; Jaffrin, A. 2003. Temperature gradients in a partially shaded large greenhouse equipped with evaporative cooling pads. *Biosystems Engineering*, 85(1): 87– 94

Montero, J.I.; Anton, A.; Biel, C. *et al*. 1990. Cooling of greenhouses with compressed air fogging nozzles. *Acta Horticulturae*, 281: 199-209

National Agricultural Statistics Service. 2005. http://www.nass.usda.gov/Publications/Ag_Statistics/agr05/05_ch4.PDF

NGMA. 1998. Standards for ventilation and cooling greenhouse structures. National Greenhouse Manufacturer Association, Littleton, CO

Noel, J.E. 2005. The U.S. specialty crop industry: significance and sustainability. http://cissc.calpoly.edu/farmbill/USSpecCropIndSigandSust.pdf

Seginer, I; Livne, A. 1978. Effect of ceiling height on the power requirement of forced ventilation in greenhouses. *Acta Horticulturae*, 87: 51–68

Seginer, I.; Willits, D. H.; Raviv M.; Peet, M. M. 2000. Transpirational cooling of greenhouse crops. BARD Final Scientific Report IS-2538-95R, Bet Dagan, Israel

Teitel, M.; Tanny, J. 1999. Natural ventilation of greenhouses: experiments and model. *Agricultural and Forest Meteorology*, 96: 59-70Teitel, M. 2005. Personal communication

Walker, J. N. 1965. Predicting temperatures in ventilated greenhouses. *Transactions of the ASAE*, 8 (3): 445– 448

Wang, S. 1998. Measurement and modeling of natural ventilation in a large scale Venlo-type greenhouse. PhD dissertation. Gembloux, Belgium

Willits, D.H. 2003. Cooling fan ventilated greenhouses: a modeling study. *Biosystems Engineering*, 84(3): 315–329

Willits, D.H.; Li, S. 2005. A Comparison of naturally ventilated vs. fan ventilated greenhouses in the southeastern U.S. ASAE paper No. 05-4155. American Society of Agricultural and Biological Engineers, St. Joseph, MI

Chapter 2 Comparing Low-Pressure and High-Pressure Fogging Systems in Naturally Ventilated Greenhouses

Abstract The cooling performance of low-pressure and high-pressure fogging systems was evaluated. Two month long experiments were conducted in two empty, naturally ventilated greenhouses under summer conditions. One greenhouse was used as the treatment greenhouse (fogged house) and the other was used as the control house (unfogged house). Cooling efficiency was defined as the ratio of the temperature difference between the unfogged and fogged greenhouses to the difference between the temperature in unfogged house and the wet bulb temperature in the fogged greenhouse. Evaporation efficiency was defined as the ratio of evaporation rate to spray rate. Cooling efficiency and evaporation efficiency were compared for low-pressure and high-pressure systems after accounting for differences in weather conditions. It is suggested that evaporation efficiency for the high-pressure system was at least 64% greater than the low-pressure system; cooling efficiency for the high-pressure system was at least 28% greater than for the low-pressure system on average.

2.1 Introduction

Fogging is one type of evaporative cooling that comes with a myriad of applications and configurations. Cooling, humidification, and seed propagation are some of the principal applications in protected horticulture. An important characteristic of fogging systems is the working pressure, because it determines to a large extent the performance of fogging systems (size of fog droplets, cooling effect) and the associated costs (installation and operational costs). Low-pressure fogging systems typically work at the line pressure (3-4 atm) without requiring additional pressure boosting. The size of droplets produced by low-pressure systems is typically 50 to 100 μm. The working pressure of high-pressure systems is much higher (35-70 atm) than low-pressure systems and high-pressure pumps are typically utilized.

The droplet size produced by high-pressure systems is typically 2 to 60 μm.

High-pressure systems generally provide better cooling than low-pressure systems since the finer droplets produced by high-pressure systems evaporate faster. However, better cooling of high-pressure systems comes at the price of much higher initial investment and operational costs. A quantitative evaluation and comparision of the two fogging systems is required if a choice is to be made between them.

Previous studies (Walker *et al*, 1968; Montero *et al*, 1981; Montero *et al*, 1990; Giacomelli *et al*, 1985; Giacomelli and Roberts, 1989; Arbel *et al*, 1999; Arbel *et al*, 2003; Ozturk, 2003) focused on one or the other of the two systems, and none of them examined them in contrast. To rectify this, the current study tested a low-pressure and a high-pressure fogging system at the same time. Cooling efficiency and evaporation efficiency were compared after accounting for differences in weather.

2.2 Materials and Methods

2.2.1 Experiment Setup

The experiments were conducted in two naturally ventilated, east-west oriented, freestanding gutter-connected greenhouses at the Horticultural Field Laboratory of North Carolina State University, Raleigh, NC (35°47′N; 78°39′W). The greenhouses were 6.4 x 11 m (width by length); the gutter height was 3.45 m and the ridge height was 5.36 m. Three vents were installed at the north and south sides. The total opening area accounted for 35% of the ground area. The two greenhouses (NV1 and NV2) shared a common end wall made of double-polyethelene. Further details can be found in Appendix A.

Low-pressure fogging systems were installed in both NV1 and NV2 in 2004. These

consisted of 24 nozzles (Black EXL, Dig Corp) configured in three rows (two side rows and a mid-row) in parallel with the ridge, eight in each row and suspended from the roof structure. The nozzles in the mid-row were about 5.0 m above the ground and those in the side rows were about 4.0 m above the ground. Two solenoids controlled the side rows and the mid row separately. A booster pump maintained the line pressure at 4 atm. Anti-drip devices at every nozzle prevented dripping once the line pressure dropped below the threshold of 2.4 atm. The nominal flowrate of the nozzles was 3.79 liter per hour.

A high-pressure fogging system was installed in NV1 at the end of the summer of 2005. The system was composed of 24 nozzles (Item #00002, Ecologic Technologies, Inc.) installed at a height of 2.36 m. The nozzles were configured in seven rows normal to the ridge, three or four in each row. City water was filtered and decalcified before the pressure being boosted to 68 atm with a high-pressure pump (Fogco System Inc.). A valve system was installed, enabling two levels of fogging, each with 12 nozzles. The nominal flowrate was 5.49 liter per hour. Further details can be found in Appendix A.

A computer controlled the fogging on the basis of 15-second intervals. Fog level and duty cycle (number of 15-second intervals when fog was on during each 10-minute duration) of the fogging systems were measured. Details of the fog control algorithms can be found in Appendix A. For this study, both the high-pressure and low-pressure systems were operated in NV1 (called fogged greenhouse hereafter). The other house, NV2, was used as the control greenhouse (called unfogged greenhouse hereafter). The high-pressure system was run from 6/04 to 7/3 of 2006. The low-pressure system was run from 7/20 to 8/22 of 2006.

2.2.2 Measurements

Air temperature and relative humidity were measured with twelve shielded aspirated

enclosures, each containing a type-T thermocouple and humidity sensor (HM50U, Vaisala). These were mounted in potential canopy area at three heights in each house (Willits *et al.*, 2006). The data were recorded with a CR23X datalogger (Campbell Scientific, Inc., Utah).

Outside dry bulb and wet bulb temperatures, solar radiation, wind speed and direction were monitored by a weather station located nearby (~26 m north of the test greenhouses) and recorded by a datalogger (Helios I, Fluke Corporation). All data were recorded as 10-minute averages of 1-minute readings.

Three to five low-pressure and high-pressure nozzles were selected and their flowrates were measured *in situ* during the experiments. By collecting fog with a cup and measuring the increase in weight during three to five minutes with a digital scale, the actual flowrates were derived. The spray rate of fogging systems was calculated based on the measured flowrates of the nozzles, fog level and the duty cycle of fogging.

2.2.3 Data Processing

The dataset included air temperatures and relative humidities in both the fogged greenhouse and the unfogged greenhouse, outside weather (dry and wet bulb temperatures, solar radiation, wind speed and direction) and fog spray rate. Inside air temperatures and relative humidities were averaged for each greenhouse. The inside humidity ratio, enthalpy and wet bulb temperature were calculated based on the average temperature and relative humidity. The outside humidity ratio, enthalpy, and specific volume were calculated with the dry bulb and wet bulb temperatures. The equations by Albright (1991) were used for the psychrometric calculations.

Cooling efficiency of fogging systems can be defined as (Li *et al*., 2006; Bottcher *et*

al., 1991)

$$\eta_{cool} = \frac{t_{unfog} - t_{fog}}{t_{unfog} - t_{wb,fog}} \tag{2.1}$$

where η_{cool} is the cooling efficiency of fogging system; t_{unfog} is the air temperature in the unfogged greenhouse, ^{o}C; t_{fog} is the air temperature in the fogged greenhouse, ^{o}C; and $t_{wb,fog}$ is the web bulb temperature in the fogged greenhouse, ^{o}C.

The evaporative efficiency was defined as the ratio of fog evaporation rate to spray rate, i.e.

$$\eta_{evap} = \dot{m}_e / \dot{m} \tag{2.2}$$

where η_{evap} is the evaporation efficiency; $\dot{m}_e$ is the fog evaporation rate, g m^{-2}[floor] s^{-1}; and $\dot{m}$ is the spray rate, g m^{-2}[floor] s^{-1}. The fog evaporation rate was

$$\dot{m}_e = Q \cdot (\psi_i - \psi_o) \tag{2.3}$$

where Q is the ventilation rate, m^3 m^{-2} s^{-1}; and ψ_i and ψ_o are the inside and outside water vapor concentrations, g m^{-3}. Ventilation rate was calculated according to Arbel *et al.* (1999) as

$$Q = \frac{S \cdot \tau \cdot \alpha - U(t_i - t_o) A_c / A_g}{(h_i - h_o)} v_o \tag{2.4}$$

where S is the outside solar radiation intensity, Wm^{-2}; τ is the transmissivity of the greenhouse covers; α the proportion of inside solar radiation that contributes to the increase of enthalpy of greenhouse air; U is the overall heat transfer coefficient, Wm^{-2} ^{o}C^{-1}; t_i and t_o are the inside and outside air temperatures, ^{o}C (t_i either t_{fog} or t_{unfog}); A_c and A_g are greenhouse cover area and ground area, m^2; v_o is the specific volume of the outside air, m^3 kg^{-1}; h_i and h_o

are the inside and outside enthalpies, J kg^{-1}. According to the measurement by Zamir *et al*. (1969), the product of τ and α was taken as 0.5. The overall heat transfer coefficient, U, was taken to be 4 $Wm^{-2}\,{}^{o}C^{-1}$ for double-polyethelene covers (ASAE, 2003).

To compare the low-pressure and high-pressure systems on a fair basis, the differences in weather conditions and spray rate were accounted for using the least square means procedure in GLM of SAS (SAS Institute Inc., 1989). The evaporation and cooling efficiencies were regressed against the outside weather and spray rate as linear first-order functions.

The data from days when extreme weather (storm, windy days) disrupted the experiment for significant portion of daytime were excluded. The data compromised by sensor breakdown and human misoperation were also assumed to be invalid and not used. Details can be found in Appendix B.

2.3 Results and Discussion

2.3.1 Running Examples

2.3.1.1 Low-pressure system

The data from 7/31/2006 are presented to illustrate the effects of the low-pressure system on the indoor environment. Solar radiation, S, reached 800 Wm^{-2} and outside temperature, t_o, reached 34.5 ^{o}C. The data for t_{fog}, t_{unfog}, $t_{wb,fog}$, and t_o are presented in Fig.2.1. The low-pressure system resulted in t_{fog} being 5.0 ^{o}C less than t_{unfog} on average during the day. The maximum difference between t_{fog} and t_{unfog} was 7.0 ^{o}C. Cooling efficiency, defined in Eqn.2.1, was about 0.5 (Fig.2.1).

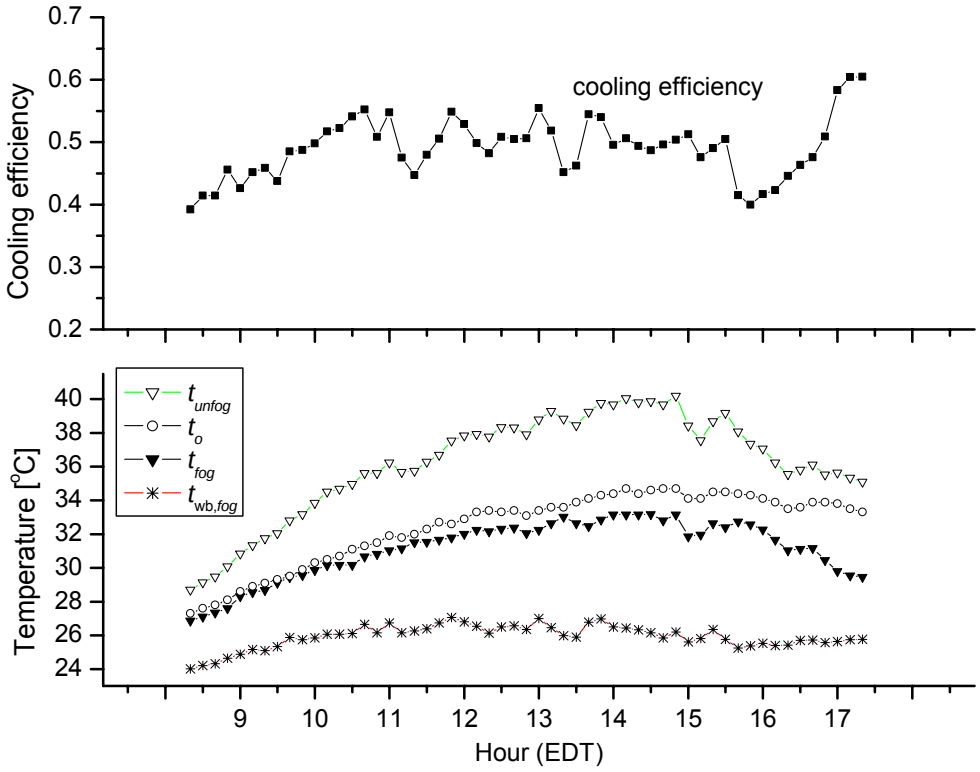

Figure 2.1 Cooling efficiency and temperatures for the low-pressure system. Time was Eastern Daylight Time (EDT).

Figure 2.2 shows the relative humidities in the fogged and the unfogged greenhouses and the outside relative humidity. Relative humidity was increased by 26%, on average, from 41% in the unfogged greenhouse to 67% in the fogged greenhouse due to low-pressure fog. It is also shown that the inside relative humidity in the fogged greenhouse was greater than the outside.

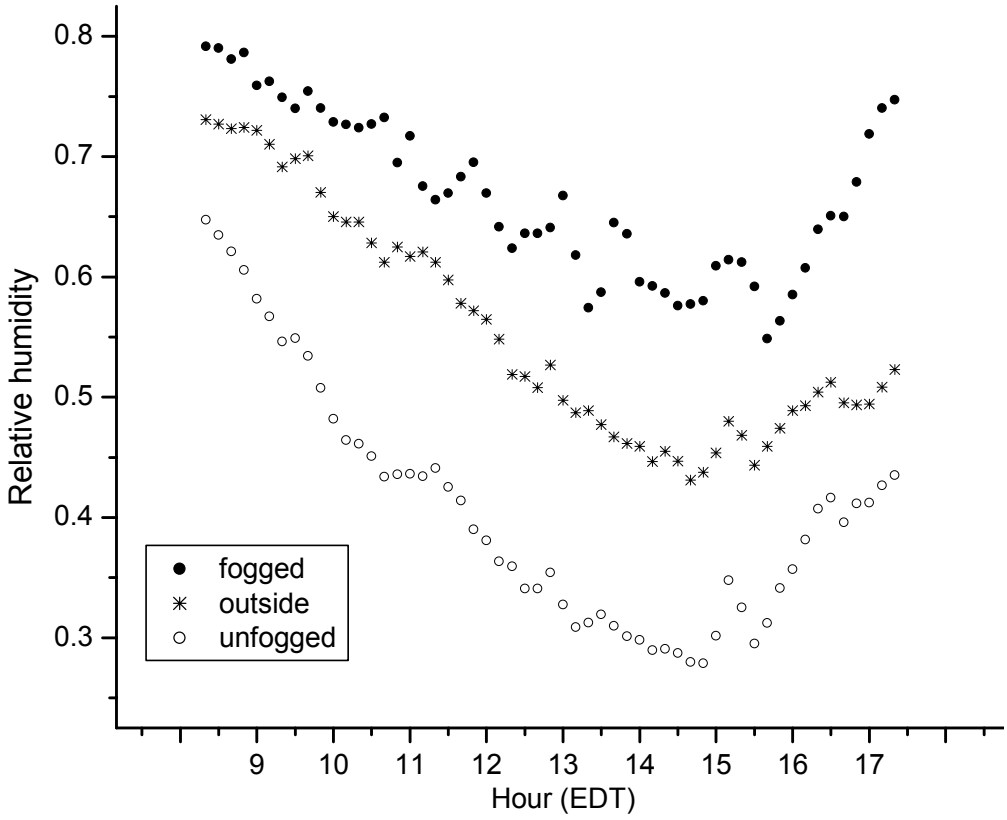

Figure 2.2 Relative humidities in the fogged, unfogged greenhouses and the outside for the low-pressure system. Time was Eastern Daylight Time (EDT).

Figure 2.3 shows the spray rate, $\dot{m}_e$; evaporation rates, $\dot{m}$; and evaporation efficiency, η_{evap}, i.e. the ratio of evaporation rate to spray rate. The average η_{evap} during that day was 0.38, indicating 38% of the sprayed fog had contributed to the cooling while 62% of the sprayed fog was either blown out of the greenhouse or drained off.

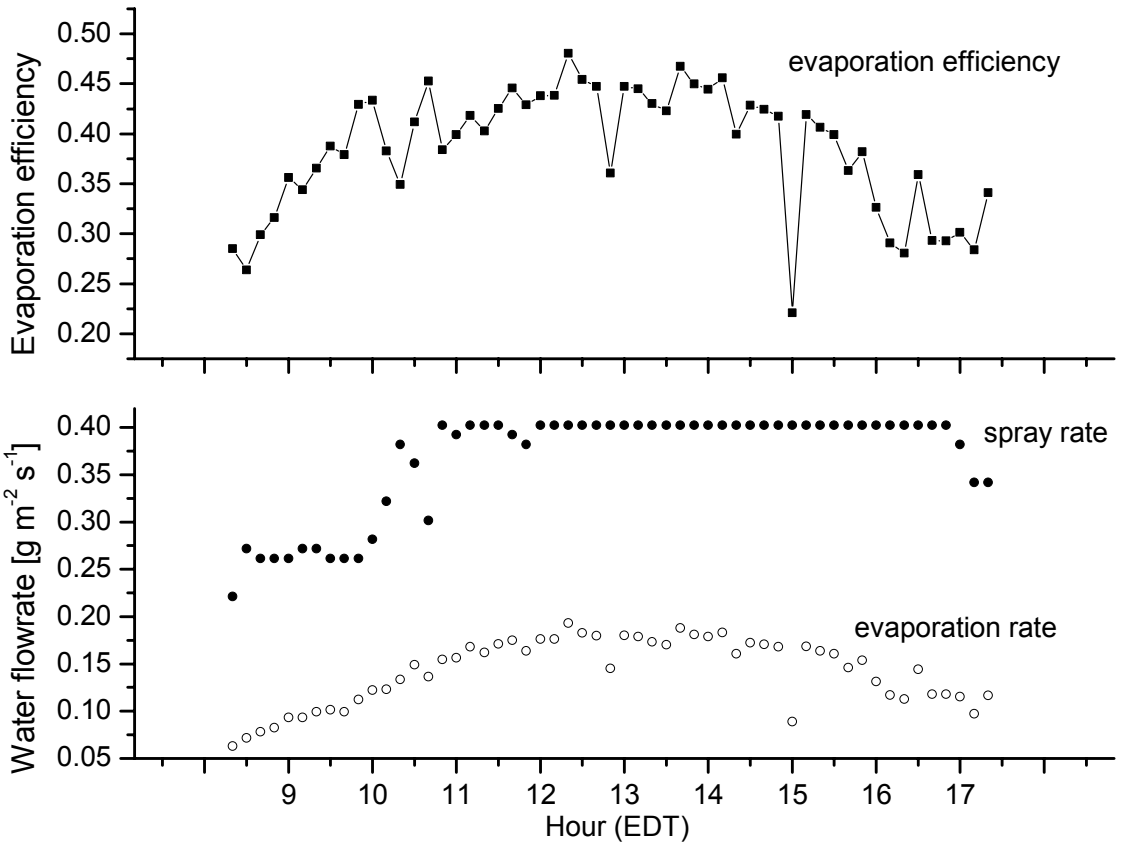

Figure 2.3 Evaporation efficiency, spray rate and evaporation rate for the low-pressure system. Time was Eastern Daylight Time (EDT).

Descriptive statistics for the low-pressure system are given in Table 2.1. The experiment encompassed a relatively wide range of outside weather conditions. The average air temperature reduction caused by the low-pressure fog was 4.3^{o}C; relative humidity increased by 22% on average.

The average cooling efficiency was 0.42 and the average evaporation efficiency was 39%. The cooling effect observed in this study was much more significant than the previous study (Li *et al.*, 2005). Examination of the spray rate indicated that the control algorithm used by Li *et al*. (2005) was conservative, resulting in lower spray rates and less significant cooling. As will be discussed below, the cooling effect of low-pressure fog was closely

related to spray rate.

Table 2.1 Statistics of outside weather, spray rate, environment differences between the fogged and unfogged greenhouses, cooling and evaporation efficiencies for the low-pressure system

Variable		Unit	Mean	Std Dev	Min	Max
Weather	air temp.	^{o}C	31.7	2.3	25.9	36.6
	solar radiation	W m^{-2}	540	206	94	905
	RH	-	0.55	0.08	0.37	0.78
	$\psi_o^* - \psi_o$	kg kg^{-1}	0.0143	0.0038	0.0052	0.0239
	wind speed	m s^{-1}	2.29	0.97	0	5.12
	wind direction	degree	240	84	0	360
Spray rate		g m^{-2} s^{-1}	0.334	0.065	0.184	0.402
Performance	Δt	^{o}C	4.3	1.5	0.7	9.1
	ΔRH	-	0.22	0.06	0.05	0.39
	η_{cool}	-	0.42	0.10	0.08	0.70
	η_{evap}	-	0.39	0.09	0.10	0.79

Note: Δt is the air temperature in the unfogged greenhouse minus that of the fogged greenhouses, i.e. t_{unfog}-t_{fog}; ΔRH is the relative humidity in the fogged greenhouse minus that of the unfogged greenhouses, i.e. RH_{fog}-$RH_{unfogged}$.

2.3.1.2 High-pressure system

Data from 6/20/2006 for the high-pressure system are presented in Figs 2.4 to 2.6. Outside solar radiation that day exceeded 800 Wm^{-2} and the highest outside air temperature was over 32 ^{o}C. The data for t_{fog}, t_{unfog}, $t_{wb,fog}$ and t_o are shown in Fig.2.4. Comparing t_{fog} with t_{unfog} shows that the cooling effect was very significant, with t_{fog} 6.4 ^{o}C less than t_{unfog}, on average, during the day. The greatest difference between t_{fog} and t_{unfog} was 9.0 ^{o}C. Cooling efficiency, η_{cool}, shown in Fig.2.4, was 57% on average.

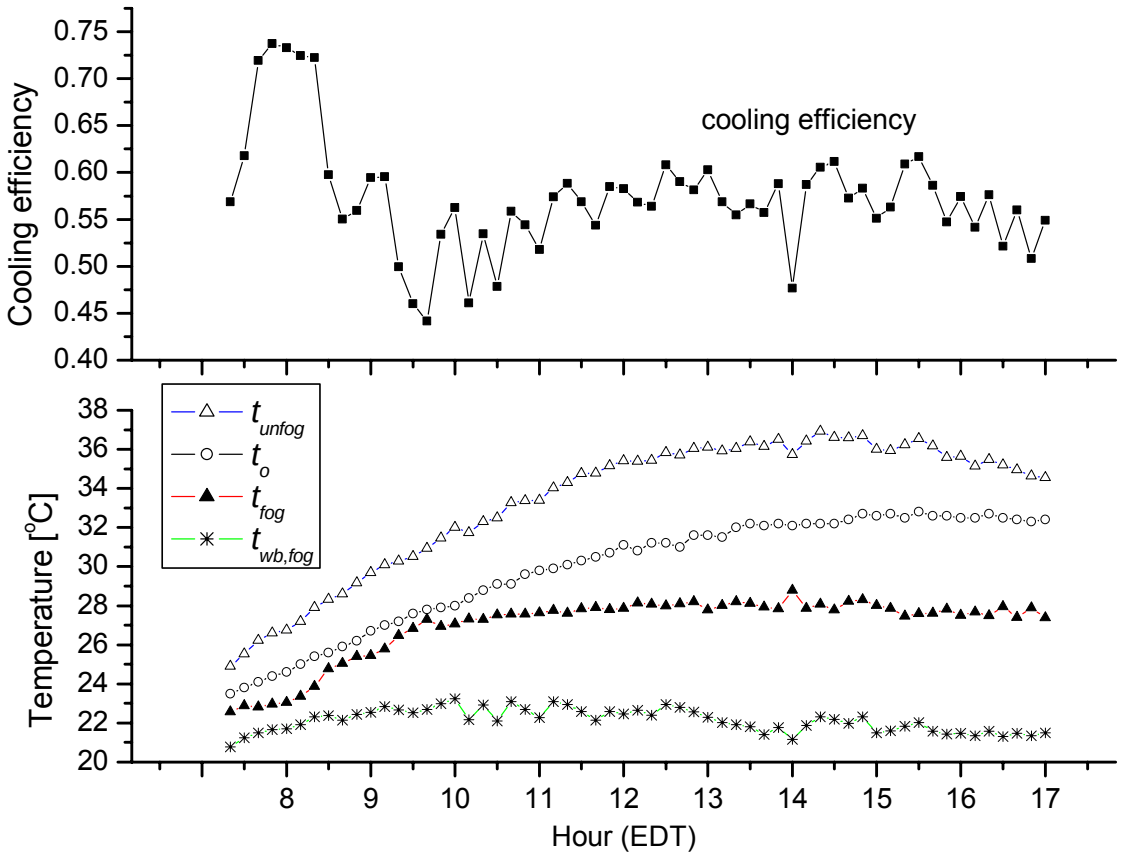

Figure 2.4 Cooling efficiency and temperatures for high-pressure system. Time was Eastern Daylight Time (EDT).

Figure 2.5 shows the relative humidities in the fogged and unfogged greenhouses and the outside. The relative humidity in the fogged greenhouse increased by 31% over the relative humidity in the unfogged greenhouse on average. Figure 2.6 shows the spray rate, evaporation rate and evaporation efficiency. Evaporation efficiency remained pretty much constant. The average evaporation efficiency was 72%, indicating that a significant proportion of the sprayed fog had contributed to the cooling.

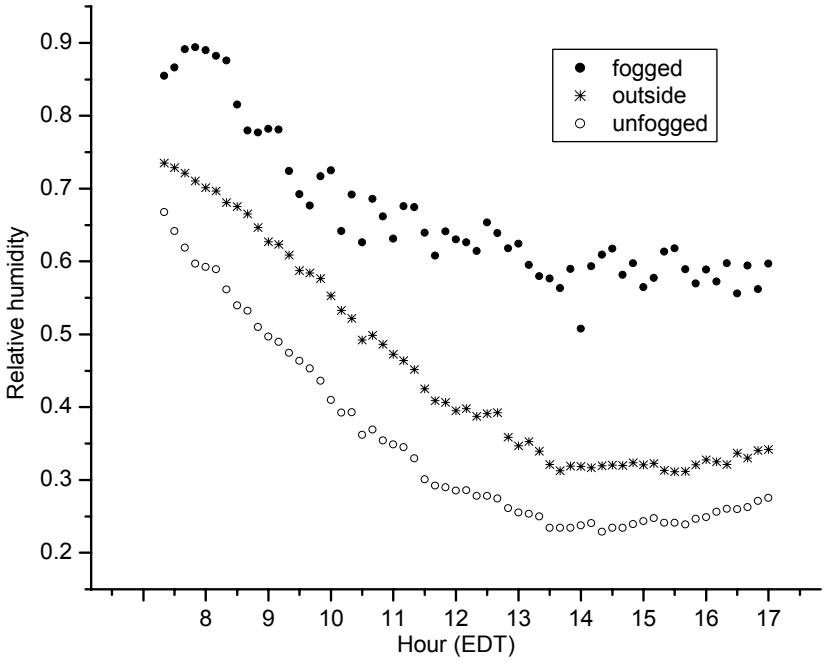

Figure 2.5 Relative humidities in the fogged, unfogged greenhouses and the outside for the high-pressure system. Time was Eastern Daylight Time (EDT).

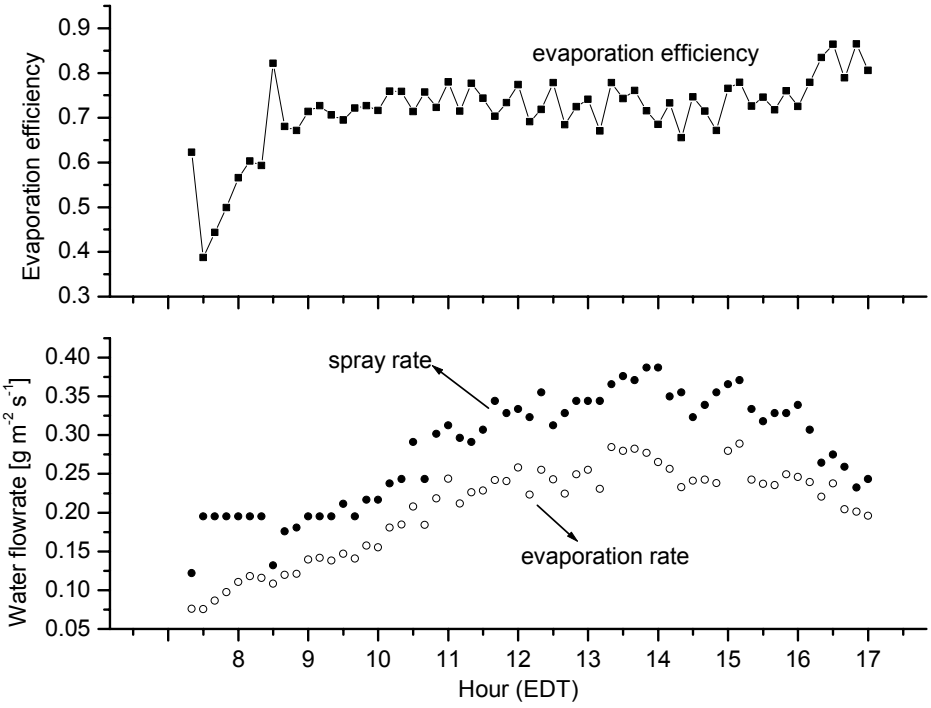

Figure 2.6 Evaporation efficiency, spray rate and evaporation rate for the high-pressure system. Time was Eastern Daylight Time (EDT).

Descriptive statistics for high-pressure system are presented in Table 2.2. The range of weather conditions for high-pressure fog was wide, with air temperature ranging from 22.4 to 34.6 ^{o}C and solar radiation ranging from 219 to 880 Wm^{-2}. The inside air temperature was reduced by 5.8 ^{o}C and relative humidity increased by 29% on average (ΔT and ΔRH in Table 2.2). The highest air temperature difference between the unfogged and fogged houses was 10.2 ^{o}C. The average cooling and evaporation efficiencies of the high-pressure system were 0.53 and 0.71 respectively.

Comparing the mean cooling efficiency (0.42 vs. 0.53) and evaporation efficiency (0.39 vs. 0.71) between the low-pressure and high-pressure systems (Tables 2.1 and 2.2) suggested better cooling performance for the high-pressure system than the low-pressure system, though this is not a rigorous comparison.

Table 2.2 Statistics of outside weather, spray rate, environment differences between the fogged and unfogged greenhouses, cooling and evaporation efficiencies for the high-pressure system

Variable		Unit	Mean	Std Dev	Min	Max
Weather	air temp.	^{o}C	28.7	2.7	22.4	34.6
	solar radiation	W m^{-2}	630	161	219	880
	RH	-	0.48	0.10	0.31	0.75
	$\psi_o^* - \psi_o$	kg kg^{-1}	0.0139	0.0040	0.0047	0.0225
	wind speed	m s^{-1}	2.68	0.91	0	5.28
	wind direction	degree	242	62	0	360
Spray rate		g m^{-2} s^{-1}	0.258	0.071	0.052	0.395
Performance	ΔT	^{o}C	5.8	2.0	1.0	10.2
	ΔRH	-	0.29	0.08	0.08	0.49
	η_{cool}	-	0.53	0.11	0.20	0.74
	η_{evap}	-	0.71	0.09	0.37	1.00

Note: Δt is the air temperature in the unfogged greenhouse minus that of the fogged greenhouses, i.e. t_{unfog}-t_{fog}; ΔRH is the relative humidity in the fogged greenhouse minus that of the unfogged greenhouses, i.e. RH_{fog}-$RH_{unfogged}$.

2.3.2 Evaporation Efficiency

The regression of evaporation efficiency for the low-pressure case resulted in

$$\eta_{evap} = 18.08\left(\psi_o^* - \psi_o\right) + 1.97Q \qquad (R^2=0.95) \qquad (2.5)$$

where ψ_o^* is saturated humidity ratio at t_o, kg kg^{-1}; $\psi_o^* - \psi_o$ is the outside humidity ratio deficit, kg kg^{-1}. Equation 2.5 suggests that increasing airflow under drier weather will promote fog evaporation.

The regression for the high-pressure case was

$$\eta_{evap} = 29.74\left(\psi_o^* - \psi_o\right) + 4.83Q \qquad (R^2=0.96) \qquad (2.6)$$

By observing the coefficients of Eqns 2.5 and 2.6, evaporation efficiency, η_{evap}, for the high-pressure system should be higher than for the low-pressure system under the same $\psi_o^* - \psi_o$ and Q. Given same ventilation rate Q, evaporation coefficiency, η_{evap}, for the high-pressure system will be at least 64% greater than the low-pressure system (29.74 vs. 18.08). Under the same $\psi_o^* - \psi_o$, the evaporation efficiency of high-pressure system would always be higher than the low-pressure system (4.83 vs. 1.97). The presentations of η_{evap} in Figs 2.7 and 2.8 give a clear contrast between the two systems and the positive dependences of η_{evap} on $\psi_o^* - \psi_o$ and Q.

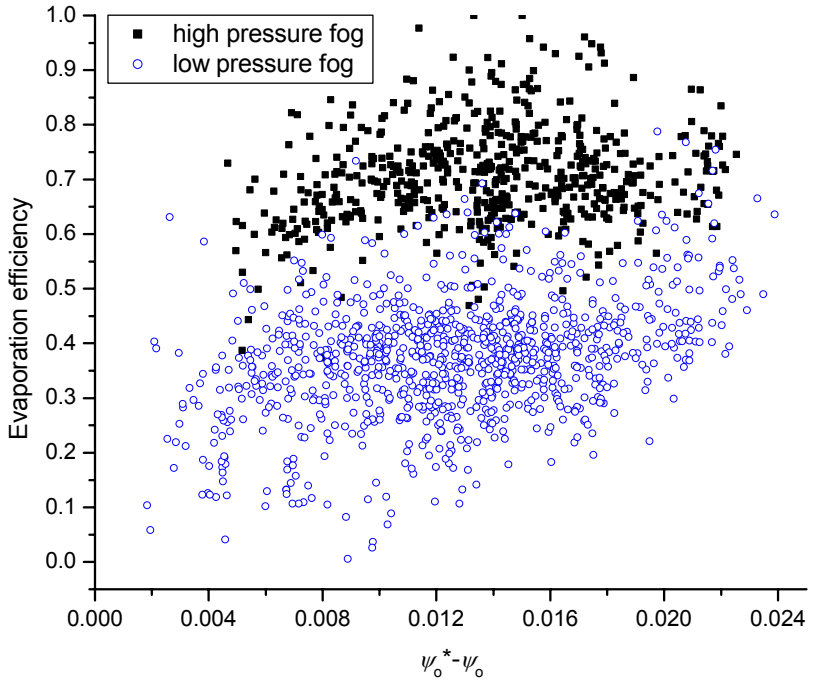

Figure 2.7 Effect of out humidity ratio deficit on evaporation efficiencies of low-pressure and high-pressure systems

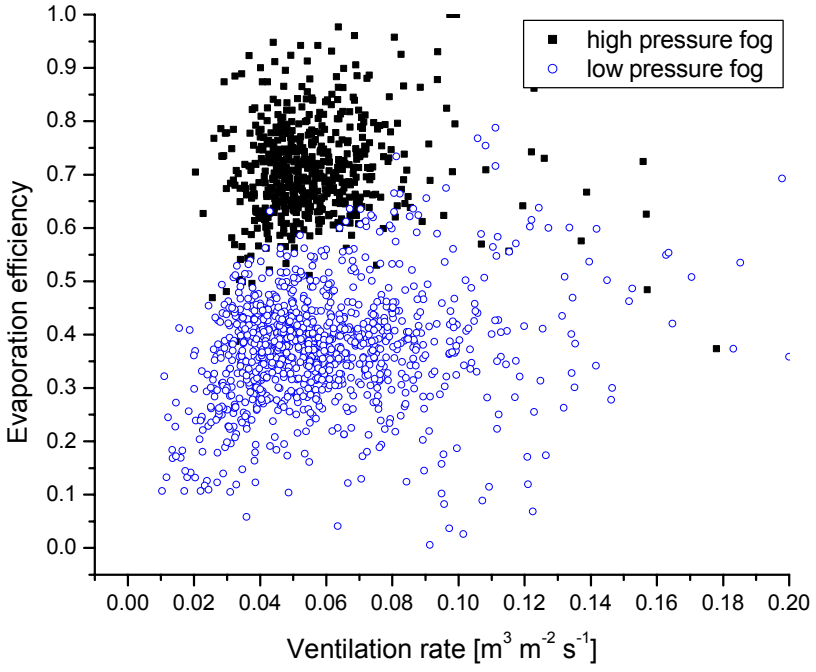

Figure 2.8 Effect of ventilation rate on evaporation efficiencies of low-pressure and high-pressure systems

2.3.3 Cooling Efficiency

Regression of η_{cool} for the low-pressure case was

$$\eta_{cool} = 1.06\dot{m} + 4.2\left(\psi_o^* - \psi_o\right) \qquad (R^2=0.96) \tag{2.7}$$

Whereas the regression for the high-pressure case was

$$\eta_{cool} = 1.36\dot{m} + 11.2\left(\psi_o^* - \psi_o\right) \qquad (R^2=0.95) \tag{2.8}$$

By comparing the coefficients of $\dot{m}$ in Eqns 2.7 and 2.8, it can be inferred that η_{cool} of the high-pressure fog will be at least 28% (1.36 vs. 1.06) greater than the low-pressure fog given the same $\psi_o^* - \psi_o$. Plotting cooling efficiency, η_{cool}, against $\dot{m}$ and $\psi_o^* - \psi_o$ in Figs 2.9 and 2.10 clearly displayed the relative significance of η_{cool} of the two systems.

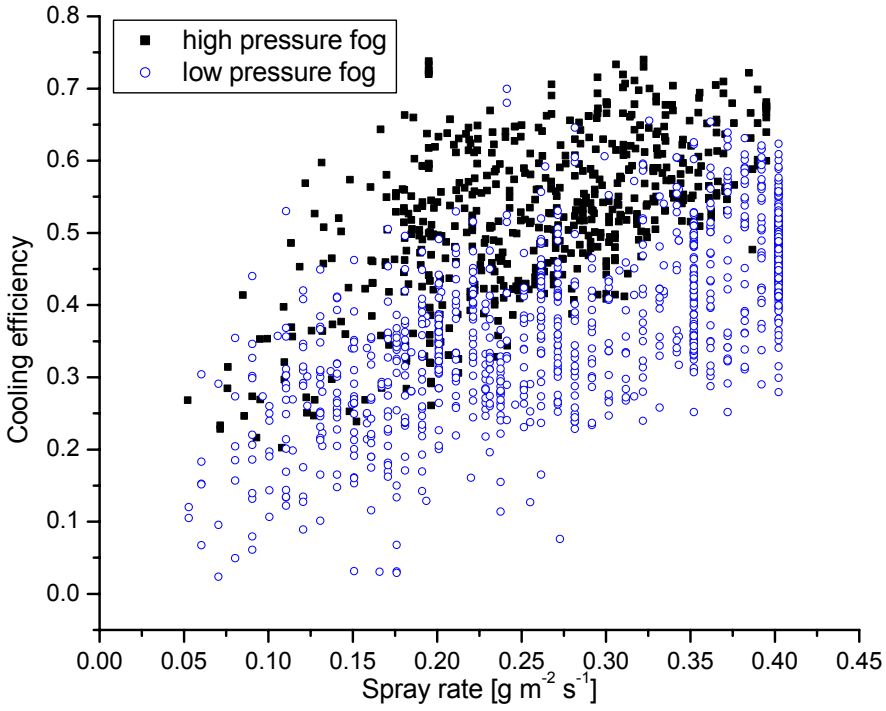

Figure 2.9 Effect of spray rate on the cooling efficiencies of low-pressure and high-pressure systems

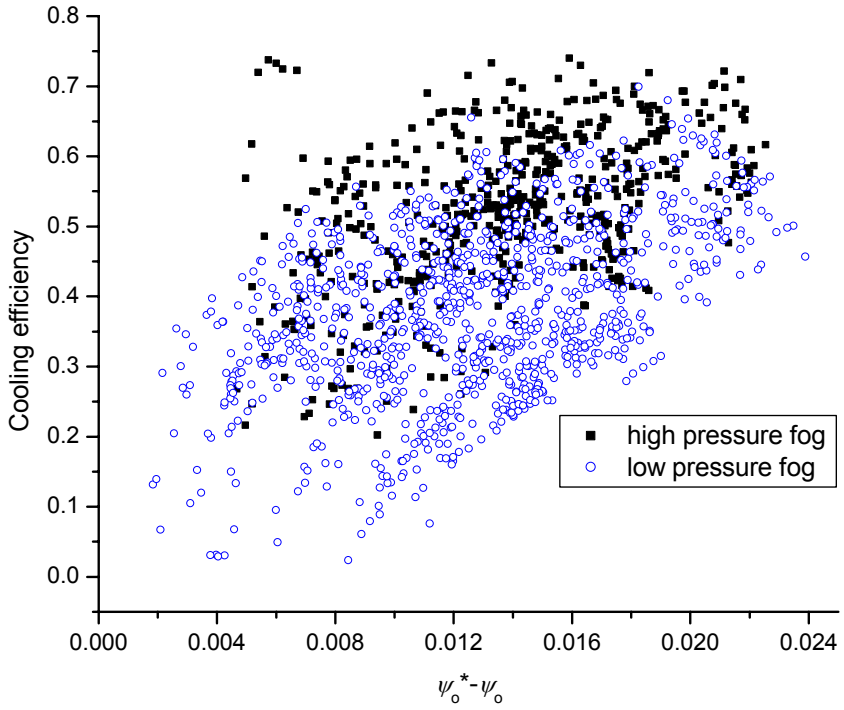

Figure 2.10 Effect of outside humidity ratio deficit on the cooling efficiency of low-pressure and high-pressure systems

2.4 Conclusions

Experiments were performed with low-pressure and high-pressure fogging systems in naturally ventilated greenhouses. The cooling and evaporation efficiencies of the two systems were compared. High-pressure system had evaporation efficiencies at least 64% higher than low-pressure system. The cooling efficiencies of high-pressure system were at least 28% higher than low-pressure system.

Nomenclature

A_c	greenhouse cover area, m^2
A_g	greenhouse ground area, m^2
$\dot{m}_e$	fog evaporation rate, g m^{-2}[floor]s^{-1}
$\dot{m}$	spray rate of fog, g m^{-2}[floor] s^{-1}

Q	ventilation rate, $m^3\ m^{-2}$[floor] s^{-1}
RH_{fog}	relative humidity in the fogged greenhouse
RH_{unfog}	relative humidity in the unfogged greenhouse
S	outside solar radiation, W m^{-2}
t_i	inside dry bulb air temperature, ^oC
t_o	outside dry bulb air temperature, ^oC
t_{unfog}	air temperature in the unfogged greenhouse, ^oC
t_{fog}	air temperature in fogged greenhouse, ^oC
$t_{wb,fog}$	web bulb temperature inside the fogged greenhouse, ^oC
U	overall heat transfer coefficient of greenhouse cover, W m^{-2} $^oC^{-1}$
ΔRH	relative humidity difference between the fogged and unfogged greenhouses, $\Delta RH = RH_{fog} - RH_{unfog}$
Δt	air temperature difference between the unfogged and fogged greenhouses, ^oC, $\Delta t = t_{unfog} - t_{fog}$
v_o	specific volume of the outside air, $m^3\ kg^{-1}$
α	percentage of inside solar radiation converted to enthalpy of greenhouses
η_{evap}	fog evaporation efficiency
η_{cool}	cooling efficiency of fog
τ	solar radiation transmissivity of greenhouse cover
ψ_i	inside humidity ratio, kg m^{-3}
ψ_o	outside humidity ratio, kg m^{-3}
ψ_o^*	saturated humidity ratio at t_o, kg m^{-3}

References

Albright, L.D.1990. Environment control for animals and plants. American Society of Agricultural Engineers, St. Joseph, MI

Arbel, A.; Yekutieli, O.; Barak, M. 1999. Performance of a fog system for cooling greenhouses. *Journal of Agricultural Engineering Research*, 72: 129-136

Arbel, A.; Barak, M.; Shklyar, A. 2003. Combination of forced ventilation and fogging systems for cooling greenhouses. *Journal of Agricultural Engineering Research*, 84(1): 45-55

ASAE. 2003. Heating, ventilating and cooling greenhouses. ANSI/ASAE EP406.2. The American Society of Agricultural Engineers, St. Joseph, MI

Bottcher, R.W.; Baughman, G.R.; Gates, R.S. *et al*. 1991. Characterizing efficiency of misting systems for poultry. *Transactions of the ASAE*, 34(2): 586-590

Giacomelli, G.; Giniger, M.S.; Krass, A.E. *et al*. 1985. Improved methods of greenhouse evaporative cooling. *Acta Horticulturae*, 1974: 49-55

Giacomelli, G.; Roberts, W. 1989. Try alternative methods of evaporative cooling. *Acta Horticulturae*, 257: 29-30

Li, S.; Willits, D.H.; Yunker, C. 2005. Experimental study of low pressure fogging system in naturally ventilated greenhouses. Paper No. 05-4139, American Society of Agricultural and Biological Engineers, St. Joseph, MI

Li, S.; Willits, D.H.; Yunker, C. 2006. Experimental study of a high-pressure fogging system in naturally ventilated greenhouses. *Acta Horticulturae*, 719: 393-400

Montero, J.I.; Short, T.H.; Curry, R.B. *et al*. 1981. The influence of various water evaporation systems in the greenhouse environment. Paper No. 81-4027, American Society of Agricultural Engineers St. Joseph, MI

Montero, J.I.; Anton, A.; Biel, C. *et al*. 1990. Cooling of greenhouses with compressed air fogging nozzles. *Acta Horticulturae*, 281: 199-209

Ozturk, H.H. 2003. Evaporative cooling efficiency of a fogging system for greenhouses. *Turk. J. Agric. For*., 27: 49-57

SAS Institute, Inc. 1989. SAS/STAT User's Guide. Version 6, Fourth Edition. Cary, NC SAS Institute Inc., 846 pp

Walker, J.N.; Cotter, D.J. 1968. Cooling of greenhouses with various water evaporative systems. *Transactions of the ASAE*, 11(1): 116-119

Willits, D.H.; Teitel, M.; Tanny, J.; Peet, M.M.; Cohen, S.; Matan, E. 2006.Comparing the performance of naturally ventilated and fan ventilated greenhouses. BARD Final Scientific Report US-3189-01, Bet Dagan, Israel

Zamir, N.; Lavav, N.; Naveh, D. 1969. Examination of the factors which influence the climate in a greenhouse. Progress report No.9. Institute of Agricultural Engineering, Agricultural Research Organization, Bet Dagan, Israel (in Hebrew)

Chapter 3 Control Strategies for High-Pressure Fog in Naturally Ventilated Greenhouses

Abstract A control strategy (NCSU control) was proposed to control both the pump and the vents in a high-pressure fog system for naturally ventilated greenhouses. The control strategy uses enthalpy (inside, outside and target) to determine vent configurations, and humidity ratio to control the high-pressure pump. NCSU control and four other control strategies were tested in a naturally ventilated greenhouse under summer conditions. Evaporation efficiency, cooling efficiency, cycle frequency of the high-pressure pump, leaf wetness duration, and water use were compared for the five control strategies. The results suggested that: 1) NCSU control and the one based on temperature and relative humidity resulted in higher cooling efficiencies than the others; 2) manipulating vents properly to regulate airflow resulted in less cycling of the high-pressure pump than keeping vents at fixed configurations; 4) control by vapor pressure deficit is a simple and effective way to reduce leaf wetting; 5) NCSU control was highly accurate in simultaneously controling the air temperature and relative humidity.

3.1 Introduction

Previous research has shown that high-pressure fogging can have a significant cooling effect in greenhouses (Arbel *et al*., 1999; Li *et al*., 2006). However, its application in commercial greenhouses is limited, possibly due to technical difficulties and side effects. One difficulty is spray rate control, which is complicated, because it is difficult to determine how much fog should be applied, especially for naturally ventilated greenhouses. Fogging also causes wetting problems and improper control makes the wetting problem worse. Excessive fog will wet the plants, ground and indoor equipment, increasing the chance of disease development and equipment deterioration. Some studies suggest that pest population

and disease development are attributable to the amount of free water on foliage (Lindquist *et al*., 1987; Peece, 1971; Hall and Burges, 1979). To overcome these difficulties in determing spray rate and mitigate the side effects, technically sound fog control is required. Ideally, control should be able to maintain inside temperature and/or humidity at desired levels. In addition, minimal water and electricity should be consumed to reduce operational costs. Also, the high-pressure pump and vents should not cycle too frequently or excessively to minimize equipment wear.

Several control strategies are used in practice and/or have been studied. One control strategy uses thermostats and humidistats to control pump activity. The logic of the control is simple: when inside temperature is higher than setpoint and humidity is lower than setpoint, the pump will be turned on and fogging will be started, otherwise the pump will stay off.

Handarto *et al.* (2006) proposed a second control strategy. They developed an algorithm that determined the required spray rate based on the inside humidity ratio, target humidity ratio and ventilation rate. The target humidity ratio was determined based on inside wet bulb temperature and target relative humidity. The ventilation rate was determined by dividing the solar radiation absorbed by greenhouse with the difference between inside and outside enthalpies.

A third method uses vapor pressure deficit (VPD) as the control variable and maintains VPD at a preset level. The idea behind this is to maintain sufficient potential for fog evaporation and plant transpiration. With a VPD large enough, fog droplets will evaporate efficiently and the physiological processes associated with transpiration will not be attenuated. Some studies that utilized VPD control are Meca *et al*. (2006), Gazquez *et al*. (2006) and Dixon (2003).

One of the limitations of the first three controls is that only one variable (temperature, relative humidity or VPD) can be controlled. It was impossible to control more than one variable simultaneously because the pump was the only control action involved, i.e., vent configuration was fixed.

A fourth control, described by Sase *et al*. (2006) controlled the pump with temperature and the vents with relative humidity. The algorithm was tested in a greenhouse and demonstrated the possibility of keeping both temperature and relative humidity within the desired range.

A fifth control strategy, NCSU control, is proposed as an alternative to the previous controls. In this control, the vent configuration will be changed to regulate the inside enthalpy. The spray rate will be controlled to get the desired humidity ratio. By manipulating the vent configuration and spray rate, the inside temperature and relative humidity can be controlled simultaneously.

The objective of this study is to test the five control strategies described above. Their performance will be evaluated and compared, and their limitations and strengths will be identified.

3.2 Materials and Methods

3.2.1 Facilities

The two greenhouses used in this study were located on the campus of North Carolina State University in Raleigh, NC. They were naturally ventilated, double-polyethylene covered and east-west oriented. The size of the greenhouses was 6.4 by 11m; the gutter height was 3.45 m and ridge height was 5.36 m. The two greenhouses shared a common end

wall made of double-polyethylene, dividing the east side from the west side. Each house was fitted with three vents, one each on the south, north and top sides. The vents were driven by rack and pinion drive systems. The opening area of the three vents accounted for 35% of the ground area. See Appendix A for more details.

A high-pressure fogging system was installed in the greenhouse on the east side (fogged house) in the late summer of 2005. The greenhouse on the west side was used as the control greenhouse (unfogged house). The fogging system was composed of twenty-four nozzles (item #00002, Ecologic Technologies, Inc.) evenly distributed across the greenhouse at the height of 2.36m (Fig.3.1). The nominal flow rate of the nozzles was 5.49 liter per hour. City water was filtered and decalcified before being supplied to a high-pressure pump (Fogco System Inc.), which elevated the water pressure to 6.8 atm. A valve system was installed enabling two levels of fogging (Fig.3.2). The high level fog involved 24 nozzles; the low level fog involved 12 nozzles. See Appendix A for details.

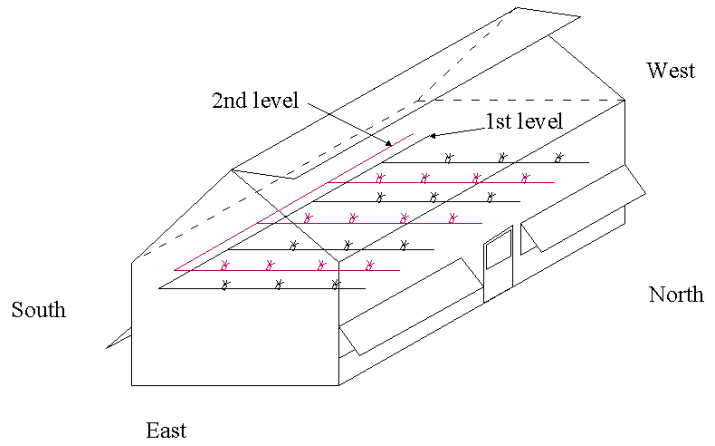

Figure 3.1 Layout of the 24 high-pressure nozzles, with 12 nozzles for each level of fogging

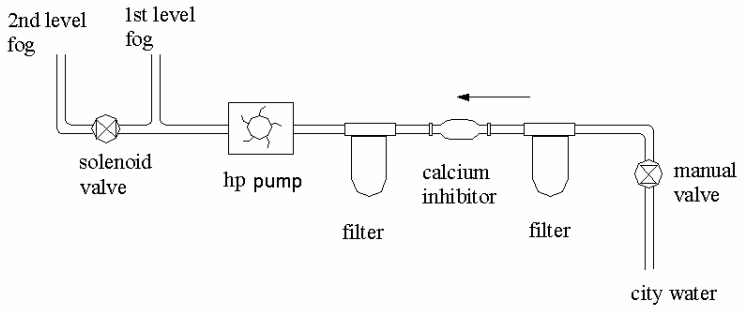

Figure 3.2 Water treatment and valve system enabling two levels of fogging

3.2.2 Control sensors

The dry bulb and wet bulb temperatures in the fogged greenhouse and outside were measured with type-T thermocouples. The two thermocouples were placed at the inlets of an aspirated plywood box. A fan was used to create sufficient airflow to minimize the effect of radiation.

Outside solar radiation on a horizontal surface was measured by a black and white Eppley Precision Pyronometer (Eppley Laboratory, Inc., Rhode Island) mounted on a stand nearby. Wind speed and wind direction were measured with an anemometer and vane set (03001-L, R.M.Young wind sentry set, R.M. Young Company) mounted at the top of a steel frame structure about 6 m high.

The data were sent to a computer, where control decisions were made. The control signals from the computer were sent to the high-pressure pump and vent motors.

3.2.3 Implementation of Control Strategies

3.2.3.1 Set-point control with temperature and relative humidity (Strategy 1)

This control is very straightforward. First, outside relative humidity was calculated from the dry bulb and wet bulb temperatures. If the outside relative humidity was high (greater than 85% in our case), indicating very muggy or rainy weather, fog was disabled

completely. Second, inside relative humidity was calculated from inside dry and wet bulb temperatures. If the inside relative humidity was high (greater than 87% in our case), the fog level was reduced by one level (i.e. if the fog level from last cycle was high, it was reduced to low; if fogging was running at low level, fog was disabled completely; if fog was off, it was kept off). Third, the fog level was modified by checking the inside dry bulb temperature, i.e. if the inside temperature was 2.8 ^{o}C higher than cooling setpoint, the fog level was increased by one level. If the inside temperature was 0.6 ^{o}C higher than cooling setpoint, the low level fog was triggered. The cooling setpoint was set on a daily basis. The code for this strategy can be found in Appendix C.

3.2.3.2 Handarto's control (Strategy 2)

The control by Handarto *et al*. (2006) adjusts spray rate based on weather conditions. His control was revised here to accommodate our experimental conditions.

For this strategy, a variable λ was defined to represent the ratio of required increase in spray rate to nominal spray rate, i.e.

$$\lambda = \frac{\dot{m}_r}{\dot{m}} \tag{3.1}$$

where $\dot{m}_r$ is the required increase in spray rate above the current spray rate, kg s^{-1}; $\dot{m}$ is the design spray rate of fogging system, kg s^{-1}. The required spray rate was calculated as

$$\dot{m}_r = \frac{m_a \cdot \left(\chi_{i,s} - \chi_i\right) \cdot A_f}{\zeta} \tag{3.2}$$

where m_a is the ventilation rate on mass basis, kg m^{-2} s^{-1}; $\chi_{i,s}$ is the target humidity ratio, kg[H_2O] kg^{-1}[air]; χ_i is the current humidity ratio, kg[H_2O] kg^{-1}[air]; A_f is the floor area, m^2; and ζ is the evaporation efficiency (i.e., the ratio of evaporated fog to the sprayed fog). The

evaporation efficiency was approximated as 0.57 for control purposes (Li *et al*., 2006).

The ventilation rate was determined as

$$m_a = \frac{\tau\alpha S_o - U\left(t_i - t_o\right) A_c / A_f}{h_i - h_o} \tag{3.3}$$

where τ is the transmissivity of greenhouse cover; α is the percentage of inside solar radiation contributed to increase of air enthalpy; S_o is the outside solar radiation, W m^{-2}; U is overall heat transfer coefficient of greenhouse cover, $Wm^{-2}\ {}^{o}C^{-1}$; A_c is cover area, m^2; t_i and t_o are the inside and outside dry bulb temperatures, ^{o}C. The product of τ and α was taken as 0.5 according to Zamir *et al*. (1969). A value of 4 $Wm^{-2}\ {}^{o}C^{-1}$ was assigned to U for double-polyethylene (ASAE, 2003). The ratio of A_c to A_f was 1.96 for the greenhouse used.

The target and current humidity ratios were

$$\chi_{i,s} = X(t_{i,s}, t_w) \tag{3.4}$$

and

$$\chi_i = X(t_i, t_w) \tag{3.5}$$

where $X(t, t_w)$ is the function to calculate the humidity ratio based on dry bulb and wet bulb temperatures; $t_{i,s}$ is the setpoint temperature, ^{o}C; and t_w is the inside wet bulb temperature, ^{o}C.

Equation 3.4 was not used in two cases where the temperature setpoint, $t_{i,s}$, would not be reasonable. The first case was that $t_{i,s}$ was set below t_w, the lowest temperature that inside temperature can reach theoretically. The second case was that the $t_{i,s}$ was set so that the resulting inside relative humidity, *RH*, would exceed 87%. For example, if t_w is 24 ^{o}C and $t_{i,s}$ is set at 25 ^{o}C, *RH* would be 91% if the inside temperature reaches the setpoint, $t_{i,s}$. In both cases, $\chi_{i,s}$ was calculated from the target *RH* (87% in this study) and t_w.

Lastly, the variable, λ, in Eqn.3.1, was used to determine the fog level. When λ was

greater than 0.05, low level fog was enabled; when λ was greater than 0.5, high level fog was enabled. The code for this strategy can be found in Appendix D.

3.2.3.3 Set-point control with VPD (Strategy 3)

Vapor pressure deficit, *VPD*, was calculated as

$$VPD=p_s*(1-RH) \tag{3.6}$$

where *RH* is the inside relative humidity; and p_s is the saturated vapor pressure at t_i. The inside relative humidity, *RH*, was calculated from t_i and t_w.

When *VPD* was higher than 1000 Pa, low-level fog was enabled; when *VPD* was higher than 1350 Pa, high-level fog was enabled. The code for this control is in Appendix E.

3.2.3.4 Sase's control (Strategy 4)

The method applied by Sase *et al*. (2006) is counterintuitive. Inside temperature was used to control fogging, while relative humidity was used to control the vents. It is not clear whether there was any theoretical thinking behind the method. Because temperature and relative humidity are both affected by spray rate and the vent configuration, it is impossible to control air temperature without affecting relative humidity or control relative humidity without affecting air temperature. The method used in this study basically followed the paper with some modifications, i.e.

1) Inside temperature, t_i, was used to determine fog level: if t_i was 2.5 ^oC higher than $t_{i,s}$, high-level fog was triggered; if t_i was 0.6 ^oC higher than $t_{i,s}$, low-level fog was triggered.The decision cycle was 15 seconds long.
2) Inside relative humidity, *RH*, was used to determine vent configuration: If *RH* was higher than 80%, all vents (south, top and north vents) were opened; if *RH* was lower than 75%, only the south and top vents were opened; if *RH* was between 75% and

80%, the vent configuration from the previous vent cycle was maintained. The inside relative humidity, *RH*, was calculated from t_i and t_w from the four previous fog decision cycles (represented by the dotted tick marks in Fig.3.3).

The durations for various cycles are shown in Fig.3.3. The decision cycle for vent control was 120 seconds; fog level and vent configuration were recorded and written to disk every 10 minutes. The code for this control can be found in Appendix F.

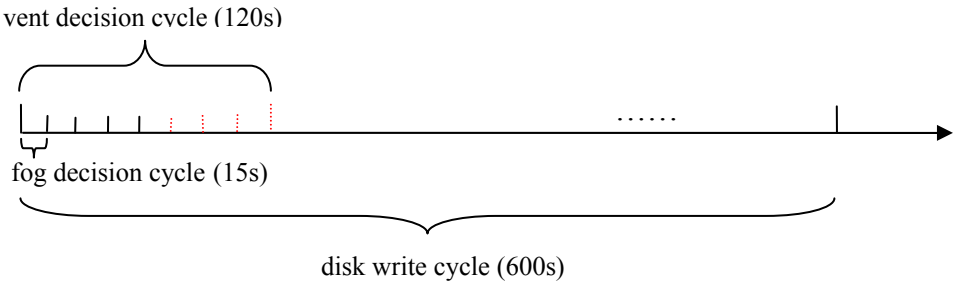

Figure 3.3 Durations for cycle of vent control, fog control (pump) and disk write for strategy 4

3.2.3.5 NCSU control (Strategy 5)

Basic concept

Two assumptions were made in this control: 1) fog evaporation is an adiabatic (isoenthalpic) process; and 2) when ventilation rates change, the state point of inside air on psychometric chart moves on the line that connects the original state points of the inside air and outside air.

Based on the facts that the inside enthalpy and humidity ratio are greater than outside and the assumptions made above, five zones can be identified on a psychrometric chart (Fig.3.4) when targeting a setpoint. Each zone is characterized by its enthalpy and humidity ratio relative to the setpoint and the outside air. Specific control action needs to be taken if the state point of the inside air is in each zone.

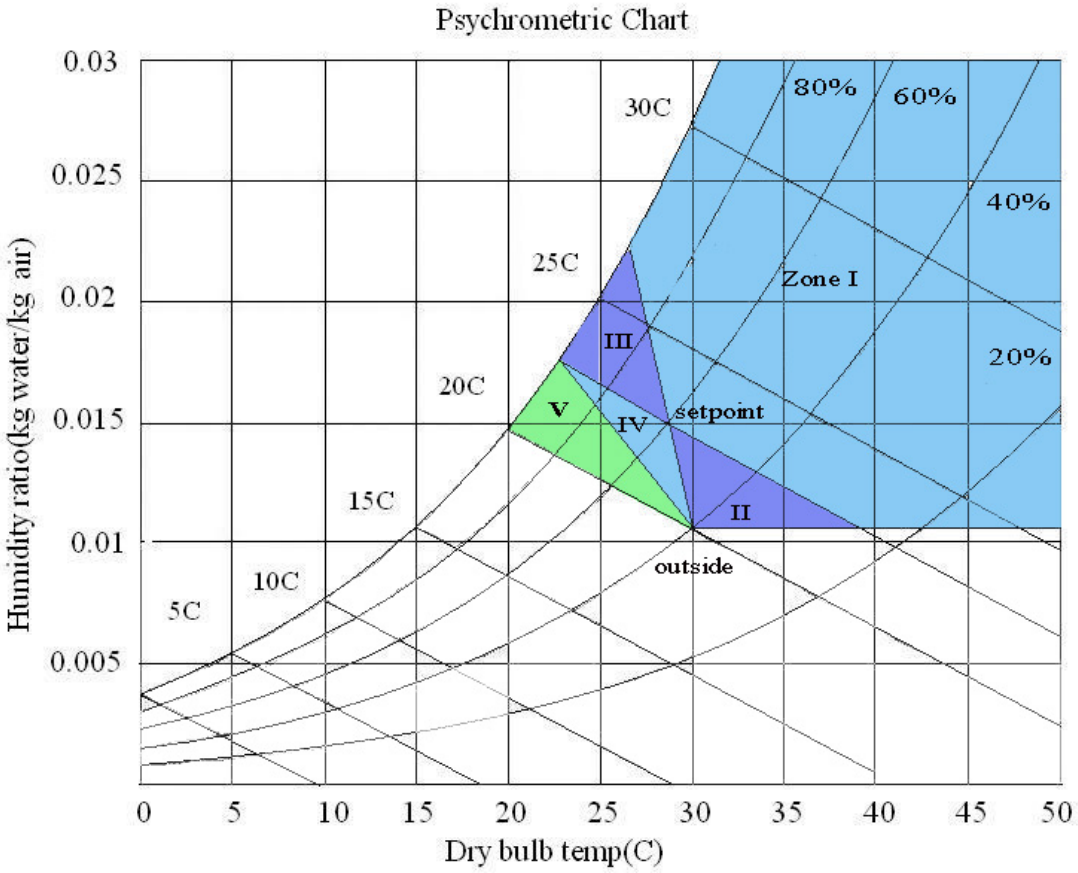

Figure 3.4 Zone classifications when targeting a setpoint

As shown in Fig.3.4, Zone I has greater enthalpy than the setpoint. It lies in the upper-right to the isoenthalpic line connecting the state points of the outside air and the setpoint. The mathematical definition of Zone I is

$$h_i > h_s \tag{3.7}$$

and

$$\chi_o + \frac{\chi_s - \chi_o}{t_s - t_o}\left(t_i - t_o\right) < \chi_i \tag{3.8}$$

where h_s is the enthalpy corresponding to setpoint, kJ kg^{-1}; χ_o is the outside humidity ratio, kg kg^{-1}; χ_s is the humidity ratio corresponding to setpoint, kg kg^{-1}; and χ_i is the inside humidity ratio, kg kg^{-1}. If the state point of inside air is in Zone I, inside enthalpy has to be reduced. It can be achieved by increasing airflow rate. To this end, more vents must be opened to get

more airflow. If airflow can be manipulated in a precise manner, then inside enthalpy can be adjusted to be exactly equal to setpoint and the state point of the inside air should be on the isoenthalpic line through the setpoint; then, the state point must move along the isenthalpic to reach the setpoint. This can be achieved by increasing fog level. Similarly, the mathematical definitions for the other four zones are

Zone II

$$h_i < h_s \tag{3.9}$$

and

$$\chi_o + \frac{\chi_s - \chi_o}{t_s - t_o}\left(t_i - t_o\right) < \chi_i \tag{3.10}$$

Zone III

$$h_i > h_s \tag{3.11}$$

and

$$\chi_o + \frac{\chi_s - \chi_o}{t_s - t_o}\left(t_i - t_o\right) > \chi_i \tag{3.12}$$

Zone IV

$$h_i < h_s \tag{3.13}$$

$$\chi_o + \frac{\chi_s - \chi_o}{t_s - t_o}\left(t_i - t_o\right) > \chi_i \tag{3.14}$$

and

$$\chi_o + \frac{\chi_{s,w} - \chi_o}{t_{s,w} - t_o}\left(t_i - t_o\right) < \chi_i \tag{3.15}$$

Zone V

$$\chi_o + \frac{\chi_{s,w} - \chi_o}{t_{s,w} - t_o}\left(t_i - t_o\right) > \chi_i \tag{3.16}$$

The actions to bring the state point of the inside air to the setpoint for Zones I to IV are listed in Table 3.1. Note that for Zone V, it is impossible for the inside air to reach the

setpoint no matter how the airflow and fog level are manipulated.

Table 3.1 Control actions taken for each zone when targeting a setpoint

	Airflow	Spray rate
Zone I	↑	↑
Zone II	↓	↑
Zone III	↑	↓
Zone IV	↓	↓

Practical constraints

This concept would be an ideal solution to fog control if both spray rate and airflow can be controlled in a precise manner; however, in practice, this is difficult to realize, especially for airflow. First of all, airflow in naturally ventilated greenhouses depends on outside wind speed and direction, so it is not controllable. The motors that drive the vents in our experimental greenhouse are not stepwise driven, which means the status of the three vents can only be either open or closed. The only way airflow can be manipulated is to switch among several vent configurations. Secondly, the spray rate can not be varied continually because our system worked at a single pressure. The spray rate can be switched only among level 0 (no fog), level 1 (low) and level 2 (high). To cope with the practical constraints, empirical approaches were adopted. To create staged airflows, three vent configurations, 's', 's+t', 's+t+n', were allowed, which represent south vent open only; south plus top vents open; and south, top and north vents open, respectively. According to the tracer gas study conducted in this greenhouse (Willits *et al*., 2006), the airflow rates of the three vent configurations can be approximated as 1: 3: 3.33 at wind speed of 2 m s^{-1} with wind speed normal to the vent openings.

Vent control

To implement vent control, a dimensionless index, β, was defined as

$$\beta = \frac{h_i - h_o}{h_s - h_o} \tag{3.17}$$

Because inside enthalpy is greater than outside, β will always be greater than or equal to zero. The vent configuration of the next vent decision cycle depends on β and the current vent configuration. That dependence is shown in Table 3.2.

Table 3.2 Dependence of vent configuration of next decision cycle on β and the current vent onfiguration

vent config. of current cycle	vent config. of next decision cycle		
	s	s+t	s+t+n
s	$\beta < 1.5$	$1.5 \le \beta \le 3.6$	$3.6 < \beta$
s+t	$\beta < 0.67$	$0.67 \le \beta \le 1.06$	$1.06 < \beta$
s+t+n	$\beta < 0.45$	$0.45 \le \beta \le 0.95$	$0.95 < \beta$

Table 3.2 can be interpreted in the following way: 1) the current vent configuration was pinpointed in the first column in the table; 2) in the row corresponding to the current vent configuration, the range of β was determined. The vent configuration of the next decision cycle would be that corresponding to the range in the same column. For example, if the current vent configuration is 's+t' and the value of β is equal to 1.5, the vent configuration of the next cycle will be 's+t+n'.

Fog control

Fog control was similar to that described in section 3.2.3.2. The fog level for the next decision cycle depended on the current fog level and the value of λ. The dependence is

tabulated in Table 3.3. It can be interpreted in the same manner as Table 3.2. In the row corresponding to the current fog level, the range of λ was identified. The fog level of the next cycle was that corresponding to the range in the same column.

The code for this strategy can be found in Appendix G.

Table 3.3 Dependence of spray rate of next decision cycle on the value of λ and the current spray rate

spray rate of current cycle	Spray rate of next cycle		
	none	low	high
none	$\lambda < 0.05$	$0.05 \le \lambda \le 1.5$	$1.5 < \lambda$
low	$\lambda < -0.5$	$-0.5 \le \lambda \le 0.5$	$0.5 < \lambda$
high	$\lambda < -1.5$	$-1.5 \le \lambda \le -0.5$	$-0.5 < \lambda$

3.2.4 Oberved Data Measurement and Processing

The experiment was conducted from June 27 to Sept. 29 of 2006. Strategy 1 was tested from June 27 to July 7; strategy 2 from July 8 to July 19; strategy 3 from Aug. 23 to Sept.4; strategy 4 from Sept.5 to Sept.16; strategy 5 from Sept.17 to Sept.29.

Air temperature and relative humidity were measured by twelve aspirated stations located in potential canopy area in each house. Each aspirated station contained a type-T thermocouple and a humidity sensor (HM50U, Vaisala). Special precautions were taken to reduce the error caused by thermal conduction along the lead wires to thermocouples. Further details can be found in Appendix A.

Leaf wetness was measured with five wetness sensors (237-L, Campbell Scientific Inc., Utah) supported and positioned at fixed orientation and tilt angle (~45 degree) to mimic real leaves. The sensors were calibrated at three wetness levels: the first represented the totally dry condition; the second represented a moderate level of moisture within the paint

layer, but no visible droplets present on sensor surface; the third represented visible droplets sitting on sensor surface. The details of leaf wetness sensor calibration can be found in Appendix H. The second and third wetness levels were regarded as 'wet'. The percentage of 'wet' periods during each 10-minute was examined.

Air temperatures and relative humidity were averaged for each greenhouse. Other psychrometric variables were calculated using the average temperature and relative humidity and the equations by Albright (1991).

Cooling efficiency was calculated with Eqn 2.1; evaporation efficiency was calculated with Eqns 2.2 to 2.4; water use was determined based on the spray rate of nozzles, fog level and the duty cycle of the high-pressure pump.

To account for the effects of outside weather, cooling efficiency, evaporative efficiency, water use, leaf wetness duration were regressed against weather conditions with the least square means procedure of the GLM procedure of SAS (SAS Institute Inc., 1989),

$$X = function(S_o, t_o, t_{wo}, u, \theta, C) \tag{3.18}$$

where X represents cooling efficiency η_{cool}; evaporative efficiency η_{evap}; water consumption m_w, g hr^{-1} m^{-2}; and the percentage of wetness duration; t_{wo} is outside wet bulb temperature, ^oC; u is wind speed, m s^{-1}; θ is wind direction, degree; and C is the class variable representing control strategy. Least square means of X for the class variable C were used to compare the performance of the five control strategies.

3.3 Results and Discussion

Table 3.4 lists the cooling efficiency, evaporation efficiency, water use, cycle frequency of the pump and percentage of wetting duration for the five control strategies. It shows that cooling efficiency ranged from 34% to 63%. Strategy 5 had the highest cooling

efficiency while strategy 3 had the lowest.

Table 3.4 Least square means of the cooling efficiency, evaporation efficiency, water use, action frequency of high-pressure pump and the percentage of wetting duration for the five control strategies

Performance	unit	strategy 1	strategy 2	strategy 3	strategy 4	strategy 5
Cooling Efficiency η_{cool}	%	41	38	34	50	63
Evaporation Efficiency η_{evap}	%	49	59	70	66	80
Water use m_w	g hr^{-1} m^{-2}	296	351	418	395	479
Pump cycle frequency ω	h^{-1}	62	30	49	20	12
Percentage of wetting duration	%	22	13	1	7	13
$\eta_{cool} \div m_w$		0.138	0.108	0.081	0.127	0.132

Note: strategy 1 is the set-point control with temperature and relative humidity; strategy 2 is handarto' control; strategy 3 is the setpoint control with VPD; strategy 4 is Sase's control; strategy 5 is NCSU control.

In terms of water use, strategy 5 (NCSU control) used the highest amount of water, while strategy 1 used the lowest amount. However, simply comparing cooling efficiency and water use seems unfair, because more water use should result in more cooling. To fix this, cooling efficiency was divided by water use. The result is listed in the last row of Table 3.4. It turned out strategy 1 had the highest cooling efficiency normalized for water use, and strategy 5 had second highest. Strategy 3, on the other hand, had the lowest. It was expected that the order of this normalized cooling efficiency should match the order of evaporation efficiency. The reason is that for more water evaporates, more cooling should result. They obviously did not match and it was not clear why. However, more trust should be given to the normalized cooling efficiency than evaporation efficiency, because calculation of the latter was based on a parameter (greenhouse heating efficiency, i.e. percentage of solar radiation transformed into internal energy of greenhouse) that does not have a commonly accepted value.

When it comes to the cycle frequency of the pump, strategy 5 (NCSU control) had the

lowest while strategy 1 had the highest frequency. The other three were intermediate. It is important to note that strategies 4 and 5 are capable of manipulating vent configurations. These resulted in less cycle frequency than the other three strategies, suggesting that manipulating vents properly can trigger the high-pressure pump less frequently. The cycling of vents was not examined in the current study because vent configuration was switched much less frequently than the pump.

As to wetting duration, strategy 3 had the shortest wetting duration, while strategy 1 had the longest duration. It makes sense considering that strategy 3 was based on VPD, which directly affects the evaporation of fog droplets. Maintaining VPD large enough ensured there was sufficient potential for droplets to evaporate and the wetting period was reduced.

To facilitate understanding of how the NCSU control worked, a running example is presented to illustrate the way in which the fog and vents were controlled. Figure 3.5 shows a one-hour snapshot of the evolution of inside enthalpy, target enthalpy and the outside enthalpy. Note that the inside enthalpy fluctuated around the target enthalpy, which is the normal pattern of controlled variables.

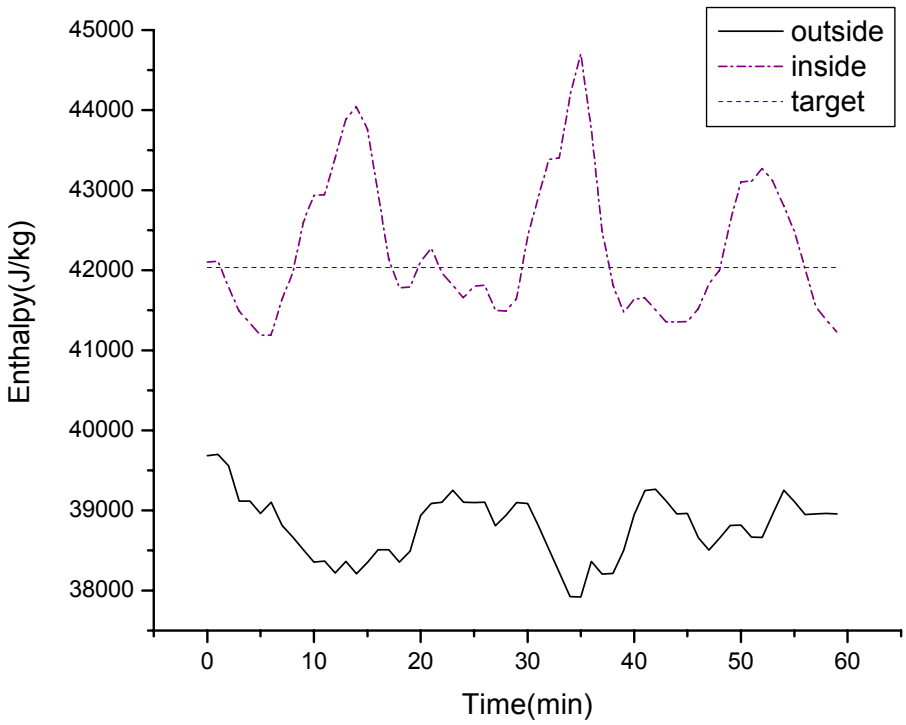

Figure 3.5 Outside, inside and target enthalpies at 5:00-6:00PM on Sept. 21, 2006 when strategy 5 was in effect

Figure 3.6 shows the normalized index β, which is the ratio of the inside-outside enthalpy difference to the target-outside enthalpy difference (Eqn.3.17). When β was greater than unity, the inside enthalpy was greater than the target value, and more airflow was required. When β was less than unity, the inside enthalpy is less than the target value, and airflow should be reduced. It can be seen from the Fig.3.6 that the vent configuration was switched between 's+t' and 's+t+n' responding to the change of the inside enthalpy.

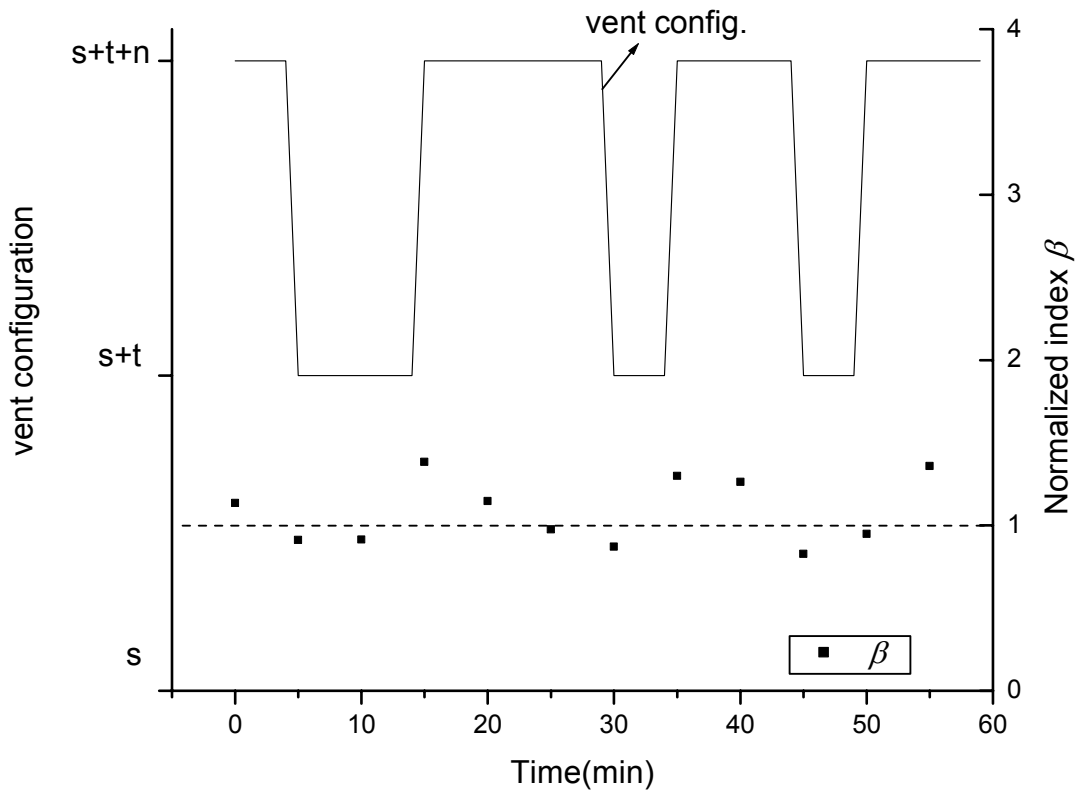

Figure 3.6 Evolution of the ventilation configuration affected by the normalized index β. β >1 indicates more airflow was required to adjust inside enthalpy to the target value; β <1 indicates less airflow was required.

The inside and target humidity ratios and the fog level are presented in Fig.3.7. When the inside humidity ratio was higher than the target value, the fog level was reduced from 1 to 0 (no fog). Note the fog level did not change instantaneously once the inside humidity ratio dropped below or rose above the target line, because of the buffer zone (deadband) that was included in this control.

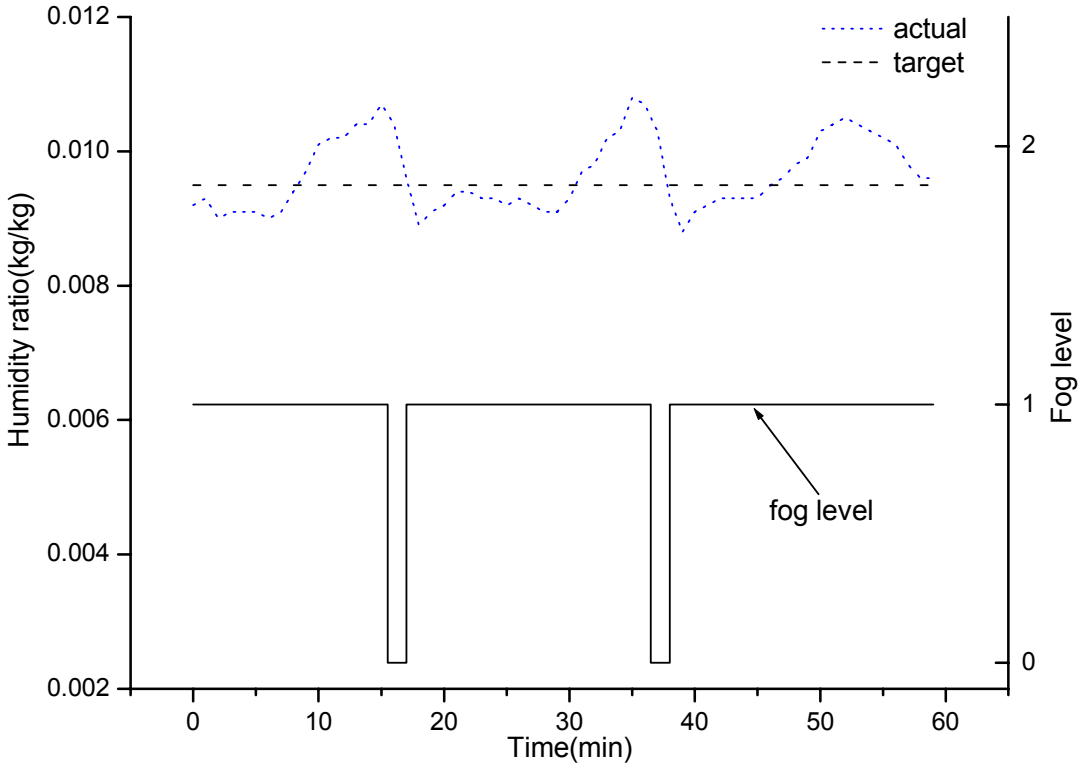

Figure 3.7 Actual, target humidity ratio and change of fog level at 5:00-6:00PM on Sept. 21, 2006

The resulting inside air temperature and relative humidity and their setpoints are presented in Fig.3.8. The quality of a control algorithm can be reflected in some sense by the deviations of the actual value from the target values. The average deviation of temperature from the target value (17.8^{o}C) was 0.6 ^{o}C and the maximum deviation was 1.5 ^{o}C. The amplitude of air temperature fluctuation was 2.7 ^{o}C. For inside relative humidity, the average deviation from the target value (75%) was 6%, and the maximum deviation was 16%. The amplitude of fluctuation was 26%. The average temperature was essentially equal to the setpoint and the average relative humidity was 2% above the setpoint. Obviously, variations of the temperature and relative humidity were reasonably small and the control results were deemed satisfactory.

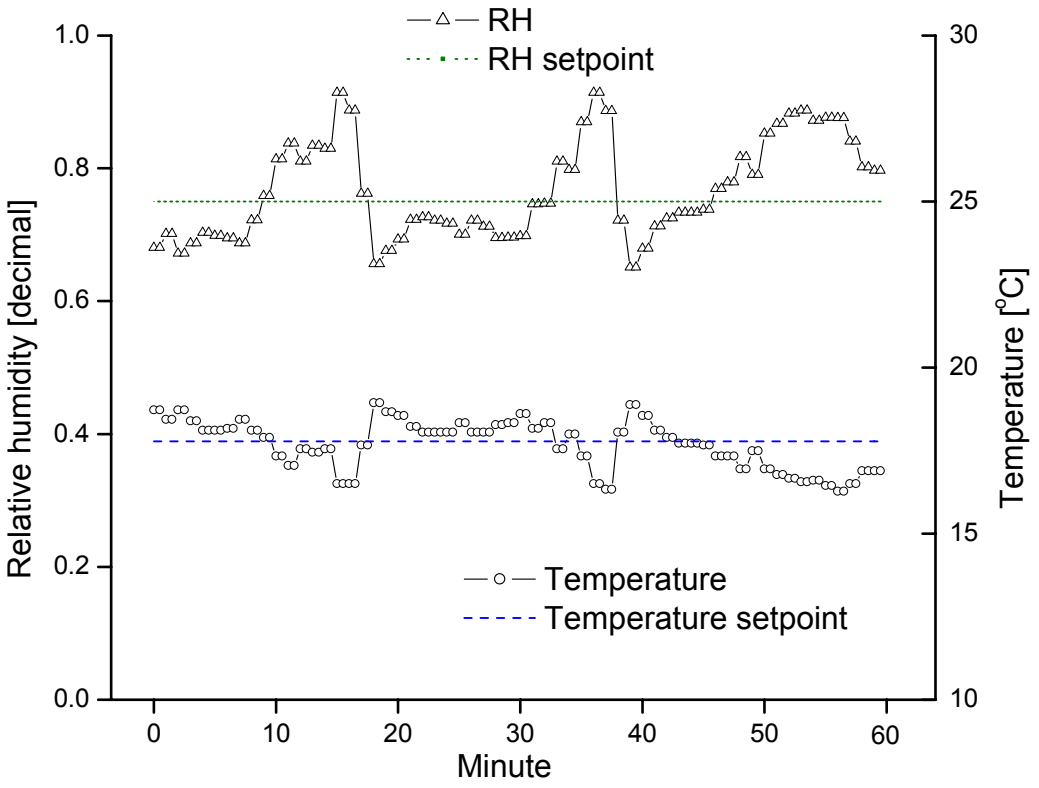

Figure 3.8 Inside temperature, relative humidity and the target values

3.4. Conclusions

A control strategy, NCSU control, was proposed to control the pump and vents in a naturally ventilated greenhouse. Five fog control strategies, including NCSU control were tested in a naturally ventilated greenhouse. The results suggest that:

1) set-point control with temperature and relative humidity and NCSU control resulted in higher cooling efficiency after being normalized for water consumption;

2) properly manipulating vents resulted in less cycling of the high-pressure pump;

3) set-point control with vapor pressure deficit was effective in minimizing leaf wetting;

4) NCSU control was shown to control the air temperature and relative humidity

simultaneously at high accuracies.

Nomenclature

A_c greenhouse cover area, m^2

A_f greenhouse floor area, m^2

C class variable representing performance of control strategy

h_i inside enthalpy, J kg^{-1}

h_o outside enthalpy, J kg^{-1}

h_s enthalpy corresponding to setpoint temperature and humidity, J kg^{-1}

$\dot{m}$ nominal spray rate of fogging system, kg s^{-1}

m_a ventilation rate on mass basis, kg m^{-2} s^{-1}

$\dot{m}_r$ required increase in spray rate above the current spray rate, kg s^{-1}

m_w water consumption, g hr^{-1} m^{-2}

p_s saturated water vapor pressure at t_i, Pa

RH relative humidity

So outside solar radiation, Wm^{-2}

t_i inside temperature, ^oC

t_o outside temperature, ^oC

t_s setpoint temperature, ^oC

$t_{s,w}$ wet bulb temperature corresponding to setpoint temperature and setpoint relative humidity, ^oC

t_w wet bulb temperature inside greenhouse

t_{wo} outside wet bulb temperature, ^oC

u outside wind speed, m s^{-1}

U overall heat transfer coefficient of greenhouse cover, W m^2 $^oC^{-1}$

VPD vapor pressure deficit

X dummy variable representing the performance of control strategy

Greek symbols

α percentage of inside solar radiation contributed to increase of air enthalpy

β index indicating the ratio of inside-outside enthalpy difference to that of target-outside

ζ approximate evaporation efficiency used in fog control

τ transmissivity of greenhouse cover

λ index representing the ratio of required increase in spray rate to nominal spray rate

θ outside wind direction, degree

η_{cool} cooling efficiency

η_{evap} evaporative efficiency

χ_o outside humidity ratio, kg kg^{-1}

χ_i inside humidity ratio, kg kg^{-1}

χ_s humidity ratio corresponding sepoint temperature and humidity, kg kg^{-1}

$\chi_{s,w}$ saturated humidity ratio at $t_{s,w}$, kg kg^{-1}

ω pump cycle frequency, hr^{-1}

References

Arbel, A.; Yekutieli, O.; Barak, M. 1999. Performance of a fog system for cooling greenhouses. *Journal of Agricultural Engineering Research*, 72: 129-136

ASAE. 2003. Heating, ventilating and cooling greenhouses. ANSI/ASAE EP406.2. American Society of Agricultural Engineers, St. Joseph, MI

Bottcher, R.W.; Baughman, G.R.; Gates, R.S. *et al*. 1991. Characterizing efficiency of misting systems for poultry. *Transactions of the ASAE*, 34(2): 586-590

Dixon, M.A. 2003. Humidity control algorithm in the greenhouse. http://www.microcool.com/cooling/brochures/HumidityControl.pdf

Gazquez, J.C; Lopez, J.C.; Baeza, E. *et al*. 2006. Yield response of a sweet pepper crop to different methods of greenhouse cooling. *Acta Horticulturae*, 719: 507-514

Hall, R.A.; Burges, H.D. 1979. Control of aphids in glasshouses with the fungus *Verticillium lecanii*. *Annals of Applied Biology*, 99(3): 235-246

Handarto, M.H.; Katsumi O.; Hiromi, T. *et al*. 2006. Developing control logic for a high-pressure fog cooling system operation for a naturally ventilated greenhouse. *Environmental Control in Biology*, 44(1): 1-9

Li, S.; Willits, D.H.; Yunker, C. 2006. Experimental study of a High-pressure Fogging System in Naturally Ventilated Greenhouses. *Acta Horticulturae*, 719: 393-400

Lindquist, R.K.; Casey, M.L.; Bauerle, W.L. and Short, T.L. 1987. Effects of an overhead misting system on thrips population and spider mite-predator interactions on greenhouse cucumber. *Rose Incorporated Bulletin* (Oct.): 97-100

Meca, D.; Gazquez J.C.; Baeza, E. *et al*. 2006.Evaluation of two cooling systems in parral type greenhouses with pepper crops: low pressure fog system verses whitening. *Acta Horticulturae*, 719: 515-519

Preece, T.F. 1971. Some environmental and microscopical procedures useful in leaf surface tudies. In Ecology of leaf surface micro-organisms, 245-253. Preece, T.F. and Dickinson, C.H., eds. London, U.K.: Academic Press

Sase S.; Ishii M. Moriyama H. *et al*. 2006. Effect of natural ventilation rate on relative humidity and water use for fog cooling in a semiarid greenhouse. *Acta Horticulturae*, 719: 385-392

SAS Institute, Inc. 1989. SAS/STAT User's Guide. Version 6, Fourth Edition. Cary, NC SAS Institute Inc., 846 pp

Willits, D.H.; Yunker, C; Li, S. 2006. Air exchange rates in a naturally ventilated greenhouse using different vent configurations. Paper No. 06-4095, American Society of Agricultural and Biological Engineers, St. Joseph, MI

Zamir, N.; Lavav, N.; Naveh, D. 1969. Examination of the factors which influence the climate in a greenhouse. Progress report No.9. Institute of Agricultural Engineering, Agricultural Research Organization, Bet Dagan, Israel (in Hebrew)

Chapter 4 Thermal Stratification in Fan-Ventilated Greenhouses-Experimental Study

Abstract Experiments were performed to investigate air velocity and vertical air temperature distributions in a fan-ventilated greenhouse. The effects of ventilation rate and canopy size on the distribution of air velocity and allocation between canopy and non-canopy areas were examined. It was found that air velocity was more uniform at high ventilation rates and when large canopy stands were present. The ratio of the velocity within canopy to the mean velocity of the entire greenhouse cross-section depended on not only the area ratio of canopy to greenhouse cross-section area, but also ventilation rate. The velocity ratio of canopy to non-canopy area was lower if ventilation rate increased. The effects of outside solar radiation, ventilation rate, evaporative pad cooling and presence of a canopy on the vertical temperature distribution were also investigated. The vertical temperature variation increased approximately linearly with solar radiation. Use of an evaporative pad increased the temperature variation. Increasing ventilation rate resulted in reduced temperature variation. The presence of a canopy modified the vertical temperature distribution and reduced temperature variations as well.

4.1 Introduction

Recent studies have shown that the air temperature varies considerably between canopy and non-canopy areas (Willits, 2006). Experimental data have indicated that the temperature variation in the vertical direction in a fan-ventilated greenhouse was considerable, reaching as high as 10 ^{o}C under certain circumstances (Li, 2007). Understanding the vertical temperature distribution could potentially improve environmental control. A representative location needs to be selected to place a temperature sensor. If the temperature sensor is placed in an improper location, more or less cooling will be called for

than necessary.

There have been few previous studies on airflow and vertical temperature distribution in fan-ventilated greenhouses except some micrometeorological studies on crop canopy in open fields and forests (Goudriaan, 1977; Barfield and Gerber, 1979). Unlike open fields, the airflow in a greenhouse is confined to a limited space and the resulting environment may have a different distribution. It is necessary to find out what factors affect the distribution and how. A closer look at the spatial distribution of the variables of interest may result in possible improvements in system design and control which might not be possible if the variables of interest were considered homogeneous.

As a preliminary effort, this study presents the experimental results of the air velocity and vertical temperature distributions in a fan-ventilated greenhouse. The effects of outside weather, operational characteristics of greenhouse (ventilation rate, evaporative cooling) and presence of a canopy on airflow and vertical temperature distributions will also be reported.

4.2 Method and Material

4.2.1 Greenhouses

The study was conducted in 2005 and 2006 in two 6.7 × 12.1 m, fan-ventilated greenhouses at Raleigh, North Carolina (35°47′N; 78°39′W). The greenhouses were covered with double-layer polyethylene. They were oriented on a north-south axis, with evaporative pads at the north end and exhaust fans located in the south end. The evaporative pads were sized for a face velocity of 1.27 m s^{-1} at the maximum ventilation rate of 0.087 m^3 m^{-2} s^{-1}. Refer to Appendix A for description.

4.2.2 Plants

In early June of 2005, sweet pepper plants were transplanted into the two greenhouses. The crop was configured in 8 rows with 26 plants in each row, as shown in Fig.4.1. Toward the end of the 2005 season, plants in one greenhouse were removed and those in the other were kept to highlight the effects of canopy on thermal stratification. No plants were grown in 2006.

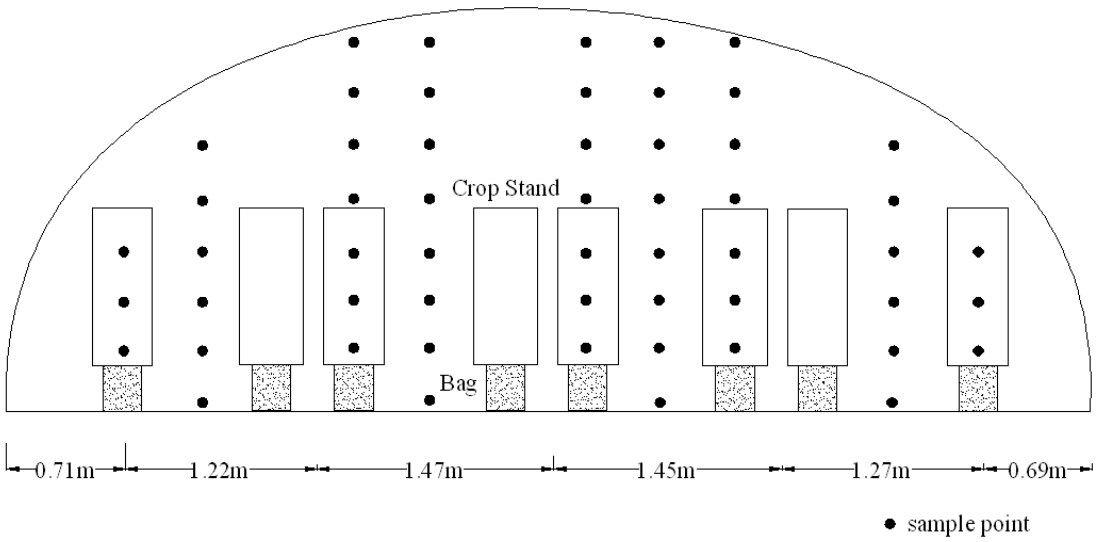

Figure 4.1 Crop configuration and positions of the air velocity sample points

4.2.3 Treatments

Two levels of ventilation rate (0.041 and 0.087 $m^3m^{-2}s^{-1}$), denoted as 'LV' and 'HV', were delivered by two exhaust fans. The status of the evaporative pads was either on or off. Four treatments of canopy sizes were imposed by trimming the plants to the desired sizes: no canopy, canopy size 1, canopy size 2 and canopy size 3. The average size of the double-rows in the middle (Fig.4.1) for each treatment is shown in Fig.4.2. The canopy areas of treatments 1 to 3 were approximately 20%, 29% and 45% of the greenhouse cross-section area respectively.

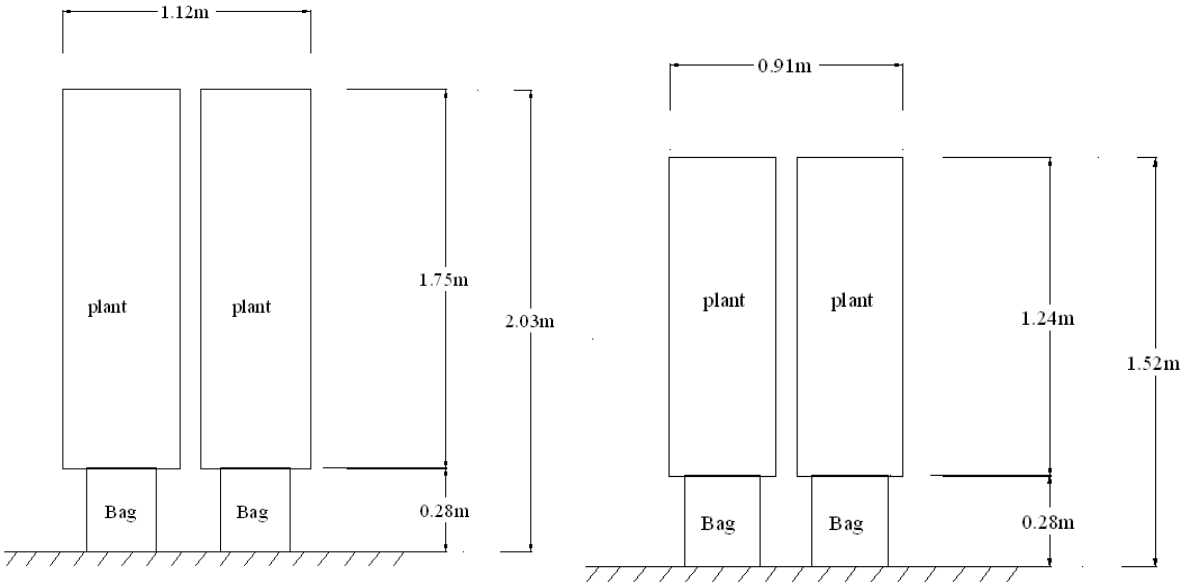

(a) canopy size 3

(b) canopy size 2

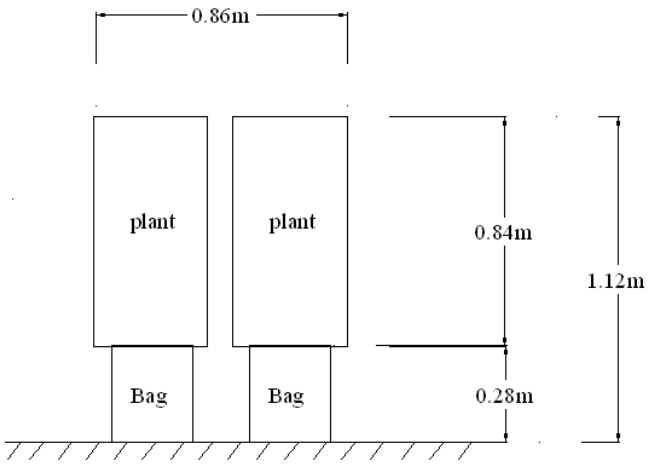

(c) canopy size 1

Figure 4.2 Double-row size for each canopy treatment

4.2.4 Measurements

Inside air temperatures and relative humidity were measured with fourteen aspirated stations, with each station housing a relative humidity sensor (HM50-U Vaisala) and a type-T thermocouple. Only the data from stations 3 to 7 are presented. The heights of the five

stations were 0.46 m, 0.94 m, 1.40 m, 1.84 m and 2.32 m above the floor. They were located 7.3m downstream from the evaporative pads.

Floor temperatures were measured with 36 gauge type-T thermocouples at three locations along a walking aisle. The thermocouple wires were covered by 25x25cm landscape cloth to minimize solar radiation exposure. More details can be found at Seginer *et al*. (2000).

Leaf temperatures were measured using type-K thermocouples glued to the underside of leaves in the upper canopy on selected plants. Eighteen leaves at various locations and heights were monitored. More details can be found at Willits *et al*. (2006).

Outside solar radiation on a horizontal surface, outside dry bulb and wet bulb temperatures, wind speed and wind direction were measured as described in Willits *et al*., (2006).

The air velocity inside the greenhouse was measured with a handheld anemometer (Testo 425, Davis Inotek Instruments, LLC). Measurements were taken at three cross sections, as shown in Fig.4.3. At each cross-section, there were 55 sample points (Fig.4.1) from ground to roof with heights of 0.13, 0.38, 0.89, 1.40, 1.91, 2.16, 2.41 and 2.67m. For each sample point, airflow velocity was measured at 1-second intervals and the 25-second average was taken as the steady velocity.

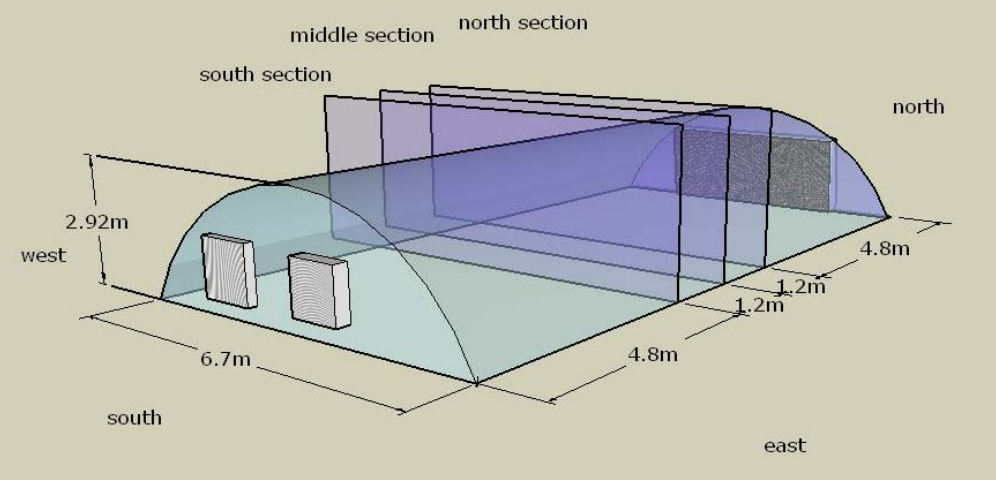

Figure 4.3 Greenhouse geometric parameters and three sections where air velocities were measured

4.3 Results and Discussion

4.3.1 Airflow Patterns

Figure 4.4 shows the vertical profile of the horizontal velocities for LV without canopy. The apparent pattern was that the velocities were generally higher near the ground than near the roof. Figure 4.5 shows the profile for HV without canopy. The velocity peaked at the height of 0.89m, roughly one third of the roof height, and decreased toward both ends. The pattern was similar to jet flow, but it was not strictly symmetrical over the central line.

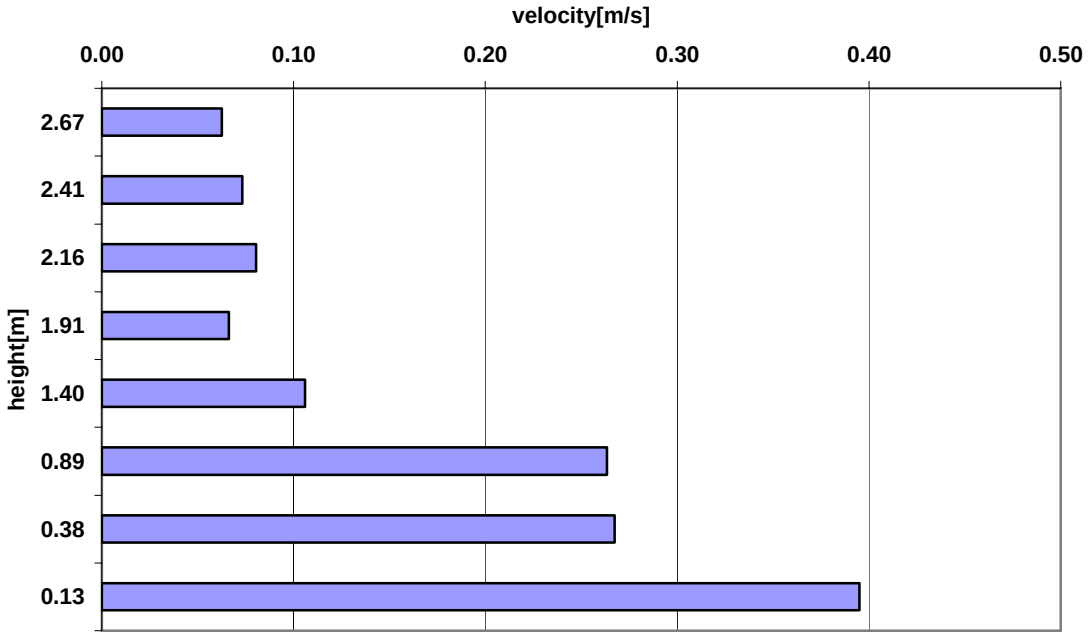

Figure 4.4 Velocity profile for treatment of LV and no canopy

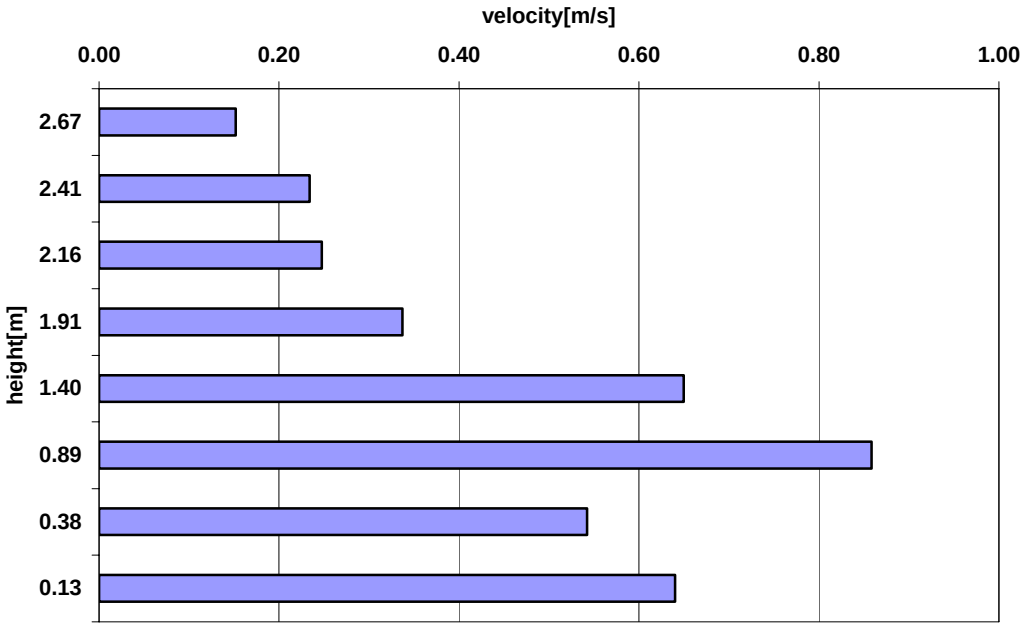

Figure 4.5 Velocity profile for treatment of HV and no canopy

To visualize the velocity profile when the ventilation rate is between LV and HV, interpolation and fitting were performed on the data. First, interpolations were performed at

the first, second and third quarters for each pair of velocities for LV and HV. Then, third order polynomial fittings were performed with the velocity-vs-height data of LV, HV and the three intermediate ventilation rates, namely Q_1, Q_2 and Q_3, approximately 0.0525, 0.064, and 0.0755$m^3m^{-2}s^{-1}$. The profiles for the five ventilation rates are shown in Fig.4.6. The evolution of the profile from LV to HV is obvious: at the low airflow rate, the velocity decreases approximately with height. As the flow rate is increased, the profile becomes more like a parabola, with the maximum flow velocity moving higher off the ground.

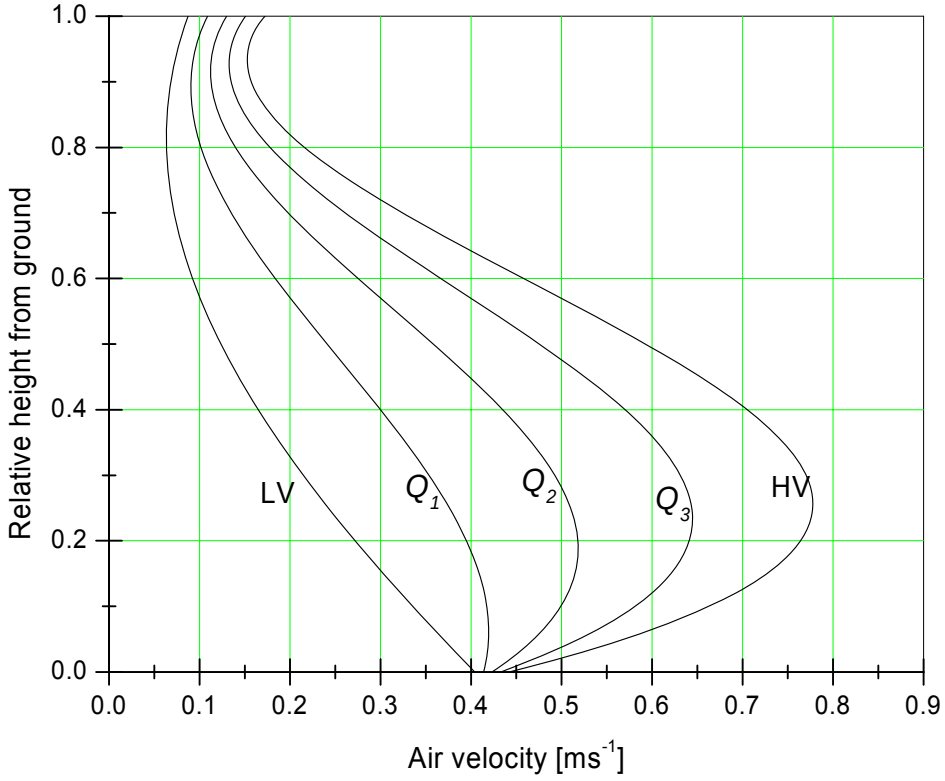

Figure 4.6 Projected velocity profiles for five ventilation rates from LV to HV

Figures 4.7 to 4.12 showed the velocity profiles for various treatments of ventilation rates (LV and HV) and canopy size (1, 2 and 3). The free space refers to the free space above canopy and the walking aisles. As expected, velocities within canopy were significantly

lower than the free space. Comparing each pair of plots for various canopy sizes, it appeared that HV was more uniform than LV. The velocities appeared much more uniform within canopy.

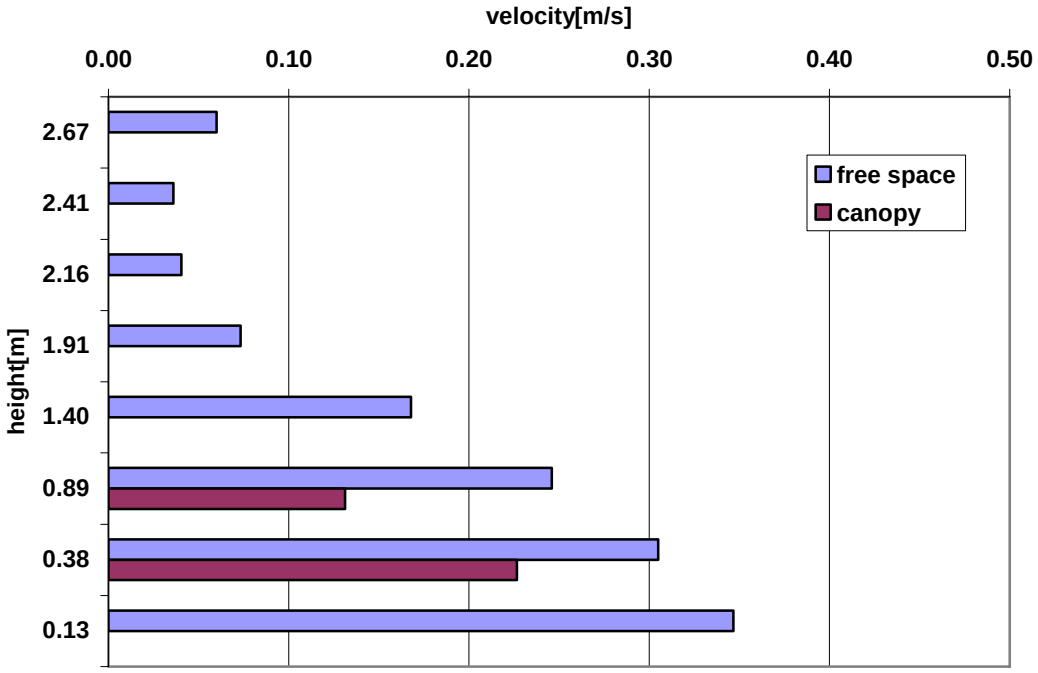

Figure 4.7 Velocity profile for treatment LV and canopy size 1

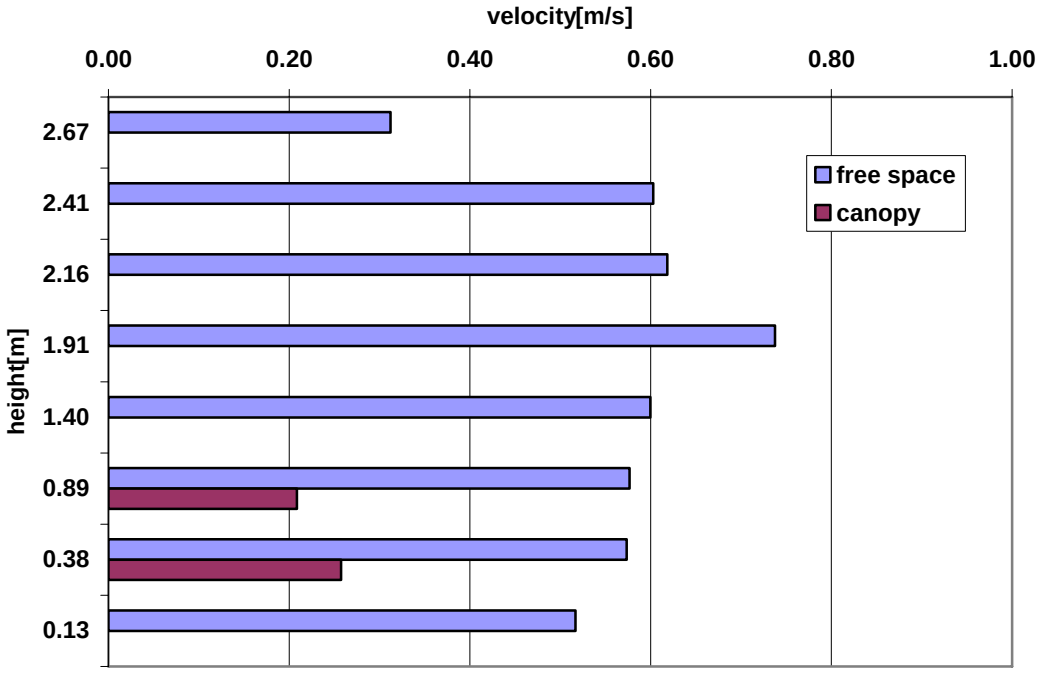

Figure 4.8 Velocity profile for treatment HV and canopy size 1

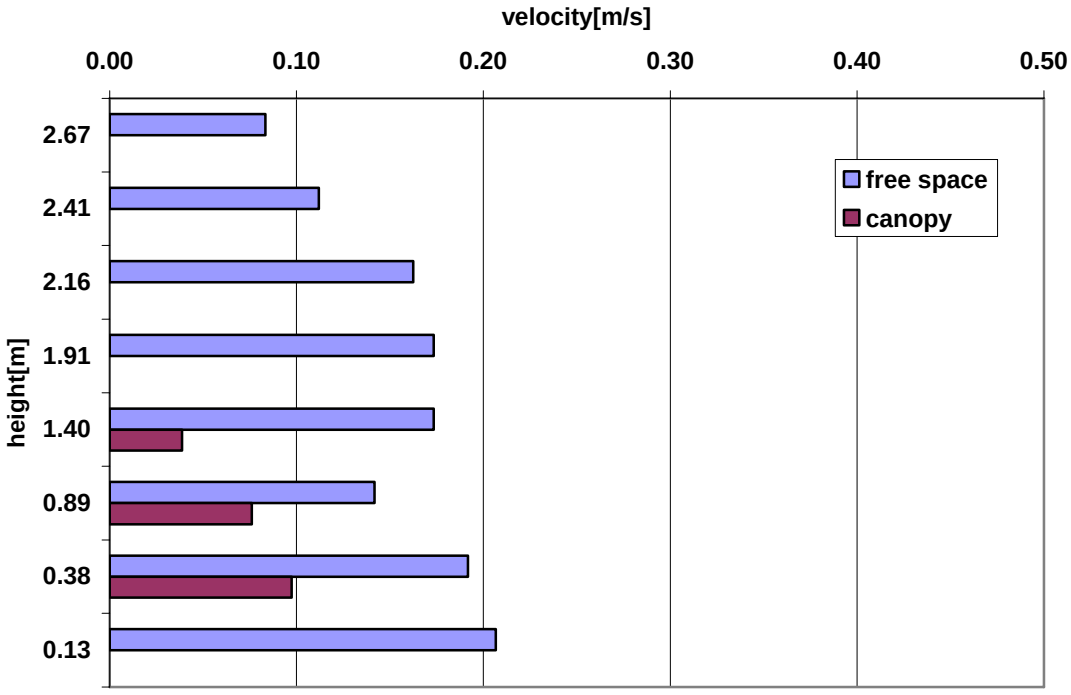

Figure 4.9 Velocity profile for treatment LV and canopy size 2

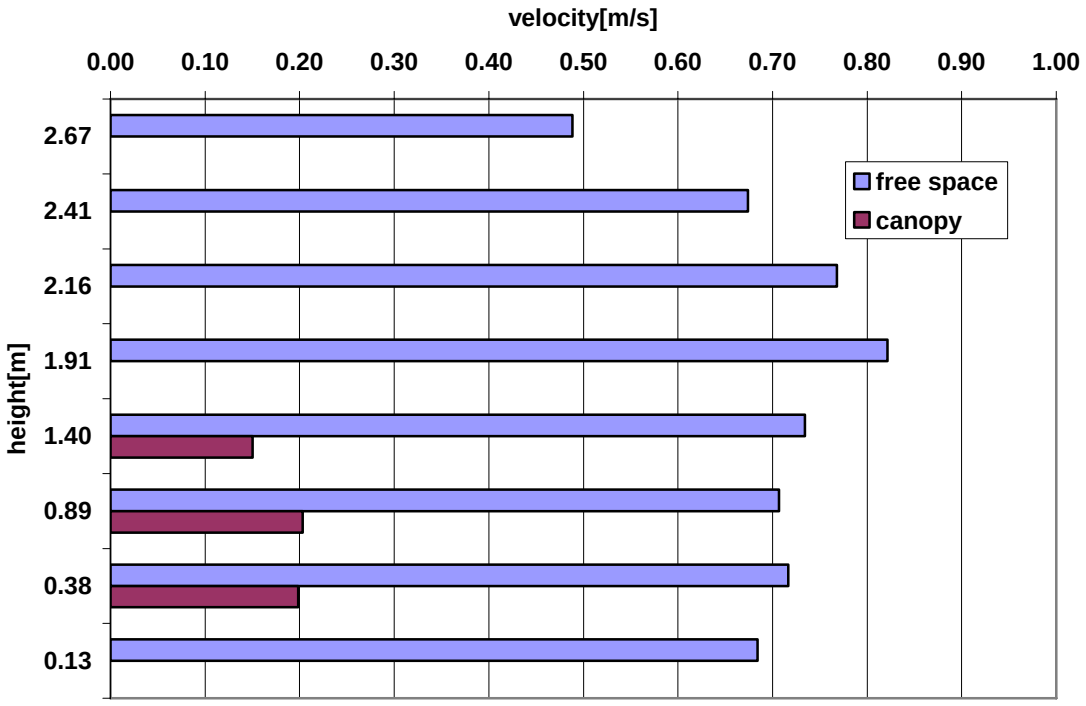

Figure 4.10 Velocity profile for treatment HV and canopy size 2

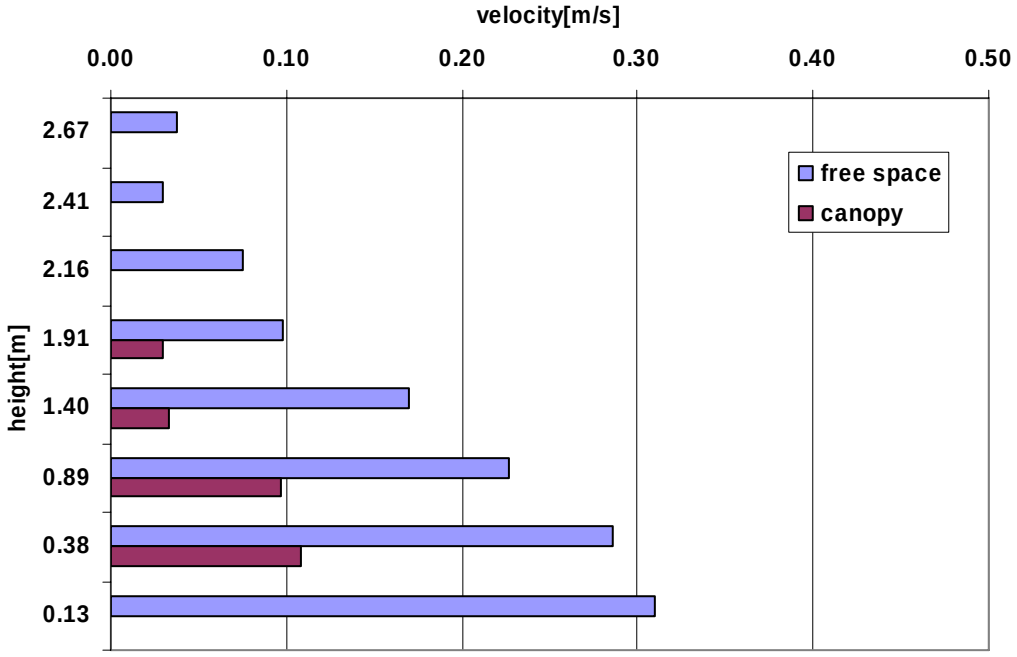

Figure 4.11 Velocity profile for treatment LV and canopy size 3

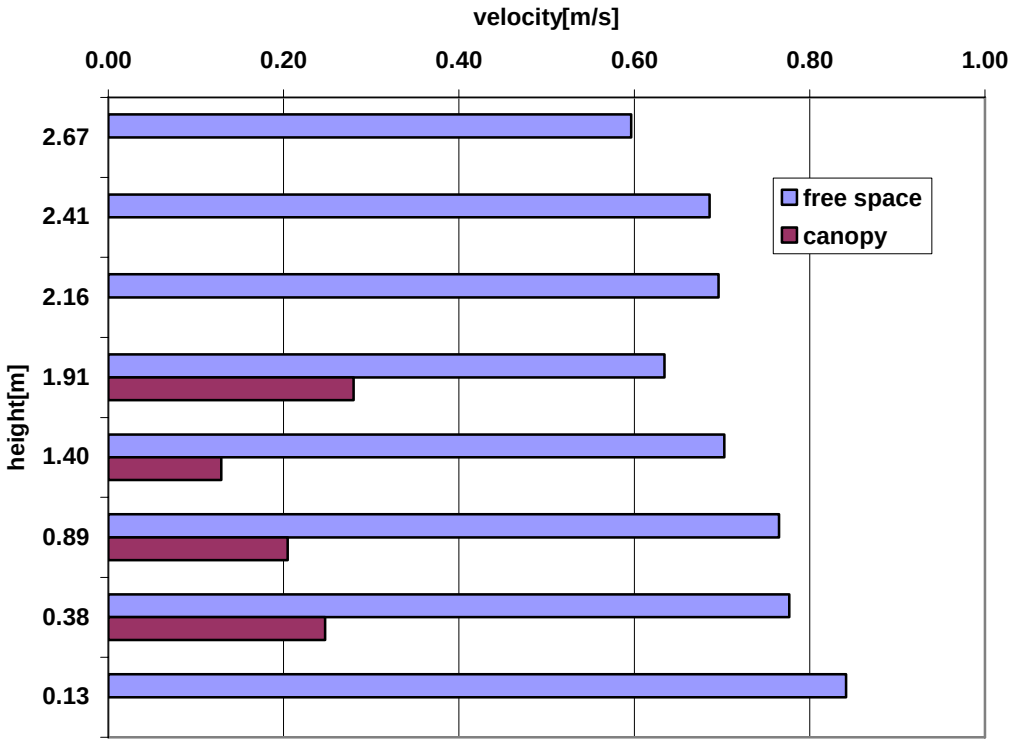

Figure 4.12 Velocity profile for treatment HV and canopy size 3

A general relationship between the velocities within the canopy and in the free space is useful for simulation, since the canopy velocity is essential for the calculation of the convective heat transfer from canopy to ambient air. The relationship was considered in two previous studies and empirical formulae were put forward on the calculation of canopy velocity. The velocities within canopy and the free space were assumed uniform in both studies. The study by Seginer and Livne (1978) adopted the empirical relationship from Rosenzweig (1976),

$$\frac{u_c}{u_m} = \left(\frac{d}{D}\right)^{(1+\eta)/2} \tag{4.1}$$

where u_c is the mean canopy velocity, m s^{-1}; u_m is the mean velocity of the entire greenhouse cross section perpendicular to the airflow direction, m s^{-1}; d is the canopy height, m; D is the

roof height, m; and η is an empirical parameter determined to be 1.3 for a rose greenhouse with bedding area approximately half of the floor area.

Kindelan (1980) proposed another relationship between the canopy velocity and the mean velocity in greenhouse. The relationship is

$$\frac{u_c}{u_m} = \left(\frac{A_c}{A} \right)^{2/3} \tag{4.2}$$

where A_c is the canopy cross section area, m^2 ; and A is the greenhouse cross section area, m^2.

To examine how well the two formulas agree with experimental data, the greenhouse mean velocity, u_m, was calculated by averaging all the measurement at the three cross sections. The mean canopy velocity, u_c, was derived by averaging the measurements taken within the canopy. The canopy section area, A_c, excluded growing media bags and the small gaps between the two single rows between a double-row stand, because they were negligible with a tall canopy. Canopy heights instead of the canopy areas were used when applying Eqn 4.1.

Figure 4.13 presents the ratio of the canopy velocity to the greenhouse velocity u_c/u_m as a function of the ratio of the cross section area of canopy to greenhouse at LV and HV. It can be seen that u_c/u_m depended not only on A_c/A, but also the ventilation rate. The velocity ratio u_c/u_m was lower with HV than LV. The formula by Rosenzweig (1976) and Kindelan (1980) agreed well with the measurements for the cases with LV and canopy size 2 and canopy size 3. However, u_c/u_m was underestimated for case of HV and canopy size 1.

One possible explanation for the underprediction of Eqns 4.1 and 4.2 was that the drag coefficient of canopy, which relates the canopy velocity and the pressure gradient in the direction of flow, is not constant. Instead, it is a variable increasing with the canopy velocity.

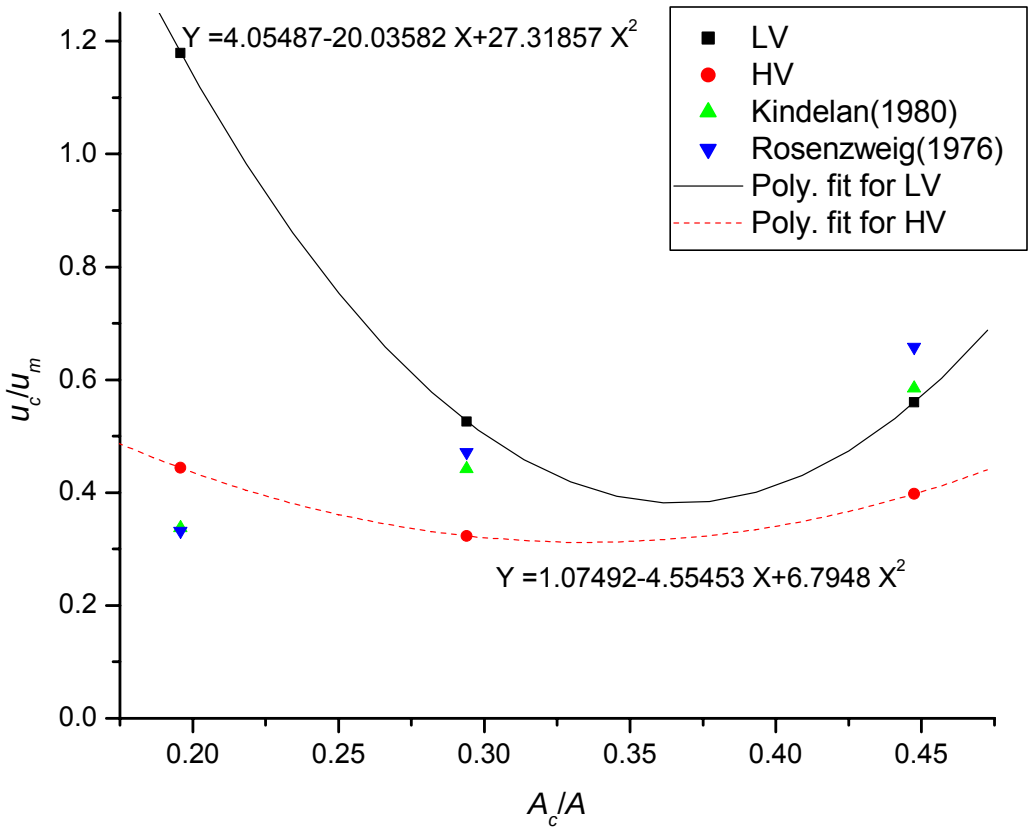

Figure 4.13 Ratio of canopy velocity to mean velocity (u_c/u_m) as the function of the ratio of canopy area to greenhouse cross-section area (A_c/A) and ventilation rate

To overcome the limitation of Eqns 4.1 and 4.2, an alternative relationship is proposed: u_c/u_m is calculated for LV and HV as a function of A_c/A respectively using the following regression equations,

$$R_l = 1.07 - 4.55(A_c / A) + 6.79(A_c / A)^2 \tag{4.3}$$

and

$$R_h = 4.05 - 20.04(A_c / A) + 27.32(A_c / A)^2 \tag{4.4}$$

where R_l and R_h are the velocity ratios u_c/u_m corresponding to LV and HV. The velocity ratio u_c/u_m at an intermediate ventilation rate Q will be

$$u_c / u_m = \frac{R_h - R_l}{0.087 - 0.041}(Q - 0.041) \tag{4.5}$$

As opposed to the general appreciation, Fig.4.13 shows that u_c/u_m exceeds one (i.e. canopy velocity higher than greenhouse velocity) at LV and canopy size 1. The seeming contradiction can be resolved by observing Fig.4.7, where the velocities near the ground were considerably higher than the free space above with LV. As the canopy was small in size, and it occupied the space near ground where the velocity was higher, the canopy velocity was still higher than mean greenhouse velocity even though the canopy imposes the drag force on the airflow.

4.3.2 Effects of Ventilation Rate and Evaporative Pad on Thermal Stratification

4.3.2.1 LV and pad off

Figure 4.14(a) shows the outside solar radiation and dry bulb temperature on August 17, 2006, when the cooling treatment was LV and the evaporative pad was off. It was cloudless in the morning and partially cloudy in the afternoon, with outside temperature between 21 ^{o}C and 31^{o}C. Figure 4.14(b) shows the change of inside temperatures measured with aspirated stations 3 to 7. The temperatures at the five heights gradually diverged from the early morning and became more spaced apart toward the afternoon. After 14:00, Eastern Daylight Time (EDT), the trend reversed and the temperatures converged gradually until they were barely distinguishable from each other at about 18:00. This pattern led to the obvious conclusion that the vertical temperature variation is closely related to outside solar radiation. This makes sense considering solar radiation is the primary driving force for all the thermal processes taking place in greenhouses. Plotting the temperature variation (maximum minus minimum temperature of the five readings) against the outside solar radiation, as shown in Fig.4.14(c), clearly shows that the vertical temperature variation Δt increased approximately

linearly with solar radiation.

However, a hysteresis pattern appeared with respect to noon of Eastern Daylight Time (EDT), i.e. the Δt were higher in the afternoon than in the morning under the same solar radiation. The hysteresis pattern occurred repeatedly throughout the experiment. Plotting ground temperatures against solar radiation resulted in the same hysteresis pattern as the Δt. Considering that the air temperature is directly influenced by ground temperature while solar radiation affects air temperature indirectly, it was probably the thermal inertia of the ground that caused the hysteresis pattern. A snapshot of the vertical temperature distribution at 12:50 is presented in Fig.4.14 (d). Temperature increased with height with the lowest temperature occurring near the floor and the highest temperature near the roof.

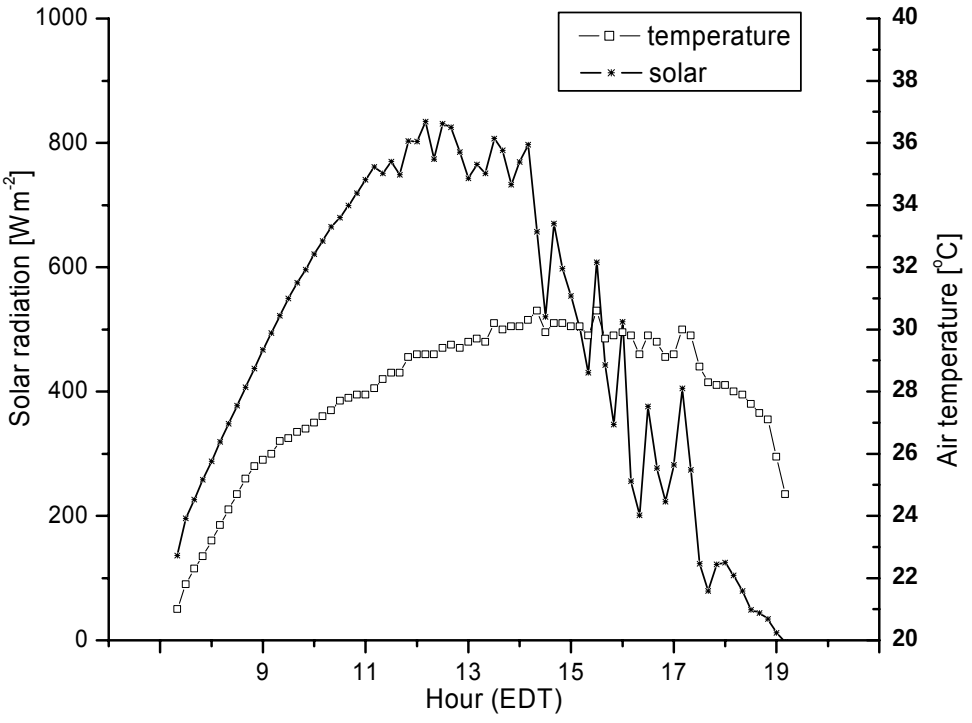

Figure 4.14(a) Outside solar radiation and dry bulb temperature (LV, pad off)

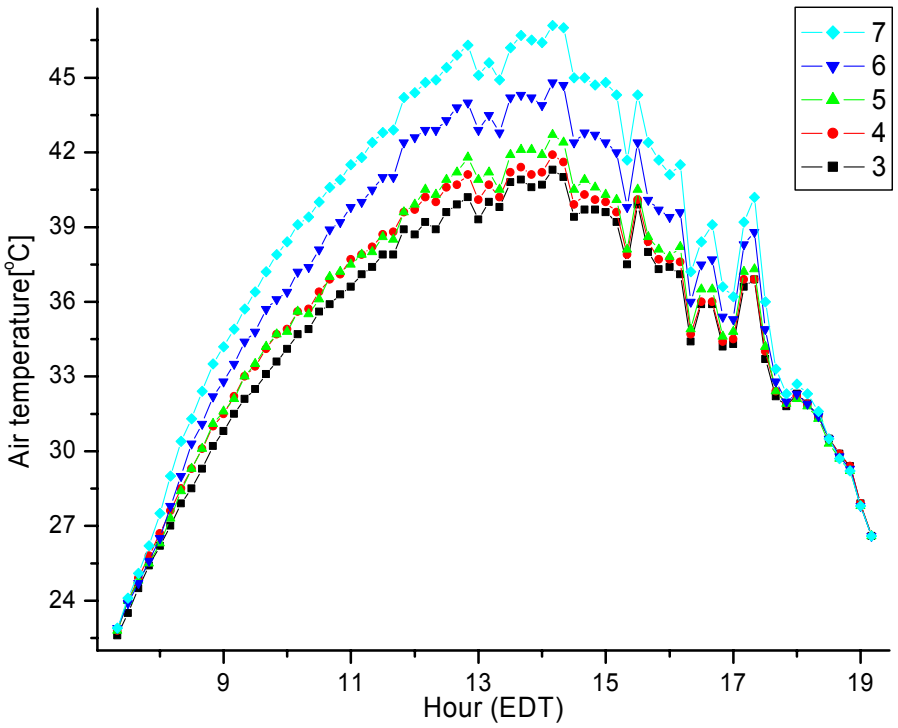

Figure 4.14(b) Temperatures measured by aspirated stations 3 to 7 (LV, pad off)

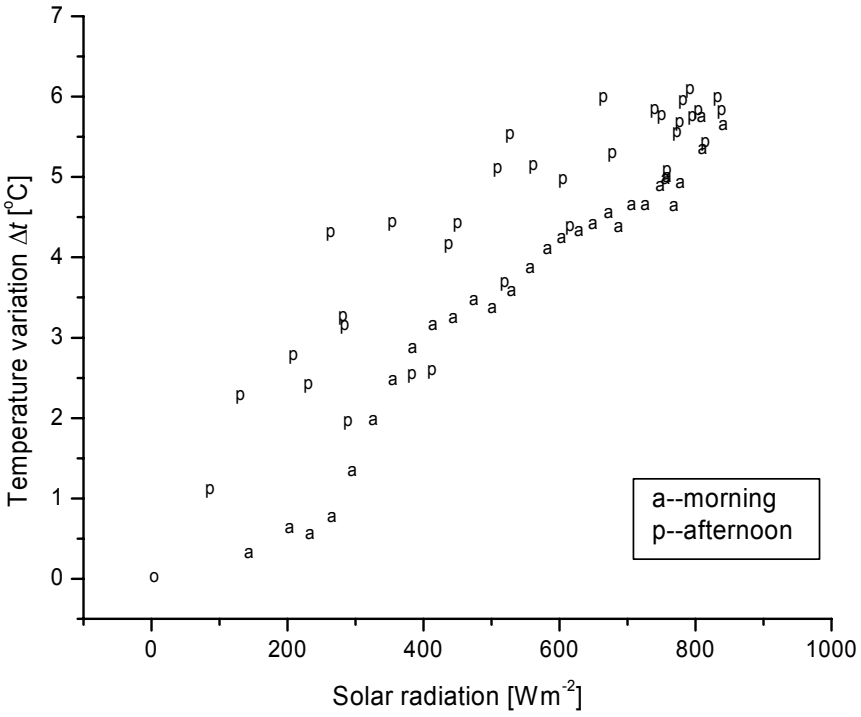

Figure 4.14(c) Vertical temperature variation vs. outside solar radiation (LV, pad off)

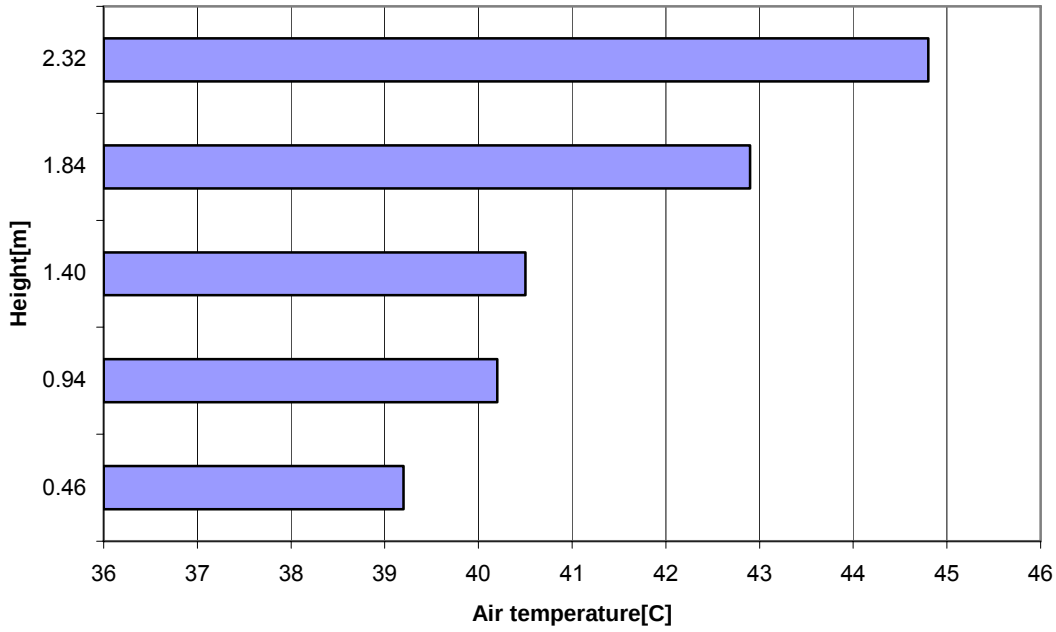

Figure 4.14(d) Vertical air temperature profile at 12:50 PM, EDT (LV, pad off)

4.3.2.2 HV and pad off

The treatment on Aug.4, 2006 was HV and pad off. The outside solar radiation and air temperature are shown in Fig.4.15 (a). The change of the five temperatures during the daytime is presented in Fig.4.15 (b). As previously, the temperatures diverged with increasing solar radiation. The order was $T_5 < T_6 < T_4 < T_7 < T_3$ for most times. Plotting Δt against solar radiation (Fig.4.15(c)) shows the positive dependence of Δt on solar radiation. As was the case with LV+pad off treatment, Δt in the morning was less than in the afternoon with HV+pad off.

Comparing Fig.4.14(c) and Fig.4.15(c) indicates that Δt with HV was less than LV. This suggests that greater Δt will be more pronounced with lower ventilation rate, or that increasing ventilation helps reduce Δt. Figure 4.15(d) shows the vertical temperature profile at 12:50. On contrast to the LV+pad off treatment, the temperature did not increase with height. Instead, the lowest temperature occurred at the middle point and the temperature

increased towards the floor and roof.

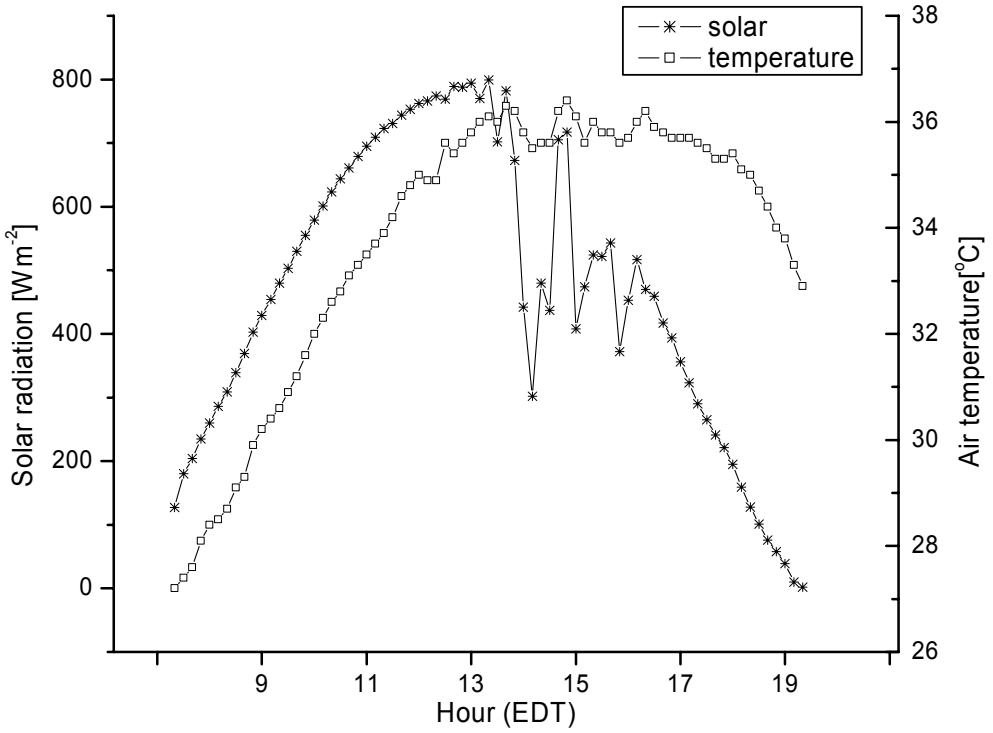

Figure 4.15(a) Outside solar radiation and dry bulb temperature (HV, pad off)

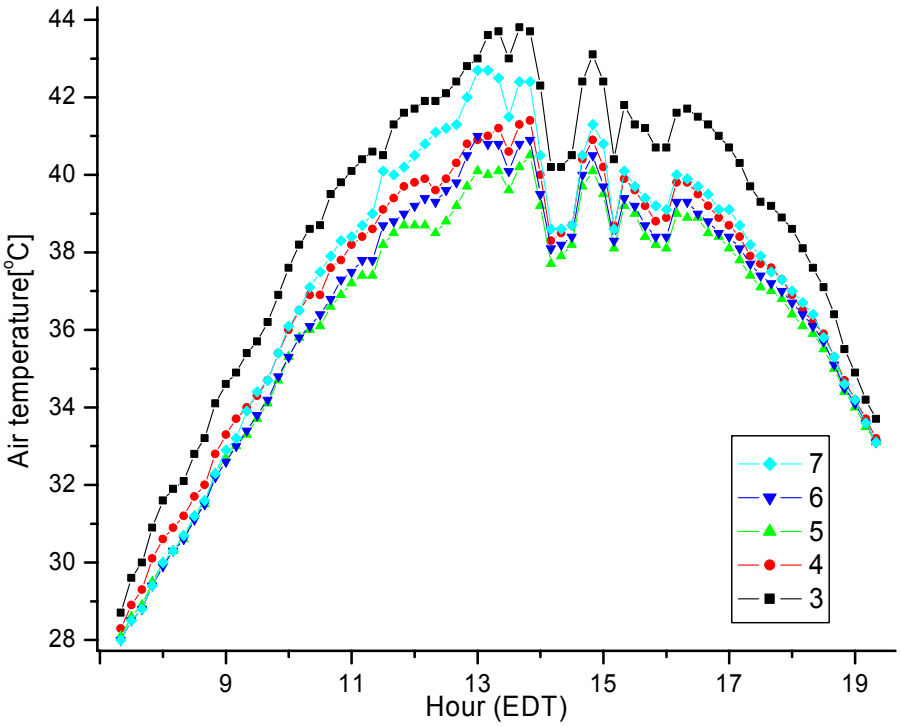

Figure 4.15(b) Temperatures measured by the aspirated station 3-7 (HV, pad off)

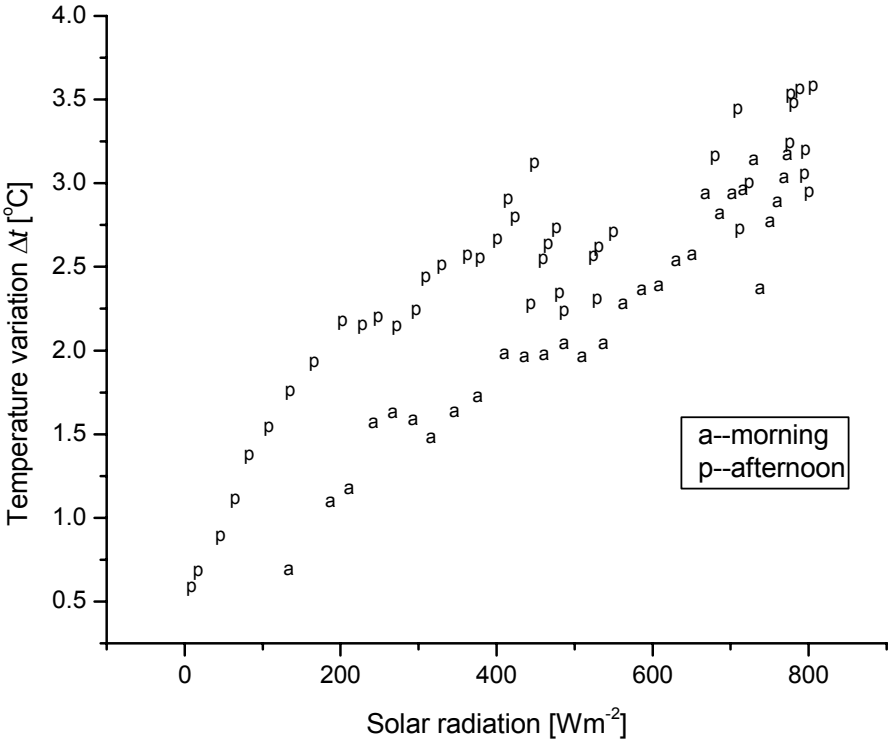

Figure 4.15(c) Vertical temperature variation vs. outside solar radiation (HV, pad off)

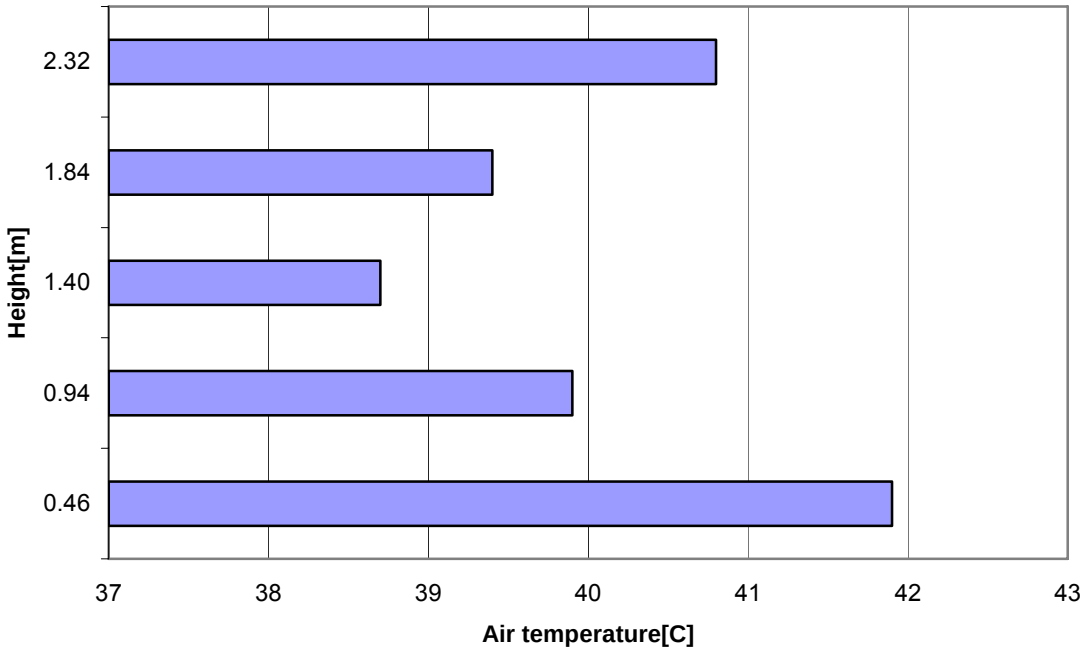

Figure 4.15(d) Vertical air temperature profile at 12:50 PM, EDT (HV, pad off)

4.3.2.3 LV and pad on

The weather conditions on June 20, 2006, are shown in Fig.4.16 (a). The inside air temperatures are presented in Fig.4.16 (b). The relative order of the temperatures was $T_4 <= T_3 < T_5 < T_6 < T_7$, where T_3 and T_4 were roughly the same. Shown in Fig.4.16(c) is Δt plotted against solar radiation. It clearly shows that Δt increased almost linearly with solar radiation, and the hysteresis pattern occurred with respect to noon EDT. Figure 4.16(d) shows the vertical temperature profile at 11:40AM. The profile was almost the same as in the LV+pad off treatment (Fig.4.14 (d)), but Δt was larger with pad on than off, suggesting that the evaporative pad may have increased Δt.

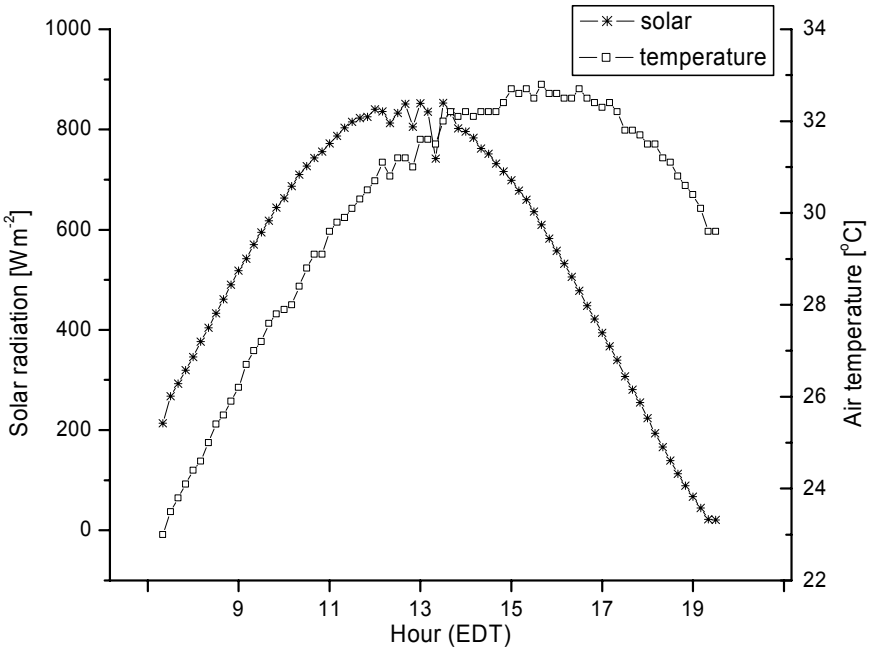

Figure 4.16(a) Outside solar radiation and dry bulb temperature (LV, pad on)

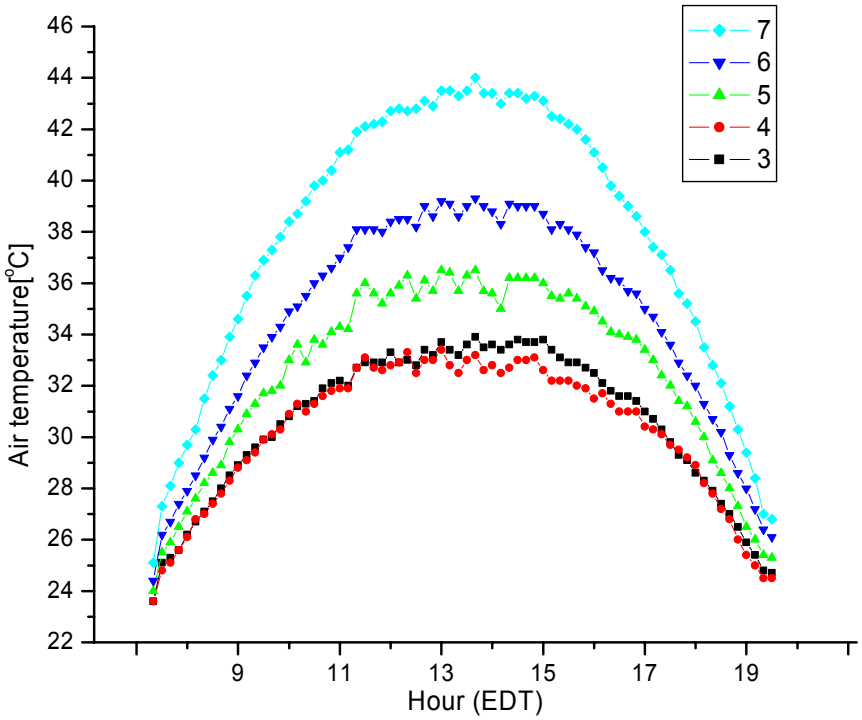

Figure 4.16(b) Temperatures measured by aspirated stations 3 to 7 (LV, pad on)

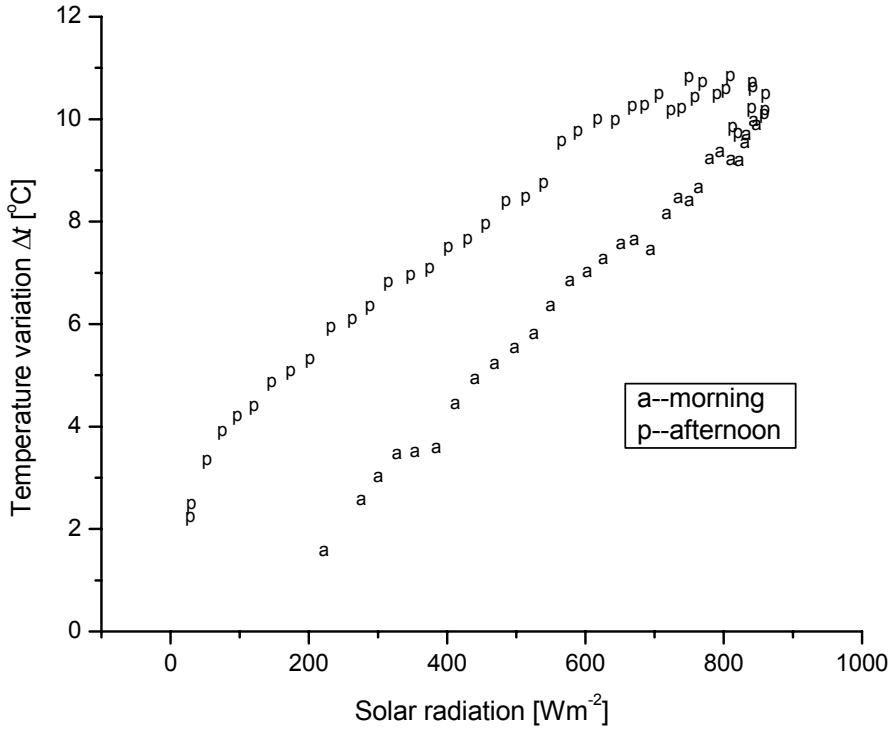

Figure 4.16(c) Vertical temperature variation vs. solar radiation (LV, pad on)

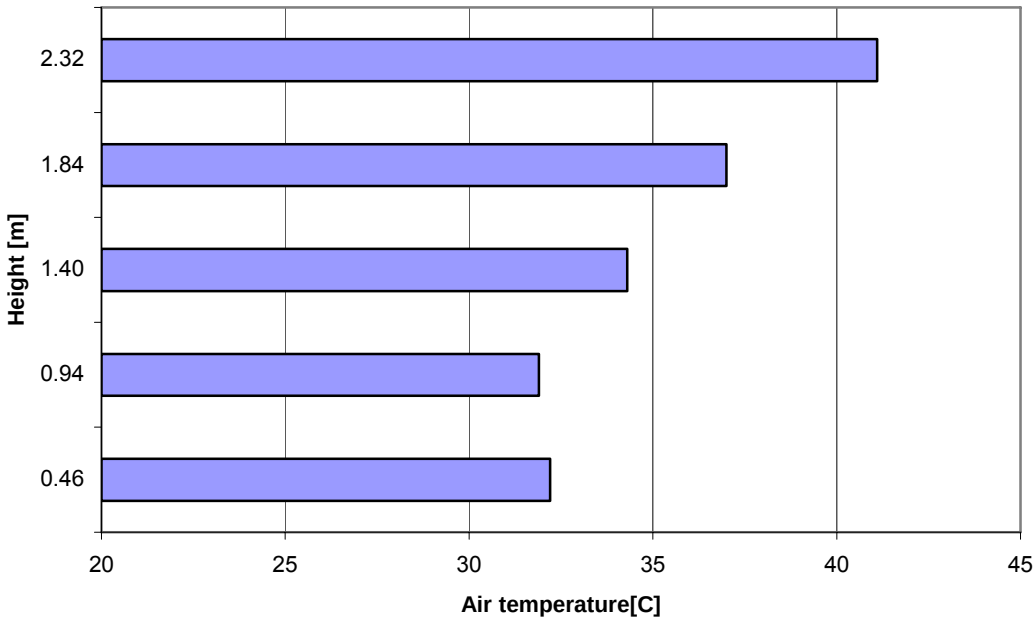

Figure 4.16(d) Vertical air temperature profile at 11:40 AM, EDT (LV, pad on)

4.3.2.4 HV and pad on

The outside solar radiation and air temperature on Aug. 25, 2006, are presented in Fig.4. 17(a), when the treatment was HV+ pad on. Observed from Fig.4.17 (d) and 4.15 (d), the temperature profile was almost the same as with the treatment of HV + pad off. However, the temperatures at upper part of the greenhouse were higher than bottom part in the pad on treatment. When pad was off, the temperatures at upper part were lower than bottom part. Inversion of the high and low temperature region was probably attributable to the cooling effect of air jet from the pad. This suggests that the temperature at the bottom was reduced more than the upper when the evaporative pad was turned on.

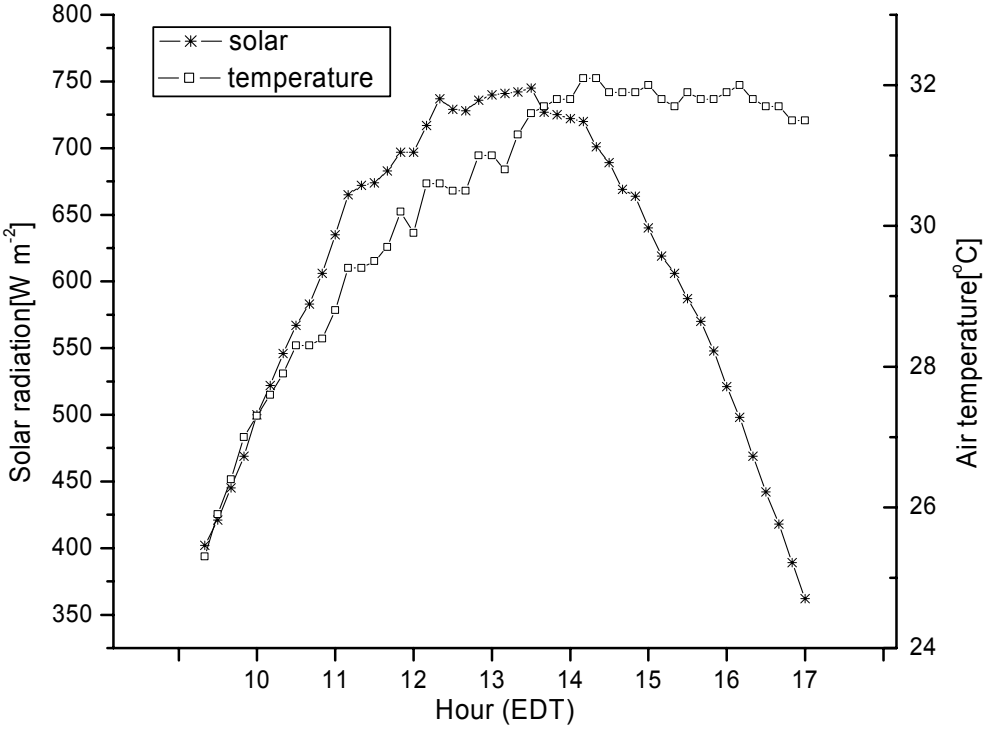

Figure 4.17(a) Outside solar radiation and dry bulb temperature (HV, pad on)

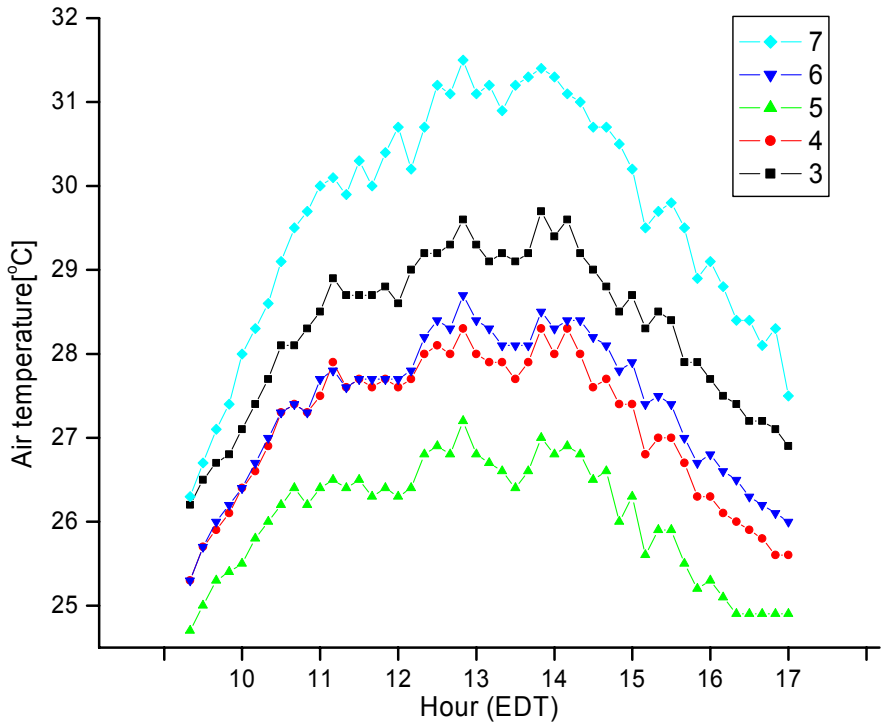

Figure 4.17(b) Temperatures measured by aspirated stations 3 to 7 (HV, pad on)

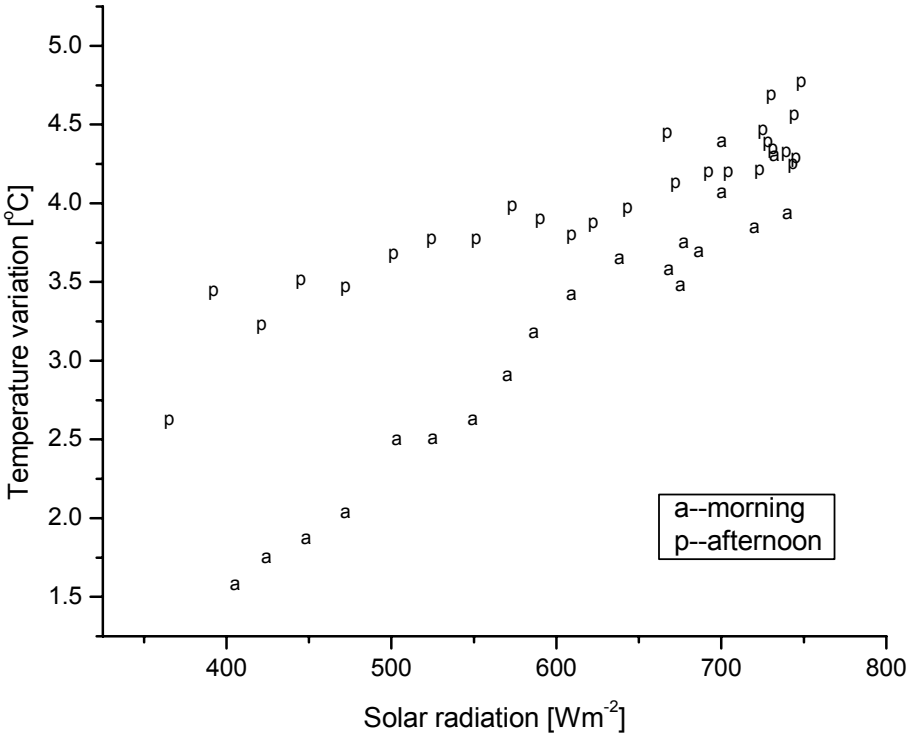

Figure 4.17(c) Vertical temperature variation vs. outside solar radiation (HV, pad on)

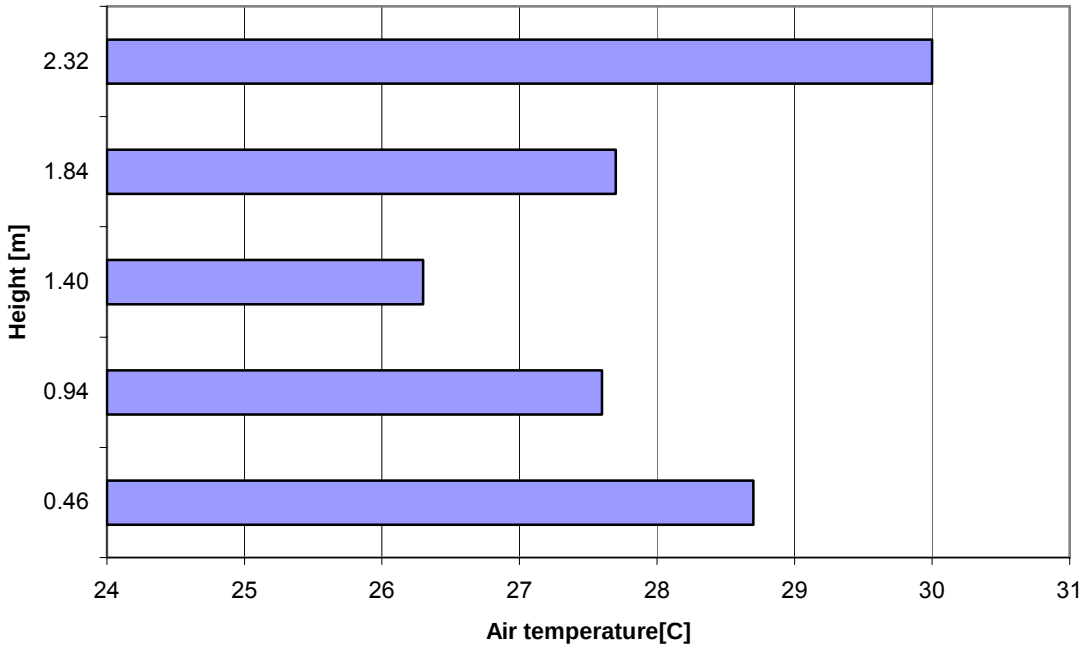

Figure 4.17(d) Vertical air temperature profile at 12:00PM, EDT (HV, pad on)

The effect of ventilation rate on temperature variation is presented in Figs 4.18 and 4.19. The presented data were confined to 8:00AM to 12:00PM in order to avoid any complication caused by the hysteresis pattern described above. The effect of solar radiation was isolated by regressing Δt against solar radiation. Comparing the slopes for HV and LV shows that HV resulted in lower Δt. This was true no matter whether the evaporative pad was on or off.

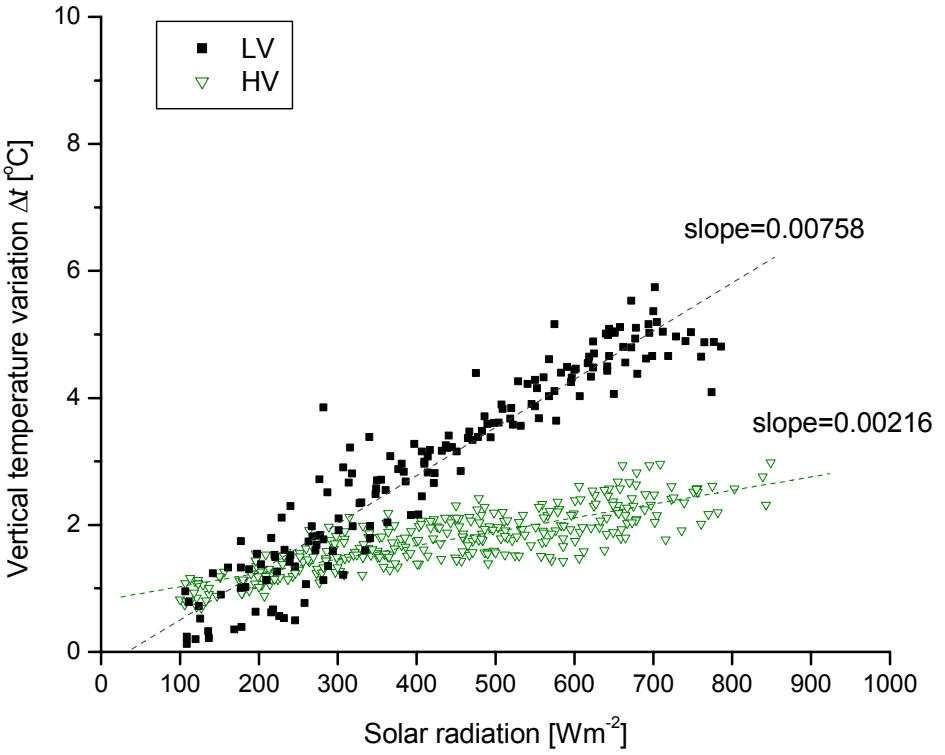

Figure 4.18 Vertical temperature variations for LV and HV with pad off

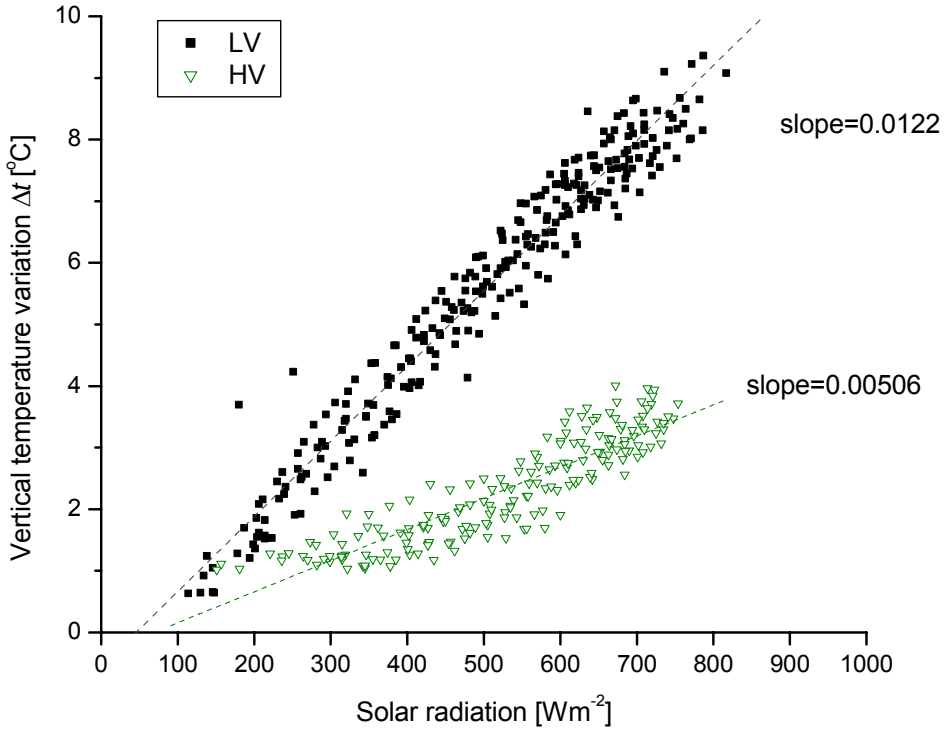

Figure 4.19 Vertical temperature variations for LV and HV with pad on

The effect of the evaporative pad is displayed in Figs 4.20 and 4.21. They clearly show that Δt with evaporative pad cooling was greater than without. It holds true for both LV and HV. It should be mentioned that increasing Δt does not suggest that the temperature at one spot decreases and the temperature at the other increases. What actually happened was that temperatures at all heights dropped, but not by the same amount. The originally cool spots benefited more from the evaporative pad than the originally warm spots, resulting in a larger Δt with the evaporative pad.

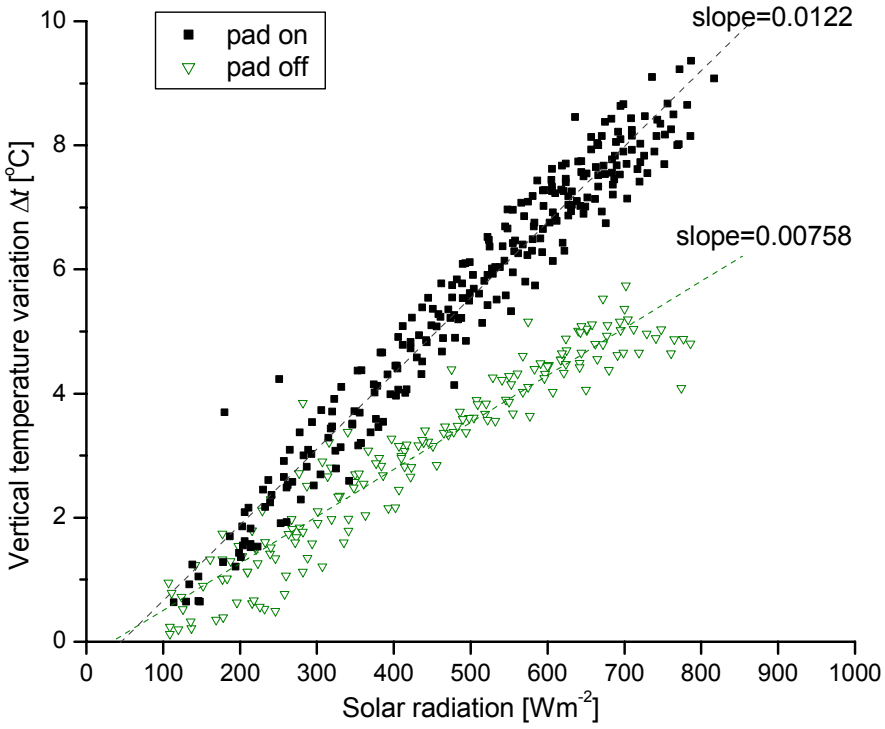

Figure 4.20 Vertical temperature variations vs. solar radiation with LV

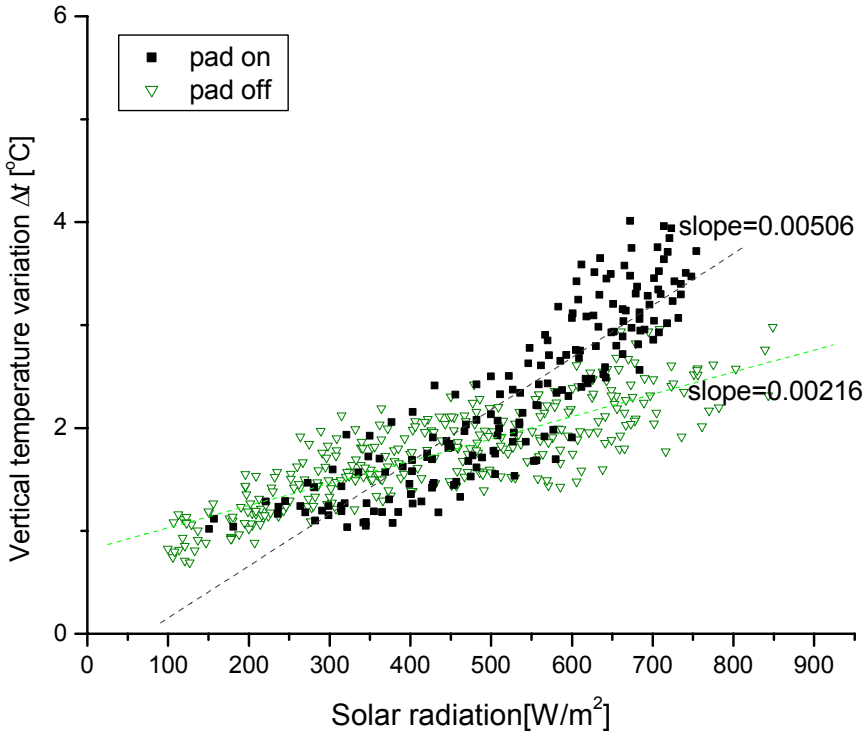

Figure 4.21 Vertical temperature variations vs. solar radiation with HV

4.3.3 Effects of Canopy on Thermal Stratification

Plant canopies alter the greenhouse environment significantly. First of all, the presence of plants modifies the flow field and further affects the temperature field, since the flow and temperature are closely related to each other. Secondly, all or partial of the sensible heat will be converted into latent heat through plant transpiration, thus reducing the temperature and increasing the humidity ratio.

Figure 4.22 shows Δt of the two greenhouses on Sept. 23, 2005: one was filled with fully developed plants and the other was empty. The height of the plants was about 1.71m and three aspirated stations (stations 3 to 5) were submerged in the canopy. Both greenhouses were operated with HV and evaporative pads. The plot shows that the Δt in the planted greenhouse (about 1.5 ^{o}C) was significantly lower than the unplanted greenhouse (about 4.0 ^{o}C).

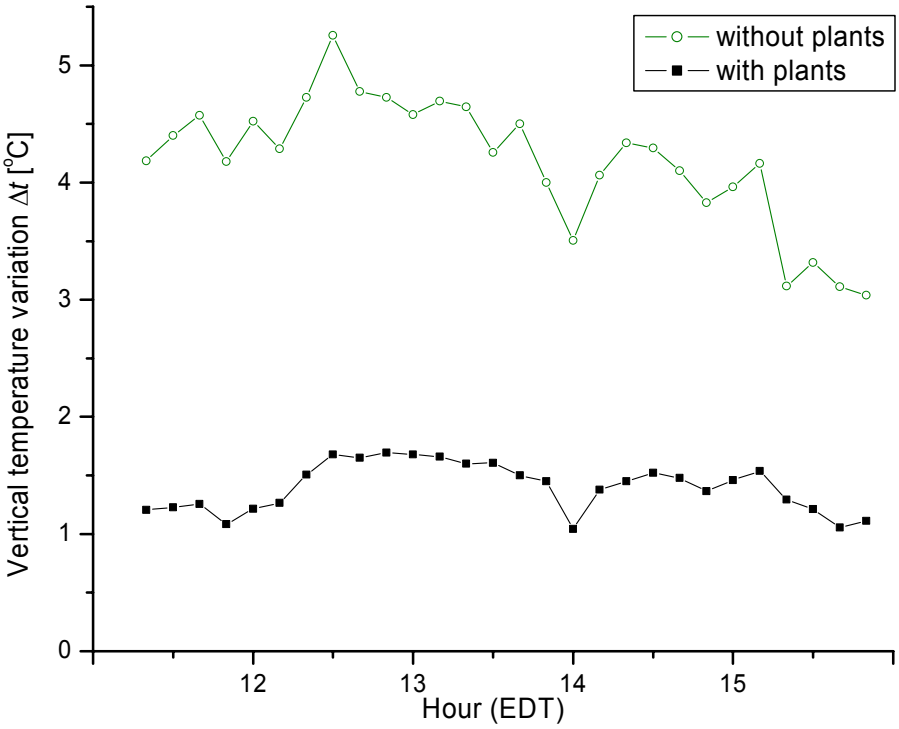

Figure 4.22 Vertical temperature variations for the greenhouses with and without plants

Shown in Fig.4.23 are the vertical air temperature distributions for the two greenhouses. These are average values of T_3 to T_7 over the period of 12:00 PM to 17:00 PM, EDT. It shows that the presence of plants reduced air temperature at all the measurement locations, due to the transpirational cooling of plants. The concave vertical temperature distribution pattern in the empty greenhouse (also shown in Fig.4.23 and Fig.4.17 (d)) did not occur in the greenhouse filled with plants. Instead, the distribution curve was flattened, therefore the temperature variation decreased. It can be observed that T_5 (top of canopy, 1.71m) was higher than T_3 and T_4 within canopy. It was also slightly higher than T_6.

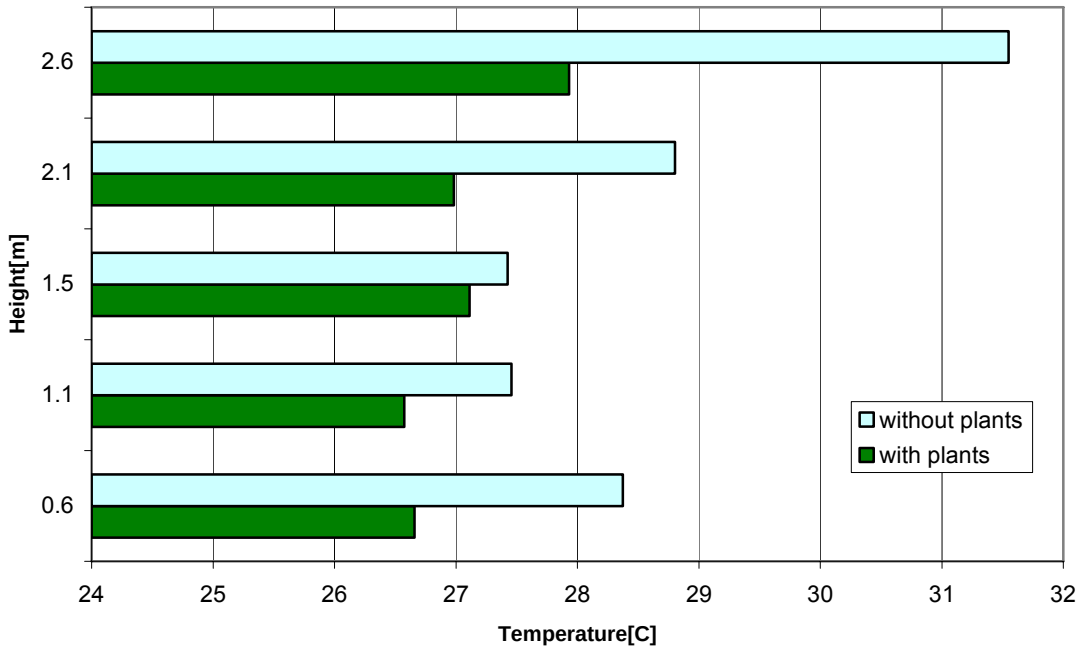

Figure 4.23 Vertical temperature distributions for two greenhouses: one with plants and the other without

Figure 4.24 shows the air and leaf temperatures at the bottom, middle and top of the canopy. The heights of the three leaf thermocouples were 0.5, 1.0, and 1.3m, approximately the same heights as the three aspirated stations measureing T_3, T_4 and T_5. At the bottom of canopy, the leaf temperature was lower than the air temperature (Fig.4.24 (a)), while at the middle and top positions, the leaf temperature was higher than air temperature (Figs 4.24 (b) and 4.24(c)) most of the time. The air-leaf temperature difference at the middle position reached as much as 6^{o}C. Fig.4.24 (d) shows that the leaf temperatures varied greatly with height, with the temperature much higher at the top of the canopy than the bottom. The data suggest that like air temperature, leaf temperature was not uniform vertically. Also, leaf-air temperature difference varied with height, possibly due to different solar radiation received at different depths into the canopy.

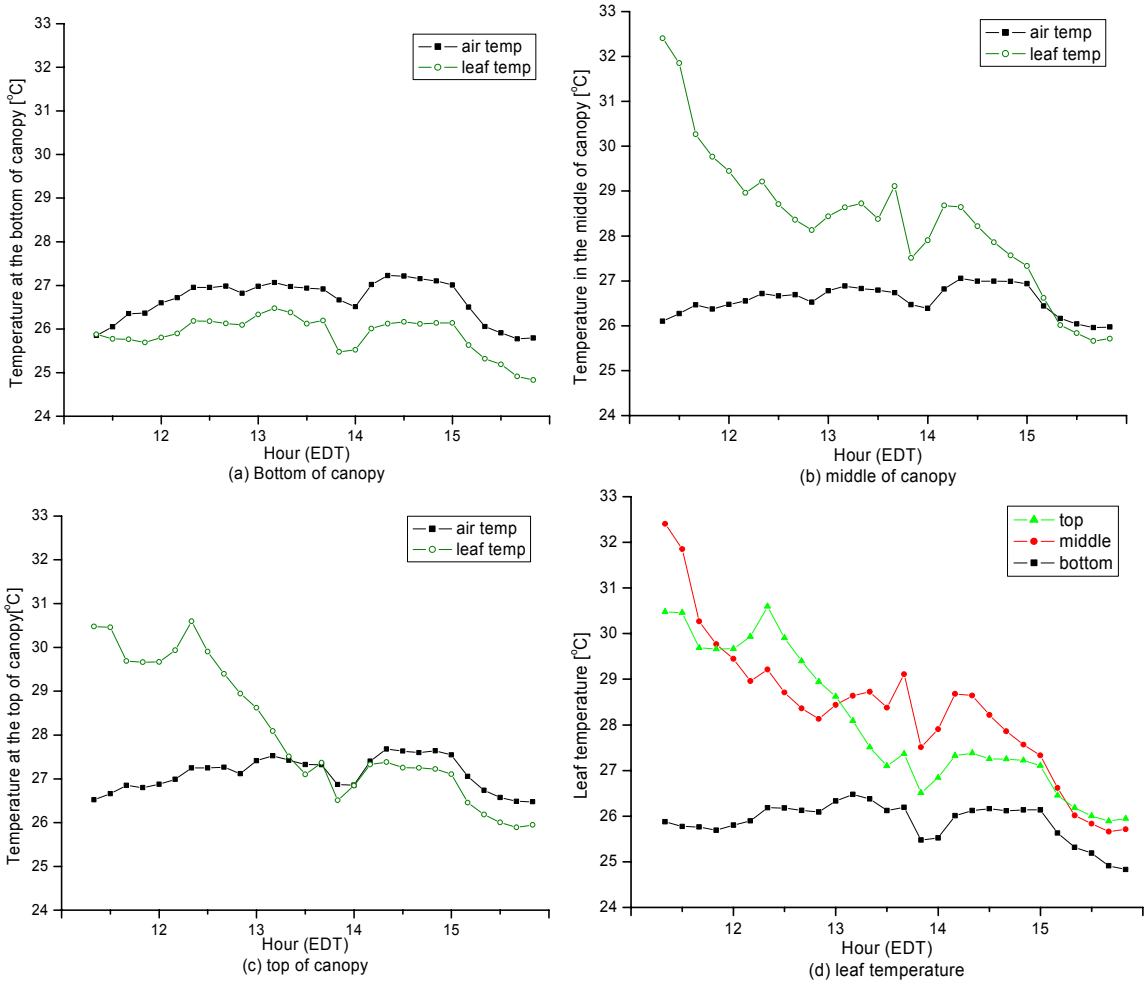

Figure 4.24 Air and leaf temperatures at top, middle and top sections of canopy

Shown in Fig.4.25 is the evolution of vertical air temperature distributions with different canopy sizes ranging from transplant seedlings to fully developed plants. The treatment was HV + pad on. Observation of the plots reveals that presence of canopy significantly modified the distribution patterns. As canopy size increased, the temperature variation decreased.

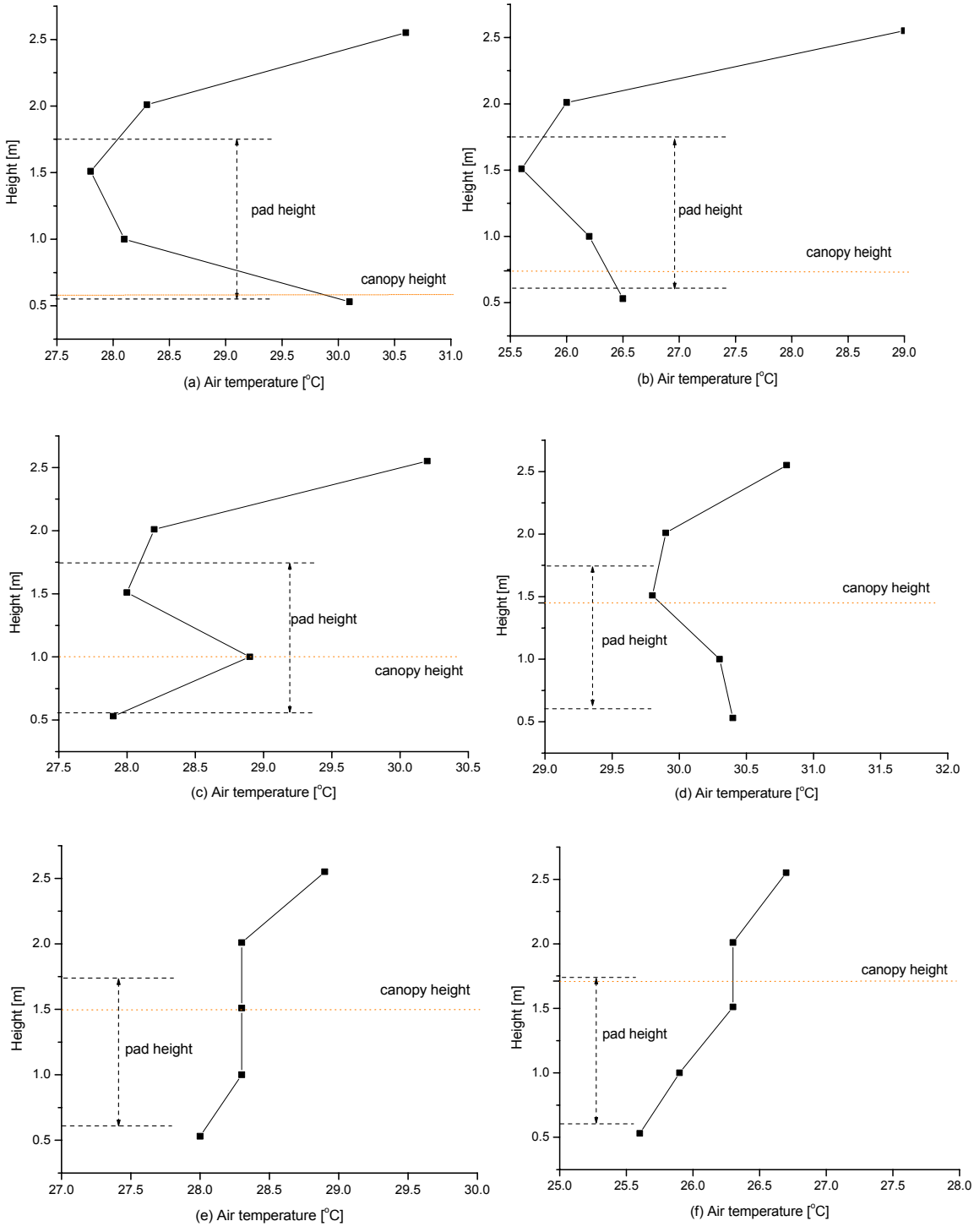

Figure 4.25 Vertical air temperature distributions with various canopy heights

4.4 Conclusions

The experimental data on air velocity in fan-ventilated greenhouses suggest

following: 1) the air velocity within canopy was lower than in the free space; 2) the ratio of the air velocity within the canopy to the mean airflow velocity of greenhouse, u_c/u_m, depended not only on canopy-to-greenhouse cross-section area ratio A_c/A, but also on ventilation rate, with higher ventilation rate resulting in smaller u_c/u_m; 3) the dependence of u_c/u_m on A_c/A was not linear; and 4) air velocities were more uniform with the high ventilation rate in the canopy.

Air temperatures had following patterns: 1) vertical temperature variation increased with solar radiation; 2) high ventilation rate resulted in less vertical temperature variation; 3) using the evaporative pad increased vertical temperature variation; and 4) the canopy altered the vertical temperature profile and reduced the vertical temperature variation.

References

Barfield, B.J.; Gerber, J.F. 1979. Modification of the aerial environment of plants. American Society of Agricultural Engineers, St. Joseph, MI

Goudriaan, J. 1977. Crop micrometeorology: a simulation study. Center for Agricultural Publishing and Documentation, Wageningen, Netherlands

Hatfield, J.L.; Baker, J.M. 2005. Micrometeorology in agricultural systems. American Society of Agronomy, Crop Science Society of America and Soil Science Society of America, Madison, WI

Kindelan, M. 1980. Dynamic modeling of greenhouse environment. *Transactions of the ASAE*, 23 (5): 1232-1239

Li, S. 2007. unpublished data.

Rosenzweig, D. 1976. Canopy flow in a ventilated greenhouse. PhD dissertation. Technion University, Haifa, Israel

Seginer, I; Livne, A. 1978. Effect of ceiling height on the power requirement of forced ventilation in greenhouses. *Acta Horticulturae*, 87: 51–68

Seginer, I.; Willits, D. H.; Raviv M.; Peet, M. M. 2000. Transpirational cooling of greenhouse crops. BARD Final Scientific Report IS-2538-95R, Bet Dagan, Israel

Willits, D.H. 2006. Fan ventilated greenhouses cooling: some considerations for design. *Acta Horticulturae*, 719: 83-96

Willits, D.H.; Teitel, M.; Tanny, J.; Peet, M.M.; Cohen, S.; Matan, E. 2006.Comparing the performance of naturally ventilated and fan ventilated greenhouses. BARD Final Scientific Report US-3189-01, Bet Dagan, Israel

Chapter 5 Thermal Stratification in Fan-Ventilated Greenhouses - Modeling Study

Abstract A two dimensional thermal model was built to describe the distribution of air temperature in fan-ventilated greenhouses. Prediction of air temperature was satisfactory. Model simulations suggest that increasing ventilation rate reduced the vertical temperature gradient. Increased ventilation reduced air temperature more at the top than the bottom of the greenhouse. Greater air temperature variation was produced when using evaporative pad cooling than not. Air temperature was reduced more at the bottom than at the top with evaporative pad cooling. The presence of a canopy altered the vertical air temperature distribution and reduced the temperature variation.

5.1 Introduction

In fan-and-pad cooled greenhouses, fans are installed in one wall and pads on the opposite wall. When air flows through the greenhouse, energy is exchanged between the air and greenhouse structure, floor, and plants by convection. Meanwhile, energy is also transferred within the airflow. Temperature variations will be developed along the airflow (x) and vertical (z) directions (Fig.5.1).

Temperature variation in the direction of airflow has long been recognized and studied (Seginer and Livne, 1978; Kittas *et al.*, 2003; Willits, 2003). However, the significance of vertical temperature variation was not recognized until recently (Willits, 2006). The existence of a vertical temperature gradient exposes different parts of plants to different temperatures. In practice, a representative location needs to be selected to place the temperature sensor for greenhouse control. If not properly placed, the control device may call for more or less cooling than necessary. The center of greenhouse in the airflow direction is usually the recommended location to place the temperature sensor, but no information is

available on what height is appropriate. Therefore achieving an in-depth understanding of the vertical temperature distribution has the potential to improve greenhouse control.

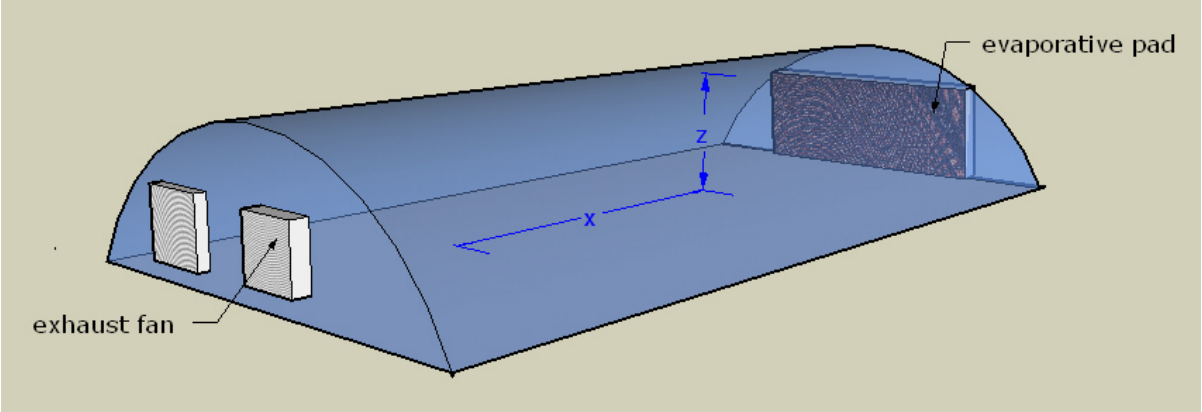

Figure 5.1 Directions *x* and *z* where temperature variation is likely to develop

Vertical profiles of greenhouse environment have been investigated in several studies. Yang *et al*. (1990a, 1990b) investigated the heat and water vapor transfer between plants and the ambient air. A model was set up to predict the vertical profiles of air temperature and humidity; leaf temperature and transpiration rate. The input conditions were air velocity in canopy and free space; incident solar radiation; cover and ground temperatures. Verification was performed with the data from a naturally ventilated greenhouse. It was shown that the agreement between predicted and measured air and leaf temperatures and transpiration rate was good and the agreement for solar radiation and humidity was reasonable. Zhang *et al*. (2003) further developed Yang's model by revising the subroutine on solar radiation that enabled the handling of double-row crop stands and incorporating a subroutine to predict the moisture condition at the leaf surfaces.

The models by Yang *et al*. (1990a, 1990b) and Zhang *et al*. (2003) are basically of same nature: the information above the canopy (cover temperature, air temperature, humidity, air velocity etc) and beneath the canopy (floor temperature) are the boundary conditions. The thermal and radiative properties of canopy, ground and cover are the model parameters.

Vertical profiles of air and leaf temperatures and humidity and near-leaf-surface microclimate are the model outputs. The models neglected the environmental variations in the airflow direction, which may be reasonable for naturally ventilated greenhouses, but not for fan-ventilated greenhouses.

As to the horizontal profiles of air temperature and other variables, the studies by Seginer and Livne (1978), Kittas *et al.* (2001) and Willits (2003) are representative. Seginer and Livne (1978) sketched a steady state model to describe the horizontal air temperature and humidity distribution in the airflow direction assuming the sensible heat from cover and floor input is known. However, the model was not calibrated or validated.

In the study by Kittas *et al.* (2003), heat balance was established for each slice of greenhouse section element by applying the cooling design equation given in the ASAE standard (2003). The resulting first-order differential equation was solved to get the horizontal profiles of air temperature. The model was simple and easy to use. Weather data, the model inputs, are readily available. Nevertheless, the response of plant transpiration to environment was oversimplified and therefore the model shared the same limitation as the ASAE equation (2003). The evaporation coefficient, a key parameter, must be estimated empirically.

Willits (2003) overcame this difficulty and established the heat balance for plants, cover, and soil, so the temperatures of these elements were predicted as outputs instead of inputs. Also, the incoming air stream was split into two streams, one through canopy and the other through the free space. The way the air stream was handled was justified by experimental data that suggested that the microclimate within canopy is different than free space.

The objective of this work is to combine capabilities of previous models, making it able to predict the distributions of air and leaf temperatures and relative humidity in airflow and vertical directions. The model will be used to examine the effects of ventilation rate, evaporative pad cooling and canopy on the vertical distribution of air temperature.

5.2 Model Description

The airflow was split into two air streams, one through and above the canopy (AS-I) and the other through the walking aisles (AS-II). As heat and water vapor transfer take place inside each air stream, they also happen between the two air streams. To reflect that, conservation equations were established for each of the two air streams and the interaction between them was incorporated. The configuration and geometric parameters of canopy and greenhouse structure are shown in Fig.5.2. The canopy rows are normally the same in size. They are spaced equally and repeat themselves in the greenhouse width direction. In this study, half of a canopy row and walking aisle were singled out for study. The distance between the centerlines of the canopy and walking aisle is W_1, m; the half-width of the canopy is W_2, m; the canopy height is H_2, m; and the height of roof is H_1, m. To simplify the model, the airflow and the associated heat transfer in the vertical direction due to buoyancy was not considered separately, but was combined with eddy diffusion in the same direction. The ground was covered with an impermeable layer therefore the evaporation from ground was neglected.

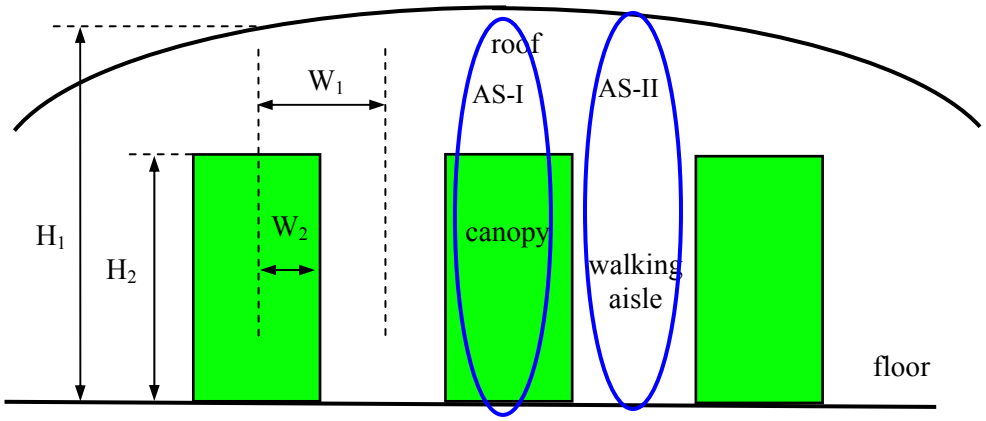

Figure 5.2 Model configuration and geometric parameters

5.2.1 Sensible Heat Conservation of Air

The heat conservation equation can be found in numerous heat transfer textbooks (Kreith and Bohn, 2001; Cengel, 2003). Taking into consideration the heat exchange between the canopy and the air stream through it, and that between AS-I and AS-II, the sensible heat equation for AS-I can be written as

$$u\rho_a c_{p,a}\frac{\partial t_{a1}}{\partial x}=\frac{\partial}{\partial z}\left(k_{eff}\frac{\partial t_{a1}}{\partial z}\right)+\frac{4k_{eff}}{W_1W_2}\left(t_{a2}-t_{a1}\right)+q \tag{5.1}$$

where u is the horizontal airflow speed, m s^{-1}; ρ_a is air density, kg m^{-3}; $c_{p,a}$ is the specific heat of air, J kg^{-1} $^oC^{-1}$; t_{a1} is the temperature of air in AS-I, ^oC; t_{a2} is the temperature of air in AS-II, ^oC; x is the distance from pad, m; z is the distance from floor, m; k_{eff} is the effective thermal conductivity of the air, $Wm^{-1o}C^{-1}$; and q is the sensible heat from leaves to air of AS-I on a volumetric basis, Wm^{-3}. Similarly, the heat equation for AS-II is

$$u\rho_a c_{p,a}\frac{\partial t_{a2}}{\partial x}=\frac{\partial}{\partial z}\left(k_{eff}\frac{\partial t_{a2}}{\partial z}\right)+\frac{4k_{eff}}{\left(W_1-W_2\right)W_1}\left(t_{a1}-t_{a2}\right) \tag{5.2}$$

The sensible heat from leaves to air of AS-I on a volumetric basis, q, is

$$q = h_{c,a1} \cdot \zeta \left(t_c - t_{a1} \right) \tag{5.3}$$

where $h_{c,a1}$ is the convective coefficient for sensible heat transfer between leaves and the ambient air, $Wm^{-2}\,{}^{o}C^{-1}$; ζ is the foliage density, i.e. leaf area per unit volume, $m^2\,m^{-3}$; and t_c is leaf temperature, ^{o}C. The sensible heat from leaves to air, q, is zero for the free space above the canopy since there are no leaves in the space. Foliage density can be expressed as

$$\zeta = \frac{\Lambda}{H_2} \tag{5.4}$$

where Λ is the leaf area index based on the normally projected canopy area on the floor and H_2 is the height of the canopy, m. The convective coefficient for sensible heat transfer between leaves and air, $h_{c,a1}$, was adopted after Seginer and Livne (1978), but the so-called 'shelter factor' was not used because the air velocities in the present study were locally measured velocity instead of that outside the canopy. The convective coefficient is calculated as

$$h_{c,a1} = 2\left[5.2\left(\frac{u}{\delta} \right)^{0.5} + 1.9\left(\frac{\left| t_c - t_{a1} \right|}{\delta} \right)^{0.25} \right] \tag{5.5}$$

where δ is the characteristic length of leaves, m; and u is the air velocity in the vicinity of leaves, $m\,s^{-1}$.

5.2.2 Water Vapor Conservation of Air

Since evaporation from ground is negligible, the only source of water vapor is plant transpiration. The conservation of water vapor is described as

$$u\frac{\partial \psi_{a1}}{\partial x} = \frac{\partial}{\partial z}\left(D_{eff}\frac{\partial \psi_{a1}}{\partial z} \right) + \frac{4D_{eff}}{W_1 W_2}\left(\psi_{a2} - \psi_{a1} \right) + q' \tag{5.6}$$

where ψ_{a1} is the water vapor concentration of AS-I, $kg\,m^{-3}$; D_{eff} is the effective water vapor

diffusivity, $m^2\ s^{-1}$; q' is the water vapor flux density from plant transpiration, kg $m^{-3}\ s^{-1}$.

Water vapor transfer for AS-II is similarly expressed as

$$u\frac{\partial \psi_{a2}}{\partial x}=\frac{\partial}{\partial z}\left(D_{eff}\frac{\partial \psi_{a2}}{\partial z}\right)+\frac{4D_{eff}}{\left(W_1-W_2\right)W_1}\left(\psi_{a1}-\psi_{a2}\right) \tag{5.7}$$

The water vapor transpired from leaves q' is

$$q'=h'_{c,a1}\cdot\zeta\left(\psi_c^*-\psi_{a1}\right) \tag{5.8}$$

where $h'_{c,a1}$ is the convective coefficient for water vapor transfer from leaves to the air in AS-I, m s^{-1}; ψ_c^* is the saturated water vapor concentration at leaf temperature, kg m^{-3}. The convective coefficient $h'_{c,a1}$ combines the stomatal resistance and the boundary layer resistance from leaf surface to the ambient air. It was calculated as

$$h'_{c,a}=\frac{2}{\frac{2\rho_a c_{p,a}}{h_{c,a1}}+r_s} \tag{5.9}$$

where r_s is stomatal resistance, s m^{-1}. Though r_s is regulated mainly by photosynthetically active radiation (PAR), a constant value (100 s m^{-1}) was used instead, since the current study focuses on noon when PAR is high. Stomatal resistance, r_s, should remain relatively constant at a minimum level under this condition.

Eddy diffusivity for heat, k_{eff}, and water vapor, D_{eff}, are not inherent properties of the fluid (air in this case) but rather properties of turbulent flow, therefore turbulence should be equally effective in enhancing the heat and water vapor transfers. Therefore the eddy water vapor diffusivity, D_{eff}, was calculated as

$$D_{eff}=D\frac{k_{eff}}{k} \tag{5.10}$$

where D is the diffusion coefficient of water vapor in air, 2.54×10^{-5} m^2 s^{-1} at 300K; and k is the thermal conductivity of air, 0.02623Wm^{-1} $^oC^{-1}$ at 300K (Lienhard IV and Lienhard V, 2004).

5.2.3 Heat Conservation of Canopy

The heat fluxes involving the canopy include the sensible heat, latent heat, thermal radiation and solar radiation. Neglecting the heat storage capacity of the canopy, the heat balance for a leaf of unit area is

$$\phi_{c,sw}+\phi_{c,lw}+h_{c,a1}\left(t_{a1}-t_c\right)-h_{c,a1}^{'}\left(\psi_c^{*}-\psi_{a1}\right)\lambda=0 \tag{5.11}$$

where $\phi_{c,sw}$ is the short wave radiation absorbed by unit leaf area, W m^{-2}; $\phi_{c,lw}$ is the net long wave radiation absorbed by unit leaf area, Wm^{-2}; and λ is the latent heat of water vaporization, taken as 2.5×10^6 J kg^{-1}.

The short wave and long wave radiation absorbed by a leaf depends on the location of the leaf within the canopy. It will be discussed in Section 5.3.1. Only total radiation absorbed by canopy is discussed here. The short wave radiation, $\phi_{c,sw}$, absorbed by the canopy is

$$\phi_{c,sw}=\left(a_{c,sw}+a_{c,sw}\rho_{f,sw}\tau_{c,sw}\right)\tau_{cv,sw}s_o \tag{5.12}$$

where $\alpha_{c,sw}$ is the short wave absorptivity of canopy, $\rho_{f,sw}$ is the short wave reflectivity of soil surface (0.25), $\tau_{c,sw}$ is the short wave transmissivity of canopy and $\tau_{cv,sw}$ is the short wave transmissivity of cover (0.69).

The long wave radiation, $\phi_{c,lw}$, absorbed by the canopy is

$$\begin{aligned}\phi_{c,lw}=&\phi_{sky,lw}\left(\alpha_{c,lw}+\alpha_{c,lw}\rho_{f,lw}\tau_{c,lw}\right)\\&+\varepsilon_{cv,lw}\sigma T_{cv}^4\left(\alpha_{c,lw}+\alpha_{c,lw}\rho_{f,lw}\tau_{c,lw}\right)\\&+\varepsilon_{f,lw}\sigma T_f^4\left(\alpha_{c,lw}+\alpha_{c,lw}\rho_{cv,lw}\tau_{c,lw}\right)\\&-2\varepsilon_{c,lw}\sigma T_c^4\end{aligned} \tag{5.13}$$

where $\phi_{sky,lw}$ is the downward long wave radiation from sky, Wm^{-2}; $\alpha_{c,lw}$ is the long wave absorptivity of canopy; $\rho_{f,lw}$ is the long wave reflectivity of floor (0.1); $\tau_{c,lw}$ is the long wave transmissivity of canopy; $\varepsilon_{cv,lw}$ is the long wave emissivity of cover (0.2); σ is the Stefan-Boltzman constant ($5.67\times10^{-8}Wm^{-2}K^{-4}$); $\varepsilon_{f,lw}$ is the long wave emissivity of floor (0.9); T_f is the absolute temperature of soil surface, K; $\varepsilon_{c,lw}$ is the long wave emissivity of canopy; and T_c is the absolute temperature of canopy, K.

The downward long wave radiation from sky, $\phi_{sky,lw}$, is calculated as (Swinbank, 1963)

$$\phi_{sky,lw} = \sigma\left[0.0552\left(T_o\right)^{1.5}\right]^4 \tag{5.14}$$

where T_o is the absolute temperature of outside, K. The procedure to calculate the transmissivity for short wave, $\tau_{c,sw}$, and long wave radiation, $\tau_{c,lw}$, of the canopy was after Willits (2003) and France and Thornley (1984).

5.3 Solution

Mathematically, the model is a set of partial differential equations and algebraic equations. To solve the partial differential equations, a finite difference method was adopted and Eqns 5.1, 5.2, 5.6, 5.7 and 5.11 were discretized and transformed into algebraic equations. The numerical algorithm was implemented with MATLAB (version 2006a).

5.3.1 Discretization

5.3.1.1 Discretization of Sensible Heat Conservation Equation of Air

The discretization scheme is shown in Fig.5.3. In the *x* direction, which is the airflow direction, the greenhouse space was divided into *n* slices. Vertically, the space was divided into *m* layers, so totally there were $n\times m$ elements (synonymous to cell, mesh).

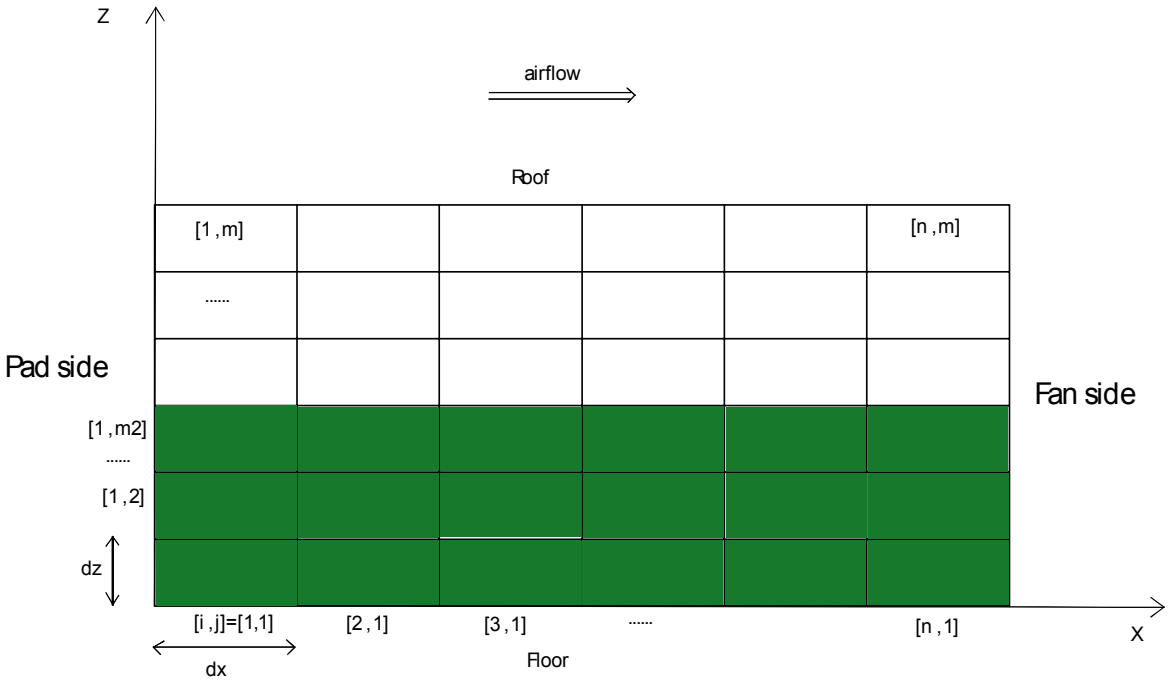

Figure 5.3 Discretization and mesh numbering

The sensible heat balance equation for AS-I, Eqn.5.1, was converted into a difference equation while substituting Eqn.5.3

$$u_j \rho_a C_{p,a} \frac{t_{a1}^{i,j} - t_{a1}^{i-1,j}}{dx} = \frac{k_{eff}^{j+1} \frac{t_{a1}^{i,j+1} - t_{a1}^{i,j}}{dz} - k_{eff}^{j} \frac{t_{a1}^{i,j} - t_{a1}^{i,j-1}}{dz}}{dz} + \frac{4k_{eff}^{j}}{W_1 W_2}\left(t_{a2}^{i,j} - t_{a1}^{i,j}\right) + h_{c,a}\zeta\left(t_c^{i,j} - t_{a1}^{i,j}\right) \quad (5.15)$$

where $t_{a1}^{i,j}$ represents the air temperature of element (i, j); k_{eff}^{j} is the effective thermal conductivity of air at the position of the element (i, j). Considering that k_{eff} depends on the velocity and the velocity was assumed independent of x, the following relationship was assumed

$$k_{eff}^{j} = a \cdot u_j^b \quad (5.16)$$

where u^j is the velocity at the height of j th elements; a and b are undetermined parameters.

Rearranging Eqn.5.15 gives

$$t_{a1}^{i,j}=\frac{u_j\rho_a C_{p,a}\dfrac{(dz)^2}{dx}t_{a1}^{i-1,j}+k_{eff}^{j+1}\cdot t_{a1}^{i,j+1}+k_{eff}^{j}\cdot t_{a1}^{i,j-1}+\dfrac{4k_{eff}^{j}(dz)^2}{W_1W_2}t_{a2}^{i,j}+h_{c,a1}\zeta(dz)^2 t_c^{i,j}}{u_j\rho_a C_{p,a}\dfrac{(dz)^2}{dx}+k_{eff}^{j+1}+k_{eff}^{j}+\dfrac{4k_{eff}^{j}(dz)^2}{W_1W_2}+h_{c,a}\zeta(dz)^2} \tag{5.17}$$

When the elements in the first slice (near the pad) were dealt with, the term $t_a^{i-1,j}$ in Eqn.5.17 was replaced with the inlet air temperature, t_{in}, since the left neighbor cells are outside air. If an element is in contact with cover or floor, the term corresponding to the air was replaced with the product of the convective coefficient and the temperature of the floor or cover. For instance, for an air element in contact with the cover and not immersed in the canopy, the difference equation for the element is

$$t_{a1}^{i,m}=\frac{u_m\rho_a C_{p,a}\dfrac{(dz)^2}{dx}t_{a1}^{i-1,m}+k_{eff}^{m}\cdot t_{a1}^{i,m-1}+h_{cv,a}dz\cdot t_{cv}^{i}}{u_m\rho_a C_{p,a}\dfrac{(dz)^2}{dx}+k_{eff}^{m}+h_{cv,a}dz} \tag{5.18}$$

where $h_{cv,a}$ is the convective coefficient between air and greenhouse cover, $Wm^{-2}\ {}^{o}C^{-1}$. Mathematically, the temperature of an air element is the weighted average of its neighboring elements.

For sensible heat of AS-II, the difference equation was derived from Eqn.5.2

$$t_{a2}^{i,j}=\frac{u_{2j}\rho_a C_{p,a}\dfrac{(dz)^2}{dx}t_{a2}^{i-1,j}+k_{eff}^{j+1}\cdot t_{a2}^{i,j+1}+k_{eff}^{j}\cdot t_{a2}^{i,j-1}+\dfrac{4k_{eff}^{j}(dz)^2}{(W_1-W_2)W_1}t_{a1}^{i,j}}{u_j\rho_a C_{p,a}\dfrac{(dz)^2}{dx}+k_{eff}^{j+1}+k_{eff}^{j}+\dfrac{4k_{eff}^{j}(dz)^2}{(W_1-W_2)W_1}} \tag{5.19}$$

5.3.1.2 Discretization of Water Vapor Conservation Equation of Air

The water vapor conservation equations were dealt with in the same fashion as the energy conservation equations. Substituting Eqn.5.8 into Eqn.5.6, discretizing and grouping similar terms yields the difference equation of water vapor for AS-I

$$\psi_a^{i,j} = \frac{u_j \frac{(dz)^2}{dx}\psi_a^{i-1,j} + D_{eff}^{j+1}\psi_a^{i,j+1} + D_{eff}^{j}\psi_a^{i,j-1} + \frac{4D_{eff}^{j}(dz)^2}{W_1 W_2}\psi_{a2}^{i,j} + h'_{c,a}\zeta(dz)^2\psi_c^{*i,j}}{u_j \frac{(dz)^2}{dx} + D_{eff}^{j+1} + D_{eff}^{j} + \frac{4D_{eff}^{j}(dz)^2}{W_1 W_2} + h'_{c,a}\zeta(dz)^2} \tag{5.20}$$

The last terms in the numerator and denominator of Eqn.5.20 vanish if no canopy element is involved. For the boundary elements that neighbor with the roof or floor, the terms that represent their upper or lower elements vanish, because the floor and roof were insulated boundaries relative to water vapor transfer. For the elements in the first slice near to the evaporative pad, the term $\psi_{a1}^{i-1,j}$ was replaced with the inlet vapor concentration, ψ_{in}.

For AS-II, the difference equation was derived similarly from Eqn.5.7

$$\psi_{a2}^{i,j} = \frac{u_{2j} \frac{(dz)^2}{dx}\psi_{a2}^{i-1,j} + D_{eff}^{j+1}\psi_{a2}^{i,j+1} + D_{eff}^{j}\psi_{a2}^{i,j-1} + \frac{4D_{eff}^{j}(dz)^2}{(W_1 - W_2)W_1}\psi_a^{i,j}}{u_{2j} \frac{(dz)^2}{dx} + D_{eff}^{j+1} + D_{eff}^{j} + \frac{4D_{eff}^{j}(dz)^2}{(W_1 - W_2)W_1}} \tag{5.21}$$

5.3.1.3 Discretization of Heat Conservation Equation of Canopy

The discretized form of the energy equation of canopy is

$$\phi_{c,sw}^{j} + \phi_{c,lw}^{i,j} + h_{c,a1}\left(t_{a1}^{i,j} - t_c^{i,j}\right) - h_{c,a1}^{'}\left(\psi_c^{*i,j} - \psi_{a1}^{i,j}\right)\lambda = 0 \tag{5.22}$$

where $\phi_{c,sw}^{j}$ is the net solar radiation absorbed by the *j*th canopy layer; and $\phi_{c,lw}^{j}$ is the net long wave radiation absorbed by the canopy element(*i*,*j*). The dependence of $\psi_c^{*i,j}$ on $t_c^{i,j}$ is nonlinear, so Eqn.5.22 is nonlinear with $t_c^{i,j}$ being the unknown variable. To simplify the algorithm and reduce computation time, the relationship between ψ^* and *t* was linearized as

$$\begin{aligned} \psi^*(t) &= a_1 \cdot t + a_2 \\ &= 0.00048761 \cdot t + 0.0053675 \end{aligned} \tag{5.23}$$

where a_1, a_2 are linear coefficients. This relationship was derived from a regression using the

data (dry bulb temperature vs. saturated water vapor concentration) produced by a psychrometric chart (Jian and Fang, 2002).

Applying Eqn.5.23 and arranging terms, Eqn.5.22 was transformed into a linear equation

$$t_c^{i,j} = \frac{\phi_{c,sw}^{j} + \phi_{c,lw}^{i,j} + h_{c,a1} t_{a1}^{i,j} + h_{c,a1}^{'} \lambda \left(\psi_{a1}^{i,j} - a_2 \right)}{h_{c1,a} + a_1 h_{c,a1}^{'} \lambda} \tag{5.24}$$

As mentioned above, the solar radiation absorbed by a leaf (or canopy element) depends on the location of the leaf in the canopy. Canopy layers of different heights should receive different amounts of solar radiation. Previous research (Goudriaan, 1977) has indicated that solar radiation intensity can be approximated as being attenuated exponentially with depth into the canopy, therefore the net solar radiation absorbed by various layers of canopy from bottom to top will be an algebraic series with a constant propagation ratio, i.e.

$$\phi_{c,sw}^{1} : \phi_{c,sw}^{2} : \phi_{c,sw}^{3} : \ \ldots \ : \phi_{c,sw}^{m_2} = 1 : c : c^2 : \ \ldots \ : c^{m_2} \tag{5.25}$$

where c is the propagation ratio. The propagation ratio depends on the extinction coefficient of canopy to solar radiation and canopy layer thickness

$$c = e^{k_{c,sw} \cdot dz} \tag{5.26}$$

where $k_{c,sw}$ is the canopy extinction coefficient to solar radiation with respect to penetration depth. It is related to the extinction coefficient with respect to Λ as follows

$$k_{c,sw} = k_{c,sw}^{'} \cdot \frac{\Lambda}{H_2} \tag{5.27}$$

where $k_{c,sw}^{'}$ is the extinction coefficient of canopy to solar radiation with respect to Λ (0.59) (Stanghellini and Jong, 1995).

As shown in Eqn.5.12, part of the net solar radiation absorbed by the canopy $\phi_{c,sw}$ is that reflected by the floor, which is $a_{c,sw}\rho_{f,sw}\tau_{c,sw}\tau_{cv,sw}s_o$. Its allocation among canopy layers follows the pattern of Eqn.5.25, but with a constant with a value of $1/c$. Due to the fact that the solar radiation reflected back from ground is insignificant compared with the downward solar radiation, it was treated in the same way as the incident solar from sky. The net solar radiation absorbed by each layer of canopy is

$$\phi_{c,sw}^{j} = \phi_{c,sw}\frac{c^{j-1}}{\frac{c^{m_2}-1}{c-1}}\frac{dz}{\zeta} \tag{5.28}$$

Long wave radiation was handled in the same manner as solar radiation. The propagation ratio, instead, is $c = e^{k_{c,lw}\cdot dz}$, where $k_{c,lw}$ is the extinction coefficient for long wave radiation with respect to penetration depth. It is related to extinction coefficient with respect to Λ by

$$k_{c,lw} = k'_{c,lw}\cdot\frac{\Lambda}{H_2} \tag{5.29}$$

where $k'_{c,lw}$ is the extinction coefficient for long wave radiation of canopy with respect to Λ, 0.80 (Stanghellini and Jong, 1995).

The air velocity, *u*, was measured *in situ* (refer to Chapter 4). In calculating k_{eff} for the terms describing the interactions between AS-I and AS-II, the average velocity of AS-I and AS-II was used.

5.3.2 Programs

Two MATLAB programs were written to handle the cases with and without canopy. When the canopy was included, all the equations listed above were used. To speed up the

convergence, the greenhouse space was discretized into a 12×12 mesh. When the canopy was not present, the energy equation for canopy and the term representing the interaction between AS-I and AS-II vanish. Only Eqns 5.1 and 5.6 were retained. The greenhouse space was refined into a 96×48 mesh for better resolution.

Six steps were executed in the following order: 1) all variables were defined; 2) values were assigned to the parameters; 3) state variables were initialized; 4) iteration was started. Air temperature, water vapor concentration and leaf temperature were updated with Eqns 5.17, 5.19, 5.20, 5.21 and 5.24. For the case without a canopy, air temperature and water vapor concentration were updated with Eqns. 5.17 and 5.20. The order of updating was from pad side to fan side, from floor to roof. Convergence criterion (the absolute differences of the air and leaf temperatures between two adjacent steps is less than 0.01 ^{o}C and that of water vapor is less than 0.001 kg m^{-3}) was checked after each iteration until it was met; 5) once convergence was reached, relative humidity was calculated based on air temperature and water vapor concentration for each element; 6) output simulation results. The two programs are included in Appendix I and J.

5.4 Calibration and Verification

Calibration data was measured in 2005 when sweet pepper plants were grown and in 2006 when no plants were grown. The plants grew from transplant seedlings to fully developed plants, resulting in different sizes of the canopy. The greenhouse was equipped with an evaporative pad. Two levels of ventilation rate (0.041 and 0.087 m^3 $m^{-2}s^{-1}$) were delivered, denoted as LV and HV respectively. Additional details on facilities, cultural practice and measurement can be found in Appendix A.

The model without canopy was calibrated and verified first. Four coefficients ($h_{f,a}$

$h_{cv,a}$ from Eqn.5.18, a and b from Eqn.5.16) were calibrated by minimizing the prediction error of vertical temperature variation. The resulting values of the parameters are listed in Table 5.1.

Table 5.1 Calibrated parameters

	LV, no pad	LV, pad	HV, no pad	HV, pad
$h_{f,a}$	19	30	10	18
$h_{cv,a}$	23	10	65	39
a	130	130	70	70
b	0.5	0.5	0.5	0.5

The model was verified with a different dataset from the one used in calibration. The comparison of the predictions and observations of air temperatures at five heights (see Chapter 4 for details) is listed in Table 5.2. The temperature variation, Δt, is the maximum of the five temperatures minus the minimum. The prediction error of air temperature was generally lower than 1^oC. The error in Δt was less than 1^oC. The model is considered accurate enough to predict the vertical distribution of air temperature, because the actual Δt is generally larger than 1^oC.

For the case with the canopy, the values of $h_{f,a}$, $h_{cv,a}$ and b were taken from Table 5.1. The value of parameter a was 10 for canopy, 40 for the interaction between AS-I and AS-II, 150 for the free space. Verification was accomplished with seven sets of data, possessing a wide range of canopy sizes. The results indicate that the absolute error of predicted air temperature was below 2 ^oC and that for Δt was below 1.4 ^oC. Relative humidity was overpredicted by about 10%. Leaf temperature was over-predicted most of time when the evaporative pad was used and under-predicted when the evaporative pad was not used.

Table 5.2 Comparison of observed and predicted air temperatures

		t_3	t_4	t_5	t_6	t_7	Δt
HV, pad	Obs.	30.4	29.3	28.5	29.3	32.3	3.7
	Pred.	30.7	28.6	27.9	28.7	31.2	3.3
	Error	0.3	-0.7	-0.6	-0.6	-1.1	-0.4
HV, no pad	Obs.	40.0	38.2	37.2	38.0	39.5	2.8
	Pred.	40.1	38.1	37.1	37.3	38.7	3.0
	Error	0.1	-0.1	-0.1	-0.7	-0.8	0.2
LV, pad	Obs.	36.9	37.2	37.8	40.6	43.6	8.4
	Pred.	34.9	35.4	37.2	39.9	44.1	9.2
	Error	-2.0	0.2	-0.6	-0.7	0.5	0.8
LV, no pad	Obs.	37.4	38.2	38.0	40.5	42.4	5.0
	Pred.	38.9	38.7	39.3	40.6	42.9	4.2
	Error	1.5	0.5	1.3	0.1	0.5	-0.8

Note: Δt is the maximum of t_3-t_7 minus the minimum; t_3-t_7 are the air temperatures measured at five heights

5.5 Simulations

5.1 Effects of Ventilation Rate and Evaporative Pad

To investigate the effects of ventilation rate and evaporative pad on the vertical temperature distribution, simulations were run with two ventilation rates (LV and HV), and with and without evaporative pad cooling. The outside dry bulb temperature was set to 32 ^{o}C. The inlet air temperature was set to 26 ^{o}C with evaporative pad cooling. Roof temperature was taken as 60 ^{o}C and ground temperature as 45 ^{o}C. The velocity profiles for LV and HV were those regressed from the observed data presented in Chapter 4.

The air temperature distributions for the four combinations of ventilation rate (HV and LV) and evaporative cooling (with and without) are shown in Figs 5.4 to 5.7. The figures show that evaporative pad cooling did not change the temperature distribution pattern significantly (compare Figs 5.4 with 5.5, Figs 5.6 with 5.7), however, increasing ventilation rate did (compare Figs 5.4 with 5.6, Figs 5.5 with 5.7). The temperature distributions with high ventilation rate were more symmetric along the horizontal centerline than with low

ventilation rate.

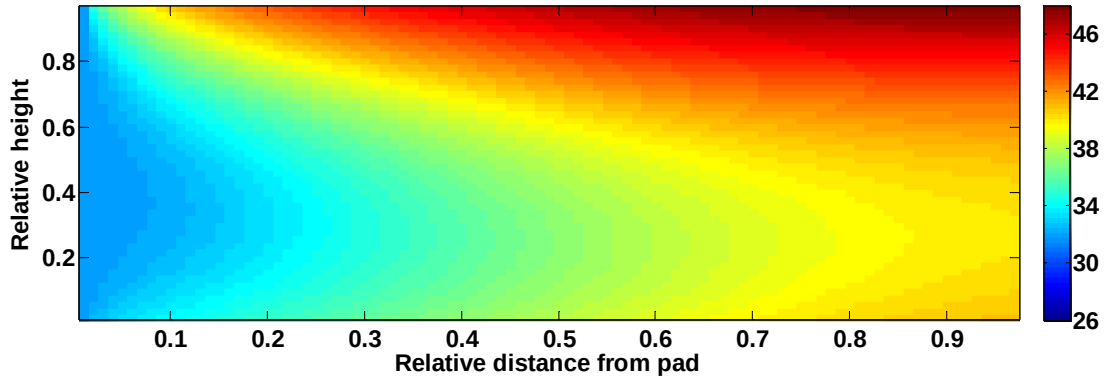

Figure 5.4 Temperature distributions for case of LV with evaporative pad off

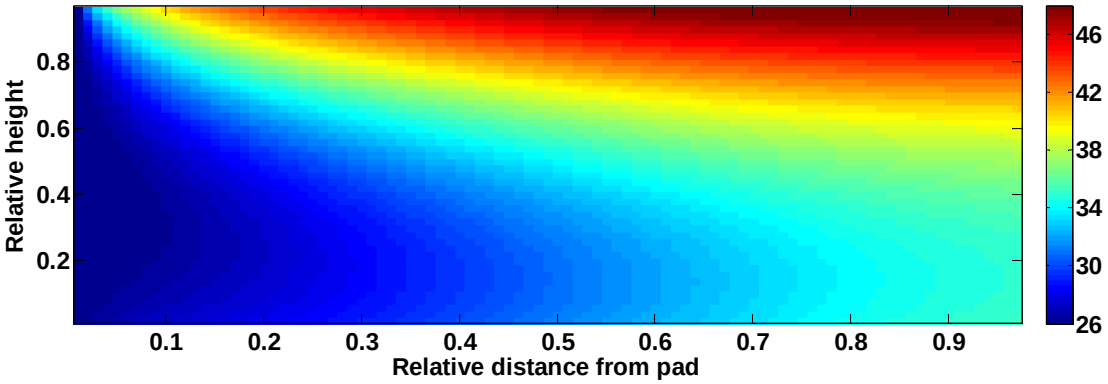

Figure 5.5 Temperature distributions for case of LV with evaporative pad on

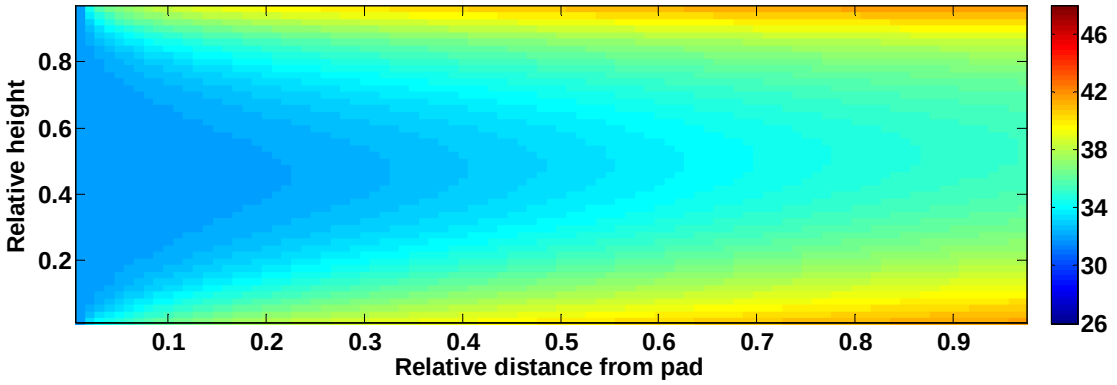

Figure 5.6 Temperature distributions for case of HV with evaporative pad off

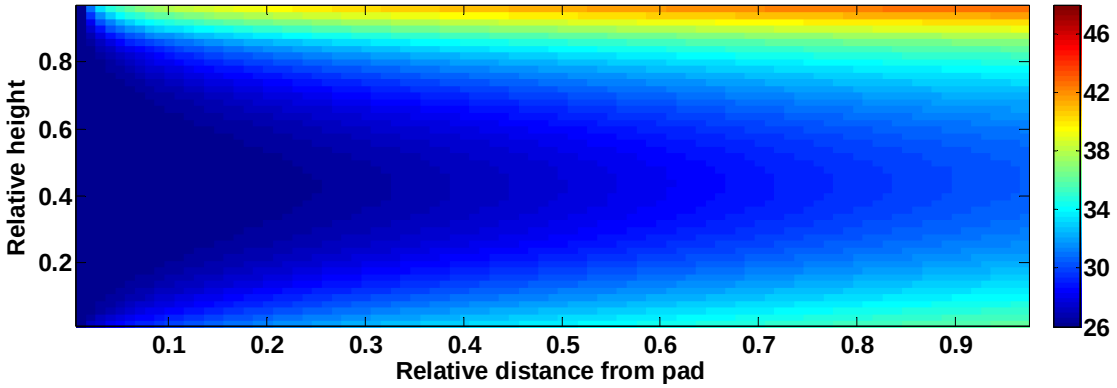

Figure 5.7 Temperature distributions for the case of HV with evaporative pad on

To get a better view of the effects of ventilation rate and evaporative pad cooling on vertical temperature distributions, the temperature profiles at the relative distance of 0.6 from the pad (x=0.6) are presented in Figs 5.8 and 5.9. Shown in Fig.5.8 is the effect of the evaporative pad on the vertical temperature distribution. A larger variation in air temperature was generated; the temperature reduction resulting from evaporative cooling was not uniform, particularly when ventilation rate was low. The temperature was reduced more at the lower part of the greenhouse than the upper part, suggesting the low part received more cooling.

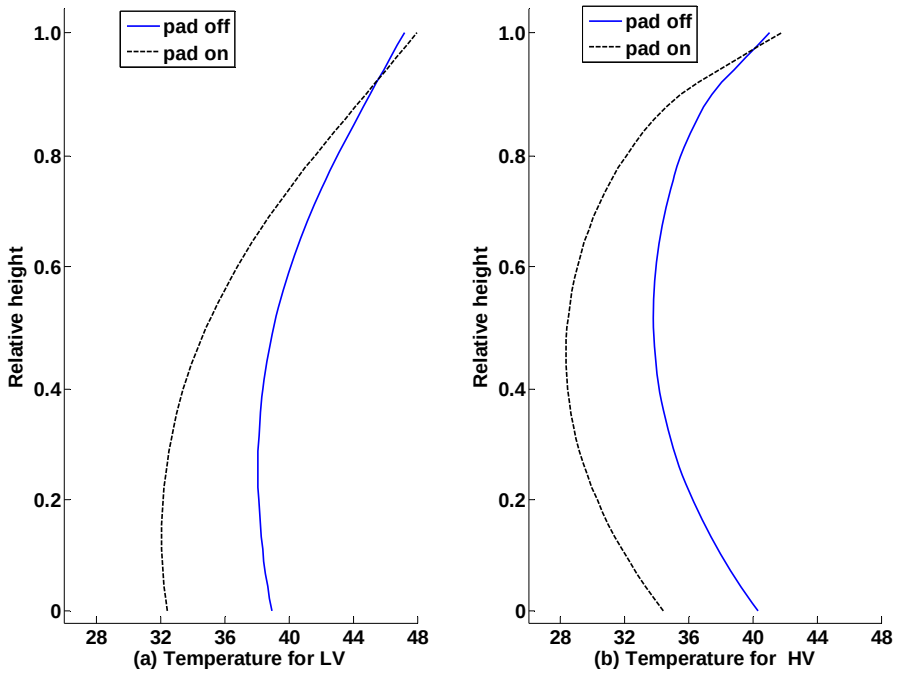

Figure 5.8 Effect of evaporative pad cooling on vertical temperature distribution: (a) vertical temperature distribution for LV; (b) vertical temperature distribution for HV.

The effect of ventilation rate is shown in Fig.5.9. The temperature reduction resulting from increasing ventilation rate was not uniform. The temperature was reduced more at the top of the greenhouse than the bottom. Figure 5.9 also shows that the temperature variation with HV was less than with LV by observing the peak and the lowest temperatures of each curve.

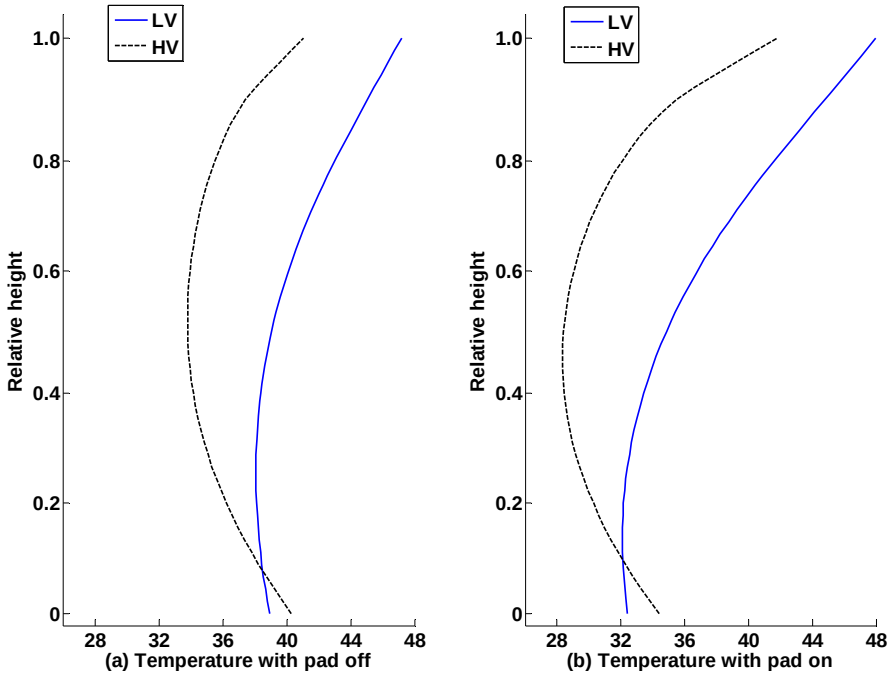

Figure 5.9 Effect of ventilation rate on the vertical temperature distribution: (a) with evaporative pad off; (b) with evaporative pad on.

To facilitate comparison, the temperature distributions of the four cases are presented in Fig.5.10. As expected, the case of HV+pad produced the lowest temperatures and the case LV+no pad produced the highest ones. By comparing the cases HV+no pad and LV+pad, it is interesting to note that the air temperature from LV+pad was cooler at the lower position, while the air temperature from HV+nopad was cooler in the upper part. The implication of such a pattern is that use of the evaporative pad and fewer fans should produce better cooling than more fans with no evaporative pad when plants are short and sparsely spaced. The commonly used control strategy in greenhouse cooling is to use the least number of fans for the lowest heat load. As the heat load increases, more fans are turned on. Evaporative pads will be typically turned on as the heat load approaches maximum. However, in light of the pattern described above, this may not be a good control strategy to handle intermediate heat loads.

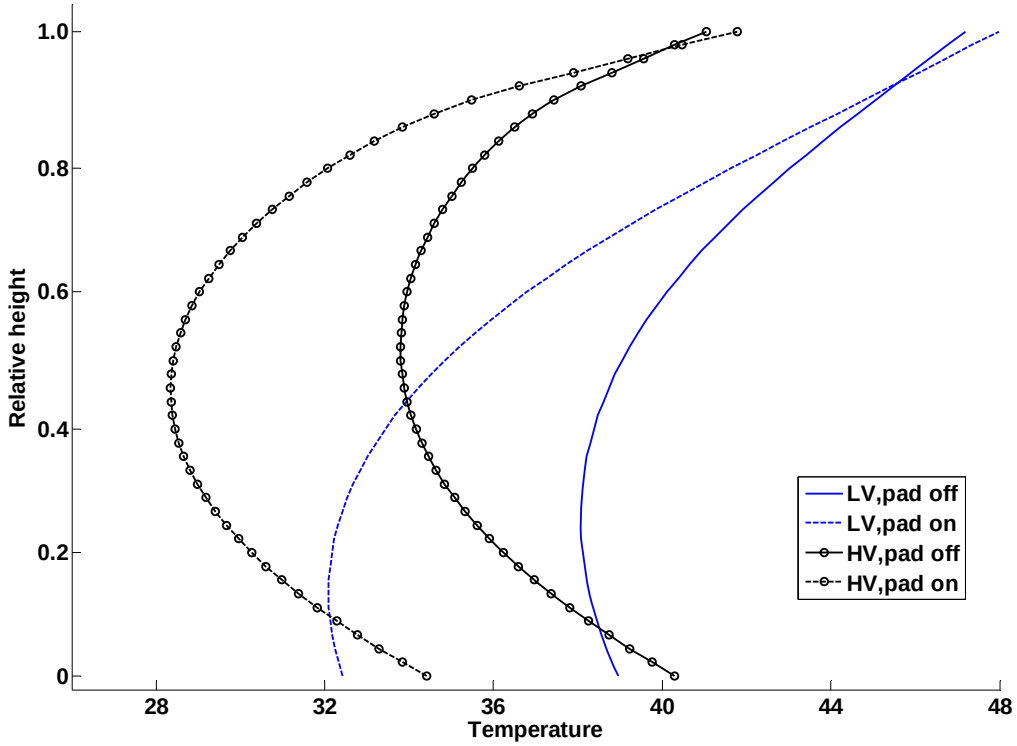

Figure 5.10 Vertical temperature distributions of the four combinations of evaporative cooling and ventilation rate

5.2 Effects of Canopy

Figures 5.11 to 5.13 show the predicted distributions of air temperature and relative humidity of AS-I, and leaf temperature. The calculation conditions were: leaf area index, A=3; canopy height, H_2=1.75 m; roof height, H_1=3.0 m; W_1=0.78 m; W_2=0.54 m; leaf characteristic length, δ=0.1 m; outside temperature, t_o=32°C; inlet air temperature, t_{in}=26°C; inlet water vapor concentration, ψ_{in}=0.0214 kg m^{-3}; and outside solar radiation s_o=720 W m^{-2}. Comparing Fig. 5.11 with Fig. 5.7 reveals that the distribution of air temperature changes remarkably with the canopy present. Figure 5.12 shows that the relative humidity within canopy was significantly higher than above canopy due, of course to plant transpiration.

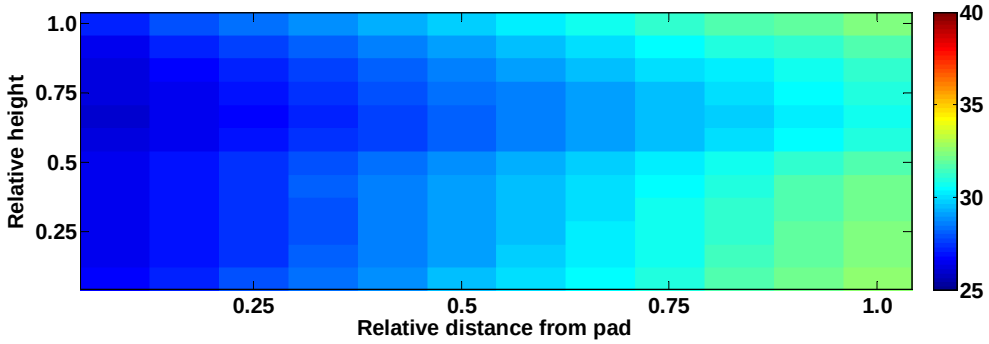

Figure 5.11 Air temperature distributions with canopy (HV, pad on)

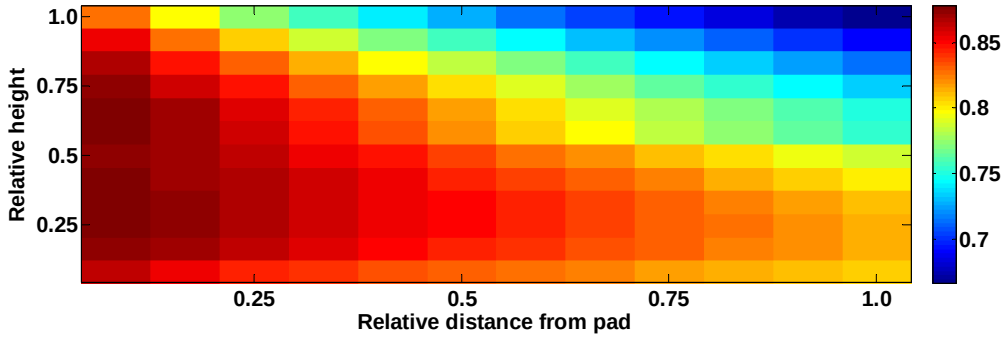

Figure 5.12 Relative humidity distributions with canopy (HV, pad on)

Leaf temperature, as shown in Fig.5.13, increases along the airflow direction. This result suggests that leaf temperature is generally lower at the bottom of canopy than the top. The reason is that the leaves at the top absorb more solar radiation than those at the bottom. Even though the higher solar radiation absorbed by the top canopy will be compensated by higher transpiration rates, thermal radiation and convection fluxes, these are not sufficient to completely offset the difference in solar radiation and the heat balance is established by increasing leaf temperature at the top of canopy.

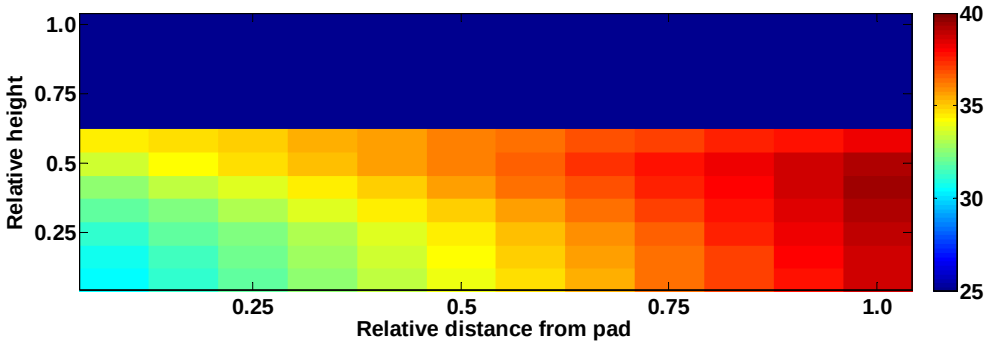

Figure 5.13 Leaf temperature distributions with canopy (HV, pad on). The blue area represents the free space above the canopy.

The effect of canopy on the vertical temperature distribution is shown in Fig.5.14. These results were extracted from Figs. 5.7 and 5.11 at x=0.6 (six tenths of the greenhouse length down from the pad). The temperature exhibits much less variation with the canopy than without. One explanation for less temperature variation is that canopy functions like a flow diffuser. The airflow straightened by a diffuser is more uniform and a uniform airflow tends to result in uniform air temperature. In addition, the presence of plant material restricts the turbulent heat diffusion within the canopy, thus the vertical heat flux decreases and so does the temperature gradient. Transpiration may also play an important role in affecting temperature distribution, but future study will be required to determine the specific mechanism involved. Note in Fig. 5.14 that for a short segment below the top of canopy, air temperature was slightly higher with the canopy than without. This is because the air velocity was reduced by the canopy and the leaf temperature was relatively high at the top.

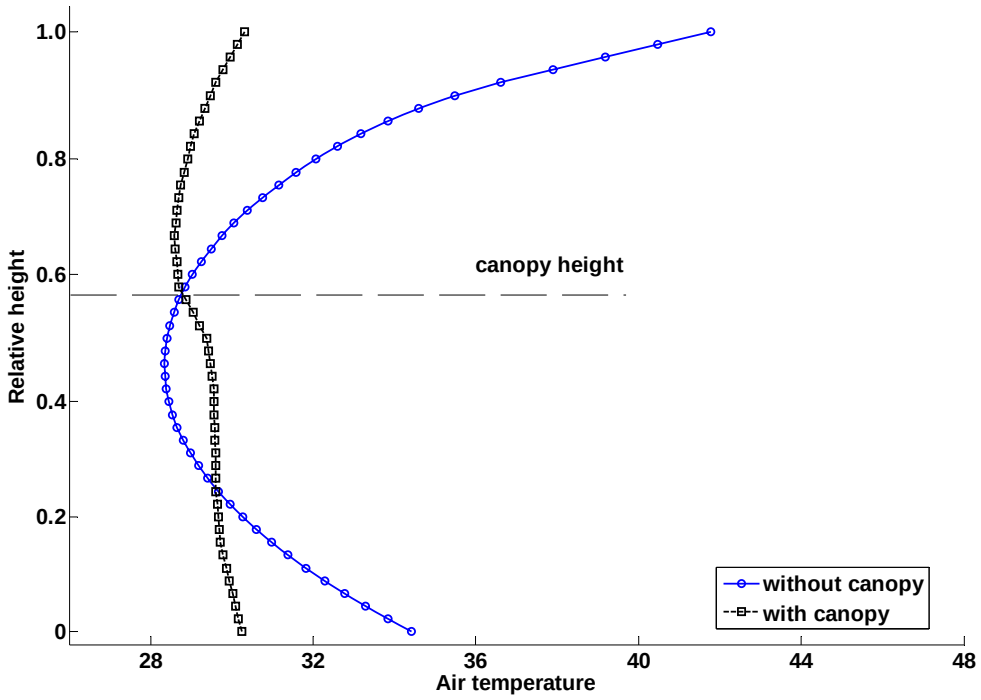

Figure 5.14 Vertical air temperature distributions with and without canopy

5.6 Conclusions

A thermal model was developed to describe the temperature distribution in the vertical and the horizontal directions in fan-ventilated greenhouses. The model was calibrated and verified with a wide range of canopy sizes and ventilation rates. Evaporative pad cooling was also investigated as a factor. The model was shown to be sufficiently accurate in predicting vertical air temperature distribution. Simulations with the model suggest the following: 1) increasing ventilation rate will result in lower vertical air temperature variation; 2) air temperature is reduced more at the upper part of greenhouse than at the lower part when ventilation rate increases; 3) using evaporative pad cooling produces larger vertical temperature variations; 4) air temperature is reduced more at the lower part of greenhouse than at the upper part with evaporative pad cooling; and 5) presence of a canopy reduces the

vertical air temperature variation, suggesting that a greenhouse occupied by fully developed plants will have less vertical temperature variation than a greenhouse with sparsely spaced small plants.

Though the preliminary verification of the model was satisfactory, the model has some limitations that need to be improved. One of them is that the velocity used by the model was taken from measurements. This will limit the predictive ability when dealing with different canopy configurations (for instance, canopy rows perpendicular to airflow). In the present model, it was assumed that the vertical velocity profile does not change along the airflow direction. This may be reasonable for long greenhouses, but not for short ones, because velocity profiles at the entry or outlet are different from the center. The prediction error for leaf temperature was larger then expected, though it is considered acceptable for the current study since air temperature is the main focus.

Nomenclature

a	undetermined parameter
a_1	linear coefficient
a_2	linear coefficient
b	undetermined parameters
$c_{p,a}$	specific heat of air, J kg^{-1} $^oC^{-1}$
D	diffusion coefficient of vapor in air, m^2 s^{-1}
D_{eff}	effective water vapor diffusivity, m^2 s^{-1}
$h_{c,a1}$	convective coefficient for sensible heat transfer between leave and air, W m^{-2} $^oC^{-1}$
$h'_{c,a1}$	convective coefficient for water vapor transfer between leaves and ambient air, ms^{-1}
$h_{cv,a}$	convective coefficient between greenhouse cover and inside air, W m^{-2} $^oC^{-1}$
$h_{f,a}$	convective coefficient between greenhouse floor and inside air, W m^{-2} $^oC^{-1}$
H_1	height of greenhouse, m

H_2 height of canopy, m

k thermal conductivity of air, W m^{-1} $^oC^{-1}$

k_{eff} effective thermal conductivity, W m^{-1} $^oC^{-1}$

k_{eff}^j effective thermal conductivity of air at the height of the jth element, W m^{-1} $^oC^{-1}$

$k_{c,sw}^{'}$ extinction coefficient of canopy to solar radiation with respect to Λ

$k_{c,lw}$ extinction coefficient for long wave radiation with respect to penetration depth, m^{-1}

$k_{c,lw}^{'}$ extinction coefficient for long wave radiation of canopy with respect to Λ

q sensible heat flux from plant leaves, W m^{-3}

q' water vapor flux from plant, kg $m^{-3}s^{-1}$

r_s stomatal resistance, s m^{-1}

t_c leaf temperature, ^oC

t_a air temperature, ^oC

$t_a^{i,j}$ air temperature of element (i, j)

t_i air temperature measured at the location of the ith aspirated station, ^oC

T_c absolute temperature of canopy, K

T_f absolute temperature of floor, K

T_o absolute temperature of outside, K

u horizontal airflow speed, m s^{-1}

u^j velocity at the height of jth elements, m s^{-1}

x distance from pad, m

z distance from floor, m

Abbreviations

HV low ventilation rate, 0.087 m^3 m^{-2} s^{-1}

LV low ventilation rate, 0.041 m^3 m^{-2} s^{-1}

Greek symbols

$\alpha_{c,sw}$ short wave absorptivity of canopy

$\alpha_{c,lw}$ long wave absorptivity of canopy

δ characteristic length of leaves, m

Δt vertical temperature variation, ^oC

$\varepsilon_{cv,lw}$ long wave emissivity of greenhouse cover

$\varepsilon_{f,lw}$ long wave emissivity of floor

$\varepsilon_{c,lw}$ long wave emissivity of canopy

λ latent heat of water vaporization, J kg^{-1}

Λ leaf area index on the basis of projected canopy area

ζ foliage density, m^2 m^{-3}

ρ_a air density, kg m^{-3}

$\rho_{f,sw}$ short wave reflectivity of floor

$\rho_{f,lw}$ long wave reflectivity of floor

σ Stefan-Boltzman constant, W m^{-2} K^{-4}

$\tau_{c,sw}$ short wave transmissivity of canopy

$\tau_{c,lw}$ long wave transmissivity of canopy

$\tau_{cv,sw}$ short wave transmissivity of cover

$\phi_{c,sw}$ short wave radiation absorbed by unit leaf area, Wm^{-2}

$\phi_{c,lw}$ net long wave radiation absorbed by unit leaf area, Wm^{-2}

$\phi_{sky,lw}$ downward long wave radiation from sky, Wm^{-2}

$\phi^j_{c,sw}$ net solar radiation absorbed by the jth canopy layer

ψ_a water vapor concentration, kg m^{-3}

ψ^*_c saturated vapor concentration at t_c, kg m^{-3}

References

ASAE. 2003. Heating, ventilating and cooling greenhouses. ANSI/ASAE EP406.2. American Society of Agricultural Engineers, St. Joseph, MI

Cengel, Y. A. 2003. Heat transfer: a practical approach. McGraw-Hill, Boston Burr Ridge, IL

France J; Thornley J.H.M. 1984. Mathematical Models in Agriculture. Butterworth & Co., Ltd., London, UK

Goudriaan, J. 1977. Crop micrometeorology: a simulation study. Center for Agricultural Publishing and Documentation, Wageningen, Netherlands

Lienhard J.H. IV; Lienhard J.H V. 2004. A heat transfer textbook. Phlogston Press. Cambridge, MA

Jian, Z.; Fang, W. 2002. Digital psychrometric chart. Dept. of Bio-industrial mechatronics Engineering, National Taiwan University, Taiwan

Kittas, C.; Bartzanas, T.; Jaffrin, A. 2003. Temperature gradients in a partially shaded large greenhouse equipped with evaporative cooling pads. *Biosystems Engineering*, 85(1): 87-94

Kreith, F.; Bohn, M.S. 2001. Principles of heat transfer. Brooks/Cole Pub, Pacific Grove, CA

Seginer, I; Livne, A. 1978. Effect of ceiling height on the power requirement of forced ventilation in greenhouses. *Acta Horticulturae*, 87: 51-68

Stanghellini, C; Jong T de. 1995. A model of humidity and its applications in a greenhouse. *Agricultural and Forestry Meteorology*, 76: 129-148

Swinbank, W.C. 1963. Long-wave radiation from clear skies. Quarterly Journal of the Royal Meteorological Society, 89(381): 339-348

Willits, D.H. 2003. Cooling fan ventilated greenhouses: a modeling study. *Biosystems Engineering*, 84(3): 315– 329

Yang, X.; Short, T.H.; Fox, R.D. *et al*. 1990a. Dynamic modeling of the microclimate of a greenhouse cucumber row-crop: Part I. Theoretical model. *Transactions of the ASAE*, 33(5): 1701-1709

Yang, X.; Short, T.H.; Fox, R.D. *et al*. 1990b. Dynamic modeling of the microclimate of a greenhouse cucumber row-crop: Part II. Validation and simulation. *Transactions of the ASAE*, 33(5): 1710-1716

Chapter 6 Environmental Comparison of Naturally Ventilated and Fan-Ventilated Greenhouses

Abstract A comparison was made of the environment in naturally ventilated (NV) and fan-ventilated (FV) greenhouses. Re-examination of the experimental data from previous studies showed that the air temperature in the FV greenhouses was less uniform than in the NV greenhouses. Neverthless, the air temperature in the FV greenhouses experienced less variation with time. Leaf temperature in the NV greenhouses was lower than air temperature, regardless of whether low-pressure fog was used or not. On the other hand, leaf temperature in the FV house was higher than air temperature when the evaporative pads were used and lower when the evaporative pad was not used. High-pressure fog in the NV greenhouse was as effective in reducing air temperature as the evaporative pad in the FV greenhouse; however, high-pressure fog produced higher relative humidity in the NV house.

6.1 Introduction

Fan ventilation (FV) and natual ventilation (NV) are two modes of ventilation in greenhouses. Fan ventilation depends on fans while natural ventilation relies on wind and/or buoyancy for exchanging air between inside and outside. Ventilation provided by FV is constant and airflows in FV houses are generally regular while ventilation provided by NV is unstable and airflows in NV houses are complex. Since the environment inside a ventilated space is affected by airflow, inside environment in FV and NV houses will be different due to different airflows. Identifying these differences in environment inside FV and NV houses will help to determine the advantages and disadvantages of the two types of ventilation.

In a three-year study carried out at NC State University between 2003 and 2005, the comparative performance of FV and NV houses was examined. The inside air temperature, relative humidity and leaf temperature were compared (Willits and Li, 2005; Willits *et al.*,

2006a).

The data from that study were reexamined in this study. The spatial and temporal variations of air temperatures and leaf-air temperature difference were compared for the FV and NV houses. In a follow-up experiment conducted in 2006, the performance of NV with high-pressure fog was compared with FV with evaporative pad cooling.

6.2 Materials and Methods

6.2.1 Structures and Facilities

Greenhouse Structure

Four double-polyethylene covered greenhouses were used throughout the study, two of which were fan-ventilated (FV1 and FV2) and two of which were naturally ventilated (NV1 and NV2). Their layout is shown in Fig. 6.1. These houses were located in Raleigh, North Carolina (35^{o}47′N; 78^{o}39′W) on the campus of North Carolina State University. The FV greenhouses were Quonset style, 6.7 by 12.1 m with a ridge height of 2.92 m. The ridges were oriented along a north-south axis. Evaporative pads were installed in the north walls and exhaust fans were situated in the south walls. The evaporative pads were sized for a face velocity of 1.27 m s^{-1} at the maximum ventilation rate of 0.087 m^3 m^{-2} s^{-1}. Details can be found in Appendix A.

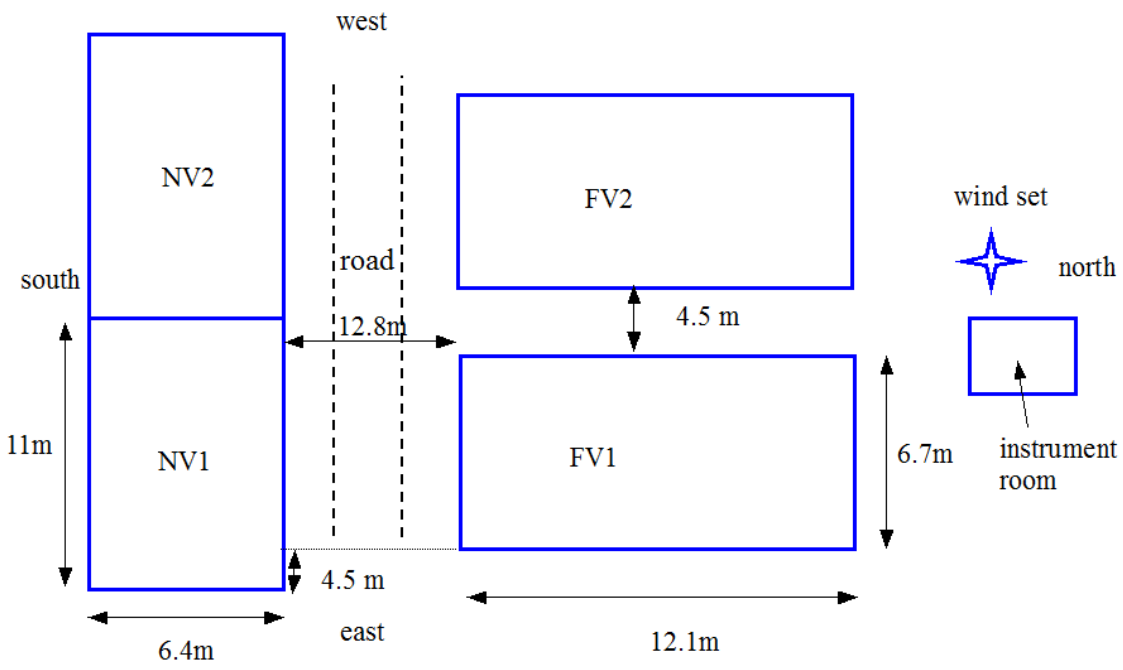

Figure 6.1 Layout of four greenhouses. Two were fan-ventilated (FV1 and FV2) and two were naturally ventilated (NV1 and NV2)

The NV greenhouses were freestanding, gutter-connected style, 6.4 by 11 m. The gutter height was 3.45 m; the ridge height was 5.36m. A double-polyethylene wall separated the NV greenhouses. The NV greenhouses were oriented along an east-west axis. Continous vents were fitted on the south, top and north sides. The vents were switched between three configurations: ‘s’, ‘s+t’ and ‘s+t+n’, representing south vent only; south plus top vents; and south plus top plus north vents open respectively. Details are shown in Appendix A.

Fogging Systems in NV greenhouses

During 2003, twelve low-pressure fogging nozzles (0.012 dia, Arizona Mist) were installed in each NV house to provide evaporative cooling. They were located above the gutter line. The spray rate of nozzles was about 1.9 liter per hour at line pressure (3-4 atm).

During 2004, a new low-pressure fogging system was installed in each of the NV greenhouses. The system consisted of 24 non-dripping nozzles (3.79 liter per hour, DIG

Corporation), configured in three rows along the ridge direction, with eight nozzles in each row. The two side rows and the mid-row were controlled separately, thus three levels of fogging were available. This allowed eight, 16 or 24 nozzles to be used at any given time. During 2005, a booster pump was added to the low-pressure fogging systems maintaining the pressure at 4 atm.

In September of 2005, a high-pressure fogging system was installed in NV1. The high-pressure fogging system utilized 24 spray nozzles (item #00002, Ecologic Technologies, Inc.) installed at the height of 2.36m. The nominal spray rate of the nozzles was 5.49 liter per hour. A high-pressure pump (FOGCO System Inc.) was used to boost the line pressure to 68 atm. Two levels of fogging were configured, each with 12 nozzles. This system was used in 2006 again and its performance was evaluated and compared with the evaporative pad in FV1.

All fogging systems were controlled on the basis of 15-second intervals. The control was similar to that of multi-stage thermostats (Appendix A). Temperature set points were adjusted by trial and error to maximize cooling while avoiding excessive wetting of plants.

6.2.2 Plants

During 2003, tomato plants (*Lycopersicon esculentum L.*) were grown in FV1 and NV2 and the other two houses were kept empty. FV1 was planted with 208 tomato plants. The plants were distributed in 8 rows parallel with the airflow, with 26 plants each. NV2 was planted with 182 tomato plants. The plants were distributed in 14 rows normal to greenhouse ridge, with 13 plants each. During 2004, tomatoes were grown in all the four houses. The crop configurations were same as 2004. During 2005, sweet peppers (*Capsicum annuum*) were grown in all houses, with the same crop configurations as 2004. No plants were grown

in 2006.

6.2.3 Measurements

Air temperatures and relative humidities were measured using aspirated enclosures containing one type-T thermocouples and one relative humidity sensor. The number and locations of the aspirated enclosures and humidity sensor model varied from year to year (Appendix A). Most aspirated enclosures were placed below the heights of fully developed plants for monitoring potential canopy area. Leaf temperatures were measured using fine gauge type-K thermocouples glued to the underside of leaves (Willits *et al*., 2006b). Eighteen leaves on six selected plants in each house were monitored. Outside weather, i.e. dry bulb and wet bulb temperatures, solar radiation, wind speed and direction were monitored by a weather station. All data were recorded as 10-minute averages of 1-min readings.

6.2.4 Data Processing

The data presented in this study were confined to the period when high cooling controls were applied in both NV and FV greenhouses. The high cooling control in NV houses represents the vent configuration of 's+t+n' or 's+t' and that in FV houses represents the maximum ventilation rate.

Spatial variation of air temperature was represented by the differences between the maximum and minimum temperature readings of the sensors that were located within the potential canopy regions. The temperature differences were then averaged over the high cooling period for each day.

To derive temporal variation of air temperature, the readings from all sensors within the potential canopy regions were averaged, then the minimum temperature during the high cooling period was subtracted from the maximum temperature.

In comparing air and leaf temperatures, the air temperatures measured in potential canopy areas and all the leaf temperatures were averaged.

6.3 Results and Discussion

6.3.1 Spatial variation of air temperature

The spatial variations of air temperatures for the two pairs of FV and NV houses in 2005 are presented in Figs 6.2 and 6.3. The spatial variation averaged over the experimental season for FV1 and NV1 were 2.4 ^{o}C and 1.4 ^{o}C, respectively. Those for FV2 and NV2 were 3.1 ^{o}C and 1.3 ^{o}C, respectively. This suggests that the air temperature in the FV houses was less uniform than the NV houses. The data from 2004 (not presented here) suggest the same pattern as in 2005. This disparity in spatial variation of air temperature could possibly be attributed to the different airflow patterns in the FV and NV houses. The airflow in FV houses was relatively regular and steady, which tended to create stratified temperatures. On the other hand, the airflow in NV houses was irregular, and thus better stirred and mixed, resulting in relatively uniform temperatures.

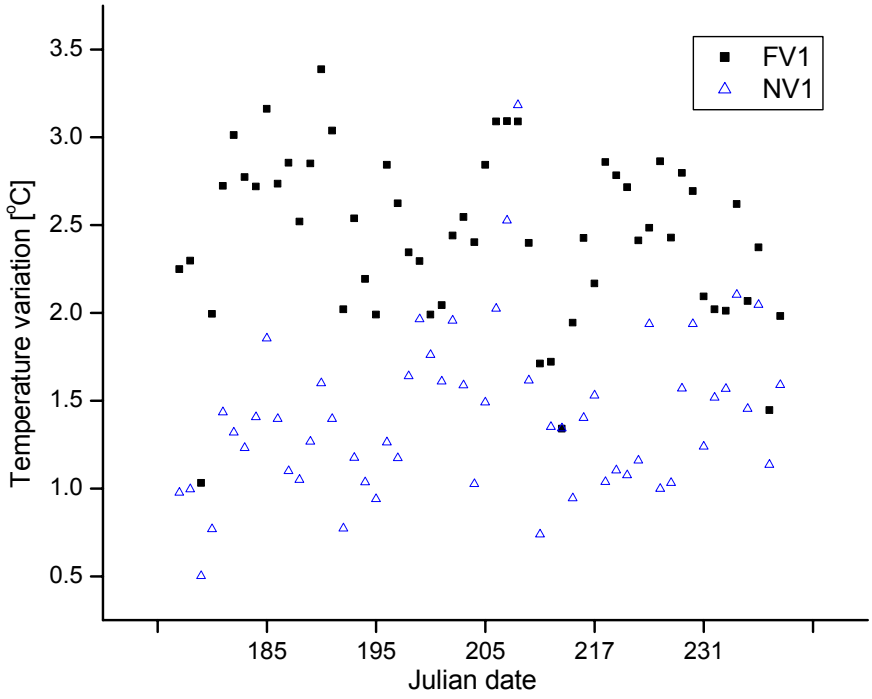

Figure 6.2 Spatial variation of air temperatures in FV 1 and NV1. Data points were the maximum temperature reading minus the minimum and then averaged on daily basis.

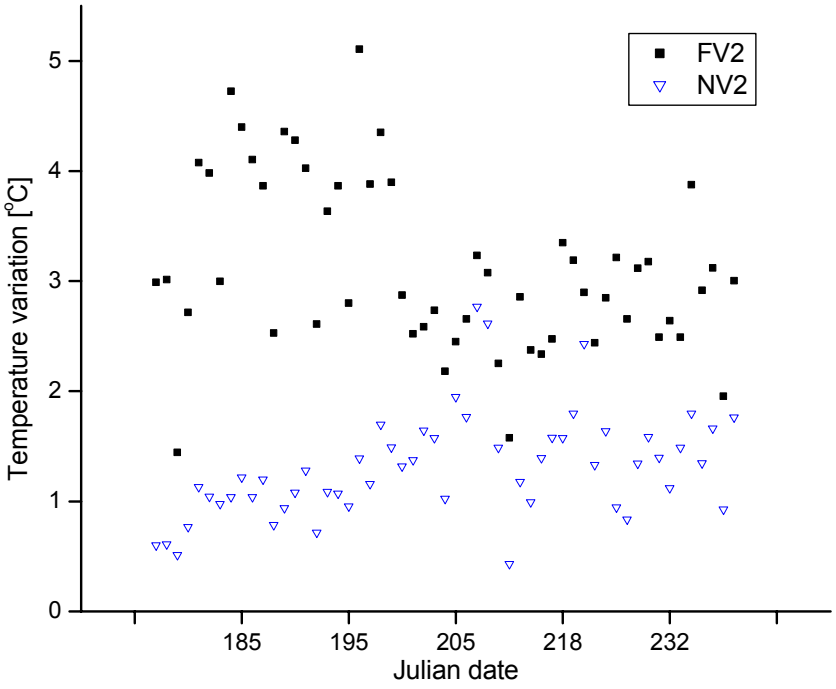

Figure 6.3 Spatial variation of air temperatures in FV 2 and NV 2. Data points were the maximum temperature reading minus the minimum and then averaged on daily basis.

6.3.2 Temporal variation of air temperature

The temporal variations of air temperatures for the two pairs of FV and NV houses in 2005 are presented in Figs 6.4 and 6.5. The temporal variation averaged over the season in FV1 and NV1 were 4.6 and 6.5 ^{o}C, respectively. Those in FV2 and NV2 were 4.6 and 7.0 ^{o}C, respectively. NV2 had higher temporal variation than NV1 likely due to the special vent configuration treatment ('s+t' vents only) periodically imposed (see Appendix A for details). It is suggested that air temperatures in the NV houses experienced greater variation than the FV houses under the same weather conditions. It is reasonable considering the ventilation rates in the NV houses depended on outside wind speed and direction, which changed rapidly, while the ventilation rates in the FV houses remained essentially unchanged.

If inside-outside temperature differences were processed in the same manner as the inside temperatures, the pattern was reversed as opposed to that in Figs 6.4 and 6.5, i.e. greater variation of inside-outside-temperature-difference occurred in FV houses than NV houses. This is because the inside temperatures of the NV houses followed the outside temperature more closely than those in the FV houses. This agrees with the general perception that the air temperatures in the FV houses are less dependent on outside weather than in the NV houses. In other words, the FV houses had more control over the air temperatures, as compared with NV houses.

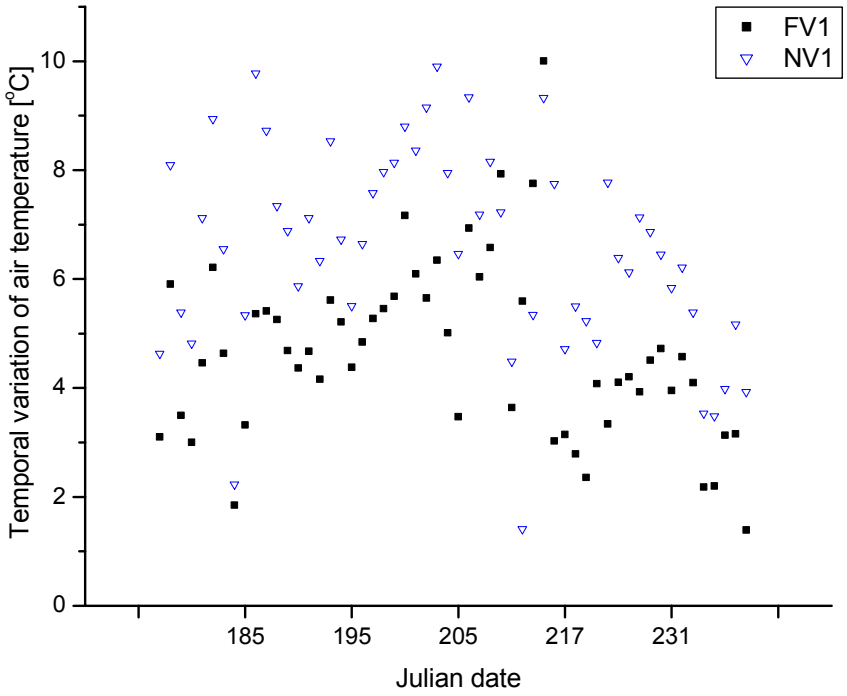

Figure 6.4 Temporal variation of air temperatures in FV1 and NV1. Data points were the maximum average temperature minus the minimum average temperature on daily basis.

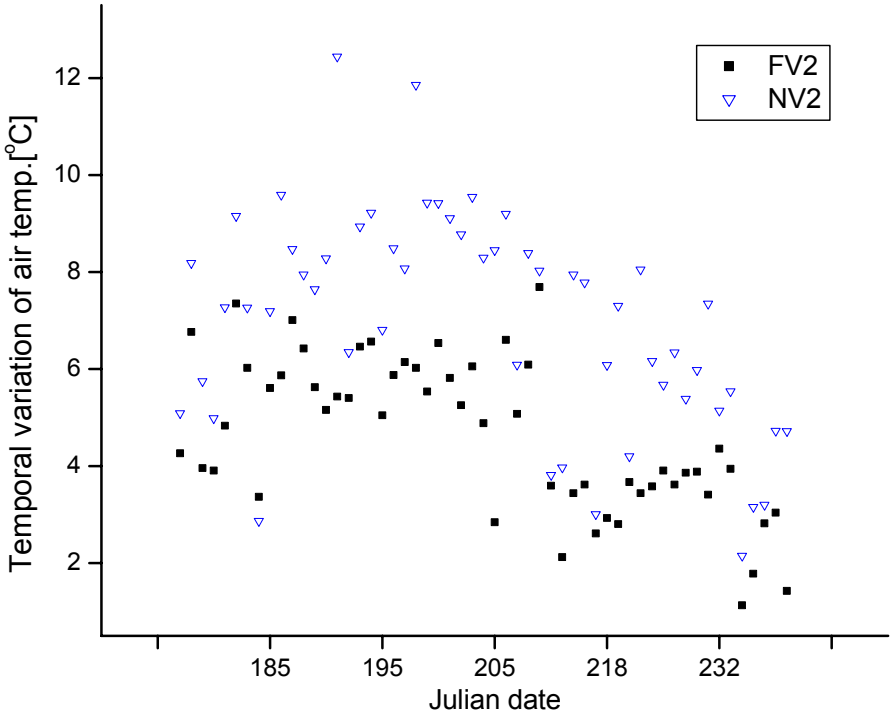

Figure 6.5 Temporal variation of air temperatures in FV2 and NV2. Data points were the maximum average temperature minus the minimum average temperature on daily basis.

6.3.3 Leaf-air-temperature difference

Figures 6.6 and 6.7 show the leaf-air temperature differences of FV1 and NV2 respectively, where tomatoes were grown in 2003. Figure 6.6 shows that with the evaporative pad on, the leaf-air temperature differences were positive in most cases, i.e. the leaf temperatures were higher than the air. When the evaporative pad was off, the leaf-air temperature differences were negative. Figure 6.7 shows that the leaf-air temperature differences were mostly negative with natural ventilation. The low-pressure fog did not change the signs of the leaf-air temperature differences. Neverthless, high-pressure fog did reverse the relative significance of air and leaf temperatures, as suggested by the experimental data from Li *et al*. (2006).

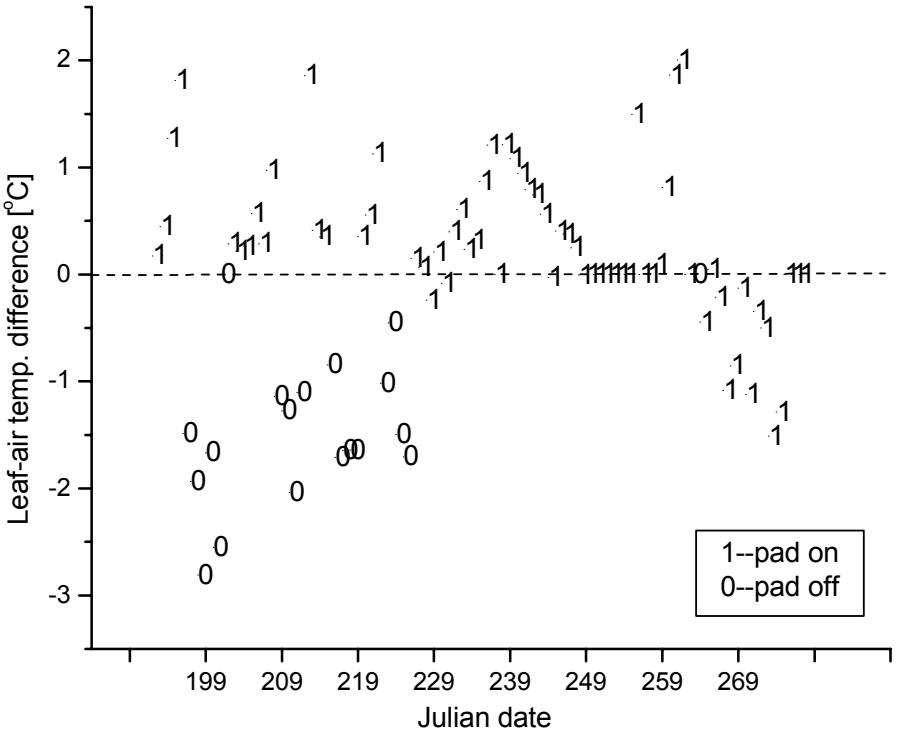

Figure 6.6 Leaf-air temperature differences in FV1 in 2003

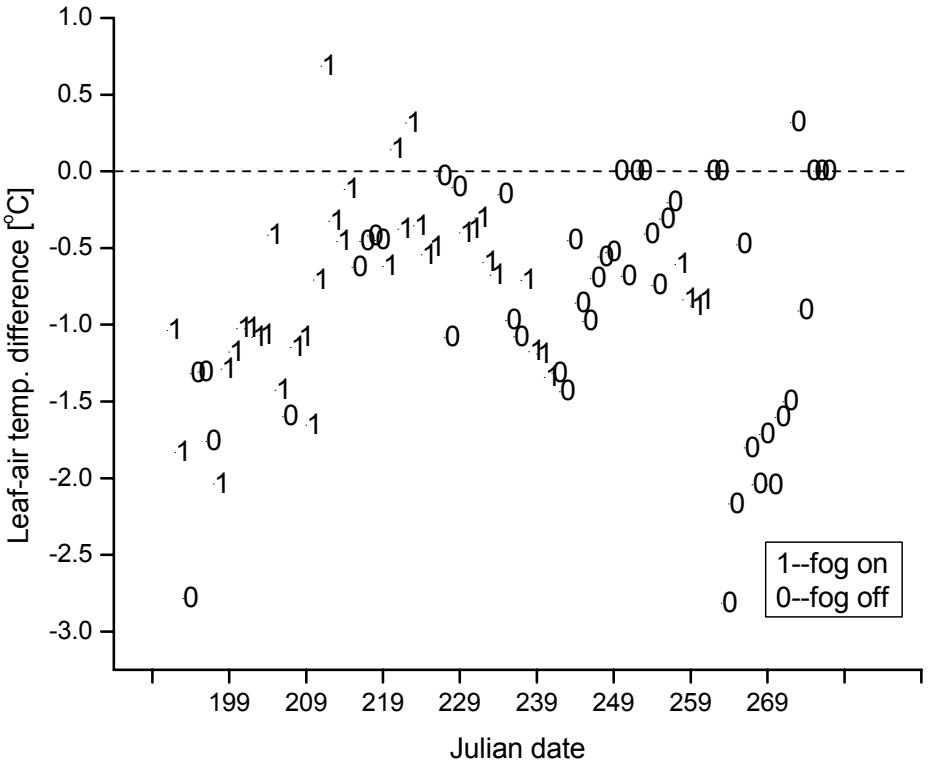

Figure 6.7 Leaf-air temperature differences in NV2 in 2003

Additional data from 2005 are presented in Figs 6.8 and 6.9 to corroborate the patterns observed above. Low-pressure fog was used in the NV houses and evaporative pads were used in the FV houses. Figure 6.8 shows the leaf-air temperature differences in FV1 and NV1. Those of FV1 were positive most of time while those of NV1 were negative almost exclusively.

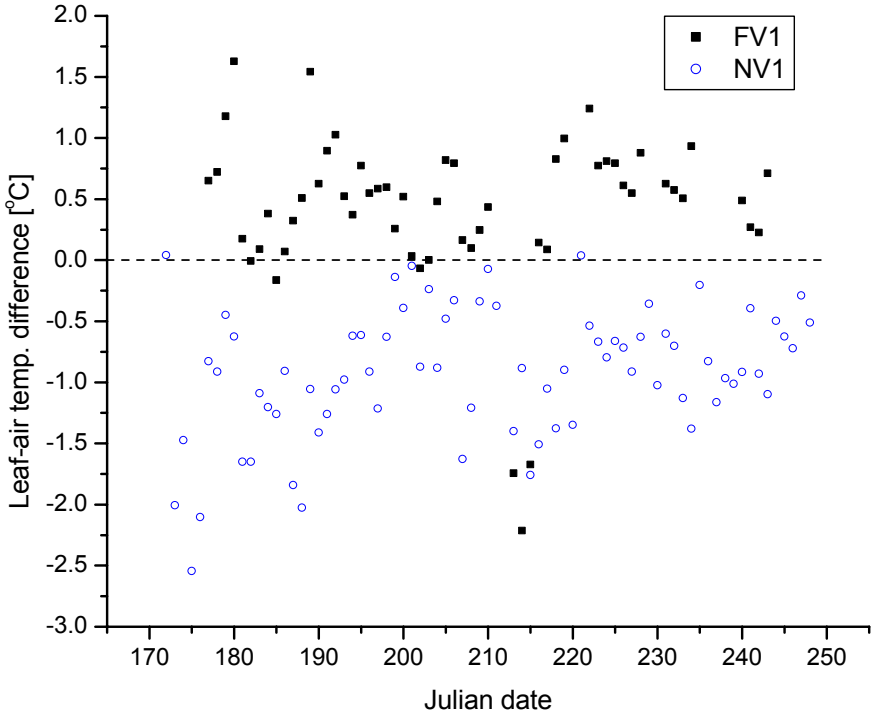

Figure 6.8 Leaf-air temperature differences in FV1 and NV1 in 2005

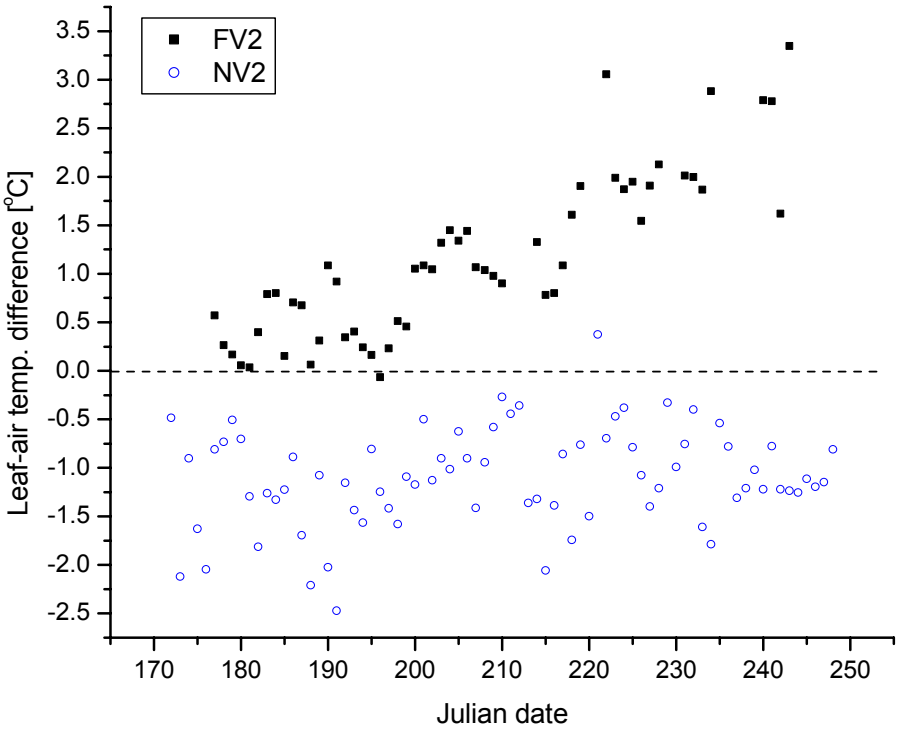

Figure 6.9 Leaf-air temperature differences in FV2 and NV2 in 2005

6.3.4 Comparison of FV+Pad and NV+hp Fog

The comparative performance of FV+pad system with the NV+hp fog system is illustrated with one day's data from July 2, 2006. The data from other days show the same trends and therefore are not presented. Outside solar radiation that day reached as high as 814 W m^{-2}; the highest air temperature was about 33 ^{o}C; the lowest relative humidity was about 42%; wind speed was approximately 2 to 4 m s^{-1}.

The comparison of the resulting inside environment is shown in Figs 6.10 to 6.13. As seen in Fig.6.10, the air temperatures resulting from both systems (FV+pad; NV+hp fog) were roughly the same. The cooling effects of both systems were significant, with the inside air temperatures as much as 5 ^{o}C lower than the outside. Relative humidities were increased above the outside with both systems, but the relative humidity resulting from NV+hp fog was much higher than FV+pad (Fig.6.11).

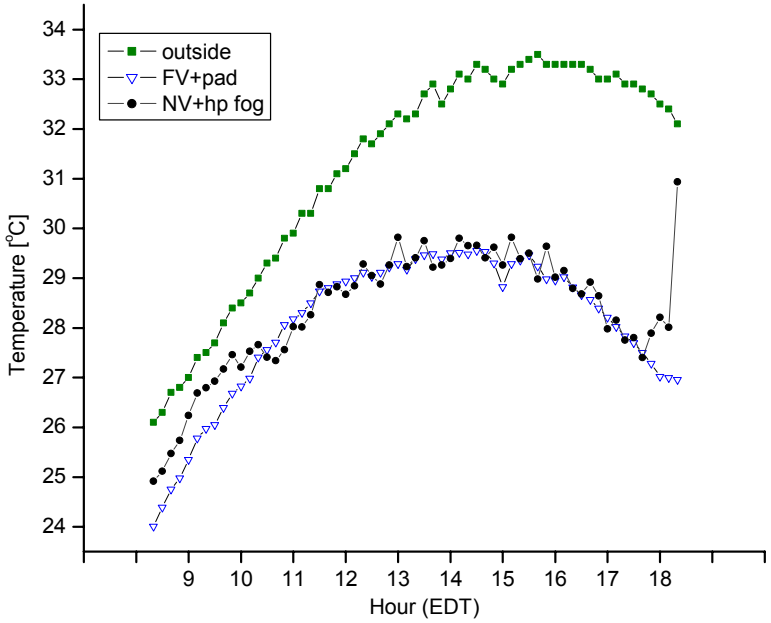

Figure 6.10 Temperatures in the FV house with the evaporative pad, the NV house with the high-pressure fog and the outside

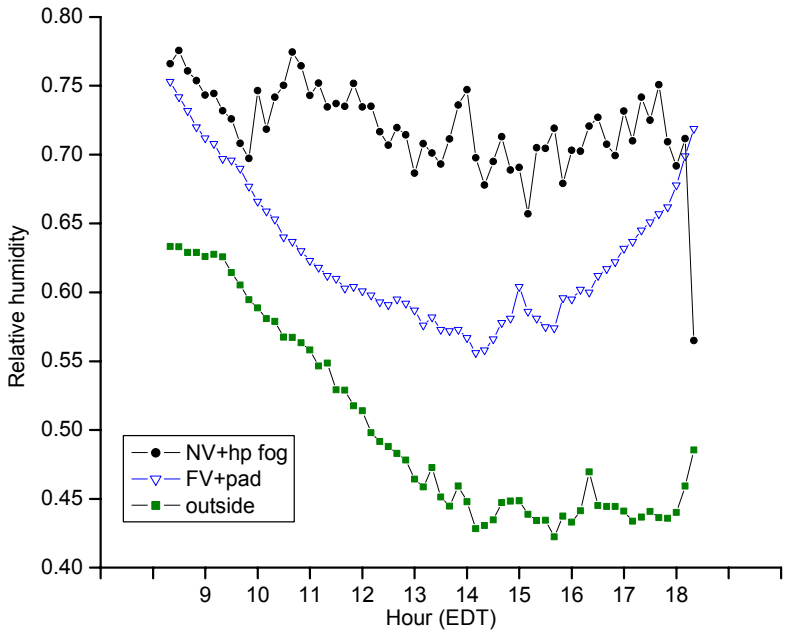

Figure 6.11 Relative humidities in the FV house with the evaporative pad, the NV house with the high-pressure fog and the outside

With roughly same air temperature but higher relative humidity, the enthalpy resulting from NV+hp fog was higher than FV+pad (Fig.6.12). It can then be inferred that the ventilation rate of the NV house was lower if both houses absorbed same amount of solar radiation. The result of this would have been higher leaf temperatures in the NV house.

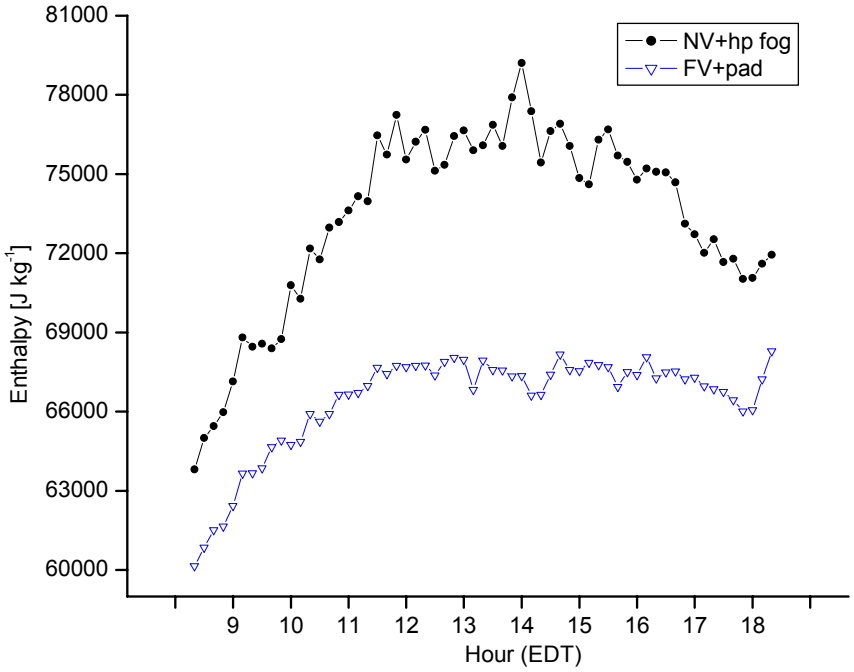

Figure 6.12 Enthalpies in the FV house with the evaporative pad and the NV house with the high-pressure fog

These results imply that it is meaningless to simply state that one system is better than the other. It depends on what aspect is to be compared, what weather conditions (especially wind speed) are to be experienced and what the fan capacity and vent size are. For example, if only air temperature is considered, either of the two systems could outperform the other. NV+ hp fog system can potentially saturate the inside air and produce lower air temperatures than FV+pad system. One the other hand, FV+pad system can produce lower temperatures if the fog spray rate is low.

6.4 Conclusions

The environmental data of the summers of 2003 to 2006 suggest that: 1) the air temperatures in FV greenhouses were generally less uniform than NV greenhouses; 2) the air temperatures in NV greenhouses experienced greater change over time than in FV greenhouses during each day; 3) the leaf temperatures in FV greenhouses were generally

higher than air temperatures when evaporative pads were used, less when not; 4) the leaf temperatures were generally lower than air temperatures in NV greenhouses no matter whether low-pressure fog was used or not (it should be noted that Li *et al*. (2006) found high-pressure fog produced air temperatures cooler than leaf temperatures, as was the case for evaporative pad cooling); 5) high-pressure fog in the NV greenhouse was as effective as the evaporative pad with fan ventilation in reducing air temperatures; however, high-pressure fog resulted in higher relative humidity.

References

Li, S.; Willits, D.H.; Yunker, C. 2006. Experimental study of a high-pressure fogging system in naturally ventilated greenhouses. *Acta Horticulturae*, 719: 393-400

Seginer, I.; Willits, D. H.; Raviv M.; Peet, M. M. 2000. Transpirational cooling of greenhouse crops. BARD Final Scientific Report IS-2538-95R, Bet Dagan, Israel

Willits, D.H.; Li, S. 2005. A Comparison of naturally ventilated vs. fan ventilated greenhouses in the southeastern U.S. ASAE paper No. 05-4155. American Society of Agricultural and Biological Engineers, St. Joseph, MI

Willits, D.H.; Li, S.; Yunker, C. 2006a. The Cooling performance of Naturally Ventilated Greenhouse in Southeastern U.S. *Acta Horticulturae*, 719: 73-82

Willits, D.H.; Teitel, M.; Tanny, J.; Peet, M.M.; Cohen, S.; Matan, E. 2006b.Comparing the performance of naturally ventilated and fan ventilated greenhouses. BARD Final Scientific Report US-3189-01, Bet Dagan, Israel

Chapter 7 The Suitability of Greenhouse Cooling Technologies under Various Climates

Abstract The suitability of four cooling technologies (fan ventilation without evaporative pad, fan ventilation with evaporative pad, natural ventilation with high-pressure fog and natural ventilation without high-pressure fog) was investigated for fifty-six locations around the world with a simulation model and weather data for these locations. The model was based on the steady heat balance of greenhouse. The weather data used were Typical Meteorological Year2 (TMY2) data. Through calculating inside air temperature with the model and weather data, and observing its distribution, a cooling technology was considered suitable if 98% of inside air temperatures were below 27.8 ^{o}C. Two values, 0.5 and 1, were used for evapotranspiration coefficient. Ventilation rates for natural ventilation were based on two empirically constructed equations, with the one twice as much as the other. It is suggested that the suitabilities of various cooling technologies depended largely on local weather. Evapotranspiration coefficient and ventilation characteristics of natural ventilation played important roles in determining the suitability of the four cooling technologies. Some locations were sensitive to evapotranspiration coefficient and ventilation characteristics of natural ventilation while some were not. The geographical pattern of suitable cooling technologies was examined for the U.S.

7.1 Introduction

Site selection is an important step in starting new greenhouse operation. There are several factors that determine suitable site selection for particular crops. These include climate, labor availability and distance to target market (Nelson, 1998; Hanan, 1998). Large greenhouse growers attempting to expand their ranges are constantly searching for the best site on a national, and even global, scale to maximize profits and reduce costs. For example, one of the major greenhouse tomato growers, Eurofresh Farm, moved from Pennsylvania to

Wilcox, Arizona to take advangte of the abundant sunshine, clean water and ready access to labor (Eurofresh Farm, 1990).

However, site selection is not a simple task, but a complex one that involves weighing several conflicting factors. Therefore, it would be helpful to narrow down the range of options from the perspective of climate. When fewer options are left, comparisons can be focused on other factors.

Cooling has to be provided for summer production, even though summer is not a favorable season for greenhouse production, because prices are low to the extent that open field grown produce is entering the market. Nevertheless, many growers have to maintain summer production in order to maintain profitability.

Various cooling greenhouse technologies exist; ventilation being a primary and essential one. This can be achieved by fans (fan ventilation) or by wind or/and air movement driven by inside-outside temperature difference (natural ventilation). Evaporative cooling is a complementary technology to ventilation providing additional cooling to assist transpiration cooling. Evaporative pads are normally used with fan ventilation, and fogging is generally incorporated with natural ventilation to provide evaporative cooling.

Since each cooling technology has its limitations, it would be helpful to assess viability from the perspective of physical environment. The study by Kittas (1996) examined natural ventilation and fan ventilation under the climate of Greece based on monthly weather data and a set of rules he developed. However, evaporative cooling was not included in his analysis.

The purpose of this study is to evaluate the suitability of two ventilation types and their accompanying evaporative cooling technologies under different climates using a

simulation model.

7.2 Methods and Materials

7.2.1 Simulation Model

The model from Seginer (1997) was used to predict the inside temperatures of greenhouses, i.e.

$$t_i = t_{in} + \frac{(1-E)\cdot\tau\cdot S_o}{\alpha\cdot U + \beta\cdot Q\cdot c_p\cdot\rho} \tag{7.1}$$

where t_i the inside temperature, ^oC; t_{in} is the inlet temperature into greenhouse, ^oC; E is the evapotranspiration coefficient; τ is the transmissivity of greenhouse cover; S_o is the outside solar radiation, Wm^{-2}; α is the cover-to-ground area ratio; U is the overall heat transfer coefficient of greenhouse cover, $W\ m^{-2}\ ^oC^{-1}$; β is the adjustment coefficient for ventilation system; Q is the ventilation rate, $m^3\ m^{-2}\ s^{-1}$; c_p is the specific heat of air, taken as 1007 $J\ kg^{-1}\ ^oC^{-1}$; and ρ is the density of outside air, taken as 1.157 $kg\ m^{-3}$ at 30 ^oC.

When an evaporative pad was used, the inlet temperature, t_{in}, was taken as

$$t_{in} = t_o - (t_o - t_{wo})\eta_p \tag{7.2}$$

where t_o is the outside temperature, ^oC; t_{wo} is the outside wet bulb temperature, ^oC; and η_p is the cooling efficiency of evaporative pads, taken as 0.75. If the evaporative pad was not in operation or if natural ventilation was used, t_{in} was set equal to t_o.

The transmissivity of greenhouse cover was set to 0.8. The cover-to-ground area ratio was assumed to be 1.5. According to Seginer (1997), the adjustment coefficient, β, was taken as 1 for natural ventilation. It was taken as 1.5 for fan ventilation based on experimental data (Li, 2007), possibly due to the non-linearity of air temperature distribution in the direction of airflow.

The evapotranspiration coefficient, E, depends on the "type, amount, age, health and/or stress level of the crops, the humidity ratio of the ventilation air at the inlet, and the amount of moisture available for evaporation from non-plant sources within the house" (ASAE, 2003). Originally, 0.5 was assumed to be a reasonable value for E (Albright, 1990). Later on, other studies (Katsoulas *et al*., 2002; Willits, 2006) found E could be much higher than 0.5, even greater than 1. As of now, it is not clear how, or to what extent, crop type and amount, humidity ratio of incoming air and other factors affect E. To deal with the uncertainty, two values of E (0.5 and 1) were selected to represent the range of conditions likely to be found in greenhouse operation.

Willits (2003) suggested that increasing Q beyond 0.05 $m^3 m^{-2} s^{-1}$ is not beneficial for cooling if an evaporative pad is not used. Even when evaporative pads are used, operating with a Q higher than 0.05 $m^3 m^{-2} s^{-1}$ is not common. To be conservative, a value of 0.06 $m^3 m^{-2} s^{-1}$ was set for Q for fan ventilation. For natural ventilation, ventilation rates mainly depend on wind speed and vent configuration. Various relationships between ventilation rates and wind speed have been developed previously for various vent configurations. Some of them are shown in Fig.7.1. To represent a moderate condition, the following relationship was assumed

$$Q = \begin{cases} 0.02u & u >= 1 \\ 0.01 + 0.01u & u < 1 \end{cases} \tag{7.4}$$

where u is the wind speed, m s^{-1}. For sensitivity analysis, ventilation rate was taken to be $2Q$ to represent highly efficient natural ventilation systems.

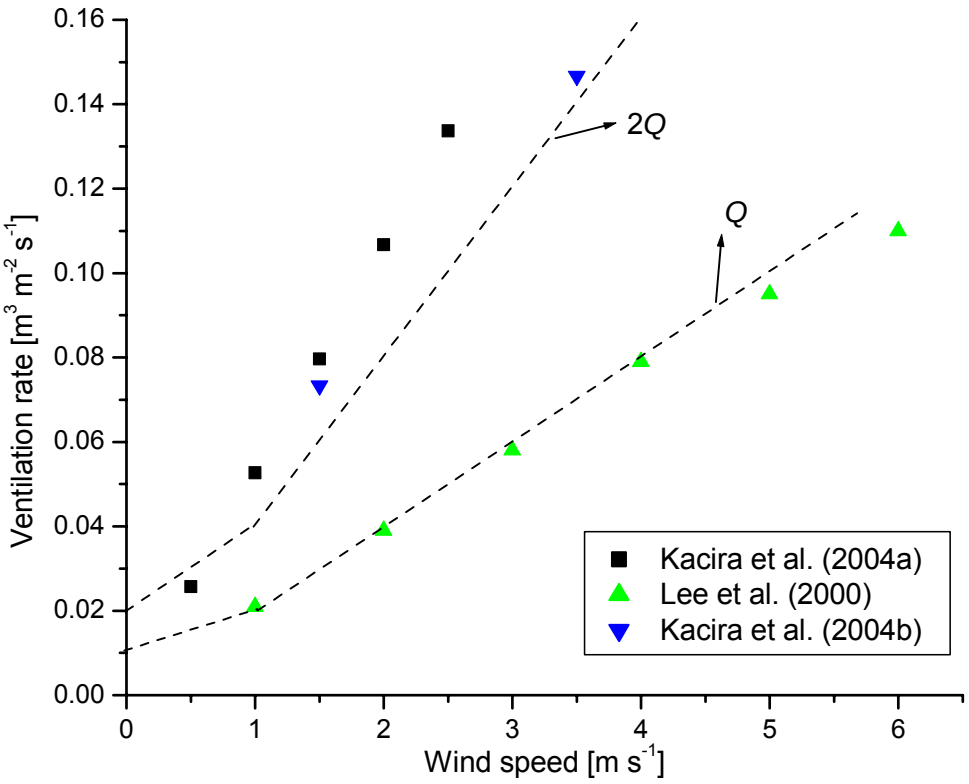

Figure 7.1 Dependence of ventilation rate on wind speed

When fogging was used, the inside temperature was predicted as

$$t_i = t_i^* - \left(t_i^* - t_{wi}\right)\eta_f \tag{7.5}$$

where t_i^* is the virtual inside temperature that would be reached without fog, ^{o}C; t_{wi} is the inside wet bulb temperature, ^{o}C; and η_f is the cooling efficiency of fogging. The virtual temperature t_i^* was calculated with Eqn.7.1. The inside wet bulb temperature, t_{wi}, was calculated with the following regression equation

$$t_{wi} = -0.0013h_i^2 + 0.4527h_i - 2.1668 \quad (R^2=0.997) \tag{7.6}$$

where h_i is the inside enthalpy, kJ kg^{-1}. Figure 7.2 shows that the wet bulb temperatures calculated with Eqn.7.6 matched well with those calculated with a psychrometric chart (Jian and Fang, 2002).

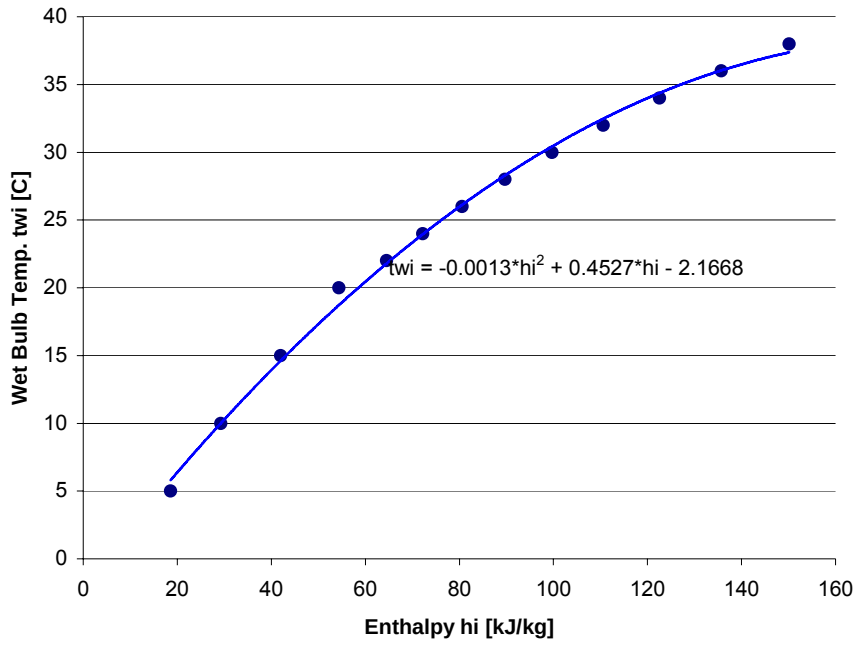

Figure 7.2 Regression relationship between enthalpy and wet bulb temperature

The inside enthalpy, h_i , was approximated as

$$h_i = h_o + \frac{\tau S_o}{Q\rho} \tag{7.7}$$

The cooling efficiency of high-pressure fogging, η_f, varies with spray rate, ventilation rate and outside humidity (Li *et al.,* 2006). To simplify the analysis, it was assumed to be a constant with a value of 0.5.

7.2.2 Locations and Weather Data

Fifty-six locations were selected, forty of which are in U.S. (Table 7.1). Each location selected for the U.S. has the lowest design wet bulb temperature in its state (ASHRAE, 1997) and TMY2 weather data (Marion and Urban, 1995) is available. Most locations selected for other countries have major greenhouse production area.

Weather data were derived from various sources. Weather data for U.S. locations are

from TMY2. Weather data for other countries were compiled by various agencies of the corresponding countries and/or international meteorological organizations (U.S. Department of Energy, 2006).

The weather data are hourly values over a 1-year period. They include dry bulb temperature, relative humidity, horizontal solar radiation and wind speed. Since summer cooling is the focus of this study, only the data from May to September were used.

Table 7.1 Locations selected for this study

	Country/State	City	County/State	City
U.S.	Alabama	Huntsville	Nebraska	Scottsbluff
	Arizona	Flagstaff	Nevada	Ely
	Arkansas	Fort Smith	New Hampshire	Concord
	California	Arcata	New Jersey	Newark
	Colorado	Alamosa	New Mexico	Albuquerque
	Connecticut	Bridgeport	New York	Binghamton
	Delaware	Wilmington	North Carolina	Asheville
	Florida	Jacksonville	North Dakota	Minot
	Georgia	Athens	Ohio	Akron
	Idaho	Pocatello	Oklahoma	Oklahoma City
	Illinois	Chicago	Oregon	North Bend
	Indiana	Fort Wayne	Pennsylvania	Bradford
	Iowa	Waterloo	South Carolina	Greenville
	Kansas	Goodland	South Dakota	Rapid City
	Kentucky	Lexington	Tennessee	Bristol
	Louisiana	New Orleans	Texas	Amarillo
	Maine	Caribou	Utah	Cedar City
	Massachusetts	Worchester	Vermont	Burlington
	Michigan	Lansing	Virginia	Roanoke
	Minnesota	Duluth	Washington	Quillayute
	Mississippi	Meridian	West Virginia	Elkins
	Missouri	Columbia	Wisconsin	Milwaukee
	Montana	Kalispell	Wyoming	Rock Springs
World	China	Beijing	Israel	Jerusalem
	China	Shanghai	Japan	Tokyo
	China	Kunming	Mexico	Mexico City
	Canada	London	Netherlands	Amsterdam
	Canada	Vancouver	Spain	Almería

7.2.3 Suitability Assessment

The suitability of four cooling options (natural ventilation without fog, natural ventilation with fog, fan ventilation without evaporative pads, fan ventilation with

evaporative pads) at the selected locations was assessed in the following way: t_i was calculated for a location when any of the four cooling options was used. By observing the distribution of t_i, the cooling option was regarded suitable if 98% of t_i were below 27.8 ^{o}C, otherwise it was regarded as unsuitable.

A '1' was used to indicate that a cooling option is suitable and a '0' indicates that a cooling option is not suitable. A four-bit number, each bit representing the suitability of one of the four cooling options, characterized each location. To group the locations with same suitable cooling number, a suitability index was defined. The definition of suitability index is tabulated in Table 7.2. A suitability index with a value of 4 means that all the four cooling options are suitable; a suitability index with a value of 3 means that all the four cooling options except NV without fog are suitable; a suitability index equal to 2 means that NV with fog and FV with pad are suitable while NV without fog and FV without pad are not suitable, and so forth.

Table 7.2 Definition of suitability index

NV+ no fog	NV+ fog	FV+no pad	FV+pad	Suitability Index
1	1	1	1	4
0	1	1	1	3
0	1	0	1	2
0	0	0	1	1
0	0	0	0	0

To examine the sensitivity of the suitability index to E and Q, the suitability assessment was performed with four calculation conditions with different E and Q. The four conditions were denoted as A, B, C and D. Condition A indicates that E was equal to 0.5 and Q was calculated with Eqn.7.4; condition B indicates that E was 1.0 and Q was calculated with Eqn.7.4; condition C indicates E was 0.5 and Q was two times greater than that from

Eqn.7.4; Condition D indicates that E was 1.0 and Q was two times greater than that from Eqn.7.4.

7.3 Results and Discussion

The suitability of various cooling options, represented by the suitability index, for the selected locations is given in Table 7.3. There were nineteen locations (marked with bold font) that had consistent suitability indices in spite of different conditions. For example, the suitability index for Arcata, California was 4, indicating all four cooling technologies are sufficient to meet the cooling need. In other words, natural ventilation would be an appropriate cooling technology for Arcata, California. Another example is Flagstaff, Arizona, which has a suitability index of 2, meaning that either FV+pad or NV+fog system is necessary to provide sufficient cooling.

Suitability indices of other locations varied with E and Q. For example, locations such as Alamosa, Colorado; Caribou, Maine; Duluth, Minnesota; Binghamton, New York; and Bradford, Pennsylvania require evaporative cooling if E was 0.5 but not if E was 1.0. For locations such as Fort Wayne, Indiana; Waterloo, Iowa; and Lexington, Kentucky, only FV+pad is a viable cooling option under condition A; however, both FV+pad and NV+fog provided sufficient cooling under conditions of B, C and D.

Some locations including London, Canada; Elkins, West Virginia; and Mexico City, Mexico were especially sensitive to E and Q. Take London, Canada for example, where only FV+pad was viable if E was 0.5, but NV+no fog would be sufficient if E was 1.0.

Table 7.3 Suitability index for all locations with different *E* and *Q*

Country/State	City	A	B	C	D	County/State	City	A	B	C	D
Alabama	Huntsville	0	1	0	1	Nebraska	Scottsbluff	1	2	2	2
Arizona	**Flagstaff**	2	2	2	2	**Nevada**	**Ely**	2	2	2	2
Arkansas	Fort Smith	0	1	0	1	New Hampshire	Concord	1	2	2	2
California	**Arcata**	4	4	4	4	New Jersey	Newark	1	2	2	2
Colorado	Alamosa	2	4	2	4	New Mexico	Albuquerque	1	2	2	2
Connecticut	**Bridgeport**	2	2	2	2	New York	Binghamton	2	4	2	4
Delaware	Wilmington	0	1	0	2	North Carolina	Asheville	1	2	1	2
Florida	**Jacksonville**	0	0	0	0	**North Dakota**	**Minot**	2	2	2	2
Georgia	Athens	0	1	0	1	**Ohio**	**Akron**	2	2	2	2
Idaho	**Pocatello**	2	2	2	2	Oklahoma	Oklahoma City	0	1	0	1
Illinois	Chicago	1	1	1	2	**Oregon**	**North Bend**	4	4	4	4
Indiana	Fort Wayne	1	2	2	2	Pennsylvania	Bradford	2	4	2	4
Iowa	Waterloo	1	2	2	2	South Carolina	Greenville	0	1	0	1
Kansas	Goodland	1	1	1	2	South Dakota	Rapid City	2	2	2	2
Kentucky	Lexington	1	2	1	2	Tennessee	Bristol	1	1	1	2
Louisiana	**New Orleans**	0	0	0	0	Texas	Amarillo	1	2	2	2
Maine	Caribou	2	4	2	4	Utah	Cedar City	1	2	2	2
Massachusetts	Worchester	1	2	2	2	**Vermont**	**Burlington**	2	2	2	2
Michigan	**Lansing**	2	2	2	2	Virginia	Roanoke	1	1	1	2
Minnesota	Duluth	2	4	2	4	**Washington**	**Quillayute**	4	4	4	4
Mississippi	Meridian	0	1	0	1	West Virginia	Elkins	1	4	2	4
Missouri	Columbia	0	1	0	1	**Wisconsin**	**Milwaukee**	2	2	2	2
Montana	**Kalispell**	2	2	2	2	**Wyoming**	**Rock Springs**	2	2	2	2
China	Beijing	0	1	0	1	Israel	Jerusalem	1	2	2	2
China	**Shanghai**	0	0	0	0	Japan	Tokyo	0	1	0	1
China	Kunming	3	4	4	4	Mexico	Mexico City	1	4	1	4
Canada	London	1	4	2	4	Netherlands	Amsterdam	3	4	4	4
Canada	**Vancouver**	4	4	4	4	Spain	Almería	1	2	2	2

Note: A indicates that *E* was 0.5 and *Q* was from Eqn.7.4; B indicates that *E* was 1.0 and *Q* was from Eqn.7.4; C indicates *E* was 0.5 and *Q* was twice of that from Eqn.7.4; D indicates that E was 1.0 and Q was twice of that from Eqn.7.4.

Figure 7.3 shows the geographical distribution pattern of suitability index under condition B. There are twelve locations in North America in addition to Amsterdam, Netherlands; Jerusalem, Israel; and Kunming, China where NV+no fog provided a sufficient cooling. The U.S. locations mainly concentrated on the West Coast and in the Great Lakes area. High altitude sometimes gives a cooling advantage. For example, the city of Kunming lies in the south of China, where the climate is semi-tropical. Owing to its high altitude (1892m), the temperature in summer is much lower than the cities at the same latitude. The monthly average temperature at noon in July is only 22-23 ^{o}C.

At the other extreme are the locations with a suitability index of 0, where none of the

cooling options were suitable. These locations include: Jacksonville, Florida; New Orleans, Louisana; and Shanghai, China. Additional cooling (such as shading) will be required for these locations.

Twenty-three locations, in addition to Almería, Spain and Jerusalem, Israel, had a suitability index of of 2. The locations span a large portion of U.S. mainland, suggesting the two evaporative cooling technologies (evaporative pads, fogging) were able to meet the cooling needs for most conditions. Most U.S. locations with suitability index of 0 or 1 are located in the southeast portion of the U.S., where summer cooling is genereally more demanding than in other areas.

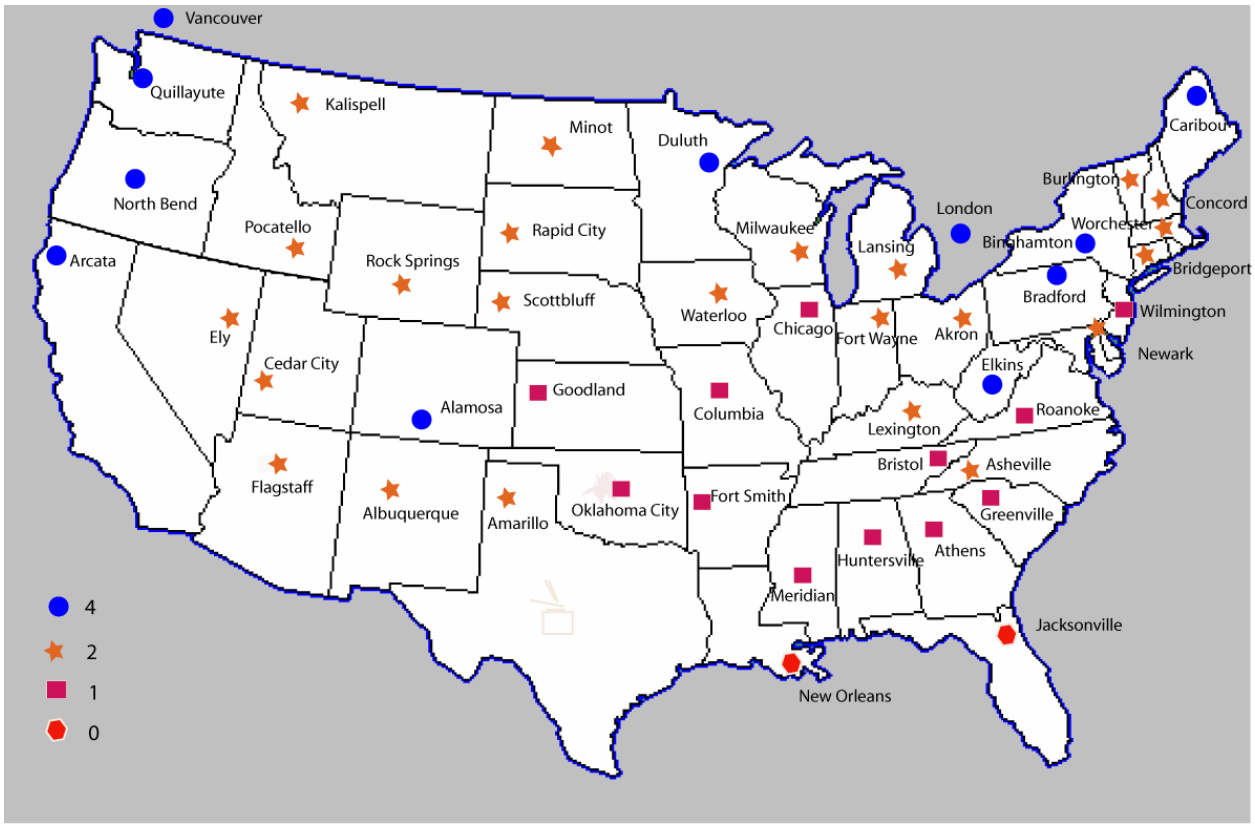

Figure 7.3 Suitability indices for the U.S. and Canadian locations. '4' indicates that natural ventilation without fog is suitable; '2 'indicates both fan-and pad system and natural ventilation with high-pressure fog are suitable; '1' indicates that only fan-and-pad system is suitable; '0' means neither of the cooling options is suitable.

These results suggest that whether the cooling technologies are suitable for a location is larged determined by the local climate, but it is also affected by crop status and greenhouse characteristics such as natural ventilation design. Validity of these results relies on the parameters and cooling criterion set. Based on the response of the suitability index to E, it is obvious that plant transpiration plays an important role in greenhouse cooling.

It should be noted that the temperature threshold (27.8 ^{o}C) in the criterion was based on the recommendation for growing tomato (Snyder, 2002). In fact, many crops have greater adaptability and many have less. If the crop to be grown is less heat tolerant than tomato, the results need to be re-evaluated.

In spite of the uncertainty surrounding the parameters E and Q, the method illustrated in this study allows cooling design to be examined from a different perspective. The normal design procedure utilizes the design conditions, such as temperature and solar radiation given in engineering stardards such as the ASHRAE handbook and applies them to design equations to specify equipment capacities. The design conditions are usually statistically derived from raw weather data, representing the harshest conditions. However, the harshest conditon for every concerned variable do not normally occur at the same time. Designs based on the extreme conditions for individual variables tend to be conservative if the correlation between the variables is not considered. If weather is regarded as random and raw weather data can represent its distribution reasonably, applying weather data to a thermal system and ensuring that the design variables remain below the desired level should result in more reasonable designs.

7.4 Conclusions

The suitability of fan and natural ventilation with evaporative cooling technologies was investigated with a simulation model for fifty-six locations in the world, mostly in U.S. The model was based on the steady heat balance of greenhouse. The weather data used are TMY2 data. It is suggested that suitability of various cooling technologies was largely determined by local climate. Evapotranspiration coefficient and ventilation characteristics of natural ventilation were also shown to be important factors affecting the suitability of the cooling technologies. Some locations were sensitive to the evapotranspiration coefficient and ventilation characteristics and some were not. Those locations with consistent suitability were identified. The geographical distribution pattern of suitable cooling technologies was examined in U.S.

Nomenclature

α	cover-to-ground area ratio
c_p	specific of air, J kg^{-1} $^oC^{-1}$
E	evaportranspiration coefficient
h_i	inside enthalpy in kJ kg^{-1}
Q	ventilation rate, m^3 m^{-2} s^{-1}
RH	outside relative humidity
S_o	outside solar radiation, Wm^{-2}
t_i	inside temperature, ^oC
$t_{i,p}$	inside air temperature with fan-and-pad system
$t_{i,f}$	inside air temperature natural ventilation with high-pressure fog
t_i^*	virtual inside temperature that would be reached without fog, ^oC
t_{in}	inlet temperature into greenhouse, ^oC
t_o	outside temperature, ^oC

t_{wo} outside wet bulb temperature, ^{o}C

t_{wi} inside wet bulb temperature, ^{o}C

U overall heat transfer coefficient of greenhouse cover, W m^{-2} $^{o}C^{-1}$

β adjustment coefficient for ventilation system

ρ density of outside air, kg m^{-3}

τ transmissivity of greenhouse cover

η_p cooling efficiency of evaporative pad

η_f cooling efficiency of high-pressure fog

Reference

Albright, L.D.1990. Environment control for animals and plants. American Society of Agricultural Engineers, St. Joseph, MI

ASAE. 2003. Heating, ventilating and cooling greenhouses. ANSI/ASAE EP406.2. American Society of Agricultural Engineers, St. Joseph, MI

ASHRAE. 1997. AHRAE handbook. Heating, ventilation, and air-conditioning systems and equipment. American Society of Heating, Refrigerating, and Air-Conditioning Engineers, Altanta, GA

EuroFresh Farms. 1990. About us. Available at: http://www.eurofresh.com/aboutus/aboutus.shtml . Accessed in Dec., 2006.

Hanan, J.J. 1998. Greenhouses-advanced technology for protected horticulture. CRC Press. Boca Raton, FL

Jian, Z.; Fang, W. 2002. Digital psychrometric chart. Dept. of Bio-industrial mechatronics Engineering, National Taiwan University, Taiwan

Kacira, M.; Sase, S. and Okushima, L. 2004a. Optimization of vent configuration by evaluating greenhouse and plant canopy ventilation rates under wind-induced ventilation. *Transactions of the ASAE*, 47(6): 2059-2067

Kacira, M.; Sase, S. and Okushima, L. 2004b. Effect of side vents and span numbers on wind-induced natural ventilation of a gothic multi-span greenhouse. *JARQ*, 38(4): 227-233

Katsoulas, N.; Baille, A.; Kittas, C. 2002. Influence of leaf are index on canopy energy partitioning and greenhouse cooling requirements. Biosystems Engineering, 83(3):349-359

Kemrati, H.; Boulard, T.; Bekkaoui, A. *et al*. 2001. Natural ventilation and microclimatic performance of a large banana greenhouse. *Journal of Agricultural Engineering Research*, 80(3): 261-271

Kittas,C. 1996. A simple climagraph for characterizing regional suitability for greenhouse crop in Greece. *Agricultural and Forest Meteorology*, 78(1-2): 133-141

Lee, I.; Short T.H. 2000. Two-dimensional numerical simulation of natural ventilation in a multi-span greenhouse. *Transactions of the ASAE*, 43(3): 745-753

Li, S. 2007. Unpublished data

Li, S.; Willits, D.H.; Yunker, C. 2006. Experimental study of a High-pressure Fogging System in Naturally Ventilated Greenhouses. *Acta Horticulturae*, 719: 393-400

Marion W.; Urban K. 1995. User's Manual for TMY2s. Golden, Colorado: National Renewable Energy Laboratory.

Nelson, P.V. 1998. Greenhouse operation and management-5th edition. Prentice-Hall, Inc. Upper Saddle River, NJ

Seginer, I. 1997. Alternative design formulae for the ventilation rate of greenhouses. *Journal of Agricultural Engineering Research*, 68(4): 355-365

Snyder, R.G. 2002. Greenhouse tomato handbook. Publication 1828. Extension Service of Mississippi State University

U.S. Department of Energy. http://www.eere.energy.gov/buildings/energyplus/cfm/weather_data.cfm

Willits, D.H. 2003. Cooling fan ventilated greenhouses: a modeling study. *Biosystems Engineering*, 84(3): 315– 329

Willits, D.H. 2006. Fan ventilated greenhouses cooling: some considerations for design. *Acta Horticulturae*, 719: 83-96

Chapter 8 Summary

This study started with an objective of comparing the cooling performance of natural ventilation (NV) and fan ventilation (FV) systems. As the study progressed, evaporative cooling was recognized as a decisive factor. Without evaporative cooling, it is impossible for NV systems to compete with FV systems equipped with evaporative pads. From then on, part of the effort of this study was devoted to finding an evaporative cooling alternative for NV systems. Initially, low-pressure fogging systems (4 atm) were installed and tested. Experimental data showed that low-pressure fogging systems did improve the cooling for NV systems, but the temperatures were still higher than FV systems. A high-pressure fogging system (68 atm) was then installed and tested for the NV systems. The cooling ability of the new system (high-pressure system) was found comparable with FV systems with evaporative pads (Chapter 6). Intuitively, this naturally led to a hypothesis that high-pressure fogging systems should be superior over low-pressure fogging systems. A comparison was made of the two fogging systems and validated the hypothesis (Chapter 2).

However, a drawback of the high-pressure fogging for NV systems was quickly realized. The high-pressure fogging system was difficult to control: leaf wetting was difficult to avoid; cooling must be compromised in order to minimize leaf wetting. The focus of the study then turned to finding an effective control strategy for the high-pressure fogging system. Various strategies were explored and tested (Chapter 3). NCSU control, a strategy developed in this study, was found to be superior in some aspects (cooling efficiency, pump cycling frequency). VPD (vapor pressure deficit) control was found to be most effective in reducing leaf wetting.

In parallel with the efforts devoted to fogging cooling for NV systems, thermal

stratification for FV systems was investigated. Thermal stratification for FV systems was brought to our attention and chosen as a focus of this study because it complicated the comparison of the two ventilation systems: significant vertical temperature gradients were found in the FV houses, causing the control computer to call for less cooling than required because of the location of the control sensor. The result was that the FV houses ended up with higher temperatures than the NV houses toward the end of the season, even though the cooling ability of the FV houses was superior to the NV houses throughout the experiment.

In order to better understand thermal stratification, the vertical temperature distribution for the FV systems was investigated. The effects of outside weather (solar radiation), operational condition (evaporative pads and airflow rate) and plant canopy were examined. Experimental data showed that vertical temperature gradients increased with solar radiation. Use of the evaporative pad also increased the gradient. However, increasing the airflow rate of fans mitigated the temperature gradient (Chapter 4). In addition, a model was developed to describe the air temperature distributions in FV systems. Simulation with the model revealed some patterns suggesting revisions to the evaporative pad control methods commonly used in commercial production (Chapter 5).

With the two issues (fogging for NV systems; thermal stratification for FV systems) reasonably well addressed, attention then returned to the main theme of this study — comparing the thermal environment of the two ventilation systems. Certain aspects were examined, i.e. spatial variation of air temperature, change of air temperature over the daily cycles, and leaf-air temperature differences (Chapter 6). Experimental data suggested that the spatial variation of air temperature was greater for the FV systems than for the NV systems; the change of air temperature over the daily cycles was less for the FV systems than for the

NV systems. When evaporative cooling, either evaporative pads or high-pressure fogging, was used, leaf temperature was higher than air temperature but otherwise it was lower. The low-pressure fogging systems did not change the relative order of leaf and air temperatures.

After evaporative cooling as one factor of the comparative performance of the two ventilation systems with their accompanying evaporative cooling was examined, climate, as another factor, was investigated as well (Chapter 7). This investigation was done by exploring the suitability of the two ventilation systems under a variety of climates. Suitability was defined as when certain cooling needs could be met. Model simulation suggests that the suitability of the various sytems depended on local climate, evapotranspiration coefficient and ventilation characteristics. A sensitivity analysis was performed and the geographical distribution pattern of suitable cooling technology was presented for the U.S.

Appendices

Appendix A Experiment Setup and Procedures

A.1 Facilities and Equipment

A.1.1 Greenhouse Structure

Four greenhouses were used throughout the study, two of which were fan-ventilated and two of which were naturally ventilated. These houses were located at the Horticultural Field Laboratory on the NC State University campus, Raleigh, NC. All four greenhouses were covered with inflated double-polyethylene. Their relative locations were shown in Fig.A.1.

The fan-ventilated (FV) greenhouses were Quonset style, 6.7m by 12.1m with a ridge height of 2.92 m. The ridges were oriented north-south. Evaporative pads were installed in the north wall and two exhaust fans located in the south wall. The evaporative pads were sized for a face velocity of 1.27 m s^{-1} at the maximum ventilation rate. The geometric dimensions of an FV greenhouse are shown in Fig.A.2.

The naturally ventilated (NV) greenhouses were free standing gutter-connected style. They were 6.4m by 11 m with a gutter height of 3.45 m and a ridge height of 5.36m. The NV greenhouses shared a common end wall made of double-polyethylene. The NV greenhouses were oriented along an east-west axis and were fitted with three vents, one on the south, one on the north and one at the top. The vents were driven by rack and pinion drive systems opening outward. The opening dimensions of the vents are shown in Fig.A.3. The vents were opened in the following sequence: the south opened first, then north and then the top.

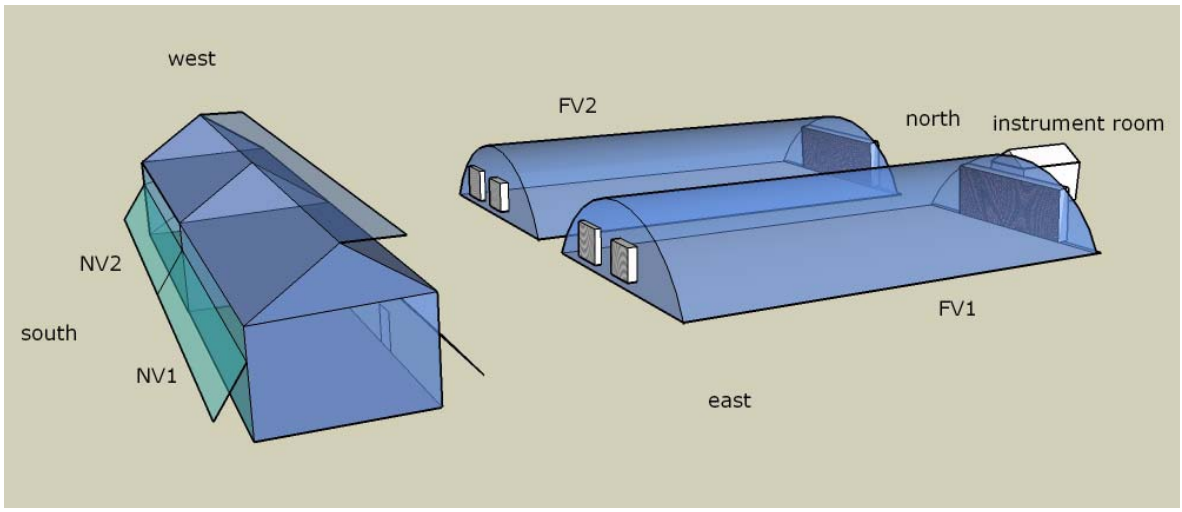

Figure A.1 Layout of four greenhouses. Two were fan-ventilated (FV1 and FV2) and the other two were naturally ventilated (NV1 and NV2)

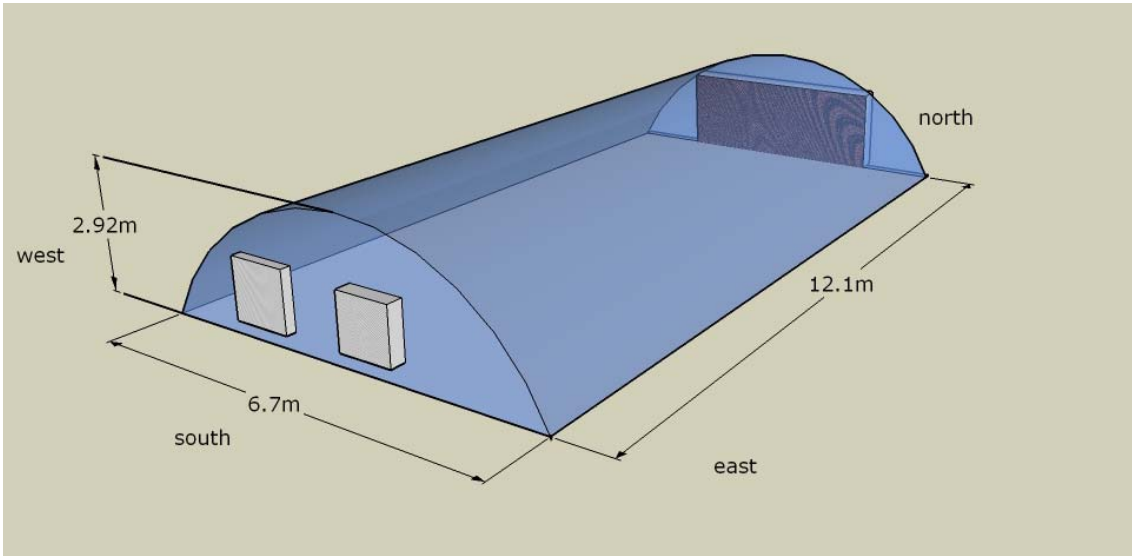

Figure A.2 Dimensions of FV greenhouses

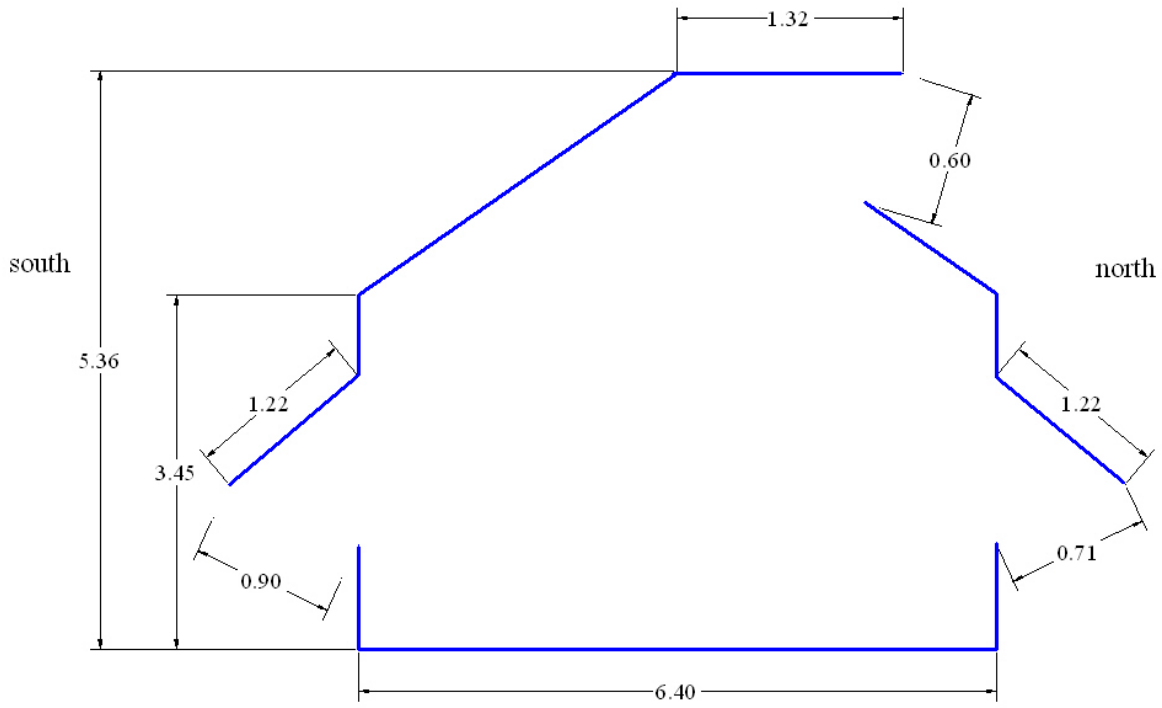

Figure A.3 Dimensions of NV greenhouses (unit: m)

A.1.2 Fogging Systems in NV Greenhouses

During 2003, evaporative cooling in the NV greenhouses was provided by 12 low-pressure (LP) fogging nozzles (0.012 inch diameter, Arizona Mist) mounted above the gutter line in each house. Each nozzle delivered about 1.9 liter per hour at line pressure.

During 2004, the low-pressure fogging system used in 2003 was replaced and new systems were designed and installed in both of the NV greenhouses. Each system contains 24 non-dripping nozzles (3.8 liter per hour, DIG Corporation) arranged in three zones spaced evenly across the house (Fig.A.4). The three zones were controlled separately so that fogging could include 8, 16 or 24 nozzles, depending upon need.

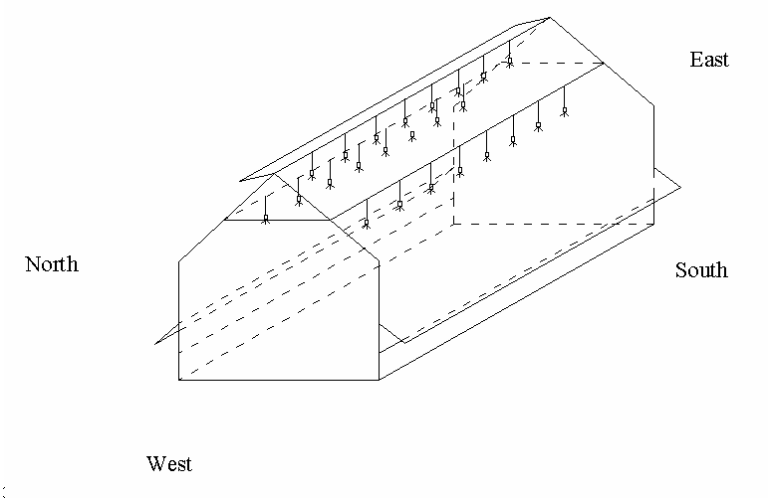

Figure A.4 Layout of nozzles of the low-pressure fogging systems. There were 24 foggers, with 8 foggers in each of three separate rows. One row is in the middle and the other two are on the both sides

During 2005, a booster pump was added to the low-pressure fogging systems. The line pressure was maintained at about 4 atm. In September of 2005, a high-pressure (HP) fogging system was installed in NV1. The system was composed of 24anti-drip nozzles (Item # 00002, Ecologic Technologies, Inc.) evenly distributed across the greenhouse at the height of 2.36m (Fig.A.5). The nominal spray rate of the nozzles were 5.49 liter per hour. Water was filtered and decalcified before being supplied to a high-pressure pump (FOGCO System Inc.). A valve system was configured to enable two levels of fogging, each with 12 nozzles (Fig.A.6).

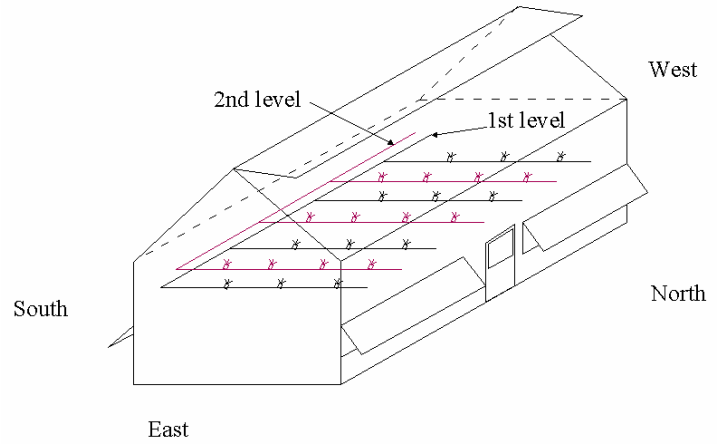

Figure A.5 Layout of high-pressure nozzles. The system consisted of 24 nozzles, with first 12 nozzles as the first level, and the last 12 as second level.

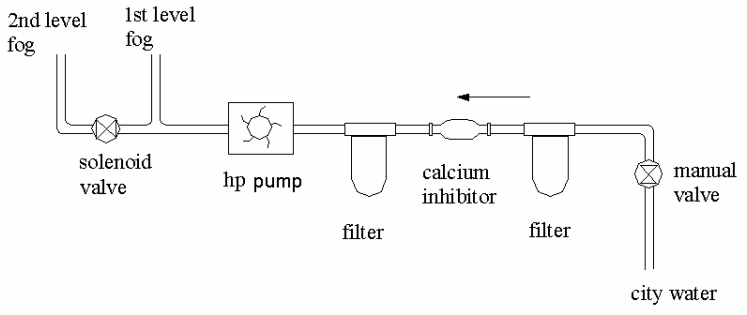

Figure A.6 Water treatment and configuration of fog levels

A computer controlled the low-pressure and high-pressure fogging systems. The control was at 15-second intervals. The control algorithms applied during the main experiment seasons were similar to that of multi-stage thermostats. The setpoints for the control variables were adjusted by trial and error to maximize cooling effect while avoiding too much wetting of the plants.

A.1.3 Growing Media and Fertigation

The growing media was composed of 50% peat and 50% aged pine bark by volume. The media was filled in 18.9 liter black polyethylene bags. The bags were pasteurized with high temperature by covering them with plastic sheets and disabling venting. The electrical conductivity (EC) was reduced to 200 - 300 ppm by flushing.

Drip emitters were placed at the top of the cultivation bags for fertilization and irrigation (also called fertigation). The chemical fertilizers (4-18-38, Ca $(NO_3)_2$, $CaCl_2$, KNO_3, $MgSO_4$) were dissolved, diluted and stored in three tanks. Based on the nutrient requirement of different crops at different ages, the solution in the three tanks were pumped and mixed in predefined ratio with injectors, further diluted with water and delivered to four greenhouses. A solenoid was installed at each greenhouse subject to the control from a control computer.

A.2 Plant Culture

2003 FV1 was planted with 208 tomato plants (cv. Trust) and NV2 house was planted with 182. The tomato seedlings were transplanted on 13 June. The plants in FV1 were distributed in 8 rows with 26 plants each. The plant rows were parallel with the airflow direction. Those in the NV2 were distributed in 14 rows with 13 plants each. The plant rows were normal to the ridge. Fertigation was once per day, usually between 6AM and 8AM. The concentrations of the solution were (ppm) 125 N, 45 P, 195 K, 185 Ca and 44 Mg. The quantity of solution delivered was determined by the predicted transpiration of tomato plants. Suckers were pruned periodically to prevent undesired branch development. The harvest started on 7 August and ended on 29 August.

2004 Tomato seedlings were transplanted into all four greenhouses on June 28. Crop configuration, variety, fertilizer recipe, pruning and other cultural practices were same as in 2003. The harvest started in early September and finished at the end of September.

2005 Peppers (*Capsicum annuum*) were grown this year. 75 *Waki* and 35 *Zamboni* were transplanted into the north end of each FV house on 8 June and 65 *Waki* and 30 *Zamboni* were transplanted into the north side of each NV house. On June 10, an additional 64 *Waki* and 32 *Walter* were added to each FV greenhouse on the south side and 63 *Waki* and 28 *Walter* were added to each NV greenhouse. Fertilization concentrations were the same as for tomatoes in 2003 and 2004. The harvest started on 9 August and ended on 6 September. Pruning was accomplished approximately every two weeks. Each plant was pruned to one main stem with two leaders. At each subsequent pruning, the strongest stem resulting from the two leaders left previously was retained and the other was removed. At the top of the plant, two leaders were again retained.

A.3 Measurements

A.3.1 Air temperature and relative humidity

NV houses

Air temperatures were measured with type-T thermocouples. Relative humidity was measured with sensors from Honeywell (HIH 3610). Due to the vulnerability of the Honeywell humidity sensors to fog, they were replaced with Vaisala HM50U humidity sensors in 2006. Each pair of thermocouple and humidity sensors was housed in an aspirated station. There were fourteen stations in each NV greenhouse. The stations were located at two vertical planes 3 m from each end wall. The locations of the seven aspirated stations on each plane are shown in Fig.A.7. The six stations below represented the potential canopy area. The top station was intended to measure the temperature and relative humidity of the air entering or leaving the top vent.

Dry and wet bulb temperatures of the air entering and leaving the side vents were measured using dry & wet bulb boxes (Fig.A.7). The two thermocouples, one with bare junction and the other wrapped in a cotton sock wet using a constant-head reservoir, were placed at the inlets of the box. A fan was used to create sufficient airflow to minimize the effect of radiation.

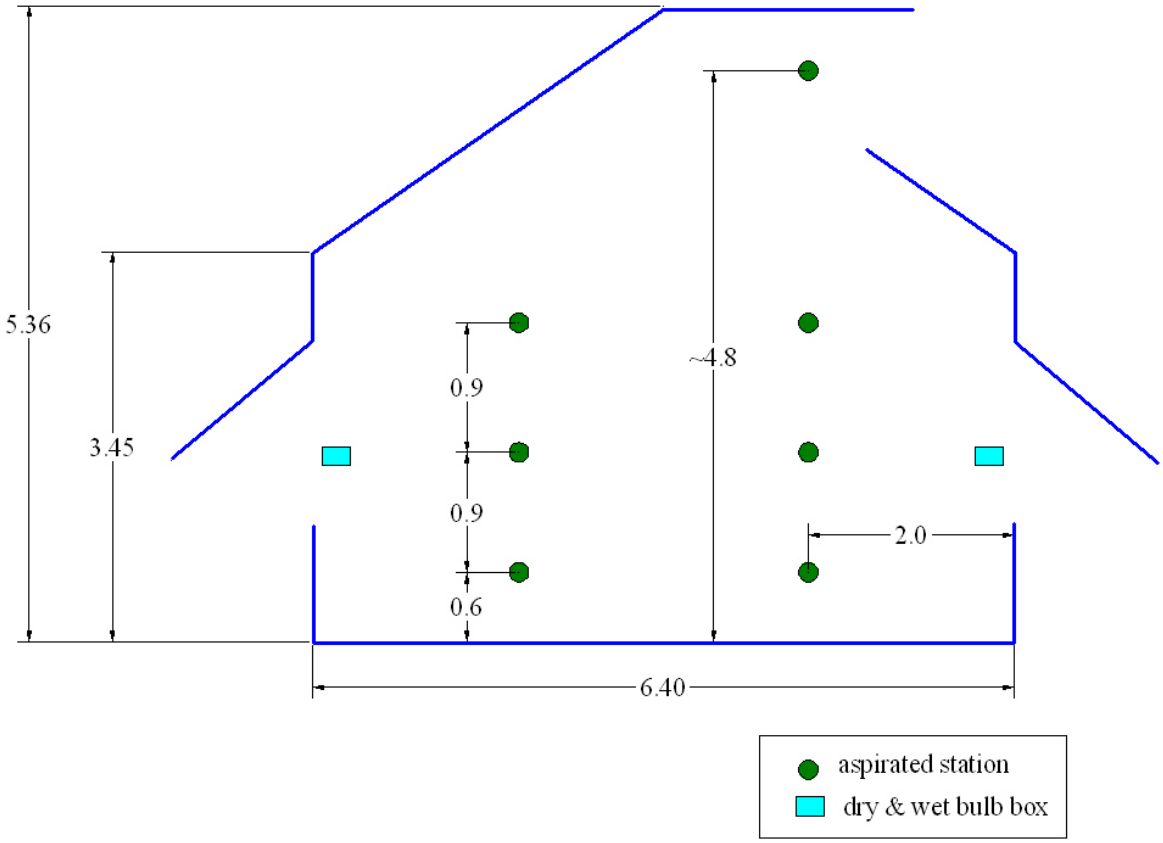

Figure A.7 Positions of aspirated stations and dry & wet bulb boxes measuring air temperatures and humidity in NV houses.

FV houses

In 2003, ten aspirated stations were used in each FV greenhouse. Two stations were located 2.44 m from the air entrance end (0.61 m and 1.22 m from the floor) on the centerline of the house, approximately 1/3 of the distance down the length of the greenhouse. At the mid-point, three stations were located at each of two locations spaced 2 m on either side of the centerline. The stations were located 0.56 m, 1.16 m and 1.72 m above the floor. The final two stations were located 10.3 m from the air entrance end, again on the centerline, at the same heights as those at the air entrance.

In 2004 and 2005, an additional four stations were added to each FV house. All stations were located on the centerline. The groupings of two were located at the upstream

and downstream edges of the canopy. The stations in these groupings were 1 m and 2 m off the floor. Those in the groupings of five were 0.46 m, 0.94 m, 1.40 m, 1.84 m and 2.32 m from the floor (Fig.A.8).

Two dry & wet bulb boxes were the dry and wet bulb temperatures of the air exiting the evaporative pad. Two other boxes were located at the intake of the exhaust fans to measure the dry and wet bulb temperatures of the exhausted air.

Both the Vaisala and Honeywell sensors were calibrated against the same Vaisala HMP45A sensor, which itself was calibrated by Vaisala to within 1% of NIST standards in February of 2003. Equations were developed from the calibrations against the HMP45A that allowed determination of relative humidity that were within 2% of each other within the range from 40% to 90%.

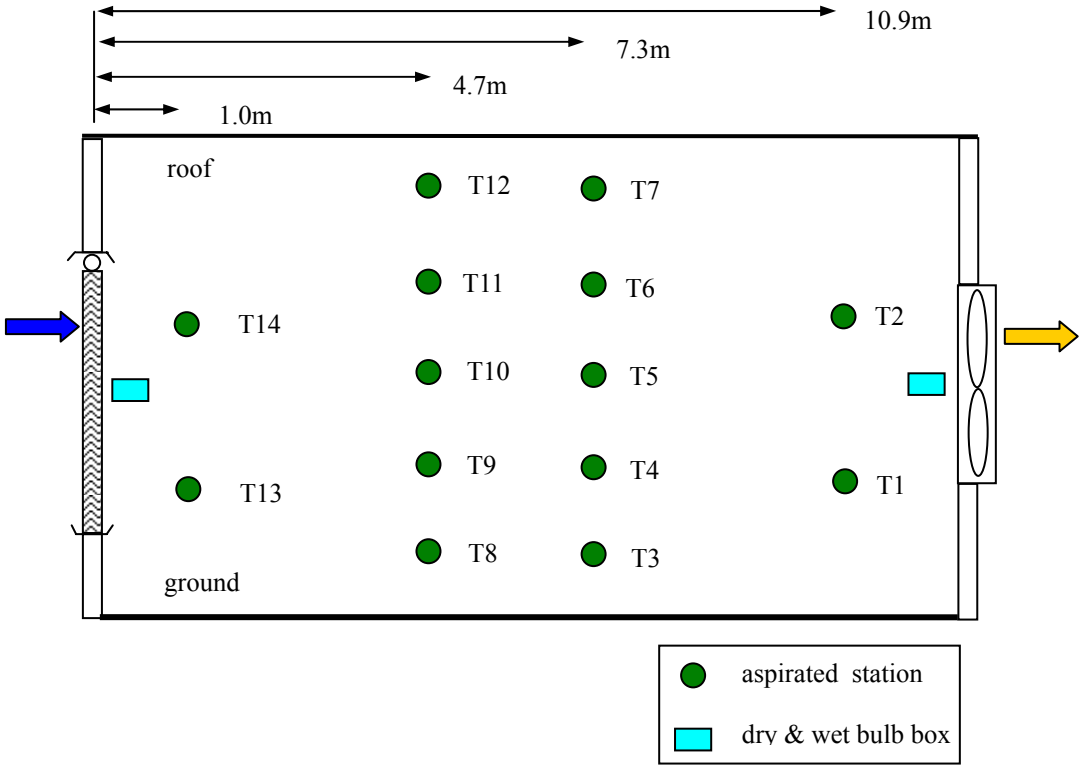

Figure A.8 Positions of aspirated stations and dry & wet bulb boxes measuring air temperatures and humidity in FV houses.

A.3.2 Leaf temperature

Leaf temperatures were measured using type-K thermocouples glued to the underside of leaves on selected plants (Fig.A.9). Eighteen leaves in each house were monitored. The thermocouples were checked at one or two-day intervals. Those that fell off from leaves or were glued to dead tissue were marked as bad measurements. Three leaf shading levels, shaded or unshaded or partially shaded, were documented. Details can be found in Seginer *et al.* (2000).

Figure A.9 Measurement of leaf temperature with fine type-K thermocouples

A.3.3 Outside weather

The outside dry bulb and wet bulb temperatures were measured with two 24-gauge (diameter is 0.51 mm) type-T thermocouples: one with bare junction and the other wrapped in a cotton sock wet using a constant-head reservoir. The two thermocouples were placed at the inlets of an aspirated plywood box. A fan was used to provide sufficient airflow to minimize the effect of radiation. Outside solar radiation on a horizontal surface was measured by a black and white pyranometer (Eppley Laboratory, Inc., Rhode Island)

mounted on a stand at the north wall of FV1. The wind speed and wind direction were measured with an anemometer and vane (03001-L, R.M.Young wind sentry set, R.M. Young Company) mounted at the top of a steel frame about 6m high at the northwest corner of FV1 (Fig.A.10).

Figure A.10 Anemometer and vane mounted on the steel frame to measure wind speed and direction

A.3.4 Data Collection

In 2003, the data monitored in the FV houses and that of outside weather were recorded by a Fluke Helios I datalogger connected to a PC. The data in the NV houses were recorded with two Campbell Scientific dataloggers, a CR23X and a CR10x, combined with three thermocouple multiplexers (AM25T) and two voltage multiplexers (AM16/32). Readings were every minute. The data were downloaded to a laptop on a daily basis.

From 2004, an additional thermocouple multiplexer was added and the CR10x was replaced. All recorded data are 10 min averages of 1 min readings.

In 2006, an additional CR23X was used to record the leaf wetness data and working status of the high-pressure pump of the high-pressure fogging system.

A.4 Treatments

2003 The treatments imposed in the FV houses consisted of ventilation rates of one of two levels, LV 0.041$m^3.m^{-2}$. [floor] s^{-1} and HV 0.087 m^3 m^{-2} [floor] s^{-1} combined with evaporative pad cooling at either full or none. In the NV houses the treatments consisted of all three vents (south, north and roof) or just the south and roof, combined with using the fogging nozzles or not. When used, the fogging nozzles were allowed only when the maximum allowed number of vents were open.

The treatments were imposed so that each treatment in a house type could be compared to all the treatments in the other house type. No one treatment was allowed to be imposed in a given house for longer than four consequentive days in order to minimize any bias on plant yield.

2004 In the FV houses, maximum cooling was provided by evaporative pad cooling and a ventilation flow rate of 0.087 m^3 m^{-2} [floor] s^{-1}. In the NV houses maximum cooling was all vents open plus all 24 fog nozzles in use. The fogging schedule was adjusted, by trial and error, to prevent excessive foliage wetting. The final result was that the first eight nozzles were employed when the inside temperature exceeded the high cooling set point by 1 C. The other 16 nozzles were triggered when the inside temperature exceeded the high cooling set point by 1.67 C and the outside temperature exceeded the high cooling set point by 2.5 C. All 24 nozzles were used when the inside temperature exceeded the maximum cooling set point by 2.5 C and the outside temperature exceeded the maximum cooling set point by 5 C. No fogging was permitted when solar radiation outside was below 650 W m^{-2}.

Only the first eight nozzles were used when the wind speed was less than 1.4 m s^{-1}. Furthermore, the nozzles were operated on a 15 s on-15 s off cycle so that the water delivery rate was 1/2 that of the maximum capacity of the nozzles.

2005 The treatments in FV greenhouses were the same as in 2004. In the NV houses, different approaches were taken in the two houses. In NV1, the use of the south and top vents was combined with the low-pressure fogging for the whole season (with a few exceptions). In NV2, the number of vents alternated on a preset schedule between two and three, coupled with fogging, for most of the season. Starting on 7/10, an additional treatment was added to the NV2 house to facilitate work with the naturally ventilated model. Venting was limited to top vent only and fogging was excluded. This was employed one day per week for the first three weeks (starting on 7/10), and two days per week for the remainder of the season. Exceptions to the above schedule were required for the period 6/13 until 6/20, shortly after transplanting, when an extremely severe heat wave severely stressed the young plants in both NV houses. During that period both NV1 and NV2 were operated with all three vents plus fogging.

Fogging was controlled by manually setting the minimum frequency for cycling the fogging nozzles. This frequency was adjusted by the computer based on inside and outside temperatures, increasing as temperatures increased. In addition, the number of nozzles available for fogging was also varied based on inside and outside temperature. The parameters and logic were adjusted by trial and error in an attempt to maximize cooling while minimizing the amount of water deposited on the leaves.

2006 Four cooling treatments were applied in FV1 house: LV without evaporative pad, LV with pad, HV without pad and HV with pad. The data were used to investigate the

thermal stratifications in FV greenhouse. The experiments were conducted in the NV greenhouses to study fog control algorithms and cooling performance of the low-pressure and high-pressure fogging systems.

Appendix B Selection of experimental data in analyzing the cooling effect of fogging systems

In comparing the low-pressure fogging and high-pressure fogging systems, only valid data were selected for the regression analyses. The data were regarded invalid if the data were from the days when fogging was disrupted by severe weather such as thunderstorms, showers, or windy weather for a significant portion of daytime. The data compromised by sensor failure, human misoperation and control program bugs were also regarded as invalid.

When the observed evaporation efficiency and cooling efficiency exhibited certain patterns that were clearly unreasonable, for example, cooling efficiency was negative or evaporation efficiency exceeded one, the data were excluded. Tables B.1 and B.2 list the days that were included for the analysis of the fogging systems.

Table B.1 Data selected for analysis of the low-pressure fogging system

Date	Julian Date	Vent Config.	Evap. Eff.	Cooling eff.	Included	Weather
7/20/06	201	S+T+N	good	good	√	
7/21/06	202	S+T	good	good	√	
7/22/06	203	S+T+N	bad	bad	X	
7/23/06	204	S+T+N	bad	bad	X	
7/24/06	205	S+T+N	good	good	X	
7/25/06	206	S+T+N	bad	bad	X	
7/26/06	207	S+T+N	good	good	√	
7/27/06	208	S+T+N	good	good	√	
7/28/06	209	S+T	good	good	√	
7/29/06	210	S+T+N	good	good	√	
7/30/06	211	S+T+N	good	good	√	
7/31/06	212	S+T+N	good	good	√	Sunny, hot
8/1/06	213	S+T+N	good	good	X	Sunny, hot
8/2/06	214	S+T	bad	good	X	
8/3/06	215	S+T+N	bad	good	√	hot
8/4/06	216	S+T	good	good	√	Sunny, very hot
8/5/06	217	S+T+N	good	good	X	Cloudy
8/6/06	218	S+T+N	bad	good	X	Sunny, warm
8/7/06	219	S+T+N	bad	bad	X	Sunny
8/8/06	220	S+T+N	bad	good	√	Sunny
8/9/06	221	S+T	bad	good	X	Cloudy
8/10/06	222	S+T+N	good	good	√	Cloudy->sunny
8/11/06	223	S+T	bad	bad	X	Cloudy
8/12/06	224	S+T+N	bad	bad	X	
8/13/06	225	S+T+N	good	good	√	
8/14/06	226	S+T+N	good	good	√	Sunny
8/15/06	227	S+T+N	good	good	√	Sunny
8/16/06	228	S+T	bad	good	X	Cloudy
8/17/06	229	S+T+N	bad	good	X	sunny, windy
8/18/06	230	S+T	bad	good	X	Cloudy->partial
8/19/06	231	S+T+N	bad	good	X	sunny warm
8/20/06	232	S+T+N	good	good	√	Part. Cloudy
8/21/06	233	S+T+N	good	good	√	Cloudy
8/22/06	234	S+T+N	bad	bad	X	Cloudy

Table B.2 Data selected for the analysis of the high-pressure fogging system

Date	Julian Date	Vent Config.	Evap. Eff.	Cooling eff.	Included	Weather
6/4/06	155		bad	bad	X	
6/5/06	156		bad	bad	X	
6/6/06	157	S+T+N	bad	bad	X	
6/7/06	158	S+T+N	good	good	√	
6/8/06	159	S+T	good	bad	X	
6/9/06	160	S+T	good	good	√	
6/10/06	161	S+T+N	good	good	X	
6/11/06	162	S+T+N	bad	good	X	
6/12/06	163	S+T	bad	bad	X	
6/13/06	164		bad	bad	X	rainy
6/14/06	165		bad	bad	X	rainy
6/15/06	166	S+T	bad	good	X	
6/16/06	167	S+T	bad	good	X	
6/17/06	168	S+T+N	good	good	√	
6/18/06	169	S+T+N	good	good	√	
6/19/06	170	S+T+N	good	good	√	
6/20/06	171	S+T+N	good	good	√	
6/21/06	172	S+T+N	bad	bad	X	
6/22/06	173	S+T+N	bad	good	X	
6/23/06	174	S+T	bad	bad	X	
6/24/06	175		bad	bad	X	rainy
6/25/06	176		bad	bad	X	rainy
6/26/06	177		bad	bad	X	rainy
6/27/06	178	S+T+N	bad	bad	X	
6/28/06	179	S+T+N	bad	good	X	
6/29/06	180	S+T+N	good	good	√	
6/30/06	181	S+T	good	good	√	
7/1/06	182	S+T+N	good	good	√	
7/2/06	183	S+T+N	good	good	√	
7/3/06	184	S+T+N	good	good	√	

Two examples are provided here to illustrate the method for distinguishing the days for which data were assumed valid. Figure B.1 shows the data from Julian day of 178, when it was cloudy and air temperature was low. The high-pressure fogging system worked at the spray rates far below its design specifications and the data did not reflect the cooling effect of

the fogging system. Also a significant portion of the data during the day were missing due to sensor failure. On the other hand, on Julian day of 170 when solar radiation and air temperature were high, the fogging system worked at spray rate near to its design condition. The data fully reflected the cooling effect of the system therefore they were used in the analysis.

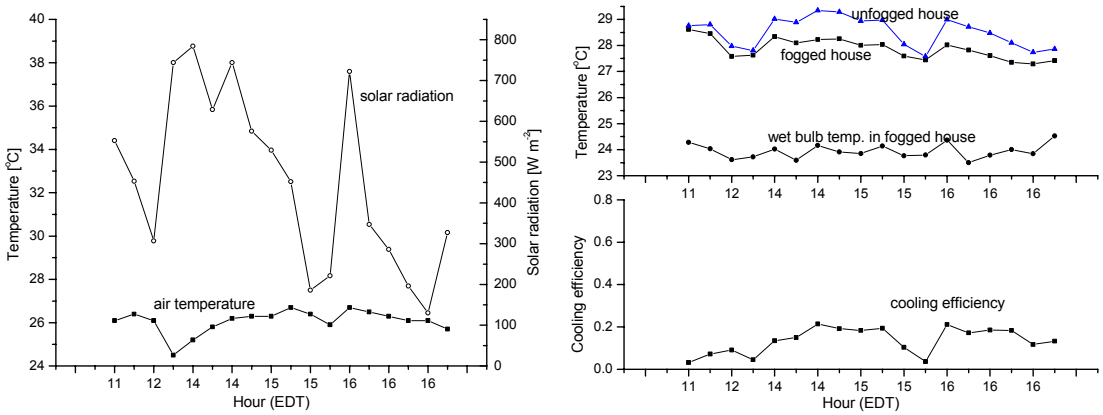

Figure B.1 Example of the days when the data were compromised and therefore not used (Julian date 178)

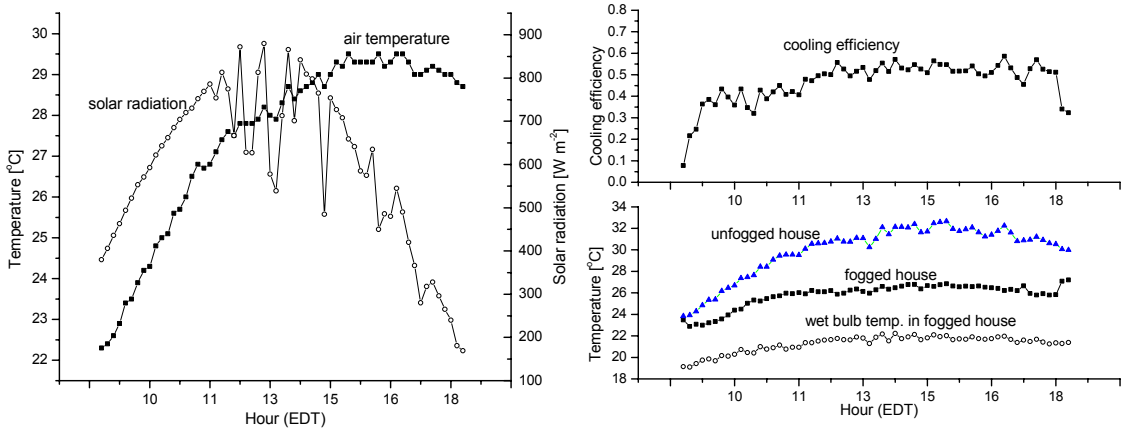

Figure B.2 Example of day when the data were regarded as valid and used (Jilian date 170)

Appendix C High-pressure fog control with temperature and relative humidity --Control strategy 1

```
/*control with temperature and relative humidity*/
/*--------------------------------*/

void chk_hpfog_level(void)
{
  float rh52;
  float rhamb;
  if (house != 3) /*if not the greenhouse with high-pressure fog*/
  {
     chk_fog_level(); /*switch to low pressure fog routine*/
     return;
  }
  if (daytime)  /*restrict fog to day time*/
  {
     if (((solar/100)/sol_cf) > 100)  /*solar check, if solar radiation greater than 100W/m2 */
      {
        /* ---------------outside humidity checking----------------------*/
        rhamb=humid(tamb,twamb);  /*calculate outside relative humidity use dry and wet bulb temps*/
        if (rhamb>=0.85)/* very muggy condition, possibly rain*/
        {
           port_stat[9]=port_stat[9]&207;  /*disable fog*/
           return;
        }

        /* ---------------inside humidity checking----------------------*/
        rh52=humid(pstmp0[house],tw52); /*if inside RH is high, reduce fog by 1 level*/

        if ((rh52>0.87) && (pst_port_stat[1][9]>=48))/*if level 2 on,shift to level 1*/
        {
           port_stat[9]=pst_port_stat[1][9]-32;
           sub_sum [MST1][house]++;
           return;
        }

        if((rh52>0.87) && (pst_port_stat[1][9]>=16))/*if level 1 on, disable it*/
        {
           port_stat[9]=pst_port_stat[1][9]-16;
```

```
            return;
        }

        if((rh52>0.87) && (pst_port_stat[1][9]<15))/* if no fog, retain state*/
        {
            port_stat[9]=pst_port_stat[1][9]&207;
            return;
        }


        /*-------------------inside temperature checking----------------------*/
        if (pstmp0[house] > hicool_stpt+5) /*if inside temperature 5 F higher than setpoint*/
        {

            if (pst_port_stat[1][9]>=16)/* if first level fog was already on*/
            {
                chk_hpfog_hi();  /*use second level fog*/
                return;
            }

            if (pst_port_stat[1][9]<16)/*if no fog was on*/
            {
                chk_hpfog_lo(); /*use the first level fog*/
                return;
            }
        }

        if (pstmp0[house] > (hicool_stpt+1)) /*if inside temp 1 F higher than setpoint*/
        {
            chk_hpfog_lo(); /*use first level fog*/
            return;
        }
    }
    return;
  }
}



/*----------------------------------------*/
/*calculate relative humidity with dry and wet bulb temps*/
/* tdb in F, twb in F*/
```

```
float humid(float tdb, float twb)
{
  float psdb;
  float pswb;
  float hvap;
  float pvest;
  float bprime;
  float pv;
  float rh;
  float patm=101325;
   int cnt = 0;
  float del = 1.0;

  if (twb > tdb) twb = tdb;

  psdb=press(tdb);
  pswb=press(twb);

  hvap = 2502535.259 - 2385.76424*(tdb-32)*5/9;
  pvest = 0.5*psdb;

   do
  {
     bprime = 1006.9254*(pswb - patm)*(1 + (0.15577*pvest/patm))/(0.62194*hvap);
     pv = bprime*(tdb - twb)*5/9 + pswb;
     del = (pv - pvest)/pvest;
     cnt = cnt + 1;
     pvest = pv;
  }while ((abs(del) >= 0.0001) & (cnt <= 100));

  if (cnt > 100)
  {
     printf("not converged\n");
     return(0);
  }
   rh = pv/psdb;
  return (rh);
}


/*---------------------------------------*/
```

```
/* calculate saturated vapor press with dry bulb temp. */
/* p is in Pa and t is in F */
float press(float t)
{
  float a1=-5.6745359e+03;
  float a2=6.3925247e+00;
  float a3=-9.677843e-03;
  float a4=0.6221570e-06;
  float a5=2.0747825e-09;
  float a6=-0.9484024e-12;
  float a7=4.1635019e+00;
  float a8=-5.8002206e+03;
  float a9=1.3914993e+00;
  float a10=-48.640239e-03;
  float a11=41.764768e-06;
  float a12=-14.452093e-09;
  float a13=6.5459673e+00;
  float p;
   t=(t-32)*5/9;  /*convert form F to C*/
  if (t>60 | t<-40)
  {
     printf("error reading");
     return(0);
  }
  t = t + 273.16;
  if (t > 273.16)
     p = (a8/t + a9 + a10*t + a11*t*t + a12*t*t*t + a13*log(t));
  else
     p = (a1/t + a2 + a3*t + a4*t*t + a5*t*t*t + a6*t*t*t*t + a7*log(t));
  p = exp(p);
  return(p);

}
```

Appendix D High-pressure fog control based on Handarto's paper---Control strategy 2

```
/*--------------high-pressure fog control based on Handarto's paper------------------*/
void chk_hpfog_level(void)
{
  float rh52;
  float ms;                 /* spray rate*/
  float mr;                 /* requred spray rate*/
  float lamda;               /* fog demand/suppy ratio*/

  if (house != 3)           /*if house no is not the one with hp fog*/
  {
     chk_fog_level();       /*switch low pressure control*/
     return;
  }

  if (daytime)
  {
     if (((solar/100)/sol_cf) > 100)  /*restrict hp fog to period when solar>100W/m2*/
      {
        /* ---------------rain checking--------------------------------*/
        if (rain==true)              /*rain is defined as rh>90%, solar<180*/
        {
           port_stat[9]=port_stat[9]&207;   /*disable fog*/
           printf("raining!fog disabled\n");
           return;
        }
        /* ---------------inside humidity checking----------------------*/
        rh52=humid(pstmp0[house],tw52); /*if inside RH is high, reduce fog by 1 level*/
        if (rh52>0.90)
        {
           printf("high inside humidity,reduce fog by 1 level\n");
           if(pst_port_stat[1][9]>=48)
           {
              port_stat[9]=pst_port_stat[1][9]-32;/*if level 2 on,switch to level 1*/
              sub_sum [MST1][house]++;
              return;
           }

           if (pst_port_stat[1][9]>=16)/*if level 1 on, disable it*/
```

```
            {
               port_stat[9]=pst_port_stat[1][9]-16;
               return;
            }

            if (pst_port_stat[1][9]<15)/* if no fog, retain state*/
            {
               port_stat[9]=pst_port_stat[1][9]&207;
               return;
            }
         }
         /*--------------use sprayrate() to determine the fog level---------*/
         if ((rh52<=0.90)&&(pstmp0[house]>hicool_stpt))
         {
            ms=0.01677;        /*design spray rate of 11 nozzles=11*3.785*1.45/3600 kg/s*/
            mr=sprayrate();
            lamda=mr/ms;
            printf("spray rate=%1.5f\n",ms);
            printf("required spray rate=%1.5f\n",mr);
            printf("demand/supply ratio=%1.3f\n",lamda);

            if (lamda>0.5)                    /*high heat load*/
            {
               chk_hpfog_hi();
               return;
            }
            else if ((lamda<=0.5) && (lamda>0.05))  /*moderate heat load*/
            {
               chk_hpfog_lo();
               return;
            }
            else
            {
               port_stat[9]=port_stat[9]&207;     /*disable fog*/
               return;
            }
         }
      }
   }
}
```

```
/*---------------determine required spray rate-----------------------------*/
float sprayrate(void)
{
  float k=4.0;        /*overall heat transfer coeff of cover,W/(m2 C)*/
  float w=1.96;       /*glazing to ground area ratio*/
  float area=72.6;    /*floor area,m2*/
  float hi,ho;        /*inside and outside enthalpies, J/kg*/
  float q;            /*ventilation rate, kg/(m2 s)*/
  float td52_new,rh52_new;    /*target inside temperature and relative humidity */
  float rh52;               /*inside relative humidity*/
  float xi,xit;       /*humidity ratio and target humidity ratio, kg/kg DA*/
   float mr;          /*required spray rate to reach setpoint temp, kg/s*/
   float t52;         /*inside dry bulb temperature*/

  t52=pstmp0[house];

  /*------determine ventilation rate-----*/
  ho=enthalpy(tamb,twamb); /*calculate outside enthalpy*/
  hi=enthalpy(t52,tw52);   /*calculate inside enthalpy*/
  printf("outside enthalpy=%5.0f \n",ho);
  printf("inside enthalpy=%5.0f \n",hi);
  if (hi<=ho) /*if inside enthalpy lower than outside*/
  {
     mr=0;
     return(mr);
     printf("inside enthalpy is lower than outside");
  }
  q=(solar*0.5+k*w*(tamb-t52)*5/9)/(hi-ho); /*calculate ventilation rate using enthalpy diff*/
  printf("ventilation rate=%1.4f \n",q);


  /*------determine spray rate------------*/
  rh52=humid(t52,tw52);    /*inside relative humidity*/
  xi=abs_humid(t52,rh52);  /*inside humidity ratio*/
  printf("current humidity ratio=%1.6f\n",xi);

  if (hicool_stpt<=tw52) /*if setpoint lower than wet bulb temp,unrealistic setpoint is set*/
  {
     rh52_new=0.87;  /*set target rh to 87%*/
     td52_new=drybulb(tw52,rh52_new); /*calculate target dry bulb temp with wet bulb temp and
```

```
target rh*/
      xit=abs_humid(td52_new,rh52_new); /*calculate target humidity ratio*/
      mr=q*area*(xit-xi)/0.57;/*the average evaporation eff. 57% is from 2005 study*/
       printf("hicool setpoint is lower than inside wet bulb\n");
       printf("use 87 per humidity to determine spray rate\n");
      printf("target humidity ratio=%1.6f\n",xit);
      return(mr);
   }
   else
   {
      rh52_new=humid(hicool_stpt,tw52);/*calculate projected rh with current wet bulb and
setpoint temp*/
      td52_new=hicool_stpt;
      if (rh52_new>0.87) /* reaching hicool_stpt will exceed 87% RH*/
      {
         rh52_new=0.87;/*set target rh as 87%*/
         td52_new=drybulb(tw52,rh52_new);/*renew target temperature*/
         printf("new targe temp=%2.1f\n",td52_new);
         xit=abs_humid(td52_new,rh52_new);/*calculate target humidity ratio*/
         printf("target humidity ratio=%1.6f\n",xit);
         mr=q*area*(xit-xi)/0.57;
         return(mr);
      }

      xit=abs_humid(td52_new,rh52_new);
      printf("target humidity ratio=%1.6f\n",xit);
      mr=q*area*(xit-xi)/0.57;
      return(mr);
   }
}
```

Appendix E High-pressure fog control with VPD---Control strategy 3

```
/*-----------high-pressure fog control using VPD---------------------*/
void chk_hpfog_level(void)
{
  float rh52;     /*relative humidity in 452,decimal*/
  float v;        /*saturated vapor pressure @ t52*/
  float vpd52;    /*vapor pressure deficit of 452*/

  if (house != 3)
  {
     chk_fog_level();
     return;
  }

  if (daytime)
  {
     /*----------------------check rain-------------------------*/
     if (rain)
     {
        port_stat[9]=port_stat[9]&207;   /*disable fog in 452*/
         printf("raining!high-pressure fog disabled\n");
        return;
     }

     /*----------------------check VPD in 452-----------------*/
     rh52=humid(pstmp0[house],tw52);
     v=press(pstmp0[house]);
     vpd52=v*(1-rh52);
     printf("absolute humidity = %3.0f\n",v);
     printf("relative humidity = %0.3f\n",rh52);
     printf("vpd52=%3.0f\n", vpd52);
     if (vpd52>vpd_foglevel2)
     {
        chk_hpfog_hi();
        return;
     }

     if (vpd52>vpd_foglevel1)
```

```
        {
            chk_hpfog_lo();
            return;
        }
    }
}
```

Appendix F High-pressure fog control based on Sase's paper--

-Control strategy 4

```
/*------------high-pressure fog control based on Sase' paper--------------------*/

void chk_hpfog_level(void)
{
  float rh52;     /*relative humidity in 452,decimal*/
  float rh52_avg; /*average rh during the last minute in 452*/
   int i,j,k;
  if (house != 3)
  {
     chk_fog_level();
     return;
  }

  if (daytime)
  {
     /*----------------------fog triggered with temp-----------------*/
      printf("temp in 452=%2.0f\n",pstmp0[house]);
     if (pstmp0[house]>(hicool_stpt+4.5))
     {
        chk_hpfog_hi();
     }else if (pstmp0[house]>hicool_stpt+1)
     {
        chk_hpfog_lo();
     }

     /*----------------------check rain-------------------------*/
     if (rain)
     {
        port_stat[9]=port_stat[9]&207;   /*disable fog in 452*/
         printf("raining!high-pressure fog disabled\n");
     }

      /*---------------------inside humidity check--------------------*/
      rh52=humid(pstmp0[house],tw52);
      if (rh52>0.87)
     {
        port_stat[9]=port_stat[9]&207;   /*disable fog in 452*/
```

```
     printf("high humidity!high-pressure fog disabled\n");
}

/*-----------------record fog action-------------------------*/
 if (hpfog_cnt>=40)
    hpfog_cnt=0;

if ((fmod(min,10.0))==0 && (sec==0)) /*restart counting from zero*/
{
    hpfog_cnt=0;
}

if (port_stat[9]==0)
{
    hpfog_stat[hpfog_cnt]=0;
}

if (port_stat[9]==16)
{
    hpfog_stat[hpfog_cnt]=1;
}

if (port_stat[9]==48)
{
    hpfog_stat[hpfog_cnt]=2;
}

 hpfog_cnt++;

 /*----------------------vent triggered with humidity--------------*/

if ((fmod(min,10.0)==0) && (sec==0))/*recount vent config from zero*/
{
    vent_cnt=0;
    vent_intvl=0;
}

if (vent_intvl>=8)
    vent_intvl=0;

if (vent_cnt>=5)
    vent_cnt=0;
```

```
        rh52_2[vent_intvl]=rh52;

        printf("rh[%1d]=%1.2f\n",vent_intvl,rh52_2[vent_intvl]);

        if ((sec==0) && (fmod(min,2.0)==0))
        {
            rh52_avg=(rh52_2[4]+rh52_2[5]+rh52_2[6]+rh52_2[7])/4;
           if (rh52_avg<0.75)
           {
              port_stat[3]=SS_OPEN + NS_CLOSE + TOP_OPEN;
              port_stat[4]=SS_OPEN + NS_CLOSE + TOP_OPEN;
           }

           if (rh52_avg>0.80)
           {
              port_stat[3]=SS_OPEN + NS_OPEN + TOP_OPEN;
              port_stat[4]=SS_OPEN + NS_OPEN + TOP_OPEN;
           }

           if ((rh52_avg>=0.75) && (rh52_avg<=0.80))
           {
              port_stat[3]=pst_port_stat[1][3];
              port_stat[4]=pst_port_stat[1][4];
           }

            vent_config[vent_cnt]=port_stat[3];
            vent_intvl = 0;
           vent_cnt++;
        }
        else
        {
           port_stat[3]=pst_port_stat[1][3];
           port_stat[4]=pst_port_stat[1][4];
        }

        /*vent_intvl is a count of the 15s intervals in 2 min period.*/
        vent_intvl++;
    }
}
```

Appendix G NCSU control ---Control strategy 5

```
/*----------------------high-pressure fog control using psychrometric chart----------------------*/
void chk_hpfog_level(void)
{
  float rh52;     /*relative humidity in 452,decimal*/
   /*float rh_setpoint; relative humidity setpoint*/
   /*float t_setpoint;  temperature setpoint*/
  float ho, hs;      /*outside and setpoint enthalpy*/
  float xo,xs;       /*outside and setpoint humidity ratio*/
   float beta,beta2;  /*ratios indicating required and current
                ventilation and spray rate*/
  float vent_ratio=1.0;
  float x52_avg, x52_avg_fog;       /*average humidity ratio during the last 4 mins
                           and 30s in 452*/
  float h52_avg, h52_avg_fog;       /*average enthalpy during the last 4 mins
                           and 30s of 452*/
  float q_avg,q_avg_fog;            /*average ventilation rate during the last 4 mins
                          and 30s of 452*/
   float ms,mr;/*nominial spray rate of 12 nozzles and required spray rate*/
  float x_new, q_new;     /*updated humidity ratio and ventilation rate*/
  float area=72.6;     /*m2*/
   float tw_setpoint;    /*wet bulb setpoint*/
   float tw_setpoint_old;
   float hs_old;
   int i,j,k;

  if (house != 3)
  {
     chk_fog_level();
     return;
  }

  if (daytime)
  {

     /*-----------------------check rain-------------------------*/
     if (rain)
     {
        port_stat[9]=port_stat[9]&207;   /*disable fog in 452*/
         printf("raining! hp fog disabled\n");
         return;
```

```
}

 /*----------------------inside humidity check--------------------*/
 rh52=humid(pstmp0[house],tw52);
 if (rh52>0.9)
{
    port_stat[9]=port_stat[9]&207;   /*disable fog in 452*/
     /*port_stat[3]=SS_OPEN + NS_OPEN + TOP_OPEN;*/
     printf("humidity is above 90% ! hp fog disabled\n");
     return;
}

 /*-------------------------------------------------------------------*/
 /*----------------------vent controlled by enthalpy--------------------*/
 /*-------------------------------------------------------------------*/

 /*if outside enthalpy is higher than setpoint,adjust setpoint*/
 ho=enthalpy(tamb,twamb);
 xo=abs_humid(tamb,humid(tamb,twamb));
hs=enthalpy(t_setpoint,humid1(t_setpoint,rh_setpoint));
 xs=abs_humid(t_setpoint,rh_setpoint);
 tw_setpoint=humid1(t_setpoint,rh_setpoint);

 if((hs<=ho)||(tw_setpoint<=twamb))
 {
    printf("Warning! unreasonable setpoint!\n");
    tw_setpoint=twamb+solar*0.003;
     t_setpoint=ceil(drybulb(tw_setpoint,rh_setpoint));
 }

 //check if the old setpoint is applicable. restore if yes
 hs_old=enthalpy(t_setpoint_old,humid1(t_setpoint_old,rh_setpoint));
 tw_setpoint_old=humid1(t_setpoint_old,rh_setpoint);
 if ((ho<hs_old) && (tw_setpoint_old>=(twamb+1)))
 {
    t_setpoint=t_setpoint_old;
 }

 printf("psychart control mode in effect\n");

 /*calculate and record current inside enthalpy,humid ratio and ventilation rate*/
h52[vent_intvl]=enthalpy(pstmp0[house],tw52);
 x52[vent_intvl]=abs_humid(pstmp0[house],humid(pstmp0[house],tw52));
```

```
 if (h52[vent_intvl]!=ho)
 {
   q[vent_intvl]=0.5*solar/(h52[vent_intvl]-ho);
 }

/*transfer vent config data to the other array and zero index vent_cnt*/
 if ((sec==0) && (fmod(min,10.0)==0))
 {
    for(i=0;i<2;i++)
    {
       vent_config2[i]=vent_config[i];
    }
    vent_cnt=0;
 }

 /*---------if clock clicks at 5 min, vent control is triggered------*/
if ((sec==0) && (fmod(min,5.0)==0))
{
    /*calculate averge enthalpy,humidity ratio and ventilation
          during past 5 mins*/
    h52_avg=0;
    x52_avg=0;
    q_avg=0;

   if ((vent_intvl2==0)&&(vent_intvl==0))
    {
       h52_avg=h52[vent_intvl2];
      x52_avg=x52[vent_intvl2];
      q_avg=q[vent_intvl2];
    }
    if ((vent_intvl2==0)&&(vent_intvl==1))
    {
       h52_avg=(h52[0]+h52[1])/2;
      x52_avg=(x52[0]+x52[1])/2;
      q_avg=(q[0]+q[1])/2;
    }
    if (vent_intvl2>=1)
    {
       for(i=0;i<=vent_intvl2;i++)
       {
          h52_avg=h52_avg+h52[i];
          x52_avg=x52_avg+x52[i];
```

```
        q_avg=q_avg+q[i];
    }
    h52_avg=h52_avg/(vent_intvl2+1);
    x52_avg=x52_avg/(vent_intvl2+1);
    q_avg=q_avg/(vent_intvl2+1);
 }

beta=(h52_avg-ho)/(hs-ho);

 /*--------------if program calling for more ventilation-----------*/
 if(beta>1)
 {
    /*if original vent configuration is South vent open only*/
    if(pst_port_stat[1][3]==(SS_OPEN + NS_CLOSE + TOP_CLOSE))
    {
        if (beta<1.5)
        {
            port_stat[3]=pst_port_stat[1][3];
          vent_ratio=1.0;
        }

        if((beta>=1.5)&&(beta<=3.6))
        {
            port_stat[3]=SS_OPEN + NS_CLOSE + TOP_OPEN;
          vent_ratio=3.0;
        }

        if(beta>3.6)
        {
            port_stat[3]=SS_OPEN + NS_OPEN + TOP_OPEN;
          vent_ratio=3.33;
        }
    }

    /*if original vent configuration is south+top open*/
    if(pst_port_stat[1][3]==(SS_OPEN + NS_CLOSE + TOP_OPEN))
    {
        if (beta<1.06)
        {
            port_stat[3]=pst_port_stat[1][3];
          vent_ratio=1.0;
        }
```

```
        if(beta>=1.06)
        {
            port_stat[3]=SS_OPEN + NS_OPEN + TOP_OPEN;
          vent_ratio=1.11;
        }
    }

    /*if original vent configuration is south+top+north open*/
    if(pst_port_stat[1][3]==(SS_OPEN + NS_OPEN + TOP_OPEN))
    {
        port_stat[3]=pst_port_stat[1][3];
       vent_ratio=1.0;
    }
}

/*--------------if program calling for less ventilation-----------*/
if(beta<1)
{
    /*if original vent configuration is South vent open only*/
    if(pst_port_stat[1][3]==(SS_OPEN + NS_CLOSE + TOP_CLOSE))
    {
          port_stat[3]=pst_port_stat[1][3];
         vent_ratio=1.0;
    }

    /*if original vent configuration is south+top open*/
    if(pst_port_stat[1][3]==(SS_OPEN + NS_CLOSE + TOP_OPEN))
    {
        if (beta>=0.67)
        {
            port_stat[3]=pst_port_stat[1][3];
          vent_ratio=1.0;
        }

        if(beta<0.67)
        {
            port_stat[3]=SS_CLOSE + NS_CLOSE + TOP_OPEN;
          vent_ratio=0.33;
        }
    }

    /*if original vent configuration is south+top+north open*/
```

```
        if(pst_port_stat[1][3]==(SS_OPEN + NS_OPEN + TOP_OPEN))
        {
            if (beta>0.95)
            {
                port_stat[3]=pst_port_stat[1][3];
              vent_ratio=1.0;
            }

            if ((beta>=0.45)&& (beta<=0.95))
            {
                port_stat[3]=SS_OPEN + NS_CLOSE + TOP_OPEN;
              vent_ratio=0.9;
            }

            if (beta<0.45)
            {
                port_stat[3]=SS_CLOSE + NS_CLOSE + TOP_OPEN;
              vent_ratio=0.3;
            }
        }
    }

    if (beta==1)
    {
        port_stat[3]=pst_port_stat[1][3];
       vent_ratio=1.0;
    }

    if (pst_port_stat[1][3]!=(SS_OPEN + NS_OPEN + TOP_OPEN) &&
        pst_port_stat[1][3]!=(SS_OPEN + NS_CLOSE + TOP_OPEN) &&
        pst_port_stat[1][3]!=(SS_CLOSE + NS_CLOSE + TOP_OPEN))
    {
       port_stat[3]=SS_OPEN + NS_OPEN + TOP_OPEN;
    }

    vent_intvl=0;
    /*record vent configuration*/
    vent_config[vent_cnt]=port_stat[3];
    printf("vent_config[%d]=%d\n",vent_cnt,vent_config[vent_cnt]);
   vent_cnt++;
    printf("vent_ratio=%1.1f\n",vent_ratio);
}
```

```
else
{
    port_stat[3]=pst_port_stat[1][3];
    vent_ratio=1.0;
}
 vent_intvl2=vent_intvl;
vent_intvl++;

 /*recount vent config from zero*/
 if (vent_cnt>=2)  vent_cnt=0;
 if (vent_intvl>=20) vent_intvl=0;

 /*-------------------------------------------------------------*/
 /*-------------fog is controlled by humidity ratio------------*/
 /*-------------------------------------------------------------*/
 h52_2[hpfog_intvl]=enthalpy(pstmp0[house],tw52);
 x52_2[hpfog_intvl]=abs_humid(pstmp0[house],humid(pstmp0[house],tw52));
q_2[hpfog_intvl]=0.5*solar/(h52[hpfog_intvl]-ho);

 /*transfer fog action history data to the other array and
zero index hpfog_cnt*/
 if ((sec==0) && (fmod(min,10.0)==0))
 {
    for(i=0;i<20;i++)
    {
        hpfog_stat2[i]=hpfog_stat[i];
    }
    hpfog_cnt=0;
 }

if (fmod(sec,30.0)==0)
 {

   /*calculate average humidity ratio and ventilation rate during 30s*/
    x52_avg_fog=0;
    q_avg_fog=0;
    if ((hpfog_intvl2==0)&&(hpfog_intvl==0))
    {
        x52_avg_fog=x52_2[hpfog_intvl];
       q_avg_fog=q_2[hpfog_intvl];
    }
    else
    {
```

```
   /*x52_avg_fog=x52_2[hpfog_intvl];
 q_avg_fog=q_2[hpfog_intvl]; */

    x52_avg_fog=(x52_2[0]+x52_2[1])/2;
    q_avg_fog=(q_2[0]+q_2[1])/2;
 }

 /*---------determine spray rate----------*/
ms=0.014;        /*spray rate of 12 nozzles
             =12*3.785*1.109523/3600 kg/s*/
if ((sec==0) && (fmod(min,5.0)==0))
 {
  x_new=xo+(x52_avg-xo)/vent_ratio;
  q_new=q_avg*vent_ratio;
   mr=q_new*area*(xs-x_new)/0.57;
 }
 else
 {
   x_new=x52_avg_fog;
   q_new=q_avg_fog;
   mr=q_new*area*(xs-x_new)/0.57;
 }
 beta2=mr/ms;
 /*------call for more water----------------*/
 if (beta2>0)
 {
    /*if fog was not on*/
    if (pst_port_stat[1][9]==0)
    {
       if (beta2>1.5)
       {
          chk_hpfog_hi();
       }
       if((beta2<=1.5) && (beta2>=0.05))
       {
          chk_hpfog_lo();
       }
       if (beta2<0.05)
       {
          port_stat[9]=port_stat[9]&207;
       }
    }
```

```
    /*if low level fog was on*/
    if (pst_port_stat[1][9]==16)
    {
        if(beta2>0.5)
        {
            chk_hpfog_hi();
        }

        if (beta2<=0.5)
        {
            chk_hpfog_lo();
        }

    }

    /*if high level fog was on*/
    if (pst_port_stat[1][9]==48)
    {
        chk_hpfog_hi();
    }
}

/*------call for less water----------------*/
if (beta2<0)
{
    /*if fog was not on*/
    if (pst_port_stat[1][9]==0)
    {
        port_stat[9]=pst_port_stat[1][9];
    }

    /*if low level fog was on*/
    if (pst_port_stat[1][9]==16)
    {
        if(beta2<-0.5)
        {
            port_stat[9]=port_stat[9]&207;
        }

        if (beta2>=-0.5)
        {
            chk_hpfog_lo();
        }
```

```
    }

     /*if high level fog was on*/
    if (pst_port_stat[1][9]==48)
    {
        if (beta2>-0.5)
        {
            chk_hpfog_hi();
        }

        if((beta2>=-1.5)&&(beta2<=-0.5))
        {
            chk_hpfog_lo();
        }

        if (beta2<-1.5)
        {
            port_stat[9]=port_stat[9]&207;
        }
    }
}

/*------------don't change spray rate---------------*/
if (beta2==0)
{
    port_stat[9]=pst_port_stat[1][9];
}

/*-----------------record fog action-------------------------*/
/*code fog level as 0,1,2 for no fog, low, high*/
if (port_stat[9]==0)
{
   hpfog_stat[hpfog_cnt]=0;
}

if (port_stat[9]==16)
{
   hpfog_stat[hpfog_cnt]=1;
}

if (port_stat[9]==48)
```

```
            {
              hpfog_stat[hpfog_cnt]=2;
            }
            printf("hpfog_stat[%d]=%d\n",hpfog_cnt,hpfog_stat[hpfog_cnt]);
            hpfog_intvl=0;
            hpfog_cnt++;
          }
          else/*if time is not on half minute,retain fog level from last 15sec*/
          {
            port_stat[9]=pst_port_stat[1][9];
          }
          hpfog_intvl2=hpfog_intvl;
          hpfog_intvl++;
          if (hpfog_cnt>=20) hpfog_cnt=0;
          if (hpfog_intvl>=2) hpfog_intvl=0;
      }
    }
```

Appendix H Calibration procedure for leaf wetness sensor

The sensors were painted with white latex paint to spread the fog droplets because the fog droplet is not large enough to touch the adjacent conducting strips. The sensors were calibrated at three wetness levels: the first represents totally dry; the second represents a moderate level of moisture, but no visible droplets present on sensor surface; the third represents wet condition where a layer of visible droplets was sitting on sensor surface. For each wetness sensor, the true resistance of the two resistors R_1 and R_2 (Fig.H.1) were measured with a multimeter.

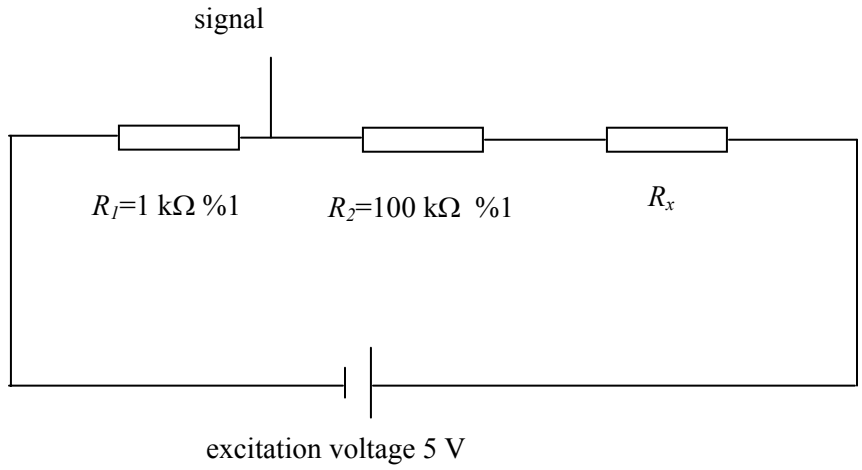

Figure H.1 Circuit diagram of leaf wetness sensor

The calibration procedure was:

1) the surface of sensor was dried with a hot air dryer, dispersing any existing moisture and letting sensor stay in room condition for 2-3 minutes and measure the resistance of the variable resistor R_x (Fig.H1) that reflects the level of wetness with a multimeter;

2) water was sprayed with a fogger on the sensor surface evenly and the steady resistance of R_x was measured;

3) the sensor was dried naturally at room condition or with a hot air dryer till all

visible water on the sensor surface disappeared, but there was still visible moisture retained in the entire paint layer, then the resistance of R_x was measured.

The process was repeated three or four times to get the average values of calibration resistances of R_x for the three different wetness levels.

During the actual measurements, a 5-volts DC power supply was applied (Fig.H.1), the voltage across R_x and of the power supply were measured and recorded at five-second intervals with a datalogger. The resistance of the R_x was calculated with voltage of power supply, across the R_x and the real values of the resistors R_1 and R_2. Then the resistance of R_x was compared with calibrated value to determine the level of wetness.

Appendix I MATLAB code for thermal stratification model without considering canopy

```
%*************************************************************************************************%
%**********************THERMAL STRATIFICATION MODEL FOR**********************%
%*****************************FAN-VENTILATED GREENHOUSES**********************%
%*************************************************************************************************%
%                                        Shuhai Li
%                                   Dept. of Bio. & Agric. Eng.
%                                  North Carolina State University
%                                        Oct. 2006
%Release note
%Oct, 2006--change effective thermal conductivity to be velocity dependent
%                 instread of multiplification ofthermal conductivity  of stagnant air with a  constant
%Oct,17, 2006- express the effective thermal conductivity as function of
%                    velocty gradient using mixing length theory.
%Dec, 15,2006-modified to compare lv and hv, pad vs nopad
%-------------------------------------------------------------------------------------------------------------------%
%-----------------------------------------------VARIABLE DEFINITION-----------------------------------------%
L=12;     %length of greenhouse, m
H=3;      %height of greenhouse ridge, m
deltx=1/8;  %cell length in horizontal direction, m
delty=0.5/8; %cell height in vertical direction, m
n=L/deltx; %number of cells in horizontal direction
m=H/delty; %number of cells in vertical direction
ta=zeros(n+1,m); %air temperature, oC
tf=zeros(n,1);  % floor temperature,oC
tc=zeros(n,1); % cover temperature, oC
u=zeros(1,m); %airflow speed in vertical velocity, m/s
keff=zeros(1,m);
keff1=zeros(1,m);
keff2=zeros(1,m);
h_sensor=[18 37 55 72.5 91.5]; % inch
h_sensor=h_sensor/115;
h_sensor=h_sensor*m;
h_sensor=int8(h_sensor);
%-------------------------------------------------------------------------------------------------------------------%
%
%-----------------------------------------------MODEL PARAMETERS-----------------------------------------%
%----------------Greenhouse Air Parameters----------%
c_a=1007;         %heat capacity of air@300k, J/(kg oC)
rho_a=1.177;     %air density, kg/m3
```

```
ka=0.02623;       %thermal conductivity of air, W/(moC)
ventrate=2;
pad=1;

%-------------------------------------------------------------------------------------------------------------%
%-----------------------------------------------INITIALIZATION-----------------------------------------------
%
%temperature of air, cover and floor
for i=1:(n+1)
      for j=1:m
            if pad==0
                  ta(i, j)=32;                  %inside temperature,oC
            end
            if pad==1
                  ta(i, j)=26;                  %inside temperature,oC
            end
      end
      if (i>=2)
            tc(i)=60;                  %cover temperature
            tf(i)=48;                   %soil temperature,oC
      end
end
%airflow velocity
for j=1:m
      if ventrate==1
            u(j)=0.4794*(j/m)^2-0.8166*j/m+0.412;   %low ventilation rate
      end
      if ventrate==2
            u(j)=-1.3511*(j/m)^2+0.6521*j/m+0.6021;  %high ventilation rate
      end
      if u(j)<0.05
            u(j)=0.05;
      end
end
%eddy (effective) thermal diffusivity
for j=1:m
      if j<m
            if j<=m/2
                  keff1(j)=0.41^2*j*abs(u(j+1)-u(j))*rho_a*c_a/0.7;
            end
            if j>m/2
                  keff1(j)=0.41^2*(m-j)*abs(u(j+1)-u(j))*rho_a*c_a/0.7;
            end
      else
            keff1(j)=keff(j-1);
      end
end

for j=1:m
      if ventrate==1
      keff2(j)=130*(u(j))^0.5;
```

```
        end
        if ventrate==2
            keff2(j)=70*(u(j))^0.5;
        end
end
ratio=0.0;
keff=keff1*ratio+keff2*(1-ratio);
%convective coefficient
if (ventrate==1) && (pad==0)
        hf=23;
        hc=19;
end

if (ventrate==1) && (pad==1)
        hf=10;
        hc=30;
end

if (ventrate==2) && (pad==0)
        hf=65;
        hc=10;
end

if (ventrate==2) && (pad==1)
        hf=39;
        hc=18;
end

%-------------------------------------------------------------------------------------------------------------%
%-----------------------------------------ITERATION-------------------------------------------------------%
ta_old=ta;
error=1;
while error>0.01
        ta_old=ta;
        for i=2:(n+1)
            for j=1:m
                if (j==1) %bottom boundary(floor)
                    %hf=4*(4.54+3.05*u(j));
                    %hf=23;
                    beta1=delty^2/deltx*rho_a*c_a*u(j)*ta(i-1,j)+keff(j+1)*ta(i,j+1)+hf*delty*tf(i);
                    beta2=delty^2/deltx*rho_a*c_a*u(j)+keff(j+1)+hf*delty;
                    ta(i,j)=beta1/beta2;
                end

                if (j==m) % upper boundary(roof)
                    %hc=16*(4.54+3.05*u(j));
                    %hc=19;
                    beta1=delty^2/deltx*rho_a*c_a*u(j)*ta(i-1,j)+keff(j)*ta(i,j-1)+hc*delty*tc(i);
                    beta2=delty^2/deltx*rho_a*c_a*u(j)+keff(j)+hc*delty;
                    ta(i,j)=beta1/beta2;
                end
```

```
                if ((j~=1) && (j~=m))
                    beta1=delty^2/deltx*rho_a*c_a*u(j)*ta(i-1,j)+keff(j)*ta(i,j-
1)+keff(j+1)*ta(i,j+1);
                    beta2=delty^2/deltx*rho_a*c_a*u(j)+keff(j)+keff(j+1);
                    ta(i,j)=beta1/beta2;
                end
            end
        end
        error_matrix=abs(ta-ta_old);
        error=max(error_matrix);
        error=max(error);
end

%print data at the postions of sensors
clc;
ta(60,h_sensor(5))
ta(60,h_sensor(4))
ta(60,h_sensor(3))
ta(60,h_sensor(2))
ta(60,h_sensor(1))
%plot temperature map
figure
climit=[26,48];
h=imagesc(ta',climit);
fontsize1=18;
fontsize2=16;
set(get(gca,'XLabel'),'String','Relative distance from pad','fontweight','bold','fontsize',fontsize1)
set(get(gca,'YLabel'),'String','Relative height','fontweight','bold','fontsize',fontsize1)
set(gca,'PlotBoxAspectRatio',[3 1 1])
set(gca,'Ydir','normal')
set(gca,'XTickLabel',{'0.1','0.2','0.3','0.4','0.5','0.6','0.7','0.8','0.9'},'fontsize',fontsize1,'fontweight','bold
')
set(gca,'YTickLabel',{'0.2','0.4','0.6','0.8'},'fontsize',fontsize1,'fontweight','bold')
colorbar('YTick',[26,30,34,38,42,46],'YTickLabel',{'26','30','34','38','42','46'},'fontweight','bold','fontsi
ze',fontsize2);
```

Appendix J MATLAB code for thermal stratification model considering canopy

```
%*************************************************************************************************%
%**********************THERMAL STRATIFICATION MODEL FOR**********************%
%*****************************FAN-VENTILATED GREENHOUSES**********************%
%*************************************************************************************************%
%                                        Shuhai Li
%                                   Dept. of Bio. & Agric. Eng.
%                                  North Carolina State University
%                                        Oct. 2006
%-----Revision note:
%10/09/2006---change effective thermal conductivity to be velocity dependent
%                 instead of multiplification of thermal conductivity  of stagnant air with a  constant

%10/11/2006---add soil and cover heat balance and rearrange the index for
%                   air temperature ta

% 10/23/2006---incoporate canopy into the model
% 12/12/2006--remove soil and cover heat balance
% 02/21/2007--tweak the model
% 02/28/2007 --add another plane of cells representing air at walking aisle

%-------------------------------------------------------------------------------------------------------------------
%
%----------------------------------------CONFIGURATION DATA----------------------------------------%

% configuration for disseration illustration, HV
c1=1.75;% H2
c2=3; % LAI
c3=0.78; % W1
c4=0.54; % W2
c5=0.7; % u
c6=0.3; %u2

c7=60; %tcv
c8=45; %ts
c9=26; %to
c10=0.88; %rh_o
c11=32; %to2
c12=720; %so

%-------------------------------------------------------------------------------------------------------------------
--%
```

```
%-----------------------------------------------VARIABLE DEFINITION-----------------------------------------
-%
L=12;     %length of greenhouse, m
H=3;      %height of greenhouse ridge, m
H2=c1;    %height of canopy, m

deltx=1;  %cell length in horizontal direction, m
deltz=1/4; %cell height in vertical direction, m

n=L/deltx; %number of cells in horizontal direction
m=H/deltz; %number of cells in vertical direction
m2=H2/deltz; %number of cell of canopy in vertical direction

ta=zeros(n,m); %air temperature at canopy row, oC
psi=zeros(n,m); %vapor concentration at canopy row, kg/m3
rhi=zeros(n,m); %relative humidity at canopy row, %

ta2=zeros(n,m); %air temperature at walking aisle, oC
psi2=zeros(n,m); %vapor concentration at walking aisle, kg/m3
rhi2=zeros(n,m); %relative humidity at walking aisle, %

tcv=zeros(n,1); % cover temperature, oC
tc=zeros(n,m2); % leaf temperature,oC
ts=zeros(n,1);   % soil temperature,oC
u=zeros(1,m); %air speed at the canopy row, m/s
u2=zeros(1,m); %air speed at the walking aisle, m/s

keff=zeros(1,m); %effective thermal conductivity in vertical direction for canopy area, W/(moC)
Deff=zeros(1,m);  %effect water vapor diffusion coefficient in air for canopy area, m2/s

keff2=zeros(1,m); %effective thermal conductivity in vertical direction for walking aisle, W/(moC)
Deff2=zeros(1,m);  %effect water vapor diffusion coefficient in air from walking aisle, m2/s

keff3=zeros(1,m); %effective thermal conductivity in vertical direction between canopy and walking
aisle, W/(moC)
Deff3=zeros(1,m);  %effect water vapor diffusion coefficient in air between canopy and walking
aisle, m2/s

h_sensor=[20 39 58.5 77.5 100]; % heights of aspirated tubes, inch
h_sensor=h_sensor/115;%relative height, 115in is the height of roof
h_sensor=h_sensor*m; %
h_sensor=int8(h_sensor);

h_sensor2=[20 40 52]; %height of leaf thermocouples, in
h_sensor2=h_sensor2/(H2/0.0254);%relative height
h_sensor2=h_sensor2*m2;
h_sensor2=int8(h_sensor2);
```

```
%-------------------------------------------------------------------------------------------------------------------
%
%-----------------------------------------MODEL PARAMETERS-----------------------------------------%

%-----------------------------------------Air Parameters-------------------------------------------------%
c_a=1007;        %heat capacity of air@300k, J/(kg oC)
rho_a=1.177;     %air density, kg/m3
k=0.02623;   %stagant air thermal conductivity, W/(moC)
D=2.54*10^-5; %water vapor diffussivity in air, m2/s
%-----------------------------------------Cover Parameters-----------------------------------------%
alpha_cv_sw=0.16;   %short wave absorptivity of cover
tau_cv_sw=0.69;       %short wave transmissivity
rho_cv_sw=1-alpha_cv_sw-tau_cv_sw;   %short wave reflectivity

epsilon_cv_lw=0.2;     %longwave emissivity
alpha_cv_lw=epsilon_cv_lw; %long wave absorptivity
tau_cv_lw=0.62*tau_cv_sw;   %longwave transmissivity
rho_cv_lw=1-epsilon_cv_lw-tau_cv_lw;    %longwave reflectivity

%-----------------------------------------Soil Parameters------------------------------------------%
rho_f_sw=0.25;   %short wave reflectivity
alpha_f_sw=1-rho_f_sw;   %short wave absorptivity

epsilon_f_lw=0.9;     %longwave emissivity
alpha_f_lw=epsilon_f_lw; %long wave absorptivity
rho_f_lw=1-epsilon_f_lw;    %longwave reflectivity

%-----------------------------------------Greenhouse Leaf Parameters-----------------------------%
LAI=c2;
cl=0.1;  %characteristic length of leaf ,m
rs=100; %stomatal resistance, s/m
w1=c3; %half of the distance of canopy rows,m
w2=c4;  %half width of canopy rows, m
zeta=LAI/H2; %foliage area density, m-1

k_c_sw=0.59;   %short wave extinction coefficient with respect to LAI
k_c_sw_prime=LAI*k_c_sw/H2;  %short wave extinction coefficient with respect to height

k_c_lw=0.59*1.35;   %long wave extinction coefficient with respect to LAI
k_c_lw_prime=LAI*k_c_lw/H2;  %long wave extinction coefficient with respect to height

rho_c_sw=0.12;   %short wave reflectivity
tau_c_sw1=0;
tau_c_sw2=exp(-k_c_sw*LAI);
tau_c_sw=tau_c_sw1+tau_c_sw2;
alpha_c_sw=1-rho_f_sw-tau_c_sw;   %short wave absorptivity

rho_c_lw=0.1; %longwave reflectivity
tau_c_lw1=0;
tau_c_lw2=exp(-k_c_lw*LAI);
tau_c_lw=tau_c_lw1+tau_c_lw2;
```

```
epsilon_c_lw=1-rho_c_lw-tau_c_lw;     %longwave emissivity
alpha_c_lw=epsilon_c_lw;

%-----------------------------------------Mics. Parameters-----------------------------------------%
to=c9;   % inlet temperature, oC
rh_o=c10;  %inlet relative humidity, decimal
psio=vaporcon(to,rh_o);%outside vapor concentration, kg/m3
to2=c11;  %outside temperature
so=c12;  % outside solar radiation, W/m2

sigma=5.67*10^-8;   %Stephan-boltzman constant
lamda=2.5*10^6;    %latent heat of evaporation, J/kg
a1=0.00048761;
a2=0.0053675;

%--------------------------------solar radiation penetration in canopy-------------------------%
% phi_c_sw_abs2=zeros(1,m2);
% for j=1:m2
%     phi_c_sw=so*tau_cv_sw*alpha_c_sw*(1+tau_c_sw*rho_f_sw); %short wave radiation
absorbed by canopy,W/m2
%     a=exp(k_c_sw_prime*deltz);
%     b=a^(j-1)*(a-1)/(a^m2-1);
%     phi_c_sw_abs2(j)=phi_c_sw*b/(zeta*deltz);
% end


%-------------------------------------------------------------------------------------------------------------%
%-------------------------------------------------INITIALIZATION-----------------------------------------------
%
for i=1:n
   for j=1:m
      ta(i, j)=c9;              %inside temperature,oC
      psi(i,j)=vaporcon(ta(i,j),c10);

      ta2(i, j)=c9;              %inside temperature,oC
      psi2(i,j)=vaporcon(ta2(i,j),c10);
   end

   for j=1:m2
      tc(i,j)=c9+1;                    % leaf temperature,oC
   end

   tcv(i)=c7;                     %cover temperature,oC
   ts(i)=c8;                     %soil temperature,oC
end

%---------------------------airflow velocity--------------%
for j=1:m
   %u(j)=0.4794*(j/m)^2-0.8166*j/m+0.412;   %low ventilation rate
   %u(j)=-1.3511*(j/m)^2+0.6521*j/m+0.6021;  %high ventilation rate
   if j<=m2
```

```
        u(j)=c6;
    end
    if j>m2
        u(j)=c5;
    end

    u2(j)=c5;
end

%---------effective vapor diffusivity or thermal conductivity----%
for j=1:m
    if j<=m2
        keff(j)=10*(u(j))^0.5;
        Deff(j)=keff(j)/k*D;

        keff3(j)=4*10*((u(j)+u2(j))/2)^0.5;
        Deff3(j)=keff3(j)/k*D;
    end

    if j>m2
        keff(j)=150*(u(j))^0.5;
        Deff(j)=keff(j)/k*D;

        keff3(j)=150*(u(j))^0.5;
        Deff3(j)=keff3(j)/k*D;
    end

        keff2(j)=150*(u2(j))^0.5;
        Deff2(j)=keff2(j)/k*D;

end

%-------------------------------------------------------------------------------------------------------------------%
%-----------------------------------------ITERATION-------------------------------------------------%
converge_all=0;
while converge_all==0
    ta_old=ta;
    psi_old=psi;
    tc_old=tc;
    ta2_old=ta2;
    psi2_old=psi2;

    for i=1:n

  %-----------------------------------------canopy row-----------------------------------------------%
        for j=1:m
            % -------------------------Convection coefficient-----------------%
            h_f_a=5;
            h_cv_a=15;
            if j<=m2
                h_c_a=(5.2*(u(j)/cl)^0.25+1.9*((abs(tc(i,j)-ta(i,j)))/cl)^0.25)*2;
```

```
        end

        % ------------------------Air  temperature at canopy row-----------------%
        if (i==1) %------------------ first column----------------

            if (j==1) %bottom boundary(floor)
                beta1=deltz^2/deltx*rho_a*c_a*u(j)*to+keff(j+1)*ta(i,j+1)+h_f_a*deltz*(ts(i)-
10)+h_c_a*zeta*deltz^2*tc(i,j)+keff3(j)*4*deltz^2/(w1*w2)*ta2(i,j);

beta2=deltz^2/deltx*rho_a*c_a*u(j)+keff(j+1)+h_f_a*deltz+h_c_a*zeta*deltz^2+keff3(j)*4*deltz^2/
(w1*w2);
                ta(i,j)=beta1/beta2;
            end

            if ((j>=2) && (j<=m2)) % in canopy
                beta1=deltz^2/deltx*rho_a*c_a*u(j)*to+keff(j-1)*ta(i,j-
1)+keff(j+1)*ta(i,j+1)+h_c_a*zeta*deltz^2*tc(i,j)+keff3(j)*4*deltz^2/(w1*w2)*ta2(i,j);
                beta2=deltz^2/deltx*rho_a*c_a*u(j)+keff(j-
1)+keff(j+1)+h_c_a*zeta*deltz^2+keff3(j)*4*deltz^2/(w1*w2);
                ta(i,j)=beta1/beta2;
            end

            if ((j>m2) && (j<m)) %above canopy
                beta1=deltz^2/deltx*rho_a*c_a*u(j)*to+keff(j-1)*ta(i,j-
1)+keff(j+1)*ta(i,j+1)+keff3(j)*4*deltz^2/(w1*w2)*ta2(i,j);
                beta2=deltz^2/deltx*rho_a*c_a*u(j)+keff(j-1)+keff(j+1)+keff3(j)*4*deltz^2/(w1*w2);
                ta(i,j)=beta1/beta2;
            end

            if (j==m) % upper boundary(roof)
                beta1=deltz^2/deltx*rho_a*c_a*u(j)*to+keff(j-1)*ta(i,j-
1)+h_cv_a*deltz*tcv(i)+keff3(j)*4*deltz^2/(w1*w2)*ta2(i,j);
                beta2=deltz^2/deltx*rho_a*c_a*u(j)+keff(j-
1)+h_cv_a*deltz+keff3(j)*4*deltz^2/(w1*w2);
                ta(i,j)=beta1/beta2;
            end

        else %-----------------second column-------------------

            if (j==1) %bottom boundary(floor)
                beta1=deltz^2/deltx*rho_a*c_a*u(j)*ta(i-1,j)+keff(j+1)*ta(i,j+1)+h_f_a*deltz*(ts(i)-
10)+h_c_a*zeta*deltz^2*tc(i,j)+keff3(j)*4*deltz^2/(w1*w2)*ta2(i,j);

beta2=deltz^2/deltx*rho_a*c_a*u(j)+keff(j+1)+h_f_a*deltz+h_c_a*zeta*deltz^2+keff3(j)*4*deltz^2/
(w1*w2);
                ta(i,j)=beta1/beta2;
            end

            if ((j>=2) && (j<=m2)) % in canopy
                beta1=deltz^2/deltx*rho_a*c_a*u(j)*ta(i-1,j)+keff(j-1)*ta(i,j-
1)+keff(j+1)*ta(i,j+1)+h_c_a*zeta*deltz^2*tc(i,j)+keff3(j)*4*deltz^2/(w1*w2)*ta2(i,j);
```

```
            beta2=deltz^2/deltx*rho_a*c_a*u(j)+keff(j-
1)+keff(j+1)+h_c_a*zeta*deltz^2+keff3(j)*4*deltz^2/(w1*w2);
            ta(i,j)=beta1/beta2;
        end

        if ((j>m2) && (j<m)) % above canopy
            beta1=deltz^2/deltx*rho_a*c_a*u(j)*ta(i-1,j)+keff(j-1)*ta(i,j-
1)+keff(j+1)*ta(i,j+1)+keff3(j)*4*deltz^2/(w1*w2)*ta2(i,j);
            beta2=deltz^2/deltx*rho_a*c_a*u(j)+keff(j-1)+keff(j+1)+keff3(j)*4*deltz^2/(w1*w2);
            ta(i,j)=beta1/beta2;
        end
        if (j==m) % upper boundary(roof)
            beta1=deltz^2/deltx*rho_a*c_a*u(j)*ta(i-1,j)+keff(j-1)*ta(i,j-
1)+h_cv_a*deltz*tcv(i)+keff3(j)*4*deltz^2/(w1*w2)*ta2(i,j);
            beta2=deltz^2/deltx*rho_a*c_a*u(j)+keff(j-
1)+h_cv_a*deltz+keff3(j)*4*deltz^2/(w1*w2);
            ta(i,j)=beta1/beta2;
        end
      end % if (i==1)
    end% for j=1:m

    % -------------------------Vapor Concentration----------------%
    for j=1:m
      h_c_a_prime=2/(rho_a*c_a/(h_c_a/2)+rs);
      if (i==1) %----------------first column------------------
        if (j==1) %bottom boundary(floor)

beta1=deltz^2/deltx*u(j)*psio+Deff(j+1)*psi(i,j+1)+h_c_a_prime*zeta*deltz^2*vaporcon(tc(i,j),1)+
Deff3(j)*4*deltz^2/(w1*w2)*psi2(i,j);

beta2=deltz^2/deltx*u(j)+Deff(j+1)+h_c_a_prime*zeta*deltz^2+Deff3(j)*4*deltz^2/(w1*w2);
            psi(i,j)=beta1/beta2;
        end

        if ((j>=2) && (j<=m2)) % in canopy
            beta1=deltz^2/deltx*u(j)*psio+Deff(j)*psi(i,j-
1)+Deff(j+1)*psi(i,j+1)+h_c_a_prime*zeta*deltz^2*vaporcon(tc(i,j),1)+Deff3(j)*4*deltz^2/(w1*w2)
*psi2(i,j);

beta2=deltz^2/deltx*u(j)+Deff(j)+Deff(j+1)+h_c_a_prime*zeta*deltz^2+Deff3(j)*4*deltz^2/(w1*w2
);
            psi(i,j)=beta1/beta2;
        end

        if ((j>m2) && (j<m)) % above canopy
            beta1=deltz^2/deltx*u(j)*psio+Deff(j)*psi(i,j-
1)+Deff(j+1)*psi(i,j+1)+Deff3(j)*4*deltz^2/(w1*w2)*psi2(i,j);
            beta2=deltz^2/deltx*u(j)+Deff(j)+Deff(j+1)+Deff3(j)*4*deltz^2/(w1*w2);
            psi(i,j)=beta1/beta2;
        end
```

```
            if (j==m) % upper boundary(roof)
               beta1=deltz^2/deltx*u(j)*psio+Deff(j)*psi(i,j-1)+Deff3(j)*4*deltz^2/(w1*w2)*psi2(i,j);
               beta2=deltz^2/deltx*u(j)+Deff(j)+Deff3(j)*4*deltz^2/(w1*w2);
               psi(i,j)=beta1/beta2;
            end

         else%--------------------second column-----------------------%

            if (j==1) %bottom boundary(floor)
               beta1=deltz^2/deltx*u(j)*psi(i-
1,j)+Deff(j+1)*psi(i,j+1)+h_c_a_prime*zeta*deltz^2*vaporcon(tc(i,j),1)+Deff3(j)*4*deltz^2/(w1*w
2)*psi2(i,j);

beta2=deltz^2/deltx*u(j)+Deff(j+1)+h_c_a_prime*zeta*deltz^2+Deff3(j)*4*deltz^2/(w1*w2);
               psi(i,j)=beta1/beta2;
            end

            if ((j>=2) && (j<=m2)) % in canopy
               beta1=deltz^2/deltx*u(j)*psi(i-1,j)+Deff(j)*psi(i,j-
1)+Deff(j+1)*psi(i,j+1)+h_c_a_prime*zeta*deltz^2*vaporcon(tc(i,j),1)+Deff3(j)*4*deltz^2/(w1*w2)
*psi2(i,j);

beta2=deltz^2/deltx*u(j)+Deff(j)+Deff(j+1)+h_c_a_prime*zeta*deltz^2+Deff3(j)*4*deltz^2/(w1*w2
);
               psi(i,j)=beta1/beta2;
            end

            if ((j>m2) && (j<m)) % above canopy
               beta1=deltz^2/deltx*u(j)*psi(i-1,j)+Deff(j)*psi(i,j-
1)+Deff(j+1)*psi(i,j+1)+Deff3(j)*4*deltz^2/(w1*w2)*psi2(i,j);
               beta2=deltz^2/deltx*u(j)+Deff(j)+Deff(j+1)+Deff3(j)*4*deltz^2/(w1*w2);
               psi(i,j)=beta1/beta2;
            end

            if (j==m) % upper boundary(roof)
               beta1=deltz^2/deltx*u(j)*psi(i-1,j)+Deff(j)*psi(i,j-
1)+Deff3(j)*4*deltz^2/(w1*w2)*psi2(i,j);
               beta2=deltz^2/deltx*u(j)+Deff(j)+Deff3(j)*4*deltz^2/(w1*w2);
               psi(i,j)=beta1/beta2;
            end
         end % if (i==1)
      end% for j=1:m

 % ------------------------------------------------------------- walking aisle-----------------------------------
------%
      for j=1:m

         if (i==1) %------------------ first column----------------
            if (j==1) %bottom boundary(floor)
               beta1=deltz^2/deltx*rho_a*c_a*u(j)*to+keff2(j+1)*ta2(i,j+1)+h_f_a*deltz*(ts(i)-
0)+keff3(j)*4*deltz^2/(w1*(w1-w2))*ta(i,j);
```

```
beta2=deltz^2/deltx*rho_a*c_a*u(j)+keff2(j+1)+h_f_a*deltz+keff3(j)*4*deltz^2/(w1*(w1-w2));
                ta2(i,j)=beta1/beta2;
            end

            if ((j>=2) && (j<m)) % in canopy
                beta1=deltz^2/deltx*rho_a*c_a*u(j)*to+keff2(j-1)*ta2(i,j-
1)+keff2(j+1)*ta2(i,j+1)+keff3(j)*4*deltz^2/((w1-w2)*w2)*ta(i,j);
                beta2=deltz^2/deltx*rho_a*c_a*u(j)+keff2(j-1)+keff2(j+1)+keff3(j)*4*deltz^2/((w1-
w2)*w2);
                ta2(i,j)=beta1/beta2;
            end

            if (j==m) % upper boundary(roof)
                beta1=deltz^2/deltx*rho_a*c_a*u(j)*to+keff2(j-1)*ta2(i,j-
1)+h_cv_a*deltz*tcv(i)+keff3(j)*4*deltz^2/((w1-w2)*w2)*ta(i,j);
                beta2=deltz^2/deltx*rho_a*c_a*u(j)+keff2(j-1)+h_cv_a*deltz+keff3(j)*4*deltz^2/((w1-
w2)*w2);
                ta2(i,j)=beta1/beta2;
            end
        else %-----------------second column-------------------
            if (j==1) %bottom boundary(floor)
                beta1=deltz^2/deltx*rho_a*c_a*u(j)*ta2(i-1,j)+keff2(j+1)*ta2(i,j+1)+h_f_a*deltz*(ts(i)-
0)+keff3(j)*4*deltz^2/(w1*(w1-w2))*ta(i,j);

beta2=deltz^2/deltx*rho_a*c_a*u(j)+keff2(j+1)+h_f_a*deltz+keff3(j)*4*deltz^2/(w1*(w1-w2));
                ta2(i,j)=beta1/beta2;
            end

            if ((j>=2) && (j<m)) % in canopy
                beta1=deltz^2/deltx*rho_a*c_a*u(j)*ta2(i-1,j)+keff2(j-1)*ta2(i,j-
1)+keff2(j+1)*ta2(i,j+1)+keff3(j)*4*deltz^2/((w1-w2)*w2)*ta(i,j);
                beta2=deltz^2/deltx*rho_a*c_a*u(j)+keff2(j-1)+keff2(j+1)+keff3(j)*4*deltz^2/((w1-
w2)*w2);
                ta2(i,j)=beta1/beta2;
            end

            if (j==m) % upper boundary(roof)
                beta1=deltz^2/deltx*rho_a*c_a*u(j)*ta2(i-1,j)+keff2(j-1)*ta2(i,j-
1)+h_cv_a*deltz*tcv(i)+keff3(j)*4*deltz^2/((w1-w2)*w2)*ta(i,j);
                beta2=deltz^2/deltx*rho_a*c_a*u(j)+keff2(j-1)+h_cv_a*deltz+keff3(j)*4*deltz^2/((w1-
w2)*w2);
                ta2(i,j)=beta1/beta2;
            end
        end % if (i==1)
    end% for j=1:m

    % ------------------------Vapor Concentration----------------%
    for j=1:m

        if (i==1) %----------------first column-------------------
```

```
            if (j==1) %bottom boundary(floor)
               beta1=deltz^2/deltx*u(j)*psio+Deff2(j+1)*psi2(i,j+1)+Deff3(j)*4*deltz^2/((w1-
w2)*w2)*psi(i,j);
               beta2=deltz^2/deltx*u(j)+Deff2(j+1)+Deff3(j)*4*deltz^2/((w1-w2)*w2);
               psi2(i,j)=beta1/beta2;
            end


            if ((j>=2) && (j<m)) % between
               beta1=deltz^2/deltx*u(j)*psio+Deff2(j)*psi2(i,j-
1)+Deff2(j+1)*psi2(i,j+1)+Deff3(j)*4*deltz^2/((w1-w2)*w2)*psi(i,j);
               beta2=deltz^2/deltx*u(j)+Deff2(j)+Deff2(j+1)+Deff3(j)*4*deltz^2/((w1-w2)*w2);
               psi2(i,j)=beta1/beta2;
            end

            if (j==m) % upper boundary(roof)
               beta1=deltz^2/deltx*u(j)*psio+Deff2(j)*psi2(i,j-1)+Deff3(j)*4*deltz^2/((w1-
w2)*w2)*psi(i,j);
               beta2=deltz^2/deltx*u(j)+Deff2(j)+Deff3(j)*4*deltz^2/((w1-w2)*w2);
               psi2(i,j)=beta1/beta2;
            end

         else%----------------------second column-------------------------%
            if (j==1) %bottom boundary(floor)
               beta1=deltz^2/deltx*u(j)*psi2(i-1,j)+Deff2(j+1)*psi2(i,j+1)+Deff3(j)*4*deltz^2/((w1-
w2)*w2)*psi(i,j);
               beta2=deltz^2/deltx*u(j)+Deff2(j+1)+Deff3(j)*4*deltz^2/((w1-w2)*w2);
               psi2(i,j)=beta1/beta2;
            end

            if ((j>=2) && (j<m)) % between
               beta1=deltz^2/deltx*u(j)*psi2(i-1,j)+Deff2(j)*psi2(i,j-
1)+Deff2(j+1)*psi2(i,j+1)+Deff3(j)*4*deltz^2/((w1-w2)*w2)*psi(i,j);
               beta2=deltz^2/deltx*u(j)+Deff2(j)+Deff2(j+1)+Deff3(j)*4*deltz^2/((w1-w2)*w2);
               psi2(i,j)=beta1/beta2;
            end

            if (j==m) % upper boundary(roof)
               beta1=deltz^2/deltx*u(j)*psi2(i-1,j)+Deff2(j)*psi2(i,j-1)+Deff3(j)*4*deltz^2/((w1-
w2)*w2)*psi(i,j);
               beta2=deltz^2/deltx*u(j)+Deff2(j)+Deff3(j)*4*deltz^2/((w1-w2)*w2);
               psi2(i,j)=beta1/beta2;
            end

         end % if (i==1)
      end% for j=1:m

      % ----------------------------------------Leaf temperature----------------------------------%
      for j=1:m2
         h_c_a=(5.2*(u(j)/cl)^0.25+1.9*((abs(tc(i,j)-ta(i,j)))/cl)^0.25)*2;
         h_c_a_prime=2/(rho_a*c_a/(h_c_a/2)+rs);
```

```
        phi_c_sw=so*tau_cv_sw*alpha_c_sw*(1+tau_c_sw*rho_f_sw); %short wave radiation
absorbed by canopy,W/m2
        a=exp(k_c_sw_prime*deltz);
        b=a^(j-1)*(a-1)/(a^m2-1);
        phi_c_sw_abs=phi_c_sw*b/(zeta*deltz);

        %---------------thermal radiation absorbed by canopy
        phi_sky_lw=sigma*(0.0552*(to2+273.16)^1.5)^4;                    %downward
longwave radiation from sky,W/m2
        tcv_avg=mean(tcv);                                               %average cover
temperatur at the top,oC
        tf_avg=mean(ts);                                              %average floor
temperature,oC
        b1=phi_sky_lw*tau_cv_lw*alpha_c_lw*(1+rho_f_lw*tau_c_lw);        %radiation from sky ,
W/m2
        b2=epsilon_cv_lw*sigma*(tcv_avg+273.16)^4*alpha_c_lw;            % radaition from cover
, W/m2
        b3=epsilon_f_lw*sigma*(tf_avg+273.16)^4*alpha_c_lw;              %radiation from floor
, W/m2
        b4=epsilon_c_lw*sigma*(tc(i,1)+273.16)^4*(-1+rho_f_lw*alpha_c_lw); %radiation emitted
by canopy, W/m2
        b5=epsilon_c_lw*sigma*(tc(i,m2)+273.16)^4*(-1+rho_cv_lw*alpha_c_lw); %radiation
emitted by canopy, W/m2
        phi_c_lw=b1+b2+b3+b4+b5;
        a=exp(k_c_lw_prime*deltz);
        b=a^(j-1)*(a-1)/(a^m2-1);
        phi_c_lw_abs=phi_c_lw*b/(zeta*deltz);

        beta1=phi_c_sw_abs+phi_c_lw_abs +h_c_a*ta(i,j)+h_c_a_prime*lamda*(psi(i,j)-a2);
        beta2=h_c_a+a1*h_c_a_prime*lamda;
        tc(i,j)=beta1/beta2;
    end

  end% i=1:n

  %residuel of air temperature between two adjacent steps
  error=abs(ta-ta_old);
  error_a=max(error);
  error_a1=max(error_a);

  error=abs(ta2-ta2_old);
  error_a=max(error);
  error_a2=max(error_a);

  error_a=max(error_a1,error_a2);

  %residuel of water vapor concentration between two adjacent steps
  error=abs(psi-psi_old);
  error_psi=max(error);
  error_psi1=max(error_psi);
```

```
    error=abs(psi2-psi2_old);
    error_psi=max(error);
    error_psi2=max(error_psi);

    error_psi=max(error_psi1,error_psi2);

    %residuel of leaf temperature between two adjacent steps
    error=abs(tc-tc_old);
    error_c=max(error);
    error_c=max(error_c);

    converge_all=(error_a<0.01) && (error_psi<0.001) && (error_c<0.01);

end %while converge_all==0


%-------------------------------------------------------------------------------------------------------%
%--------------------------CALCULATE RELATIVE HUMIDITY----------------------------------%

for i=1:n
    for j=1:m
        rhi(i,j)=psi(i,j)/vaporcon(ta(i,j),1);
    end
end
for i=1:n
    for j=1:m
        rhi2(i,j)=psi2(i,j)/vaporcon(ta2(i,j),1);
    end
end



%-------------------------------------------------------------------------------------------------------%
%--------------DISPLAY SIMULATED AIR AND LEAF TEMP. AND ---------------------------%
%--------------RELATIVE HUMIDITY AT THE SENSOR LOCATIONS--------------------------%

x=int8(n*0.6); %corresponding the location of sensor 3-7
%x=int8(n*0.4);  %corresponding the location of sensor 8-12
clc;
ta(x,h_sensor(5))
ta(x,h_sensor(4))
ta(x,h_sensor(3))
ta(x,h_sensor(2))
ta(x,h_sensor(1))

rhi(x,h_sensor(5))
rhi(x,h_sensor(4))
rhi(x,h_sensor(3))
rhi(x,h_sensor(2))
rhi(x,h_sensor(1))
```

```
tc(x,h_sensor2(3))
tc(x,h_sensor2(2))
tc(x,h_sensor2(1))

%-------------------------------------------------------------------------------------------------------------%
%---------------------------------PLOT SIMULATION RESULTS-------------------------------------%

%find minimum and maximum temperature
temp=min(ta);
min_ta=min(temp);
temp=max(ta);
max_ta=max(temp);

temp=min(tc);
min_tc=min(temp);
temp=max(tc);
max_tc=max(temp);
a1=int8(min(min_ta,min_tc))-1;
a2=int8(max(max_ta,max_tc))+1;
xlim=[a1,a2];

%plotting air temperature
imagesc(ta',xlim);
fontsize1=18;
fontsize2=16;
set(get(gca,'XLabel'),'String','Relative distance from pad','fontweight','bold','fontsize',fontsize1)
set(get(gca,'YLabel'),'String','Relative height','fontweight','bold','fontsize',fontsize1)
set(gca,'PlotBoxAspectRatio',[3 1 1])
set(gca,'Ydir','normal')
a=[0.25*m,0.5*m,0.75*m,m];
set(gca,'XTick',a)
set(gca,'XTickLabel',{'0.25','0.5','0.75','1.0'},'fontsize',fontsize1,'fontweight','bold')
set(gca,'YTick',a)
set(gca,'YTickLabel',{'0.25','0.5','0.75','1.0'},'fontsize',fontsize1,'fontweight','bold')

colorbar('fontweight','bold','fontsize',fontsize2);
%colorbar('YTick',[30,34,38,42,46],'YTickLabel',{'30','34','38','42','46'},'fontweight','bold','fontsize',f
ontsize2);

%plotting RH
rhi_c=1-rhi;
figure
imagesc(rhi')
set(get(gca,'XLabel'),'String','Relative distance from pad','fontweight','bold','fontsize',fontsize1)
set(get(gca,'YLabel'),'String','Relative height','fontweight','bold','fontsize',fontsize1)
set(gca,'Ydir','normal')
set(gca,'PlotBoxAspectRatio',[3 1 1])
set(gca,'XTick',a)
set(gca,'XTickLabel',{'0.25','0.5','0.75','1.0'},'fontsize',fontsize1,'fontweight','bold')
set(gca,'YTick',a)
```

```
set(gca,'YTickLabel',{'0.25','0.5','0.75','1.0'},'fontsize',fontsize1,'fontweight','bold')
colorbar('fontweight','bold','fontsize',fontsize2);

%plotting leaf temperature
tc2=[tc,10*ones(12,5)];
figure
a=[0.25*m,0.5*m,0.75*m,m];
imagesc(tc2',xlim)
set(get(gca,'XLabel'),'String','Relative distance from pad','fontweight','bold','fontsize',fontsize1)
set(get(gca,'YLabel'),'String','Relative height','fontweight','bold','fontsize',fontsize1)
set(gca,'Ydir','normal')
set(gca,'PlotBoxAspectRatio',[3 1 1])
set(gca,'XTick',a)
set(gca,'XTickLabel',{'0.25','0.5','0.75','1.0'},'fontsize',fontsize1,'fontweight','bold')
set(gca,'YTick',a)
set(gca,'YTickLabel',{'0.25','0.5','0.75','1.0'},'fontsize',fontsize1,'fontweight','bold')
colorbar
colorbar('fontweight','bold','fontsize',fontsize2);
```